THE INFLUENCE OF TOOL GEOMETRY ON THE PERFORMANCE OF DRILLING TOOLS

by

ABO BAKR IBRAHIM ABD EL-WAHAB

A thesis submitted to

The University of Aston in Birmingham

as part of the requirements for the degree of

DOCTOR OF PHILOSOPHY

Department of Mechanical and Production Engineering

1985

THE UNIVERSITY OF ASTON IN BIRMINGHAM

THE INFLUENCE OF TOOL GEOMETRY ON THE PERFORMANCE OF DRILLING TOOLS

A thesis submitted for the degree of Doctor of Philosophy

by

ABO BAKR IBRAHIM ABD EL-WAHAB

S U M M A R Y

The main objective of the work presented in this thesis is to investigate the two sides of the flute, the face and the heel of a twist drill. The flute face was designed to yield straight diametral lips which could be extended to eliminate the chisel edge, and consequently a single cutting edge will be obtained. Since drill rigidity and space for chip conveyance have to be a compromise a theoretical expression is deduced which enables optimum chip disposal capacity to be described in terms of drill parameters. This expression is used to describe the flute heel side.

Another main objective is to study the effect on drill performance of changing the conventional drill flute. Drills were manufactured according to the new flute design. Tests were run in order to compare the performance of a conventional flute drill and non conventional design put forward. The results showed that 50% reduction in thrust force and approximately 18% reduction in torque were attained for the new design. The flank wear was measured at the outer corner and found to be less for the new design drill than for the conventional one in the majority of cases. Hole quality, roundness, size and roughness were also considered as a further aspect of drill performance. Improvement in hole quality is shown to arise under certain cutting conditions. Accordingly it might be possible to use a hole which is produced in one pass of the new drill which previously would have required a drilled and reamed hole.

A subsidiary objective is to design the form milling cutter that should be employed for milling the foregoing special flute from drill blank allowing for the interference effect. A mathematical analysis in conjunction with computing technique and computers is used.

To control the grinding parameter, a prototype drill grinder was designed and built upon the framework of an existing cincinnati cutter grinder. The design and build of the new grinder is based on a computer aided drill point geometry analysis. In addition to the conical grinding concept, the new grinder is also used to produce spherical point utilizing a computer aided drill point geometry analysis.

Keywords: Twist Drills. Diametral Lip Drills. Flute Contour. Metal Cutting. Drilling.

LIST OF CONTENTS

LIST OF TABLES

TABLE NO.

LIST OF FIGURES

Figure No.

ACKNOWLEDGEMENTS

The author wishes to thank:

Professor R H Thornley, MSc Tech,PhD,DSc,AMCT,C.Eng.,FIMechE, FIProdE,MJSME, for permitting this work to be carried out in the Department of Mechanical and Production Engineering of the University of Aston in Birmingham. Also for his help, guidance and encouragement as Supervisor throughout the project.

The Egyptian Government and the Committee of Vice-Chancellors and Principals of the Universities of the United Kingdom for providing the financial support.

Dr J Maiden for his assistance and for the valuable discussion on the presentation of this work.

Dr T J Vickerstaff for his guidance through the early stages of this work.

All technicians in the Production Engineering Division, especially Mr G Yardley, Mr A Exton and Mr L Sharpe for their assistance and enthusiasm in the experimental part of this work.

Also, Mrs C L Wheelwright for typing the script.

Finally, his wife Mona for her assistance, patience and encouragement during the preparation of this work.

DECLARATION

No part of the work described in this thesis has been submitted in support of an application for another degree or qualification to this or any other University of Institution of learning.

It gives an account of the author's own research work performed at the Department of Production Technology and Production Management (renamed in 1983 the Department of Mechanical and Production Engineering) at the University of Aston in Birmingham and field work undertaken as described in the thesis.

It is a well-known fact that in any work of this nature the researcher must rely extensively upon the wide and ever growing body of already published and unpublished research evidence, and this work is no exception.

The material referred to in the text has been gathered from many sources and over a period of years - much of the author's experience in industry, some in visits to plants and discussions with technical staff, some from public and private institutions, and some from technical literature.

A list of references to publications and papers consulted during the course of the investigation, is given in the List of References.

A.B.I. EL-WAHAB.

NOMENCLATURE

2w	Web Thickness
w	Half Web Thickness
do	Drill Diameter
Ro	Half Drill Diameter
r	Radius at any point of the cutting edge
2P	Point Angle
Ψ	Chisel Edge Angle
γ	Lip Clearance Angle
θo	Drill Helix Angle (at Periphery)
Rc, Rcmax	Chip Disposal Capacity and max. Chip Disposal Capacity
L	Land width measured normal to the Helix
LN,LH	Actual and projected land width measured normal to the drill axis
β	Angular difference margin/heel
β_o	the same as before for Rc Equals $R_c max$
Ro,ϵ_o	Polar coordinate of the face corner of the flute
A	Drill Cross Section Area
J	Drill Cross Section Polar Moment of Inertia (second)
H	Helical Pitch of the Drill
F	Feed rate mm/rev
M	Torque, N.CM
Th	Thrust, N
r,ϵ_h	Polar coordinates of any point at radius r on the heel side
μ	Poisson's ratio
G	Shear modulus, k_g/mm^2
R,K,ξ	Coefficients to the equation of polar moment of area
ν	Relative angle of twist rad/mm

m	constant of the heel side polynomial equation
S_s	Shear stress
R_t	Chip ratio
λ	Friction angle
ϕ_s	Shear angle, degree
α	Rake Angle
F_s	Shear Force on shear plane (N)
Fn_s	Normal force on shear plane (N)
T_1	Underformed chip thickness (mm)
T_2	Deformed chip thickness (mm)
R	Resultant Cutting Force (N)
F_r	Friction Force on the rake
F_n	Normal Force on the rake
F_z	Cutting Force
F_x	Feed Force

CHAPTER 1

GENERAL INTRODUCTION

1.1 INTRODUCTION

Drilling is the production of round holes from solid material by the conversion of the material into conventional chips by the relative motion between drill and workpiece. This motion may be achieved by a rotating cutting tool, workpiece or both. According to PERA's [1]* survey 28.2% of the total general engineering industry in Britain consisted of work carried out on drilling machines. Ernst and Haggerty [2] estimated about 20% of the machine tools in the USA were drilling machines. The drilling operations can also be carried out on virtually any type of machine tool capable of providing a relative rotation of workpiece and/or cutting tool.

The twist drill is the most common, cheapest and most effective method of producing the majority of holes required by industry [3]. Such drills are made by the million of a wide range of materials from Carbon Steel to Solid Carbide. According to Billau [4], the twist drill was invented in 1863 by Martigononi, but Wiriyacosol and Armarego [5] refer to Morse as having patented a twist drill in 1863. Oxford [6] reported that among the earliest drills were those made by the Egyptians. Machine made twist drills were also first produced in the 1860's, and the basically modern twist drill became a reality with the invention of high speed steel around 1900.

* Figures in parenthesis [ ] refer to references in the Bibliography.

1.2 TWIST DRILL FEATURES

A two flute twist drill, Figure (1), is generally considered to be geometrically complex [7 - 10] and its main features are as follows:

(1) Shank

The shank fits into the chuck or spindle. The drill used in the machine shop is made with either straight or taper shanks. A straight shank drill is held in a drill chuck. A taper-shank drill has a tang at the end which fits into a slot in the spindle. The tang helps to drive the drill and prevent it from slipping, and provides a means of removing it from the taper spindle. The type of shank depends upon the method used for holding the drill, small drills (up to 10 or 12mm in diameter) have a straight shank and are held in chucks. Large drills generally have tapered shanks.

(2) Body

The body is the part between the shank and the point. It consists of the land, the margin, the web, and the flute. The drill land is the periphery portion of the drill body between adjacent flutes. A portion of the land is cut away to provide clearance, the remaining uncut narrow strip along the body forms the margin.

The margin helps keep the drill straight in the hole and determines the diameter of the hole cut. The drill is full size only across the margins. At the back of the margin the body is smaller in diameter.

The web is the thickness between the flutes. From the point to the shank the web gets increasingly thicker in the interest of greater rigidity. This increase in web thickness may be as much as 50%, therefore when a drill is sharpened a number of times it may be found to have too large a web thickness so web thinning is a necessary practice. Chip movement has been found to be far better over parallel web surfaces than over increasing web surfaces, Russell [11]. With the general purpose drills web thickness at the point will lie in the range of 11% to 22% of drill diameter. The drill flute, two channels along the body of the drill, has been defined by Galloway [12] as a chip disposal groove. Tsai [13] points out the following functions of the flute:

* form the cutting edges on the drill point;
* allow the chip to escape;
* cause the chip to curl;
* permit cutting coolant to reach the cutting edges.

According to Pais [14], the flute form affects the shape of the drilling chip. Oxford [9] refers to the

influence of flute form on lip shape, chip flute space and drill torsional rigidity. One half of the flute, the face, is commonly determined in order to yield a straight cutting edge. The other half, the heel, is chosen in such a way that drill strength, drill rigidity and space for chip conveyance are at compromise [9, 15, 16].

(3) Size

The overall length and the flute length of a drill are standardized in relation to the drill diameter.

A shorter drill length increases the torsional rigidity and consequently the drill life as suggested by many workers [15, 17 - 19]. It was reported by National Twist Drill [17] that drill life was increased by more than 8000% by shortening the drill flute length when drilling a tough high temperature alloy.

The drill diameter is chosen to obtain the required hole size. It has a strong effect on cutting forces. Galloway [12] reported that, for a given feed, torque is approximately proportional to the square of the drill diameter. The thrust is approximately proportional to drill diameter. Wiriyacosal [5] shows that the thrust increases fairly linearly and the torque increases exponentially with increase in diameter.

Drill sizes come in standard diameters which are sized according to four commonly used systems.

i) Fractional inch vary from 1/64 to 5 inches, in steps of 1/64 inch to 3/4 inch, after which the steps gradually increase.

ii) Metric size vary from 0.5 to 76mm (these sizes are not as commonly used as the fractional size).

iii) Letter size vary from A (0.234 inch) to Z (0.134 inch) in steps of 0.004 to 0.010 inch.

iv) Numbers vary from No.1 (0.228 inch) to No.8 (0.0135 inch) in steps of approximately 0.002 inch. All number size drills are smaller than letter size drills.

Because drill size and equipment are designed by imperial and metric system, it will be necessary to use the imperial system in some places in the thesis, otherwise the metric system will be considered.

(4) Point

The configuration of the drill point probably has more effect on drill performance than any other single feature of drill design. Different drill point grinding methods were used by many investigators. The plane method was reported by Armarego [7]. The cylindrical method was reported by Billau and Mcgoldrick [20]. Conical grinding, the most common method, was reported by several authors [20-25]. The point

of the drill includes the cutting lips, the chisel edge (the end of the web), and the flank (the surface of the area at the back of the cutting lip). There are three features commonly specified in handbooks for drill point to be selected by the user at the drill point grinding stage

* point angle, 2P
* chisel edge angle, ψ
* lip clearance angle, γ

The point angle is the angle included between lips. A common point angle is 118 degrees. The cutting edge (lips) will be convex or concave if the angle is decreased or increased respectively from the angle which produces straight lips. The influence of point angle variation on drill life has been investigated by Galloway [15] who reported that for each material there was a different range of point angle which gave longest drill life. PERA [26] recommended a point angle 130 degree when drilling alloy steel for better drill life. The influence of point angle on drilling forces was studied by Galloway [15], PERA [26] and Bird [27]. They came to the general conclusion that, except for a few cases, thrust increased as the point angle was increased and torque was found to decrease as the point angle was increased.

The chisel edge angle is the angle between the chisel

edge and the cutting lip, it provides clearance in the chisel edge area. The angle is from 120 to 135 degrees. A large chisel edge angle results in long chisel edge, while a small chisel edge angle results in inadequate clearance.

The clearance angle (relief angle) keeps the drill flank from rubbing with the workpiece. It is conventionally specified at the outer corner of the cutting edge and is referred to as the nominal relief angle. It's value is usually from 8 to 12 degrees. The influence of the lip clearance angle on drill life was investigated by Lorenz [28] and Kaldor [29]. Lorenz reported that drill life varies inversely with the 3.77th power of the peripheral clearance angle. The effect of relief angle on drill life and cutting forces was studied by PERA [26]. According to PERA's result it was found that drill life increases as the relief angle was increased from 4 degrees to 8 degrees, and to decrease as the relief angle was increased from 12 degrees to 20 degrees. Relief angle was found to have little effect on torque but thrust decreased as the relief angle was increased. Galloway [12] reported that smaller relief angles resulted in stronger lips and longer drill life.

(5) Drill Helix

The helix angle is defined as the outer angle between

the margin and the drill axis. It is one of the drill features which is determined at the manufacture stage. It is given by $\tan^{-1} 2\pi r/H$, where r is the radial distance from the centre and H is the pitch length. The helix angle is largest at the periphery and decreases towards the centre. Usually it is at the periphery where the helix angle is referred to. The helix angle is related to the rake angle, and is selected to suit the material to be drilled. For general purpose high speed steel drill, the helix angle ranges from 22 to 33 degrees, Bhattacharyya [30]. Waller's [16] results indicate that the 28 degrees helix angle is superior to the 20 degrees from drill life point of view. Lorenz [31] quotes Kronenberg's discussion on the effect of the helix angle from the viewpoint of the stiffness of twist drills. He emphasized that the resistance of a twisted profile to loading is approximately 85% higher than that of an untwisted bar having the same profile. Lorenz recommended 40 degrees helix angle for better drill life. Galloway [15] investigate the effect of helix angle on drill life for titanium alloy Ti150A, from his results a 25 degrees helix angle gave longer life than 10 or 42 degrees. Shaw's [32] results on SAE3245 steel shows that torque and thrust decrease slightly with increased helix angle.

As a consequence of the helix angle and the need for a web, the rake angle varies along the cutting edge from positive at the periphery to significantly negative at the centre particularly on

the chisel edge itself, Figure(2). The deformed products under the chisel edge must be wiped or extruded into the drill flute where they usually intermingle with the chips produced by the main cutting edges. Accordingly undesirably high thrust force is associated with this inefficient process.

The sharp variation in the cutting speed along the length of the cutting lip with the maximum on the periphery of the drill is the principal reason for intensive wear of this zone, thus limiting drill life.

Long coiled chips which are evident in many drilling operations can lead to clogging in the flutes of the drill, thereby limiting the depth of drilling before withdrawal, in addition these chips can cause scoring of the hole. Also the swirling of the chips, before becoming detached from the workpiece, can form a source of danger particularly when drilling the tougher materials.

Drilling by means of a twist drill is not a machining operation resulting in the highest degree of dimensional accuracy, counter-boring, honing and reaming are further operations for the improvement of initial drilled hole, [33].

The previous comments represent the main drawbacks of the two flute conventional twist drill. Hence, a number of variations on point geometry of such a tool have been devised by many inves~tigators

with the aim of improving its performance. Several modified features are explained.

1.3 SURVEY ON TWO FLUTE, CONVENTIONAL TWIST DRILL MODIFICATIONS

The survey of the different modifications and efforts to improve drilling performance of the two flute conventional twist drill includes several drill shape design features:

(1) Chip Breaker

Long coiled chips, which are evident in many drilling operations can lead to clogging in the flute of the drill, thereby limiting the depth of drilling before withdrawal, and can cause scoring of the hole in addition to being a safety hazard.

Chip breaker grooves either on the face or on the flank, Figure(3), can be provided to reduce the width of the chip. This technique is generally applied to large diameter drills. The main disadvantage of having the grooves ground in the flanks of the drill point is that they have to be re-formed after a limited number of regrinds of the drill. Crisp [34] eliminated these difficulties by providing a helical rib on the heel side of the flute which extends for the entire length of the drill flute, Figure(4). This rib impedes the normal chip flow,

deflecting the chip into a tighter curl which may cause it to break. Another chip breaker drill design is offered by many drill manufacturers and is illustrated in Figure(5). Here, the heel side of the flute is moved into a location similar to that of the rib in the Crisp design and the chip breaking action appears to be similar.

The vibratory type chip breaker consists of a special chuck which is attached to the conventional drill chuck. The chuck encloses a ball which is free to rotate in a groove around the spindle of the chuck. The groove contains a small notch in one part of its circumference. As the chuck rotates, the ball rotates and passes over the notch every three-quarters of a revolution of the chuck, thus interruping the feed and causing the chip to break. Unfortunately, the maximum drill size which can be used is only 1/2inch, so the application is rather limited.

Chip breaker drills usually require more torque than standard design drills, this represents the extra energy required to break the chips and to eject the chips through the restricted flute space of these drills. The chip breaking action may also affect the stability of the drill and produce holes which are noticeably out-of-round. Accordingly it would be of great use if a modified flute shape could provide a more compact chip without need to introduce any chip breaking

characteristics.

(2) Double Margin Drill

Another available drill variant is the double-margin configuration, Figure (6), in which a secondary margin of full diameter is left at the trailing edge of the land. This provides the extra guidance in the hole. Billau [35] used this type of drill in such a way as the second margin cuts and by virtue of its support gives an increase in tool life over a conventional twist drill and a normal double margin drill.

(3) Thinned Web

In an attempt to improve the action of the chisel edge, different types of point thinning were reported. Zhirov [36] devised a high production drill, Figure(7), for drilling cast iron. A notching cut is made on the web which removes the original chisel edge, also a double angle point is provided. Bhattacharyya [37] developed a grinding technique to generate two slots at the chisel point in a manner similar to Zhirov point drill. PERA [38] described the effect of point thinning and point relieving on the performance of H.S.S. drills. Oxford [39] enlarge the displaced distance of the main cutting edges to add extra metal to the flute face in such a manner as to increase the torsional rigidity of the drill structure while maintaining the same centre web thickness as a standard design drill, such a drill is known as 'self-thinned drill' Figure(8).

To get the maximum benefit, it is necessary to chose the optimum orientation and setting angles during web thinning. In all cases of web thinning, special drill-point grinding equipment or fixturing is necessary to ensure the point symmetricality. Lack of symmetry will cause a number of problems, such as poor starting, oversize holes and accelerated tool wear.

(4) Spiral Point Shape

Ernst and Haggerty [2] devised a method of point generation which form a characteristic S-shaped line for the chisel edge instead of the straight chisel edge of the conventional drill point, Figure (9). Although this modified shape has increased the rake angle in the sections close to the axis and also provides self-centering effect in the section along the main cutting edge there is no difference, as the rake angles here are identical to the conventional.

(5) Helical Drill

This has the same shape as the spiral drill but with a steeper heel side than that of the conventional twist drill, Figure(10) and this has the same effect of thinning the web as the thinned-web drill. Hence the helical drill possesses the advantage of the spiral drill and the thinned web drill.

(6) Split Point

The crankshaft or split point drill, Figure(11), has been developed to improve the performance of the heavy-web drills which have a longer chisel edge. The drill is first sharpened in the normal manner, yielding a long chisel edge. Then a second grinding cut is made to give a sharp secondary relief in the centre of the chisel edge, thus creating a secondary cutting lip on the opposite cutting edge. The angle between these lip segements acts like a chip-splitter, and the narrower chips produced may be somewhat easier to eject. Another significant effect is that the split point reduces web-generated thrust.

(7) Racon Drill

This point has a curved lip that gradually narrows the included point angle from the chisel edge to the outer corner, Figure(12), thus thinning the chip and spreading out the load on a longer length of cutting edge. This drill configuration is ground on a Winslow Model HC grinder [40].

(8) Helicon Drill

The Helicon drill is a combination of Helical and Racon drills. It resembles a helical drill in the part near the periphery and possesses advantages of both helical drills and racon drills. The chisel edge is S-shaped and relatively sharp. The outer corner of the cutting edge is rounded to provide smaller cutting edge angle, Figure(13).

Although some of the previous modifications give improved performance in specific applications, none of these methods has resulted in the elimination of the traditional chisel edge or modified the severe negative rake angle along the cutting edge in the vicinity of the chisel edge. The overall improvement in drilling performance can be further enhanced by optimizing and combining the techniques of cutting edge modification and chisel edge elimination.

Also it can be said that, except the attempt to impart chip breaking characteristics and to increase rigidity of the drill structure, all the modifications have been brought about only by drill user through point grinding without any consideration being given to flute shape which is produced at the manufacture stage.

As the drill geometry is determined by the combined effect of the Flank surface and the flute shape, the most interesting of twist drill design changes would be those involving modification of the flute shape. Each flute comprises two parts, the face and the heel. The flute face, leading side, is to yield the cutting edge. The cutting elements comprise two main cutting edges (or lips), lying in parallel planes displaced from each other by a distance equal to the thickness of the web. Eliminating such a distance through flute change at the manufacturing stage would yield diametrally located lips which can be extended to eliminate the chisel edge, and consequently a single cutting edge would be obtained. The advantage of extending the lip over the thinning of the web arises from the fact

that extending an existing lip is much easier than creating slots with given settings and orientations. Accordingly the operation of extending the lip could be carried out by an operator working manually.

The heel side shape is chosen in such a way that drill rigidity and space for chip conveyance have to be a compromise. Many research workers have studied twist drill rigidity. However, the author did not find any reference to the chip disposal capacity which is one of the important features of the flute shape. Clearly, therefore, an important contribution can be made if a theoretical expression can be deduced which enables optimum flute disposal capacity to be described in terms of drill parameters. Thus the optimum compromise can be made for rigidity vs disposal capacity and the heel side contoured accordingly.

A successful investigation into the flute shape of the twist drill should include the method of manufacture. A form milling cutter required to mill the helical flute allowing for the interference is mathematically described and in conjunction with a computer a helical flute with high accuracy is obtained to satisfy a given set of drill parameters.

A simplified spherical quadratic model to generate the grinding surface of a diametral-curved lip drill is described. Based on this model, a prototype drill grinder was designed and built to investigate the effect of partially spherical-diametral lip on drill performance.

CHAPTER 2

AN APPROACH TO A NEW DRILL CONFIGURATION

2.1 INTRODUCTION

The survey on the modifications of conventional twist drills reported in Chapter 1 indicates that most of the efforts have concentrated on drill point modifications through point grinding techniques. No attempts have been made toward flute design modification with the aim of improving its geometrical characteristics. Although some of these modifications give improved performance in specific applications, none of them solve the basic problem that there must be a chisel edge and consequently two cutting regions.

As the drill point geometry is determined through the combined effect of its flute shape and its point grinding, it is assumed that among the most interesting twist drill design changes are those involving modification of the flute shape. Because flute shape is a drill feature which is specified at the manufacture stage and drill user has little opportunity to introduce any further modification, it is necessary to get the manufacturer's collaboration especially in the early stages of any effort toward such modification. In this chapter one drill manufacturer's collaboration to eliminate the chisel edge is to be investigated and evaluated and as a result some modifications to the manufacturer configuration are put forward with the aim of eliminating the drawbacks of this configuration, and finally an experimental test to investigate the effect of such modifications is described.

2.2 DESCRIPTION OF THE MANUFACTURER CONFIGURATIONS

Marwin Cutting Tools Ltd, manufacture a drilling tool which consists of helically formed pieces of tungsten carbide slotted into an appropriately formed body. The important feature of this drill is that one of the two cutting edges is extending beyond the centre with the aim of eliminating the chisel edge. The other cutting edge is terminated before the centre to provide the necessary web, Figure (14). However, asymmetry of the two cutting lips and the two flutes, as well as the eccentricity of the web, lead to a difference in cutting forces over each lip and provide unnecessary extra flute space ahead of one lip and in contrast unsufficient flute space ahead of the other lip, Figure (15).

The difference in lip lengths of such a drill is similar to the difference in lip height of the conventional drills. That leads to a resultant rotary radial force of constant magnitude. This force causes static bending stress for the drill and spindle with simultaneous dynamic stress and vibration of the workpiece and fixture.

The inappropriate flute spaces allocated ahead of each lip cause non-uniform cooling, lubrication as well as chip jamming and consequently unbalanced rotary forces of variable magnitude.

As a result of the above rotary radial forces of constant or variable magnitude, poor surface finish of the hole wall and high hole

oversize were experienced while using this type of drill during the preliminary test in this work.

As a consequence it is decided, in this work, to modify the asymmetry of such a drill and to investigate the effect on the drilling performance of the proposed modification. As mentioned before because a drill user has little chance to change an existing flute, the modification reported in this chapter is limited to the alteration on the lip lengths of the existing configuration. For this purpose it is necessary first to predict cutting forces over the two lips.

2.3 CUTTING FORCE PREDICTION

The mechanics of chip formation have been studied by many authors and it is now widely accepted that chip formation is a plastic shearing process and that the deformation is extremely localised.

Basically, the chip formation process can be best explained by considering the two-dimensional simple case "orthogonal cutting" in which a single cutting edge is perpendicular to the relative motion between the tool and workpiece. In practice, actual cutting operations often involve a cutting edge which is inclined at some angle other than 90 degrees to give "oblique cutting". However, the nature of the chip formation process is similar in both cases.

The first complete analysis providing a so called "shear angle solution" was presented by Ernst and Merchant [41]. In their analysis the chip was assumed to act as a rigid body which is held in equilibrium by the action of the forces transmitted across the chip-tool interface and across the shear plane. Figure (16) shows the system of forces in orthogonal cutting with a continuous chip.

Ernst [41] and Merchant [42] support the thin shear zone model. Palmer and Oxley [43], Okushima and Hitomi [44] propose a thick deformation zone model as shown in Figure (17). Bitans and Brown [45] suggest that under different machining conditions the deformation approximates to one or other of these shear models. After examining motion picture film and photo-micrographic evidence, they conclude that, especially when the metal is in an annealed state, the "thick zone" model is more appropriate at low cutting speed. At the high cutting speed region the situation approaches the "thin zone" model.

The selection of the proper chip formation model that could be employed to predict the cutting forces of helical carbide drills is based on the cutting condition of such types of drills. Since the advantages of using tungsten carbide include potential for higher metal removal rates (higher cutting speed), then the "thin zone" model is used in this work for the cutting force prediction.

The tool angles for the element force prediction such as the rake angle α are found from the specified drill point features given in

handbooks. The basic cutting data, such as the shear stress S_s, chip ratio R_t and friction angle on the rake face are found from experimental data for this purpose. En8 steel tubes of two inch outside diameter and 2.38 mm thickness are used with the Marwin Flat ended drill as a turning tool to predict the basic cutting data. The tube is held by a lathe chuck and the drill is fixed to a three component dynamometer using a special fixture designed for this purpose. The set of the dynamometer, drill fixture and the drill is fixed to the lathe saddle, Figure (18).

The cutting force components F_z and F_x are measured simultaneously and recorded throughout the machining process. During the cutting test, the chips were collected after each test and the thickness measured using 2×10^{-4} mm clock gauge equipped with a special pointed anvil designed for this purpose. The value used for calculation of shear angle was the average of five readings. The friction angle λ, shear stress S_s, and chip ratio R_t are correlated with the basic variables (rake, angle, speed, and feed). A statistical package using the subprogram "regression" SPSS [46] was used for the regression analysis as reported in Appendix I.

The regression analysis results obtained are as follows:

$$\lambda = 26.7 + 0.77\,\alpha$$

$$R_t = 0.277 + 4.8 \times 10^{-3}\,\alpha + 1.534f$$

$$S_s = 62.4$$

where

λ = friction angle in degrees

S_s = shear stress, Kg/mm^2

R_t = chip thickness ratio = t_1/t_2

α = rake angle, degrees

f = feed rate mm/rev

The element deformation force, F_z, parallel with the velocity approach is taken as a criterion of force balance. The lip region is considered to consist of numerous single edge orthogonal cutting elements where the variations in cutting conditions within each element may be neglected and the conditions are selected at the mid-point of the elemental cutting edge. The rake face curvature away from the cutting edge is considered during the obtaining of the basic cutting data. The element deformation force, ∇F_z, is found from the force equation of the single edge orthogonal analysis as:

$$\nabla F_z = \frac{S_s \cdot b \cdot f \cdot \text{Cos}\ (\lambda - \alpha)}{\sin \phi_s \ \text{Cos}\ (\phi_s + \lambda - \alpha)}$$

where

$$\alpha = \frac{r}{R_o} \tan \theta_o$$

$$\phi_s = \tan^{-1} \frac{R_t \ \text{Cos}\ \alpha}{1 - R_t \sin \alpha}$$

$$R_t = \frac{t_i}{t_2}$$

2.4 CUTTING EDGES MODIFICATION

To improve the cutting action, firstly a force balance is required to eliminate the resultant rotary radial force and secondly the flute space of the small lip has to be modified to improve chip disposal capacity. (This aspect to be considered in the following chapter.)

A Force balance can be achieved by reducing the length of the long lip by the amount which yields equal cutting forces over the two lips. The lip is considered to consist of 50 elements, the summation of the elemental deformation force starting from the outside for the short lip and from the inside for the long lip is done to find the radial distance at which the two summations are equal. That radial distance will define the length of each lip. For a 3/4 inch diameter, that radius is found to be 4.34 mm that means the long lip has to be shortened by 5.185 mm however, if this is done, cutting will not take place over an annular portion of 1.885 mm (the difference between the reduced amount and the length of the short lip). Due to this constraint, the outer lip is shortened by 3.3 mm to provide a partial elimination of rotary radial force, Figure(19).

2.5 EXPERIMENTAL TEST TO INVESTIGATE THE PERFORMANCE OF CUTTING LIP MODIFICATION

A series of tests and measurements were designed to investigate to what extent the limited modification will improve drilling performance. Comparison with a drill as received from the drill manufacturer and with a conventional drill is provided.

2.5.1 Instrumentation

The force components of thrust, radial force and torque were measured using a system comprising of a Kistler quartz four-component dynamometer, charge amplifier with built in galvo and a U-V recorder. The system is set out in Figure (20). For hole size measurement, a Tesa internal micrometer with a range of 1/2 to 1 inch was used. A series of five readings were taken from entry to exit of the diameter of each hole. A talyrond machine, Figure (21), was used to measure the out of roundness. Three readings were taken down the length of the hole at the entry, middle and exit of the hole.

(1) Dynamometer

A Kistler four-component dynamometer type 9273, Figure (22), was used to measure the axial and radial forces as well as torque in the drilling tests. It consists of two two-component load washers fitted under high pre-load one above the other

between a base plate and a cover plate. Each load washer contains two sets of quartz discs which are arranged directionally-orientated according to their sensitivity. The measuring principle of the dynamometer is to convert the applied physical variable into proportional electric output charge when the force acts upon a quartz element in the load washer. Calibration charts were provided by Kistler Instruments before the test programme started.

The technical specification for the dynamometer is as follows:

Components		F_x, F_y	F_z	M_z
Range	kN	-5...5	-5...20	Nm-100...100
Overload	kN	-6/6	-6/24	Nm-120/120
Threshold	N	0.02	0.02	Ncm 0.02
Sensitivity	pC/N	-3.65	-1.95	PC/Ncm 1.58
Linearity	% full scale output	$\leq \pm 1$	$\leq \pm 1$	$\leq \pm 1$
Hysteresis	% full scale output	1	1	1
Rigidity	kN/um	0.1	.2	Ncm/µrad 30
Natural frequency	KHz	1.5	3	
Cross talk		F_z $F_{x,y}$	%	$\leq \pm$ 1
		F_x F_y	%	$\leq \pm$ 3
		$F_{x,y}$ F_z	%	$\leq \pm$ 3
		F_z M_z	Ncm/N	$\leq \pm$ 0.02
		M_z F_z	N/Ncm	$\leq \pm$ 0.01
Operating temperature range		0 to 70°C		
Weight		Kg 3.3		

(2) Charge amplifier with galvo output

The charge amplifier converts the charge yielded by a piezo electric transducer into proportional voltage by a first stage with capacitive feedback. In the amplifier the signal is finally scaled for voltage output. This output signal is furthermore converted into a proportional current for deflecting a galvanometer by the galvopart of the amplifier.

The coefficient for the conversion of mechanical units into electrical charge is entered with the potentiometer for adjusting the TRANSDUCER SENSITIVITY and the setting ring.

The amplifier operates with fixed scales of 1, 2, 5.10^n mechanical units per volt. When a galvanometer is connected to the galvo output, the measuring signal is recorded to the same scale.

The technical data for charge amplifier used (model 5006) is as follows:

Measuring ranges 12 steps	1:2:5...PC		± 10....±500000
Transducer sensitivity		Pc/M.U	0.1....11000
Voltage output, 100		V/mA	± 10/< ± 5
Galvo output		mA	⩽ 60
Frequency range		KHz	0....180
Time constant	long	s	1000...100000
	Medium	s	1...5000
	Short	s	0.01...50
Linearity		%	< ± 0.05
Accuracy of ranges		%	< ± 1
Calibration input		PC/mv	1 ± 0.5%
Operating temperature range		^{o}C	0....50
Power supply		V	220/110 ± 20%
Dimensions		mm	74 x 145 x 216
Weight		Kg	1.5

(3) Direct recording ultra-violet oscillograph

The model 1300 U-V oscillograph can record up to ten channels. On each channel used (two) a SMI/L type tubular galvanometer was inserted. As the input current is fed into the circuit it produces an angular deflection of the mirror inside the galvanometer and reflects the light onto sensitised paper. The image is be developed by exposure to light. Time marks can be marked on the paper at

adjustable intervals during recording.

2.5.2 Test Specimens

The specimens were made from En8 steel (Grade D) of 2 inch diameter and 1.5 inch thickness (2.d). The preparation of test specimens consisted of three stages. Firstly the 2 inch diameter long bars were parted off using a capstan lathe, secondly the parted off specimens were face turned both sides using a centre lathe and finally a surface grinding machine was used to make the two faces completely parallel.

2.5.3 Test Variables

Three variables were selected: speed, feed and drill type

speed: 690, 1060, 1600 r.p.m.

feed: 38 - 137 x 10^{-3} mm/rev

tool: three types of tools are used in the test (3/4 in dia.)

i) conventional

ii) drill as received (asymmetric)

(iii) drill with partial lip modification (asymmetric & modified

During the drilling operation the thrust force, radial force and torque were monitored continuously during each test. After all the tests had been completed further measurements were taken for hole roundness and hole oversize.

2.6 RESULTS AND DISCUSSION

Three readings for hole roundness measurement were taken down the length of each hole at top, middle and bottom. Each specimen had to be individually centred on the talyrand machine, Figure(21), three times, one for each reading due to the error in parallelism of the hole. The average of the three readings was taken.

Hole measurement was taken for each hole using an internal micrometer. Five readings were taken in a sequence from entry side to exit side and the average of these five readings was taken. The data and results obtained from these tests are represented in Tables 1 - 5 and graphically shown in Figures(23)-(37) to represent the influence of a limited modification of lip lengths on radial force, out of roundness and hole oversize as well as drilling thrust and drilling torque at three speeds 690, 1060 and 1500 r.p.m. and different feed rates ranging from 38 to 137 x 10^{-3} mm/rev.

It may be seen from these results that the difference between drill as received (asymmetric) and drill with partial lip modification (Asymmetric & modified) is considerable in terms of radial force, Figures(23)-(25). Accordingly considerable improvement of out of roundness, Figures(26)-(28), and hole oversize, Figures (29)-(31),are obtained as a result of the reduction in the rotary unbalanced radial force which displaces the drill out of its axis of rotation. However, although the limited modification on lip lengths

provides a considerable improvement as mentioned, the values are higher than with the conventional drill.

2.7 CONCLUSION

Although the drill configuration proposed by a drill manufacturer provided advantages over a conventional drill in terms of drilling thrust and torque as shown in Figures(32)~(37), due to the elimination of chisel edge, the hole quality deteriorated due to the severe run out caused by the rotary radial force. This force is a result of asymmetric lip configuration and inappropriate flute allocation ahead of each lip.

As a general conclusion the main two aspects to be emphasised for any drill design modification are firstly the necessity of providing the proper chip disposal capacity, and secondly the necessity of symmetric configuration.

These two aspects, chip disposal capacity and symmetry configuration to eliminate the chisel edge are considered in the following chapters.

CHAPTER 3

SOME ASPECTS OF DRILL CROSS SECTION

3.1 INTRODUCTION

As mentioned in the previous chapter, the proper selection of flute space is of great importance in any drill design to allow the proper flute space and the proper chip disposal capacity. The requirements guiding the design of a twist drill flute shape are that on the one hand the area of the flute should be large enough to allow good chip removal and on the other hand the drill cross section should be sufficient to provide adequate rigidity to withstand the cutting forces. These are two contradictory conditions the fulfilment of which requires a compromise.

In many works in literature, no information has been found related to chip disposal capacity. It is the purpose of this chapter to provide a fundamental understanding of these two contradictory conditions (flute capacity and drill rigidity) and how they are affected by different drill parameters. Furthermore, a discussion on how to come to a compromise between them is included.

3.2 ANALYSIS OF CHIP DISPOSAL CAPACITY

A consideration of the flute space required leads to the conclusion that its total area is not the significant factor because a typical drill chip is conical in shape and hence only the inscribed circle of the flute cross section will be occupied. Consequently the inscribed circle diameter is considered in this work as the critical

parameter.

The radius R_c of the circle A and B in Figure(38) which could be inscribed in the flute space normal to the axis of drill are considered to be a good index of chip disposal capacity, because the chip which is formed is a curled-conical shape and will occupy a circular part of the flute space. When the radius of the chip cone tends to be larger than R_c, the chip is crushed in order to permit it to pass up the flute.

In this work a fundamental analysis is to be carried out to represent the chip disposal capacity by a mathematical model which defines the effect of various drill parameters (R_o, L, W, P, θ_o) on R_c.

In the normal cross section, Figure(39) the flute space a-c-e is approximately represented in this analysis by the space a-b-c-d-e. The circle which could be inscribed in that space is that circle, Figure (40), which meets the following conditions:

i) is tangent to o-a at point f

ii) is tangent to o-e at point g

iii) is tangent to a-e at point h

iv) its centre O_c lies along the radius oh which bisects angle β (angular difference margin/heel)

v) it has a radius R_c

vi) its maximum radius for given value of R_o and W is $(\frac{R_o - W}{2})$

From Figure (39)

$$LH = R_o[\sin\varepsilon_o + \sin(\varepsilon_o + \beta)] \; ; \qquad 3.1$$

$$LN = \frac{LH}{\sin\left(\varepsilon_o + \frac{\beta}{2}\right)} \qquad 3.2$$

$$\therefore L = LN \cdot \cos\theta_o$$

$$\therefore L = 2 R_o \cos\theta_o \cos\frac{\beta}{2} \qquad 3.3$$

from which

$$\beta = 2\cos^{-1}\left(\frac{L}{2 R_o \cos\theta_o}\right) \qquad 3.4$$

from Figure (40)

$$\sin\frac{\beta}{2} = \frac{R_c}{R_o - R_c} \qquad 3.5$$

$$R_c = \frac{R_o \sin\frac{\beta}{2}}{1 + \sin\frac{\beta}{2}} \qquad 3.6$$

or

$$R_c = \frac{R_o\left[(2 R_o \cos\theta_o)^2 - L^2\right]^{\frac{1}{2}}}{2 R_o \cos\theta_o + \left[(2R_o\cos\theta_o)^2 - L^2\right]^{\frac{1}{2}}} \qquad 3.7$$

Equations 3.6 and 3.7 represent the mathematical representation of chip disposal capacity in terms of angle β and land L respectively.

Reducing land width (increasing angle β) to the limit shown in

Figure(41) provide a chip disposal R_c equal to $R_{c\max}(\frac{R_o - W}{2})$.

The condition whereby this model starts to obtain is shown in Figure (42), from which the land width and angle β at which R_c remain constant for any further increase in angle β or reduction in land width equal:

$$L_o = \frac{4\ R_o\ \text{Cos}\ \theta_o \sqrt{W\ R_o}}{W + R_o} \qquad 3.8$$

and

$$\beta_o = 2\ \sin^{-1} \frac{R_o - W}{R_o + W} \qquad 3.9$$

Also, increasing the web thickness to the limit shown in Figure (43) provides a similar condition ($R_c = \frac{R_o - W}{2}$). The web thickness, for given land, at which this condition starts to obtain is given from Figure(42)as:

$$W_o = \frac{R_o\ (1 - \sin \frac{\beta}{2})}{1 + \sin \frac{\beta}{2}} \qquad 3.10$$

Accordingly for a given web thickness W and drill diameter $2R_o$ the value of chip disposal capacity R_c remains constant and equal to $\frac{R_o - W}{2}$ for $L \leqslant L_o$ $(\beta \geqslant \beta_o)$

Also, for a given land L (or β) and drill diameter $2R_o$ the value of chip disposal capacity R_c remains constant and equal to $\frac{R_o \sin \frac{\beta}{2}}{1+\sin \frac{\beta}{2}}$ for $W \leqslant W_o$.

3.3 DRILL RIGIDITY

The bigger the ratio of chip disposal capacity R_c to drill radius R_o, the better the chip removal and the less the friction between upward moving chips and the tool and thus the less the drilling forces. However, the bigger this ratio the lower the drill rigidity of the drill.

Drill torsional rigidity affects drill life as referred to by several workers [8, 16, 17, 28, 34, 36]. Because of its explicit effect on drill life and its implicit effect on chip disposal capacity, the drill rigidity needs to be studied with the aim of finding how it correlates with the twist drill parameters. Because of drill shape complexity some research workers give different definitions for drill rigidity. For example, Oxford [8] considered the diameter of the circle which could be inscribed in the cross section normal to the drill axis as a good index of the torsional rigidity. However, a study of the range of twist drills shown in Table 6 indicates that for some cases the inscribed diameter is not consistent with the change in polar second moment of area which is proportional to drill rigidity. Spur [47] relies on visual description of the cross section polar second moment of inertia which provides no accurate assessment. Kirilenko [48] relied on an empirical formula to calculate the polar second moment of inertia which does not include the effect of helix angle and point angle.

From the previous comments, it becomes clear that neither the visual description by Spur nor the index suggested by Oxford are entirely valid. The drill rigidity must be accurately defined and greatly simplified if an empirical equation is to be deduced which includes the effect of various drill parameters, such as diameter, land, web as well as the helix angle and point angle. For this purpose a detailed analysis to calculate the cross section area and second polar moment of area is presented in Appendix II and in conjunction with a regression analysis the following empirical equations were obtained

$$\text{Area } A = 16.9 \times 10^{-2} L^{1.286} do^{.57} {}_{2W}{}^{.142} {}_{2p}{}^{.169} \theta_o^{.275} \qquad 3.11$$

second
Polar moment of inertia

$$J = 2.6 \times 10^{-2} do^{2.74} L^{1.194} \theta_o^{.33} {}_{2W}{}^{.063} {}_{2p}{}^{.034} \qquad 3.12$$

A comparison of the actual and predicted values are shown in Tables 8 and 9 for the variables in Table 7. From which it can be seen that a good accuracy of prediction is obtained using these empirical equations.

To analyse a complete drill structure, section compliance is integrated along the drill length taking into account the helical arrangement of the drill flute which has a considerable influence on drill torsional stiffness. Kirilenko [48] proposed the following formula

$$J_p = J\,(1 + \nu^2 \cdot \frac{K}{R}) - 2(1 + \mu)\nu^2\,\xi \qquad 3.13$$

where

J_p = provision polar second moment of area

$\nu = \dfrac{\tan\theta_o}{R_o}$

μ = poisson ratio

R, K and ξ are constants which are calculated from the formulae

$$R = \int_0^{R_0} \frac{r\,\psi(r)\,dr}{(1 + \nu^2 r^2)^2}$$

$$K = \int_0^{R_0} \frac{r^3\,\psi(r)\,dr}{(1 + \nu^2 r^2)^2}$$

$$\lambda = \int_0^{R_0} \frac{r^5\,\psi(r)\,dr}{(1 + \nu^2 r^2)^2}$$

$$\xi = \frac{K^2}{R} - \lambda$$

The value of function $\psi(r)$ is equal to the sum of angles α_1 and α_2 in Figure 46 which determine the points of intersection of the circle radius r with the cross section profile. For a symmetrical section, $\alpha_1 = \alpha_2$, instead of the graphical method to determine $\psi(r)$ used by Kirilenko, an analytical method is devised in this work. The advantage of providing such an analytical method is to facilitate the introducting of computer-aided design to handle the numerical work. The analytical method can be explained as follows:

In Figure 46:

$$\alpha_1 = \alpha_2 = \varepsilon + \theta \qquad 3.14$$

where

$$\varepsilon = \sin^{-1}\frac{W}{R} + \frac{\tan\theta_0 [R^2 - W^2]^{\frac{1}{2}}}{R_o \tan P} \qquad \text{(after Galloway)}$$

The angle θ can be calculated by knowing the constant m of the heel side polynomial equation.

$$Y = mx^2 + W \qquad 3.15$$

For point P_o in Figure 46

$$x = R \cos\theta \quad \text{and} \quad Y = R \sin\theta \qquad 3.16$$

From 3.15 and 3.16

$$R \sin\theta = m (R \cos\theta)^2 + w \qquad 3.17$$

Angle θ can be calculated from equation 3.17 using the value of constant m from appendix II,.

$$m = \frac{\sin(\beta + \varepsilon_o) - \frac{W}{R_o}}{R_o \cos^2(\beta + \varepsilon_o)}$$

and the value of angle β from equation 3.4

$$\beta = 2 \cos^{-1}\left(\frac{L}{2R_o \cos\theta_o}\right)$$

A Computer-aided design is used to handle these calculations and a comparison of the computer output of the analytical method with those obtained by the Kirilenko graphical method are shown in Figure(46). There is good coincidence between the two methods.

The calculated value of function $\psi(r)$ is used to calculate the provisional polar moment of inertia Jp. Example shown in Figure 47.

3.4. SELECTION OF DRILL PARAMETERS TO MAKE CHIP DISPOSAL CAPACITY AND DRILL RIGIDITY ON COMPROMISE

Using the foregoing analysis, the drill parameters such as land width L, angular difference margin/heel β, and web thickness 2W can be selected to provide optimum compromise of drill rigidity and chip disposal capacity. Alternatively the rigidity and chip disposal capacity which are the main features of cross section, can be predicted for certain drill parameters.

The influence on second polar moment of inertia (rigidity) and chip disposal capacity of land width L, angular difference β, and web thickness W, are presented graphically in Figures(48)-(50). The observations which can be made out of these Figures are, first the polar moment of inertia increases with the increase of the land

width L, web thickness W and the decrease of angular difference β. The second observation is that the chip disposal capacity is constant for a certain range of these parameters beyond which its value is dependant on these parameters. The values for L, β and W at which this change on Rc trend (from constant to variable), is determined from equations 3.8, 3.9 and 3.10 respectively. As a result of these observations the optimum compromise of polar second moment of inertia Vs chip disposal capacity can be found as follows:

For given web thickness

$$L \geqslant L_o \geqslant \frac{4R_o \cos\theta_o \sqrt{W R_o}}{W + R_o}$$

$$\beta \leqslant \beta_o \leqslant 2 \cos^{-1} \frac{L_o}{2 R_o \cos\theta_o}$$

or

$$\beta \leqslant \beta_o \leqslant 2 \sin^{-1} \frac{R_o - W}{R_o + W}$$

and for a given land width L or angular difference

$$W \geqslant W_o \geqslant \frac{R_o (1 - \sin \frac{\beta}{2})}{1 + \sin \frac{\beta}{2}}$$

or

$$W \geqslant W_o \geqslant \frac{R_o \{2R_o \cos\theta_o - [(2 R_o \cos\theta_o)^2 - L^2]^{\frac{1}{2}}\}}{2 R_o \cos\theta_o + [(2 R_o \cos\theta_o)^2 - L^2]^{\frac{1}{2}}}$$

(The equality sign is for Rc maximization)

These results can be explained in accordance of Figures(48)~(50) as follows: either reducing land width beyond Lo (Figure 48) or increasing angle β beyond β_o (Figure 49) or reducing the web thickness W beyond W_o (Figure 50) provides a reduction in polar moment of inertia while the chip disposal capacity remains constant, this means a sacrifice in drill rigidity without a

corresponding gain in chip disposal capacity. A summary of these results is represented graphically in Figure(51) which shows the minimum optimum land width and angular difference margin/heel corresponding to a range of web thickness.

3.5 APPLICATIONS

Traditionally, some drill manufacturers consider the land width to equal the flute width. Accordingly the land width $L = \sqrt{2}\ R_o \cos \theta_o$. However according to comparison between this assumed ratio and the optimum minimum value as in Figure(52) this land width selection by the drill manufacturer is not entirely valid especially at higher values of $\frac{W}{R_o}$.

As a practical application to the previous comment, Waller [16] tested the tendency for chips to clog in the drill flutes. The test consisted of mounting the workpiece on a torque dynamometer and, at a suitable speed and feed, drilling successive holes with equal increments of depth. The point of clogging was recognised by a sudden increase in torque recorded on the dynamometer. The comparison of clogging performance was measured by the depth of hole that could be drilled prior to clogging.

The test conditions and results are:

Drill identification	Drill I	Drill II
Area of cross section (mm^2)	3.549	3.097
Area of flute (mm^2)	4.387	4.839
Land Width (mm)	2.033	1.88
Average maximum depth of hole drilled before clogging	16.5	11.9

Drill size = 1/8 inch (3.18mm)

Web Thickness = 0.66 mm

Helix Angle = 23 degrees

The experimental results lead to an interesting conclusion: that the drill with small flutes has less tendency to clog, although Waller did not explain this result, the theoretical investigation presented in this chapter can provide the required explanation as follows:

The land width, L_o, at which maximum chip disposal capacity Rc is attained, is calculated from equation 3.8 and found to equal 2.208mm. This value and the values of chip disposal capacity Rc as well as the Polar moment of inertia J as a function of land width L for the tested drills are shown in Figure(53). From which it can be seen that drill II has bigger flute space and accordingly should have better chip disposal. But this is not true because the two drills have a value of land width L less than the optimum minimum value Lo. As a result both drills sacrifice drill rigidity. While both drills have the same chip disposal capacity,

Drill II sacrifices more rigidity which could explain its higher tendency to clogging even with its larger flute area.

Two important issues can be deduced from the above example. First that the theoretical model can be successfully applied to explain some phenomena which could not be explained before. Secondly that the drill manufacturer's selection of certain drill parameters are not entirely valid. Accordingly the optimum selection of some drill parameters which may be required for further flute modification can be based on the developed theoretical model as suggested in the following chapter.

CHAPTER 4

AN APPROACH TO FLUTE SHAPE MODIFICATION

4.1 INTRODUCTION

Drill geometry is determined by the combined effect of the flank surface and the flute shape. Because most of the previous investigations have been directed mainly at point grinding techniques it is assumed that flute changes are considered as one of the most interesting drill design changes. Pais [14] developed a new flute shape to yield a more uniform wedge angle along the drill lips and thus to provide uniform wear. However, the analysis of the drill wear results reveal that the expectations built upon that hypothesis did not succeed as reported by Pais. This was attributed to the convex nature of such drill lips which set up a tensile force in addition to an outward force between the chip and the wall of the hole. This force increases the heat to be dissipated while impairs the performance of the drill. Accordingly it seems that lip straightness is an essential aspect for any drill modification. Another requirem. which is deduced from the investigation in Chapter II is the symmetrical configuration. These two aspects (straightness and symmetry) are under consideration for the development of an alternative flute form with the aim of improving the drill geometry.

The new flute contour is designed to yield straight-diametral lips which can then be extended to provide a single cutting edge and to eliminate the chisel edge with its disadvantages of lack of centring and poor cutting action. Also it provides a more uniform rake angle along the cutting edges of the new drill.

The objectives of this chapter are to investigate the conventional twist drill flute design and to provide new guidance for the selection of some of its parameters. This investigation is then extended to provide the new flute contour and its modification.

4.2 CONVENTIONAL TWIST DRILL FLUTE DESIGN

The twist drill flutes are the grooves in the body of the drill which provide lips and permit the removal of chips and allow cutting fluid to reach the lips. The oblique flute figure (54) is the flute contour in a plane normal to the helical direction of the drill flute. The oblique flute is of practical importance as the profile of the form milling cutter that should be employed for milling the helical flute from drill blanks can be determined from this (this to be investigated in the following chapter). The Flute contour on the plane normal to the drill axis is defined as the orthogonal flute, Figure 55. It comprises two sides the face and the heel.

(1) Flute Face

For certain drill parameters including the drill diameter, point angle, helix angle, web thickness and land width, the conventional flute face is designed to produce a straight cutting edge. This side of the flute can be presented by the parametric equations developed by Galloway [15] from which Tsai

and Wu [49] deduced the mathematical model of the flute shape.

From Figure 44 it can be seen that

$$\varepsilon = \varepsilon_1 + \varepsilon_2 \qquad 4.1$$

where

$$\varepsilon_1 = \sin^{-1} \frac{W}{R} \qquad 4.2$$

$$\varepsilon_2 = \frac{\tan\theta_o \, [R^2 - W^2]^{\frac{1}{2}}}{R_o \tan P} \qquad 4.3$$

$$\therefore \quad \varepsilon = \sin^{-1}\left(\frac{W}{R}\right) + \frac{\tan\theta_o [R^2 - W^2]^{\frac{1}{2}}}{R_o \tan P} \qquad 4.4$$

where

W : half the web thickness

R_o : radius of the drill

θ_o : helix angle

P : half the point angle

It can be seen from equation 4.4 that the orthogonal flute shape is dependent on the helix angle, the point angle, the radius of the drill and the web thickness. The helix angle is given by

$$\theta_o = \tan^{-1} \frac{2 \pi R_o}{H} \qquad 4.5$$

where H is the pitch of the helix.

As the helix angle is constant, the pitch is proportional to the radius of the drill.

Substituting the value of θ_o from equation 4.5 into 4.4 we get

$$\varepsilon = \sin^{-1}\left(\frac{W}{R}\right) + \frac{2 \pi [R^2 - W^2]^{\frac{1}{2}}}{H \tan P} \qquad 4.6$$

If H in equation 4.6 is constant, then the flute shape is independent of the radius of the drill and the helix angle. The orthogonal flute faces in different sections along the drill axis are the same, but the directions are rotated by the helix angle. The flute shape in two cross sections at distance H apart are rotated by 360 degrees relative to each other. If the rotation of the drill flute is taken into consideration, equation 4.4 becomes

$$\varepsilon = \sin^{-1}\left(\frac{W}{R}\right) + \frac{[R^2-W^2]^{\frac{1}{2}}}{R_o \tan P}\tan\theta_o + \frac{2\pi Z}{H} \qquad 4.7$$

where Z is the coordinate along the drill axis.

The pitch of the helix can be obtained from equation 4.5.

$$H = \frac{2\pi R_o}{\tan\theta_o} \qquad 4.8$$

substituting 4.8 into 4.7 we get

$$\varepsilon = \sin^{-1}\left(\frac{W}{R}\right) + \frac{[R^2-W^2]^{\frac{1}{2}}}{R_o \tan P}\tan\theta_o + \frac{Z \tan\theta_o}{R_o} \qquad 4.9$$

Equation 4.9 is the mathematical model for the drill flute in the cylindrical coordinate system (R, ε, Z) with R_o, W, θ_o and P as paramters. In the X-Y coordinate system, the coordinates can be represented as

$$X = R \cos\varepsilon \qquad \text{and} \quad Y = R \sin\varepsilon \qquad 4.10$$

(2) Flute Heel

While the flute face is fully specified, the flute heel shape and the heel corner position are not fully specified,

these are determined by the drill manufacturer. Chitale [50] reported that this portion of the flute profile is not critical and is chosen so as to provide extra strength while still leaving sufficient space for chip disposal. From his observation Armarego [7] found the heel corner to be about 90 degrees to the face corner (β = 90 degrees). This observation is confirmed by the fact that drill manufacturers consider the land width to be equal to the flute width. However, by using a theoretical analysis developed in chapter 3 it is now considered possible that a full specification of drill heel shape is possible. The selection of the heel corner position can be based on :

(i) the new definition of chip disposal capacity represented by the radius, R_c, of the circle inscribed in the drill flute.

(ii) the drill cross section rigidity represented by the polar moment of inertia.

This may be illustrated by an example considering a drill having the following dimensions:

Diameter = 3/4 inches

Web Thickness = 3.81mm (20% diameter)

Point Angle = 118 degrees

Helix Angle = 32 degrees

Fig 56 shows the characteristic diagram of such a drill constructed from the mathematical analysis of chapter 3. It can be seen from this figure and from Table 10 that the manufacturer's selection of flute heel side through the selection of angular difference margin/heel (angle β) is not valid. A 6% sacrifice in drill rigidity without any gain in chip disposal capacity is due to the drill manufacturer selection of angle β equal to 90 degrees. The authors selection of angle β to be 83.6 degrees will provide the same chip disposal capacity as the manufacturer while the polar moment of inertia is 6543.6 mm^4 compared with 6143.3 mm^4 for the manufacturers selection.

Once the proper selection of the heel corner position is defined through the proper selection of angular difference margin/heel (angle β), the shape of the contour between the end points of the heel flute may be represented by a polynomial equation.

4.3 AN APPROACH TO A NEW FLUTE FORM

The main cutting edges of the conventional drill are offset from a parallel radial line (a head of the centre) by an amount approximately equal to one half of the Web thickness. These are connected by a secondary cutting edge (chisel edge) which has unfavourable geometrical parameters, furthermore along the main cutting edges, the rake angle varies from positive at the periphery to

significantly negative at the centre.

These difficulties can be eliminated if a flute contour is designed to yield diametrally-straight lips when the drill is sharpened with a conventional drill point. These lips can then be extended to provide a single cutting edge. Fortunately the development of such a flute does not present any particular problem and the respective analysis can be described as follows:

From Figure 57, the flute face shape required to produce the diametrally-straight lip drill is designed so that if the drill point angle is 2P, the point N of the drill flute before grinding becomes the point Q on the diametral-straight cutting edge.

Since ON = OQ = R:

then polar coordinates of the point N are R, ε .

The difference of elevation between point N and Q is t which is given by;

$$t = R \text{ Cot } P. \qquad 4.11$$

The drill flute is rotated by angle ε since from point N to point Q the elevation is changed by t. The angle ε is proportional to t and will equal 2π when t = H.

Hence

$$\varepsilon = \frac{2\pi}{H} \cdot t = \frac{2\pi}{H} R \text{ Cot } P \qquad 4.12$$

The peripheral helix angle is given by

$$\theta_O = \tan^{-1} \frac{2\pi R_O}{H} \qquad 4.13$$

By substituting equation 4.13 into equation 4.12 we get

$$\varepsilon = \frac{R \tan \theta_o}{R_o \tan P} \qquad 4.14$$

Equation 4.14 is the drill flute cross section for $Z = o$. If $Z \neq o$ the drill flute is rotated by the angle $Z \tan \frac{\theta_o}{R_o}$, hence the drill flute cross section for $Z \neq o$ is given by

$$\varepsilon = \frac{R \tan \theta_o}{R_o \tan P} + \frac{Z \tan \theta_o}{R_o} \qquad 4.15$$

Equation 4.15 is the mathematical model of the diametrally-straight lip flute face represented in the cylindrical coordinates (R, ε, Z).

Because of its critical effect on the chip disposal capacity and cross section rigidity, the heel surface is approached in this work based on the optimum compromise of these two aspects through the proper selection of the angular difference margin/heel and the mathematical representation of the heel contour. In the orthogonal plane XY, the heel contour is given in this work, the law

$$Xl\,(Xl^2 + Yl^2) - A\,Yl^2 = o \qquad 4.16$$

where

$$Xl = R \cos \varepsilon - X$$

$$Yl = Y - R \sin \varepsilon$$

$$A = \text{constant}$$

X,Y are the cartesian coordinates of any point on the heel surface relative to the XY reference system. Substituting the value of Xl, Yl in equation 4.16 we get:

$$(R\cos\varepsilon - x)\left((R\cos\varepsilon - x)^2+(Y-R\sin\varepsilon)^2\right)-A(Y-R\sin\varepsilon)^2 = o \qquad 4.17$$

which proved to describe satisfactorily the following requirements

i) provide the required angle of the heel contour corner from the face corner. This angle is to be determined from the analysis reported in Chapter 3 to provide the optimum compromise of cross section aspects, chip disposal vs rigidity.

ii) to join the face contour near the central web, thus reducing the amount of metal to be removed during the extending of the two lips.

iii) has a common tangent with the central web to provide the required web thickness.

To determine numerically and geometrically the shape of the heel contou it is necessary to find A, R and ε to equation 4.17 which satisfy the conditions established above.

The design procedure begins by the selection of an assumed radius R from which the angle ε is calculated from the relationship

$$\varepsilon = \frac{R \tan \theta_o}{R_o \tan P}$$

The second step is to apply equation 4.17 for the heel corner where:

$X = R_o \cos (\varepsilon_o + \beta)$

$Y = R_o \sin (\varepsilon_o + \beta)$

$\varepsilon_o = \frac{\tan \theta_o}{\tan P}$

β = angular difference margin/heel

Accordingly the value of constant A is given by·

$$A = \frac{[R\,Cos\,\varepsilon - R_o Cos(\varepsilon_o+\beta)]^3}{[R_o sin(\varepsilon_o+\beta) - R\,sin\,\varepsilon]^2} + R\,Cos\varepsilon - R_o Cos\,(\varepsilon_o + \beta) \qquad 4.18$$

Finally, the assumed value of R is be checked and changed (if necessary) until condition (iii) above is achieved through the relation.

$$x^2 + Y^2 \geqslant W^2 \text{ for } R\,Cos\varepsilon \leqslant x \geqslant R_o Cos\,(\varepsilon_o+\beta) \qquad 4.19$$

where

$$Y = \left[\frac{(R\,Cos\,\varepsilon - X)^3}{A - R\,Cos\,\varepsilon + X}\right]^{\frac{1}{2}} + R\,sin\,\varepsilon$$

Figure 58 shows a flute profile plotted after being computed according to the mathematical approach presented above for the heel side and according to the criterion of diametrally located lip for the face side.

Drill prototype manufacture involved the collaboration of drill manufacturers and was controlled by the author through the design of the form cutter that will cut the new flute shape. A subsequent simple grinding operation shown in Figure 59 to extend the diametral lips was done and the final shape is presented in Figure 60.

The mathematical analysis of the flute cutter design and the performance test on the new flute design will be presented in the following chapters.

4.4 THE INFLUENCE OF THE NEW FLUTE SHAPE ON DRILL GEOMETRY

The twist drill is geometrically the most complex tool to be found in the workshop [7-10]. Drill angles have been defined by many workers. The clearance angle is determined by drill point grinding and is affected by flute shape to a lesser degree. Thus its value for the new drill is nearly as that for the conventional drill for the same point grinder. The rake angle which is mainly determined by the flute shape design is to be treated in a different way. Expressions for the calculation of the rake angle have been presented by several workers. The most common expressions are those developed by Oxford [8], Shaw [51-53], and Galloway [15]. From his investigation the author found that although different expressions have been developed, it can be proved that each one can be trigonometrically transformed to the other (Appendix III). Following Shaw's approach who represented the drill angles in terms of equivalent lathe tool angles, Fig.61, we get:

$$\alpha_b = \theta = \tan^{-1} \frac{R \tan \theta_o}{R_o} \quad ; \qquad 4.20$$

$$C_s = \mathrm{Cos}^{-1} \frac{\mathrm{Cos}\ P}{\mathrm{Cos}\ i} \quad ; \qquad 4.21$$

$$i = \sin^{-1} \left(\frac{W \sin P}{R}\right) \quad ; \qquad 4.22$$

$$\alpha_s = \tan^{-1} \left[\frac{\tan \theta}{\tan C_s} - \frac{\tan i}{\sin C_s}\right] \quad ; \qquad 4.23$$

$$\alpha_n = \tan^{-1} \left[(\tan\alpha_s \mathrm{Cos}\ C_s + \tan\alpha_b \sin C_s)\ \mathrm{Cos}i\right] \quad ; \qquad 4.24$$

$$\sin\alpha_e = \sin^2 i + \mathrm{Cos}^2 i \sin\alpha_n \qquad 4.25$$

where

α_b : back rake angle, the angle between the ground top face of the tool and the top plane of the tool

α_s : side rake angle,

C_s : side cutting edge angle

i : inclination angle

α_n : normal rake angle, the angle measured from a normal to the finished surface in a plane perpendicular to the cutting edge

α_e : effective rake angle

With the conventional twist drill, the main cutting edges are offset ahead of centre by an amount approximately equal to one half of the web thickness. As a result the cutting edges are oblique to the direction of motion and consequently the surface produced is a hyperboloid of revolution. However the diametrally located cutting lips, the surface of the cut produced is conical so that the inclination angle i is eliminated along the cutting lip. Substituting i = o for the diametral drill in equations 4.21-4.25 the angles for 3/4inch diameter drill may be computed at different radii and compared with these for the conventional drill as shown in Figures 62 and 63 for the normal and effective rake angles respectively. It can be seen from these figures that the negative normal rake angle near the centre zone has been improved to positive and its variation along the cutting edge becomes more gradual. Also the effective rake angles have been increased over the cutting edge for the diametral lip drills.

4.5 FLUTE SHAPE FOR DIAMETRALLY-CURVED DRILLS

One of the problems associated with the twist drill is the sharp variation in the cutting speed along the length of the cutting edge with the maximum on the periphery of the drill, this is the principal reason for intensive wear of this zone, thus limiting drill life.

Curved lip drills help to compensate the uniform rise of the cutting speed by gradually decreasing the true feed along the cutting edges and thus enhance the overall life of the drill.

In this section the flute shape required to provide diametrally partial-curved drills, Figure 64 have been analysed. Since the method of point grinding in which the lips are curved controls the design of the flute form, it is necessary first to describe the process of point grinding.

4.5.1 Generation of grinding surface

One of the methods of grinding curved lip drills has been described by Lyubimov [54]. However flank backing is insufficient and the chisel edge angle is unsuitable and additional grinding was necessary to eliminate these faults. Giddings & Lewis Co., provides a drill pointer [40] to offer the so called racon drill, Figure 12. Tsai [55] describes the generation of a grinding surface for this type of drill as an

ellipsoid. However, this model is not simple and is difficult to use.

The author's objective was to investigate the validity of applying the spherical quadratic model with the aim of applying this model to manufacture a simple point grinder. In his investigations the author found that this quadratic spherical model can be used as a simple method to provide the required drill angles similar to that produced by the ellipsoidal moodel.

The drill flank configurations of the spherical curved drill, Figure 65 can be described by a quadratic equation in the form

$$X^{*2} + Y^{*2} + Z^{*2} = a^2 \qquad 4.26$$

Where a is the sphere radius and the (X^*,Y^*,Z^*) is the coordinate system selected with the origin O^* of the coordinate system located at the centre of the spherical surface, with the Y^* axis perpendicular to the drill axis. In addition to the parameter a, the drill flank configuration also depends upon three other parameters d, s and ø which determine the location of the drill point on the quadratic grinding surface and the direction of the drill axis.

For analytical simplicity, the (X,Y,Z) referential system is considered such that the origin of the coordinate system O is to be located at the centre of the drill point and the Z-axis

coincides with the drill axis. The x-axis is chosen to be parallel to the projection of the cutting edge on the plane perpendicular to the drill axis when the cutting edge is straight from Figure 65.

$$Y_0^* = -S$$

$$Z_0^* = d$$

The value of X_o^* which makes point O lies on the spherical surface can be obtained from equation 4.26, viz:

$$X_o^* = (a^2 - d^2 - S^2)^{\frac{1}{2}}$$

Also from figure 65.

$$X^* = X_o^* + X \cos\phi + Z \sin\phi$$

$$Y^* = Y - s$$

$$Z^* = d - X \sin\phi + Z \cos\phi$$

substituting X^*, Y^* and Z^* in equation 4.26 it results an equation of the form

$$F(X,Y,Z) = X^2 + Y^2 + AX + BY + C = 0 \qquad 4.27$$

where

$$A = 2 x_o^* \cos\phi - 2 d \sin\phi$$

$$B = -2 S$$

$$C = Z^2\sin^2\phi + (x_o^*)^2 + 2 Z \sin\phi X_o^* + s^2 - a^2 + (Z \cos\phi + d)^2$$

This equation represents the model of the spherical flank whose parameters are a, d, s and ϕ.

For partially curved drill, Figure 64 with $\frac{R_J}{R_o} = 0.5$ the parameter d can be calculated in terms of the other parameters and the selected point angle P over the straight part of the cutting edges. As can be seen from the geometry of Figure 66.

$$d = oq \sin (P - \phi) + \frac{R_J}{2 \sin P \ \text{Cos} \ (P-\phi)}$$

$$= [a^2 - s^2]^{\frac{1}{2}} \sin (P - \phi + \overset{*}{\theta}) \qquad 4.28$$

where

$$\overset{*}{\theta} = \sin^{-1} \frac{R_J}{2 [a^2 - s^2]^{\frac{1}{2}} \sin P}$$

Therefore, for partial curved lip drills with curved portion over $R = R_J$ to R_o and point angle P over the straight lip portion, the number of parameters can be reduced to three, a, S and ϕ.

The validity of the spherical quadratic model was investigated in two issues, experimentally and geometrically. The first issue was investigated through a drilling test represent in following chapter. The later involved comparing the drill angles for spherical drill with that when a well established model (ellipsoidal model) was used.

The relationship between the drill angles and the grinding parameters for ellipsoidal quadratic model were derived by Tsai [24].

The drill angles for the spherical model are derived as follows:

The included angle as shown in Figure 67a is given by:

$$P = \tan^{-1} \left(\frac{\partial Z}{\partial X}\right) - \frac{\pi}{2} \qquad 4.29$$

where:

$Z = F(X,Y)$ and can be found from Equation 4.27.

The chisel edge is obtained as shown in Figure 67b. From the tangent line to the contour circles passing through the point O.

$$\psi = \pi - \tan^{-1} \frac{\overset{*}{O}\ \bar{O}}{S} \qquad 4.30$$

where:

From Figure 66 $\overset{*}{O}\ \bar{O}$ is given by

$$\overset{*}{O}\ \bar{O} = \overset{*}{O}\ b \sin \phi$$
$$= [a^2 - s^2]^{\frac{1}{2}} \cos(\phi + \theta)$$

and

$$\theta = \sin^{-1} \frac{d}{[a^2 - s^2]^{\frac{1}{2}}}$$

The clearance angle δ at any point G on the curved cutting edge is shown in the plan view of the spherical grinding model in Figure 67c. The drill axis OZ is offset froom the grinding axis $\overset{*}{O}\ \overset{*}{Z}$ by an amount S. Any point on the cutting edge is at distance W from axis.

From the geometry of Figure 67c:

$$\sin\delta = \sin \widehat{G\ \overset{*}{O}\ \overset{*}{Z}}$$

$$= \frac{S - W}{a}$$

$$\therefore \text{clearance angle } \delta = \sin^{-1} \frac{S\_W}{a} \qquad 4.31$$

For diametral lip

$$\text{clearance angle } \delta = \sin^{-1} \frac{S}{a} \qquad 4.32$$

Investigating the geometry of Figure 67c and the expression for the calculation of the clearance angle in equation 4.31 shows that lip clearance angle, δ, for a spherical grinding model is constant along the cutting lip.

Therefore, the number of parameters for partial curved drills can be reduced again to two a and ϕ or s and ϕ for a given clearance angle.

A comparison of the drill angles obtained from equations 4.29 to 4.32 for a 1 inch diameter spherical drill with that when an ellipsoidal model was used is represented in Table 11. From which it is clear how close are the angles for the chisel edge and clearance. The included angles range from 57° at the centre and 27.4° at the periphery for the spherical compared with 46° at the centre and 30° at the periphery for the ellipsoidal.

The above analysis proves the validity of the spherical quadratic model suggested in this work as an alternative to the more difficult to maintain ellipsoidal model . Beside providing very close angles to that obtained by the ellipsoidal model, the spherical model reduces the required number of

grinding parameters to two compared with five for the ellipsoidal model.

4.5.2. Mathematical model for partially curved drill flute shape with diametrally located lips

The drill flute should be so shaped as to facilitate a straight cutting lip to be ground on the drill for a given helix angle and grinding parameters. The flute face for the straight portion of the diametrally cutting edge is to be represented as reported in Section 4.3.

The flute face for the curved portion is shown in Figure 68 when viewed normal to the drill axis. The orthogonal flute should be so shaped so that any point Q on the cutting edge has corresponding point N on the orthogonal flute. The coordinates of N in the orthogonal reference system X Y can be expressed as·

$$X = R \cos \varepsilon \quad \text{and} \quad Y = R \sin \varepsilon \qquad 4.33$$

where R is the radial distance of point N and ε is the angle that the flute is rotated from point N to point Q. The elevation is changed by t, the angle ε is proportional to t and will equal 2π when t = H, hence

$$\varepsilon = \frac{2\pi}{H} \cdot t = \frac{t}{R_o} \tan \theta_o \qquad 4.34$$

Referring to Figure 69, the length of radius $\bar{a}$ of the circle which represents a cross section A - A on the spherical grinding surface can be given by:

$$\bar{a} = [a^2 - s^2]^{\frac{1}{2}}$$

a and S are grinding parameters.

From the geometry of Figure 66 the following relationships can be obtained

$$t = OO' - GG' \qquad 4.35$$

$$GG'^2 = \bar{a}^2 - [R + \bar{a}\ \text{Cos}\ (\phi + \theta)]^2$$

$$OO' = \bar{a}\ \sin\ (\theta + \phi)$$

substituting the value of GG' and OO' into equation 4.35

$$\therefore\ t = \bar{a}\ \sin\ (\theta+\phi) - \{\bar{a}^2 - [R+\bar{a}\ \text{Cos}\ (\phi+\theta)]^2\}^{\frac{1}{2}} \qquad 4.36$$

where

$$\theta = \sin^{-1}\ \frac{d}{\bar{a}}$$

Substituting the value of t from equation 4.36 into equation 4.34 to find the value of ε and consequently the orthogonal flute coordinates from equation 4.33. Apply for a different points to complete the flute face contour. The heel contour can be found as reported in section 4.3. A typical flute shape based on the above mathematical analysis is shown in Figure 70.

CHAPTER 5

THE PREDICTION OF CUTTER PROFILE FOR PRODUCING HELICAL TWIST DRILL

5.1 INTRODUCTION

The increased demand for new types of drill emphasised the need for an accurate method to predict the cutter form used to cut drill flute. Traditionally either trial and error or empirical description methods are used to compensate for the amount of interference caused by the helical nature of the flute.

To provide an accurate prediction and to produce drills with previously selected parameters, a mathematical analysis and computing technique have been developed in this work to provide the profile of the form cutter that will cut a helical flute of any kind.

To obtain the cutter profile, firstly it is necessary to find the oblique "normal to the helix" flute which will produce straight cutting edges as viewed from the drill point. Secondly, it is necessary to compensate for the additional material removal from the flute due to the interference effect during cutting. Also the flute shape produced by a certain form cutter can be predicted. A computer program is developed to handle the analysis.

5.2 OBLIQUE FLUTE PREDICTION

Since the flute milling cutter is to be set at an angle (the helix angle) to the drill axis, the oblique flute profile has to be determined to obtain the required milling cutter. Due to the helical

geometry of the flute, the transformation between the orthogonal and oblique flute profile is not simple and direct.

Radhakrishnan [56] mathematical approach to obtain the oblique flute for the conventional drill required firstly to find out the orthogonal flute profile using the Galloway [15] method as reported before, and secondly, the transformation between the orthogonal and oblique flute is obtained through coordinate transformation and coordinate rotation. That makes the matter complicated. Graphical methods such as that given by Chitale [50] are over simplified and hence inaccurate.

The author's objective was to present a mathematical approach to obtain the oblique flute with a simple, accurate and direct method without any need to determine the orthogonal flute. This method can be applied for the conventional and non-conventional drills. As shown in Figures 71 and 72, for the straight and curved lip drills respectively, the oblique flute for drill face should be so shaped as any point A on the straight (as viewed normal to the drill axis) cutting edge has a corresponding point B on the oblique flute. The coordinates of B in the oblique section can be expressed as;

$$X = R \frac{\text{Cos}(\varepsilon+\delta)}{\text{Cos } \theta_o}$$

$$Y = R \sin (\delta + \varepsilon) \qquad 5.1$$

where R = radial distance of point B

$\delta = \sin^{-1} \frac{W}{R}$ (δ = o for diametral drills)

ε = the angle that the flute is rotated from point A to point B.

The drill flute is rotated by the angle ε since from point B to point A the elevation is changed by Z. The angle ε is proportion to Z and will equal 2π when Z = H, hence;

$$\varepsilon = \frac{2\pi}{H} Z = \frac{Z.\tan\theta_o}{R_o} \qquad 5.2$$

where

H = helix lead

θ_o = helix angle at periphery

From the geometry of figure (71) or (72)

$$Z = Z1 - Z2 \qquad 5,3$$

and

$$Z1 = (R^2 - W^2)^{\frac{1}{2}} \tan\theta_o + t; \qquad 5.4$$

$$Z2 = R \tan\theta_o [\cos\delta - \cos(\varepsilon + \delta)] \qquad 5.5$$

substitution of Z in terms of ε from equation 5.2, Z1 from 5.4 and Z2 from 5.5 the equation 5.3 yields;

$$\frac{\varepsilon R_o}{\tan\theta_o} = (R^2 - W^2)^{\frac{1}{2}} \tan\theta_o + t - R\tan\theta_o [\cos\delta - \cos(\varepsilon + \delta)] \qquad 5.6$$

where:

$$t = \frac{(R^2 - W^2)^{\frac{1}{2}}}{\tan P} \qquad \text{(straight lip)}$$

$$t = \bar{a}\sin(\theta + \phi) - [\bar{a}^2 - (R + \bar{a}\cos(\phi+\theta))^2]^{\frac{1}{2}} \qquad \text{(curved lip)}$$

$$\theta = \sin^{-1}\frac{d}{\bar{a}}$$

$\bar{a}$, d, ϕ are grinding parameters.

Using an iterative technique, ε can then be solved for. The solution of ε yield X and Y from equation 5.1 which is the mathematical model of the drill flute face normal to the helix. The oblique flute for drill heel can be presented in similar way as shown in Figures (71) and (72).

For any point E on the orthogonal flute there is a corresponding point D on the oblique flute. The coordinates of D in the oblique section can be expressed as:

$$X = R \frac{\text{Cos } (\varepsilon_h + \delta_h)}{\text{Cos } \theta_o}$$

$$Y = R \sin (\varepsilon_h + \delta_h) \qquad 5.7$$

$$\delta_h = \tan^{-1} \frac{Y_c}{X_c} \qquad 5.8$$

where

X_c, Y_c the coordinate of point E on the drill heel and can be found from the analysis presented in Chapter 4 for drill heel side;

$R = [X_c^2 + Y_c^2]^{\frac{1}{2}}$

The angle ε_h is the angle the drill flute is rotated since from point E to point D. The elevation is changed by Z_h, hence

$$Z_h = \frac{\varepsilon_h R_o}{\tan \theta_o} \qquad 5.9$$

From the geometry of figures (71) and (72)

$$Z_h = R \text{ Cos } (\delta_h + \varepsilon_h) \tan \theta_o \qquad 5.10$$

From 5.9 and 5.10

$$\frac{\varepsilon_h R_o}{\tan\theta_o} = R \cos(\delta_h + \varepsilon_h) \tan\theta_o \qquad 5.11$$

Again an iterative technique can be used, ε_h can then be solved for. The solution of ε_h yield X and Y from equation 5.7 which is the mathematical model of the drill heel side normal to the helix.

The equations dealt with in the present section were implemented in a computer program which handles the computing methods. Computer plots of the oblique flute cross-section for several values of angular difference margin/heel are shown in Figures (73) and (74) for diametral-straight and partial curved drills respectively.

5.3 CUTTER-PROFILE ANALYSIS

5.3.1 The prediction of cutter profile for milling the flute shape

The interference produced when milling a helical flute with a disc type cutter can critically affect the flute face and the heel face profiles. Interference taking place at the flute face side will affect the geometry of the cutting lip. Interference at the flute heel side will affect the compromise of drill rigidity vs flute disposal capacity as investigated in Chapter 3.

The proper cutter profile is obtained by allowing for the additional metal removal as a result of interference action. To investigate interference all motions of flute milling operation are assumed to be frozen and the intersection between the cutter and the drill blank at different sections is studied. Through coordinate transformation and coordinate rotation the location of the cutter at different sections can be related to the actual required flute at each particular section.

To simplify the matter, the cutter profile is considered as a number of points and the analysis is applied for each point separately. To eliminate any additional metal removal as a result of interference action, a correction to the location of the point under investigation is required. According to this correction, which takes place at any particular plane, a modification is required to the cutter central section. Application to other planes for the same point and for all the other points yields the final cutter profile.

Based on the above analysis, the following steps are necessary:

(1) The oblique flute (in the plane normal to the helix) is determined using the analysis presented in the previous section.

(2) As a first assumption, any point b, Figure (75), in the oblique flute is considered as a point of the cutter central sections C.C.S. (section B-B). This assumption is checked and corrected if necessary as will be explained later.

(3) At any other section (section C-C) parallel and further from the C.C.S. by distance w, the coordinate of point C corresponding (on the same cutter annular circle) to point b can be expressed in the reference system u v w as shown in Figure (76) by:

$$u_c = U_b \qquad 5.12$$

$$v_c = Rw + W - [(Rw + W - V_b)^2 - w^2]^{\frac{1}{2}} \qquad 5.13$$

where:

Rw = maximum cutter radius

W = half the web thickness

(4) It may be noted that the flute profile in plane C-C has the same shape as the flute profile in plane B-B, but is rotated by angle ε which given by $\varepsilon = \frac{w.\tan\theta_o}{R_o}$. Accordingly through coordinate transformation and coordinate rotation, the coordinate of point C can then be expressed relative to the flute profile reference system in plane C-C (system m n q). To help with the coordinate transformation and rotation, an auxillary referential system KLq was introduced. The coordinate of point C relative to

the auxillary referential system is;

$$k_c = U_c + \bar{w} \cdot \tan \theta_o \qquad 5.14$$

$$\ell_c = V_c \qquad 5.15$$

The coordinate of the same point can hence be expressed relative to the flute profile reference system $\acute{m}\ \acute{n}$ as;

$$m_c = k_c \cos \varepsilon - \ell_c \sin \varepsilon \qquad 5.16$$

$$n_c = k_c \sin \varepsilon + \ell_c \cos \varepsilon \qquad 5.17$$

A computer plot of the location of five points C_1, C_2, C_3, C_4 and C_5 at different sections parallel and farther from the C.C.S. by distance - 4.0 to 12.0 in step 2.0 are shown in figure (77).

(5) Check and correct (if necessary) the assumption in 2. If the predicted location of point C lies outside the required flute contour at a particular section, no correction is required otherwise correction is required to avoid any additional removal of material. The correction (if required) is done by shifting the location of point C to be point d to provide no interference, Figure (75). The coordinate of point d relative to the coordinate system m n is defined as m_d and n_d.

(6) According to the correction made, the assumption used in 2 is modified now to suit the shift in 5. Accordingly the coordinate of the corresponding point (on the same cutter annular circle), point e, to the new corrected location,

point d, can then be found relative to the coordinate system u v w as;

$$u_e = -\bar{w}.\tan\theta_o + m_d \cos\varepsilon + n_d \sin\varepsilon$$

$$v_e = Rw+W - [\bar{w}^2+(Rw+W + m_d\sin\varepsilon - n_d\cos\varepsilon)^2]^{\frac{1}{2}}$$

(7) Repeat the same procedure for different planes at different distances from the C.C.S. to find if there is any further interference to be eliminated.

(8) Apply for different points to form the required cutter profile.

A computer program was developed to describe the profile of the form cutter based on the analysis presented above. A HARRIS computer was employed for the computations with Fortran as the programming language. Cutter profile was plotted by a T4662 graph plotter in conjunction with the computer. The computer program consisted of three main parts : (a) the design of the drill flute, (b) the prediction of the form cutter profile allowing for the interference action, and (c) the graphical routines using GINO-F library [57]. The computer program flow chart is shown in figure (78). The computer program (Appendix IV) follows closely the analysis developed above. Two sample cutter profiles were determined and plotted in figures (79) and (80) for diametral, straight lip drill and diametral, partial curved lip drill respectively.

5.3.2 The prediction of flute shape produced by a certain form cutter

The drill flute is designed to provide a drill having certain required parameters. It is important to make sure that the flute produced by using a certain form cutter is the proper one. By using the analysis in this section and the computer program in Appendix V, the drill flute produced by using a certain form cutter can be predicted. Such contribution enables drill manufacturers to predict the flute shape produced by a certain form cutter without an actual flute milling.

The analysis can be explained through the following steps;

(1) The given cutter is presented as shown in Figure (76). It's contour is assumed to consist of a number of N points. The coordinate of each point relative to the coordinate system XYZ, with the origin O coinciding with the drill blank, is defined.

(2) One of the points that form the cutter shape is traced. The coordinate of its corresponding point (on the same cutter annular circle) at another section parallel and further from the cutter central section is defined as in step 3 of section 5.3.1.

(3) The coordinates of the corresponding point relative to the flute coordinate system in such section can be found as in step 4 of section 5.3.1.

(4) Repeat the same procedure for N points, that form the cutter shape in the C.C.S, at different sections 1,2,...m Parallel and further from the C.C.S.

(5) Superpose all the points (N . m). The intersection of the outside trace of these sets of points with the ellipsoid that represent the drill blank in the C.C.S. yields the oblique flute shape. The flow chart for the computer program that handles the above analysis is shown in Figure (81). A computer plot of the flute shape produced by using a typical cutter shape, Figure (82), is shown in Figure (83).

It is interesting to notice that not any flute shape can be produced using a form cutter. Thus the above analysis and the computer program provide a comparison between the required flute and the actually produced flute shape to see how closely it fits. Another practical contribution for the drill manufacturer is to be able to store and sort the available form cutters in an accurate and simple way.

5.4 DRILL PROTOTYPE MANUFACTURE

Drills were manufactured according to the new flute design. Drill prototype manufacture involved the form cutter design as before and the collaboration of a drill manufacturer. The author has had two types of prototypes of drill, diametral-straight lip and diametral-partial curved lip . The influence on drill performance of the new design is studied in the coming chapters.

CHAPTER 6

PERFORMANCE TEST COMPARING DRILLING FORCES ON CONVENTIONAL AND NEW FLUTE DRILLS

6.1. INTRODUCTION

Drill performance concepts encompass several aspects. Ernst and Haggerty [2] investigated drill performance by considering the following aspects: (i) torque and thrust, (ii) drill life and (iii) hole size. Fujii [25] restricted the analysis of drill performance to the study of drilling forces, and so did Micheletti [58]. Galloway [15] considered drilling performance criteria as follows: (i) rate of penetration, (ii) drill life, (iii) efficiency of metal removal, (iv) hole accuracy, (v) hole surface finish.

The new drill flute (diametral drill) performance was assessed in this work through the following criteria;

(i) drilling forces (thrust and torque)

(ii) drill life

(iii) hole quality (size, roundness and surface finish)

The cutting forces, ie thrust and torque play an important part in tool life, hole quality and stress and/or strain on working elements such as the component holders, drill holders and drilling machine.

Drilling forces have been studied by many authors for the variation of helix angle [15,33,58,59,60], point angle [15,58,59,60], clearance angle [15,58]. point shape [2,13,61,62], chisel edge

[15,60,63]. The effect of a selected type of point thinning was reported by PERA [26,38,64]. Reznikov et al [65] used photo-elasticity to methods to establish the influence of thrust force on the twist drill stresses. Drilling forces can also be important to comparing drill performance for different drill designs.

6.2. EXPERIMENTAL DESIGN

An experimental programme was designed to carry out a series of drilling tests varying the cutting speed and feed rates. The main objectives of these tests were:

(1) to confirm, by comparing, that the diametral drill reduces the cutting forces

(2) to investigate the effect of cutting parameters (speed and feed) on drilling forces for conventional and diametral drills

(3) to establish a regression model for calculation of thrust and torque.

Each drill type was tested to determine the drilling forces with varying speeds and feeds. As a result of the drilling feeds and speeds range available in the machine, the combination of drilling factors shown in Table 12 were selected for testing. The measuring equipment was that described in Chapter 2 .

6.3. DRILLING FORCE TESTS

The effects of cutting speed N(r.p.m.) and feed rate F(mm/rev) on drill forces were evaluated by a 2X3X3 factorial design for the two types of drills, conventional and diametral. The objective of these experiments were to test the effect of the diametral lip drill on drilling forces.

For each set of drilling conditions and each drill type, the test was replicated to eliminate, by averaging, the effect of experimental random deviations. Drilling torques and thrusts were recorded by a UV recorder as described in Chapter 2.

6.3.1. Material

The work material, En8 steel supplied in 3 m (10 inch) lengths of 50.8 mm (2 inch) diameter bar was a nominal 45% carbon steel with the following limits to chemical composition.

	C	Si	Mn	S	P
Minimum	0.35	0.05	0.60	-	-
Maximum	0.45	0.35	1.00	0.060	0.060

The bars were cut into pieces 38 mm long and the end pieces discarded. The specimens were cleaned, ground both ends and numbered. Random samples were selected for hardness tests on each top face. A Rockwell hardness tester was

used for testing the specimens hardness . The hardness numbers obtained after the reading fell in the interval 213 HB ~ 217 HB. The pieces for drilling tests were selected in a random sequence and drilled with 38 mm (≅ 2d) deep, through hole.

6.4 ANALYSIS OF THE EXPERIMENTAL RESULTS

The drilling forces were averaged for each set of cutting conditions and presented in Table 13 (Thrust) and Table 14 (Torque). Curves from Figures (84) and (85) show that, for both drill types, drilling forces increase with feed as expected. They also show obvious differences between the conventional drill and the diametral drill.

For each feed, the thrust value relative to the conventional drill at 345 r.p.m. speed has been given the value 100 and the thrust values for the other cases have been computed accordingly, the results are shown in Table 15 and the same procedure has been adopted for the torque values and the results are shown in Table 16.

All the thrust and torque values shown in Table 15 and 16 are less for the diametral drill than for the conventional one for the same drilling conditions. Comparing the thrust values for the diametral drill with those for the conventional drill shown in Table 13, the minimum ratio was found to be 44% and the maximum 56%, on

average the values of thrust forces for the diametral drill are approximately 50% lower than those for the conventional drill, for the same speed and feed.

From the torque results, Table 14 and Figure (85), the minimum ratio of torque values of the diametral drill with those for conventional drill was found to be 72% and the maximum 90%. On average the values of the torque for the diametral drill were approximately 18% lower than those for the conventional drill.

An analysis of variance on the drilling force results has been done in order to find if the effects of the test drilling factors were statistically significant.

For drilling thrust analysis of variance, the following symbols were used:

d1 - Conventional

d2 - Diametral

F1,F2,F3, the feeds corresponding to 76.2,152.4 and $228.6 \times 10^{-3} \frac{mm}{rev}$

V1,V2,V3 the speeds corresponding to 345,490 and 690 r.p.m.

Sum of squares for feed effect (after Table 17):

$$SSF = \frac{1}{12}(12.05^2 + 19.3^2 + 26.1^2) - \frac{57.45^2}{36} = 8.2279$$

Sum of squares for drill type effect (after Table 17):

$$SSD = \frac{1}{18}(38.3^2 + 19.15^2) - \frac{57.45^2}{36} = 10.1867$$

Sum of squares for speed effect (after Table 17):

summing for the speed

S1	S2	S3
18.2	19.25	20

$$SSS = \frac{1}{12}(18.2.^2 + 19.25^2 + 20^2) - \frac{57.45^2}{36} = 0.13625$$

Sum of squares for cross effect drill type and feed:

summing for drill type and feed

	d1	d2
F1	8.05	4.0
F2	13.0	6.3
F3	17.25	8.85

$$SSDF = \frac{1}{6}(8.05^2 + 13.0^2 + 17.25^2 + 4.0^2 + 6.3^2 + 8.85^2) - \frac{57.45^2}{36}$$

$$- 10.1867 - 8.2279 = 0.801.$$

Sum of squares for drill type and speed cross effect:

summing for drill type and speed

	d1	d2
S1	11.95	6.25
S2	12.65	6.60
S3	13.70	6.30

$$SSDS = \frac{1}{6}(11.95^2 + 12.65^2 + 13.7^2 + 6.25^2 + 6.6^2 + 6.3^2) - \frac{57.45^2}{36}$$

$$- 10.1867 - 0.13625 = 0.13434$$

Sum of squares for speed and feed cross effect

summing for speed and feed

	S1	S2	S3
F1	3.8	4.0	4.25
F2	6.25	6.35	6.70
F3	8.15	8.9	9.05

$$SSSF = \frac{1}{4}(3.8^2 + 6.25^2 + 8.15^2 + 4^2 + 6.35^2 + 8.9^2 + 4.25^2 + 6.7^2 + 9.05^2) - \frac{57.45^2}{36} - 0.13625 - 8.2279 = 0.03335$$

Sum of squares for the three factors cross effect

$$= \frac{1}{2}(2.5^2 + 4.2^2\ 5.25^2 + \qquad\qquad + 2.75^2).$$

$$- \frac{57.45^2}{36} - 8.2279 - 10.1867 - 0.13625 - 0.801 - 0.13434 = 0.09858$$

Total sum of squares

$$= \frac{446.57}{4} - \frac{57.45^2}{36} = 19.96187$$

A summary of the above analysis of variance for drilling thrust, the effect of the different factors and their interactions were computed and presented in Table 18.

Proceeding in a similar way for as thrust, for the analysis of variance of drilling torque, a summary of these analysis is presented in Tables 19 and 20.

For the range of the test factors used, the analysis of variance of the drilling thrust of Table 18 reveals that the effect of drill type is highly significant at 0.1% levels, also the effect of feed is highly significant at 1% levels. The analysis also shows that the interaction between drill type and feed are also significant at 1%, whilst the speed, the interaction between the speed and the feed, and the interaction between the three factors (drill type, speed and feed) are not significant.

The results of the torque variance analysis of Table 20 shows that the drill type and feed rate are highly significant at 1% levels, whilst the speed and interaction are not significant.

The above analysis of the cutting force test performance reveals that the expectations built upon the hypothesis of better cutting performance, with a diametral lip drill, were achieved. The reduction in drilling thrust and torque obtained by the diametral lip drill may be of particular advantage when using multi-spindle drilling machines and multi-spindle attachments. Often the most economic drill penetration rate cannot be used on multi-spindle drilling operations because of power and machine rigidity limitations. Also this feature (reduction in drilling thrust and torque) is of great importance in the field of portable drilling where an operator's ability to push a tool is quite limited.

6.5 RESULTS OF REGRESSION ANALYSIS

The SPSS Package (Appendix I) was used to investigate the effect of the cutting variables on both the thrust and torque. To exclude the cutting speed as a testing factor was justified on the basis of the above analysis of variance and the reports of some workers who found the influence of the cutting speed on drill forces to be negligible [66], insignificant [5] or nil [67]. The regression results obtained were as follows:

Thrust force for conventional drills

$$Th = 15947\ F^{0.69}$$

Thrust force for diametral drills

$$Th = 8286\ F^{0.714}$$

Torque for conventional drills

$$M = 9159\ F^{0.74}$$

Torque for diametral drills

$$M = 8447\ F^{0.8}$$

The above results of regression analysis were above 98% correlation coefficient.

CHAPTER 7

PERFORMANCE TEST COMPARING DRILL LIFE FOR CONVENTIONAL AND NEW FLUTE DRILLS

7.1 INTRODUCTION

The cost of regrinding and the cost of delays at the drilling machine due to drill failure especially on some multi-spindle machines have to be taken into account when selecting drilling tools which will result in optimum drill life. The number of drilling operations carried out is so vast that even a slight improvement in the tool life will be of great value to industry. Tool life is the period of economical use of a tool before regrinding is necessary. Drill life is expressed either as a drilling time or as depth drilled between grinds, but under test conditions where all holes have the same depth the number of holes between grinds is an equivalent measure of drill life.

The fundamental difficulty is to find means whereby the end of drill life can be determined precisely. Accordingly different criteria were developed by different research workers for measuring drill life as stated below.

(i) a change in colour of the drill from shiney to a dark blue [68]

(ii) a change in sound "cry" and squeaking [26,68-70]

(iii) "screech" [71,72]

(iv) complete destruction [68,70]

(v) significant and rapid change of drilling forces and power [73]

(vi) excessive drill wear [73-75]

The first three criteria are influenced by personnal opinion rather than on any objective criterion. A drill destruction criterion is not practicable since the number of holes needed could be extremely large and considerable damage has to be done to attain this condition and consequently much work is required if the drill is to be re-conditioned for further work.

Considering these reasons the last two criteria are investigated in this work to assess drill life.

7.2 DRILLING FORCES AND POWER

Torque, thrust and power are basic process variables that depend on the cutting conditions and the tool conditions. If it is true that the torque, thrust and power vary during the life of a drill, then the changes in these variables should be significant with respect to drill life. Some workers refer to the cutting forces used as a basic for tool life criterion [12,76]. However, some others [70,72] doubt the methods. The present work monitores thrust, torque and power to find whether or not any of these variables could be used as an index of drill life.

7.3 DRILL WEAR

As any other cutting tool, a drill is subject to wear. In the general case high speed steel drills wear on the lip relief surfaces (flanks), rake surfaces, margins and chisel edge, Figure (86). Wear limit criterion is most commonly used to define tool life for most machining operations, Bhattacharyya [30]. The outer corner of the flank is subjected to intensive wear which limits drill life. This wear which has a close relationship with the drill life has been measured(Kanai[75]).Also the wear on the outer corner of the drill margin was measured and used as a drill life criterion (Lenz [74] and Kaldor [29]).

7.4 EXPERIMENTAL DESIGN

The aim for the experiments was to compare two types of drill - conventional and diametral - for drill life and to define criteria for deciding drill life. Drilling tests may be divided into three types [12,77].

- short duration tests - up to approximately 30 holes
- medium duration tests - up to approximately 40-140 holes
- long duration tests - more than 150 holes

The medium duration tests are reported by Kahng and Ham [77] and will be selected for these tests.

All of the experiments were carried out using 19 mm (3/4 inch) diameter, 230 mm long, high speed steel drills. The two types of drill are investigated to the variation of (i) speed, (ii) feed. A radial drilling machine was used, all the holes drilled were 2.5 dia. deep.

7.5 EQUIPMENT

The drilling machine, forces and power measuring equipment, drill grinding machine and wear measuring equipment involved in the test program are described in the following :

7.5.1 Drilling Machine

An Asquith radial drilling machine, figure(87), was used for drilling tests relating to this chapter. The machine was checked for alignment. The speeds were checked with a Tachometer device and the feeds by a dial gauge.

7.5.2 Drill Grinding Machine

A prototype drill grinder, Figure (88) was designed and built upon the framework of an existing Cincinnati Cutter Grinder to control the grinding parameters. The precision of the new grinder was evaluated by comparing measured drill point

geometry parameters with their expected values. The design and construction of the new grinder was based on a computer aided drill point geometry analysis. In addition to the conical grinding concept, the new grinder was also used to produce ball points utilizing the mathematic model in Chapter 4. The ground drills were then employed in an experiment to investigate and compare their tool life.

7.5.3 Drill Point Measurement

A Matrix drill point measuring instrument manufactured by Coventry Gauge and Tool Co Ltd., was used to provide a simple and convenient method of checking the point angle and lip height.

The instrument has a range of 6 to 20 mm diameter drills with point angles between 70 and 145 degrees. Standard setting pieces, ground to the required angle, are used for comparing the point angle of the ground drills to the set standards to check their accuracy. The dial gauge on the instrument can read $\pm 5^{\circ}$ deviation from the appropriate setting piece for the point angle measurements and ± 0.0001 inch for lip height difference. In each case the dial is set to zero with the standard and then the ground drill is inserted and the deviation shown by the dial.

7.6 MEASUREMENT METHODS

For the wear measurement on the flank face and margin of the drills a universal measuring machine, Figure (89) was used. The wear was measured from a reference line etched on the drill flank and drill land by a hardness indentation, Figure (90).

The wear was measured after the 5th, 10th, 15th and 20th holes and each ten holes after that. Wear measurements were carried out until the 100th hole. To measure torque and thrust a drilling dynamometer was fixed on the radial drill bed. Force traces were only recorded at intervals during the test sequence.

The power input to the drive motor of the machine was measured using a three-phase wattmeter, connected to the line between the main switch and the input connection to the drive motor.

7.7 MATERIAL

The workpiece material was the same as that used in the force measurement. Blocks of En8 (Grade D) steel in the normalised condition were used for wear test. The hardness was measured and it was found to be 210HB.

7.8 EXPERIMENTAL RESULTS

With respect to the measurement of the margin wear, it was frequently observed that this measurement was obscured by the welded or adhering materials covering the portion of interest at the drill point, and thus in many cases the attempts at measurement were abandoned.

Torque, thrust and power were recorded. An analysis of this data at the early stage of the experimental programme revealed that none of this data provided a satisfactory criterion for drill life under the conditions of this experiment. The flank wear at the outer corner which is relatively easy to measure was found closely related to the tool life.

The results for the wear loss against the number of holes drilled for each set of drilling conditions, and for both drill types are shown from Figures (91) to (94).

7.9 ANALYSIS OF THE RESULTS

With one exception, all values shown in Table 21 are to be lower for the diametral drill than for the conventional one, for the same drilling conditions. Comparing the values for the diametral drill with those for the conventional drill shown in Table 21, the minimum

ratio was found to be 0.823 and the maximum 1.0537. However, on average, the values of the wear rate for the diametral drill were approximately 10% lower than those for the conventional drill for the same speed and feed.

In order to test the statistical significance of the differences between the values shown in Table 21, an anlysis of variance has been carried out on these values.

The results are arranged in two separate blocks; one referring to the conventional drill and another to the diametral drill.

According to the factorial design, one value of each factor called low and the other high. Accordingly the symbols for factor levels were considered as in Table 22. The different combinations of the factor levels for wear testing are shown in Table 23.

To compare the wear performance of both drill types, the wear rate from Table 21 is divided by 100 (the number of holes drilled). For convenience of the calculations the values are divided by 1.5×10^{-5}, and presented in Table 24.

Sum of squares within block for conventional (refer to Tables 24 & 25)

$$228 - \frac{(28.59)^2}{4} = 23.6529$$

Sum of squares within blocks for diametral (refer to Tables 24 & 25)

$$177.1 - \frac{(25.589)^2}{4} = 13.4$$

Total sum of squares (refer to Tables 25 and 24)

$$228 + 177.1 - \frac{(54.179)^2}{4} = 38.179$$

Between blocks sum of squares :

$$\frac{(28.59)^2}{4} + \frac{(25.589)^2}{4} - \frac{(54.179)^2}{8} = 1.1257$$

Total sum of squares within blocks:

$$23.6529 + 13.4 = 37.0529$$

Analysis of variance between and within blocks is shown in Table 26.

Treatment sum of squares:

$$\frac{805.2155}{2} - \frac{(54.179)^2}{8} = 35.682$$

The sum of squares relative to residual treatment and between blocks is shown in Table 28.

The method of establishing the effects and interactions of the various factors can be done by following Moroney's method [78].

From which the effect of Factor S, for instance is:

$$(S - 1)(F + 1) = S F + S - F - 1$$

The effect of different combinations of factors are presented in Table 29. In Table 30 the analysis of variance for all factors and their interactions are presented.

For the ranges of the drilling factors tested, the analysis of Table 30 reveals that the difference between the drill types is non-significant. The effect of speed and feed is highly significant.

The above analysis of drill wear tests reveals that, with a diametral flute yielding a greater rake angle and less wedge angle, the wear loss did not increase. The observation of Figures (91) to (94) shows a better drill wear performance for the diametral drill than for the conventional one in the majority of cases.

7.10 MODIFIED DIAMETRAL DRILLS FOR WEAR AND TOOL LIFE IMPROVEMENT

The diametral drill is modified at the outer portion of the cutting lips for improvement of the tool life. The special grinding technique discussed in Chapter 4 was used to convert the outer portion of the cutting lips into curved (spherical) edges which resulted in decreasing the true feed along the cutting edges. It was expected that this modification would distribute the wear uniformly along the cutting edges and thus enhance the overall life of the drill.

Experiments have been carried out with modified diametral drills

(partial curved) using the same conditions as before. A typical results are shown in Figures (95) to (98). The wear loss values for the modified diametral drills compared with the conventional drills are shown in Table 31 from which it can be seen that all the values are lower for the modified diametral drill than for the conventional one. Comparing the values for the modified diametral drill with those for the conventional drill (Table 31), the minimum ratio was found to be 0.48 and the maximum 0.817. The average values of the wear rate for the modified diametral drill were approximately 40% lower than those for the conventional drill.

Proceeding in a similar way as for diametral drill for the analysis of variance of the wear rate for the modified diametral drill, the effects of the different factors and their interactions were computed and are presented in Table 32.

The analysis of Table 32 reveals that the difference between the drill types is significant. The effect of speed and feed is non-significant.

The above analysis of the drill wear results reveals that the expectations built upon the hypothesis of better drill wear performance with a modified diametral drill (partial curved) is confirmed.

CHAPTER 8

PERFORMANCE TEST COMPARING HOLE QUALITY FOR CONVEN-TIONAL AND NEW FLUTE DRILLS

8.1 INTRODUCTION

Drill performance varies for similar twist drills and for each set of cutting conditions. According to [8,15,28,79] such variation is due to the inaccuracies of drill geometry. This can occur at the manufacture stage, and/or at the point grinding stage. These inaccuracies of symmetry are

- relative lip height
- eccentricity of chisel edge
- unequal lip spacing
- defective drill straightness
- non equal flute
- non straight lip (concave or convex)

These drill errors can diminish drill life and influence the hole quality. In practice, drilling by means of a twist drill is not the machining operation requiring the highest degree of dimensional accuracy. Counterboring, honing and reaming are subsequent operations for improvement on an initial drilled hole. Improved quality in drilled holes results in advantages of direct economic value by giving better products, reducing production cost through reducing the amount of material left for removal by the final operation. If improvement of a high enough value can be obtained the finishing by the subsequent operations may be eliminated for many conditions.

8.2 HOLE ERRORS

Drilled holes always carry some imperfection and errors which define the quality of the hole, these are;

(1) Error in shape

The shape of the hole may not be uniform along its depth, giving rise to different hole shapes such as bell mouth, ball shaped and concave. The axis of the hole may not be straight but inclined. Hence the hole cross section at various depth will not be concentric. Galloway [15] assumed the drill as a cantilever with a concentrated load at the free end. This load arises from variation in cutting lip length. Accordingly the slope of the drilled hole was expressed by the equation:

$$S\ (\text{in/in}) = \frac{\ell_o}{\ell_1}\left(e^{\frac{3\ell_1}{2\ell_2}} - 1\right)$$

where

ℓ_o = the initial deflection of the drill

ℓ_1 = hole depth

ℓ_2 = drill projection length

(2) Error in roundness

The circularity of the hole cross section may not be perfectly round, but irregular, oval shaped or lobal. This is mainly due to the inaccuracies in the spindle bearing and drill grinding.

(3) Error in dimension

There is a concentric increase in the hole diameter and thus the dimensional accuracy of the drilled hole is influenced unfavourably because of a rotary radial force. Spur [80] related this force to the following factors:

- dissimilar length of lips
- dissimilar point angles
- dissimilar clearance angles
- non symmetric web at the point
- non symmetric flutes
- dissimilar cutting edge sharpness

The effect of unequal lip length caused by the presence of relative lip height error was investigated by Galloway [15] who showed that the drill will rotate about its true axis until the chisel edge contacts the workpiece, after that the drill will tend to rotate about a new axis approximately passing through the centre of the chisel edge at a distance equal to 1/2 K tan P from the original axis and will produce a hole oversize of an amount K tan P where:

K = relative lip height

P = half the point angle

(4) Imperfection in the hole surface

Incorrect drill grinding and imperfection in the machine tool can cause waviness and irregularities in the hole surface. The

quality of surface finish in drilled holes for any given set of cutting conditions is difficult to predict, Billau [72]. However Radhakrishnan [61,81] found a strong correlation between the dynamic characteristics of the drilling thrust and the hole surface variation. He analyzed the frequency contents of thrust and suface variation by using a dynamic data system technique [82].

(5) Burr formation

A burr will form on the periphery of the exit hole. The burr geometry (height and thickness) depends on the workpiece material, drill properties, and drill conditions. Sofronas [83] investigated the formation and control of burrs. Gribkov [84] has developed a special form of drill to ensure that the drill can be passed through without burring.

8.3 SOME ASPECTS OF HOLE QUALITY MEASUREMENTS

Aspects of the hole such as roughness of its wall surfaces, roundness of the hole cross section and hole oversize above the measured diameter of each drill were considered for the assessment of the hole quality provided by the diametral lip drills. A comparison with conventional drills was one of the objectives.

For surface finish measurement, the centre line average (C.L.A.) of the hole wall surface was determined using Taylor Hobson Talysurf 4

shown in Figure (99). The stylus is positioned to move along the specimens which are held in a magnetic fixture to obtain the C.L.A. value across the lay. The mean value of C.L.A. is taken as the average of four readings.

The hole out of roundness was measured using Taylor Hobson Talyrond Model 1 shown in Figure (21). Three traces were recorded for each hole at top, middle and bottom. Minimum rotational speed of the spindle (stylus) of 3 r.p.m. was used to reduce the fluctuations on the roundness traces by reduced inertia effect.

Hole diameter was measured using an internal micrometer. A series of five readings were made along the hole depth.

8.4 EXPERIMENT

An experiment was designed to study the effect of the diametral lip drill on hole quality. For this two types of 3/4 in. of drills were used, conventional and diametral, to drill through, a 1.5 inch deep hole using a 3VT-1000 Cintimatic NC Milling Machine Figure (100). Three speeds 345, 490 and 690 rpm and three feeds 762, 1524 and 2286 x 10^{-4} mm/rev giving nine sets of working conditions for each type of drill. The samples were fixed on a special fixture designed for this purpose. The fixture was to ensure that the sample surfaces were parallel with the machine table.

En1 A free cutting steel was used as test material. It has the following composition [85]

	C	Si	Mn	S	P
Min	0.07	-	0.80	0.20	-
Max	0.15	0.10	1.20	0.30	0.07

This material was selected as easily machineable to provide a reasonable surface, so the measuring numerical values would fall within the reading limits of the measuring equipment. Samples were cut to the required length from bar stock and the surfaces were ground.

8.5 GEOMETRICAL ERROR RESULTS

8.5.1. Hole Wall Roughness

Surface finish of the hole wall is largely a geometrically determined parameter depending on the status of the outer corner of the two lips and the nature of the tool edge in contact with the workpiece. Table 33 shows the values taken for the C.L.A. for the sample tested. It can be seen from the above table and from Figures (101-103) that a substantial improvement in surface finish is brought about by the diametral drills. In order to test the significance of the improvement in surface finish, an anlysis of variance has been carried out on the experimental

results which were obtained for surface finish. From these analysis it was found that the improvement is statistically significant, also the effect of cutting speed was found to be significant.

8.5.2. Roundness

The out of roundness results are tabulated with respect to the variable levels in Table 34. All the values were within 2.0×10^{-3} inch for the diametral drills and 2.5×10^{-3} for the conventional drills. The good results for the diametral drills were obtained at low speeds (345 and 490 rpm) while at higher speed (690 rpm) the best results were obtained by the conventional drills. This would indicate that, in some circumstances (low speeds), it might be possible to use a hole which is produced in one pass of the diametral drill which previously would have required a drilled and reamed hole. Figure 104 includes traces which demonstrated a remarkably increased accuracy in the roundness using a diametral drill compared with conventional drills.

8.5.3. Hole oversize

The average of three readings of the hole oversize above the measured diameter of each drill as measured on the top, middle and bottom of each hole are shown in Table 35. The

maximum oversize for each hole related to the variable levels is presented in Table 36 and Figures (105-107). Significance testing shows that there is significant difference between the amount of oversize between the conventional and diametral drills. Also, the statistical analysis shows significant effect of the cutting speed.

CHAPTER 9

GENERAL DISCUSSION

9.1 INTRODUCTION

This chapter presents the mathematical and the experimental programme results and deals with the new definition and models and their reflect on the twist drill design and consequently on the hole producing operation.

Mathematical models are better dealt with by computing techniques. The advantages of these techniques are:

i) To allow for mathematical model testing;

ii) To allow for reformulation of problems and hypotheses;

iii) To enlarge the field of research for the amount of information data that can be dealt with and for the complex relationship that can be analysed.

9.2 CHIP DISPOSAL

Figures (38)-(43) show the new definition, suggested in this work, for chip disposal capacity which define the inscribed circle in the flute space normal to the axis of the drill as a good index of flute disposal capacity, because the chip is formed in a curled-conical shape will only occupy a circular part of the flute space.

The requirements guiding the design of a twist drill cross section profile are that on the one hand the area of the flute should

be large enough to allow good chip removal and on the other hand the area of the drill cross section should be large enought to withstand the cutting forces. These are two contradictory conditions, the fulfilment of which requires a compromise.

The heel side of the drill flute is traditionally designed to yield a flute width equal to the land width. Unfortunately such a purely geometric and empirical criterion has in general not succeeded. As can be seen from the mathematical model in Chapter 3 for the example in Figure (48) the optimum land width should not be less than 10.88 mm because any reduction beyond this value will decrease the polar moment of area without giving any improvment to chip disposal capacity.

A comparison of the manufacturer's traditional selection and the author's mathematical selection for the face-heel spacing angle which controls the flute and land width is shown in Figure (56). Using the author's selection, the drill rigidity (polar moment of area/second) could be increased by 6.7%.

9.3 DRILL RIGIDITY

Some workers consider the diameter of the circle which could be inscribed in the cross section normal to the drill axis as a good index of the torsional rigidity, some others count upon visual

description of the cross section polar moment of area. However because polar moment of area is proportional to rigidity it follows that neither the visual description nor considering the diameter of the circle which could be inscribed in the cross section normal to the drill axis as an index of the torsional rigidity are entirely valid as proved by the results in Table 6. The following relations between the cross section area, polar moment of area and drill parameters have been deduced

$$\text{Area} = 16.9\ .10^{-2}\ L^{1.286}\ d_o^{.57}\ (2W)^{.142}\ (2P)^{.169}\ \theta_o^{.275}$$

$$\text{Polar moment of Area} = 2.6.10^{-2}\ d_o^{2.74}\ L^{1.194}\ \theta_o^{.33}\ (2W)^{.063}\ (2P)^{.034}$$

A comparison between the calculated results and the above empirical equations, Table 8 & 9, provides a good correlation which warrants its use for design purposes. The correlation co-efficient (r) exceeds 0.98 for all drills investigated.

To take into account the helical arrangement of the drill flute which has a considerable influence on drill torsional stiffness, section compliance is integrated along the drill length and the provisional polar moment of area is calculated. The relationship between the helical effect represented by the helix angle and the provisional polar moment of area has proved to be linear as shown in Figure (47). For the example shown, the provisional polar moment of area increased by about 40% due to the changing of the helix angle

from 20 to 35 degrees.

9.4 CHISEL EDGE ELIMINATION (ASYMMETRIC APPROACH)

The difference in lip lengths of the drill configuration (in Chapter 2) suggested by the drill manufactures lead to a difference in cutting forces over each lip. This is responsible for high vibration and consequently poor surface finish at the hole surface and high hole oversize. Limit modification of this type of drill based on force balance has shown considerable improvement. The radial force which is the resultant unbalance force is reduced by about 50% as shown in Figures (23)-(25). Accordingly the hole out of roundness, Figures (26)-(28) and the hole oversize, Figures (29)-(31) have been improved tremendously. The hole out of roundness has shown an average reduction of about 85% and the hole size becomes 81% closer to the nominal size.

Although a considerable improvement is obtained, all the values are higher than the conventional drill Figures (23-31) because of the remaining asymmetry in the lips. These results prove the validity of the analysis and could be considered as an early expectation of better performance for the symmetrical approach.

The basic cutting data for the element force prediction such as the shear stress S_s, chip ratio R_t and friction angle λ are found

from experimental and regression analysis. The regression analysis results obtained as follows

$$\lambda = 26.7 + 0.77\,\alpha$$

$$S_s = 62.4 \text{ Kg/mm}^2$$

$$R_t = 0.277 + 0.0048\,\alpha + 1.534\ F.$$

The thin shear zone analysis is developed for the purpose of force prediction using the above obtained cutting data.

9.5 CHISEL EDGE ELIMINATION (SYMMETRICAL APPROACH)

The flute contour is designed to yield straight-diametral lips which can be extended to obtain a single cutting edge. As a result the following features are provided·

1. Elimination of the chisel edge with its unfavourable geometrical parameters, Figure (60). Although a considerable effort has been made to improve cutting performance of the chisel edge mainly by different point thinning or different shapes, none of them eliminate the chisel edge. There must be a chisel edge and the cutting edge cannot be radial and extend to the drill centre. In the case of the diametral drill, In addition to the advantage of elimination of the chisel edge completely and extension of the cutting edge to the drill centre, the web of the new drill can be enlarged with the

aim of improving drill rigidity without any corresponding increase in chisel edge and consequently the drilling forces.

2. No negative and more gradual varition in the rake angle. Figure (62) shows the variation in the normal rake angle over the cutting lip to be 25 degrees compared with 42 degrees for the conventional drill and from Figure (63) the effective rake angle has increased by about 5 degrees over the whole cutting lip.

The geometrical analysis revealed that although the normal rake angle is highly negative along the cutting edge, near the web, the effective rake angle of the conventional twist drill is positive. This is because the main cutting edges are offset from a parallel radial line by an amount approximately equal to one half of the web thickness at the drill point. This causes the cutting edges to be oblique to the direction of motion, with the obliquity increasing toward the centre of the drill. Oblique cutting usually acts to increase the effective rake angle of the cutting tools. So far no one has yet been able to establish the magnitude of this effect on twist drill performance. However, introducing the diametral lip drill, which provides no negative but more gradual variation in the rake angle and eliminates obliquity of the cutting edge enables the establishment of reliable drill performance.

Accordingly the following advantages are obtained:-

1. A considerable amount of thrust force during drilling is due to the cutting action at the chisel edge of the drill. This is in turn due to large values of negative rake angle along with a very small cutting velocity in the zone of the chisel edge. Thrust force is reduced by 46 to 56%, Figure (84), due to the modification of the chisel edge into cutting edges with positive rake angle by extending the diametral lip to meet the dead centre in a manner similar to the Vauclain rolled drill [86].

2. The modification of the diametral drill obviates the shortcomings of the conventional drill near the drill centre as above and in the part near the periphery. The cutting edge of the diametral drill is such that the normal rake angle is more uniformly distributed and the effective rake angle is increased. A proper increase in the rake angle can facilitate cutting, decrease the deformation of the layer of material removed by the tool, facilitates chip flow and reduces the cutting forces. Accordingly torque is reduced by 10 to 28%. Such a result is expected in view of the fact that the reduction of the cutting force is mainly near the drill centre due to the elimination of the negative rake angle. This does not appreciably affect the drilling torque compared with the drilling thrust due to the small moment arm.

3. Thrust and torque values, given in Tables 13 & 14 can be used to find the net cutting power consumed at the drill point. The net cutting power is the sum of the power required to rotate the drill and to feed it. The data can also be used to find the wok done per cubic inch of metal removed, and the efficiency of stock removal.

Work done per minute = 33,000 x net cutting H.P.

$$\text{Work done per cu.in metal removed} = \frac{\text{work done per minute}}{\text{volume of metal removed per min.}}$$

The efficiency of stock removal is usually measured in terms of stock removal in cu.in per H.P. hour, which permits comparsion between different drilling tools.

$$\text{Efficiency of stock removal} = \frac{\text{stock removed per hour}}{\text{H.P.}}$$

The power required to feed the drill is only less than 1% of the total, so it can be neglected in the power calculation and the power required to rotate the drill is considerd as the net cutting power. Accordingly the power reduction, using the diametral lip drill will be from 10to 28% as in the case of torque reduction. It is clear that the reduction in torque has a corresponding reduction on drilling power, while the reduction in thrust which could be obtained by different point thinning has no contribution to the power reduction.

4. The importance of drilling force reduction derives from its influence on the stress, strain and temperature on the drilling tool and temperature distribution on the drill flank.

The specific energy in cutting and the chip/tool interface temperature rise rapidly as the inclination angle increased. The elimination of obliquity by diametrally located lip provides an orthogonal cutting system.

The uniform distribution of the rake angle on the cutting edge provides more even stress and heat distribution. Because cutting temperature and stress, have a detrimental effect on tool wear and tool life, the above stress strain and temperature distribution and reduction provided by the diametral lip drill explain the 10% increase in the tool life.

5. The drilling operation is generally used to rough out the hole, which is finished by boring or reaming. The normal practice is, wherever possible, to drill the hole with sufficient accuracy. Results of test with asymmetric drills, in Chapter 2, show their detrimental effect on hole quality, Figures (26) - (31) however using symmetrical diametral lip drills improvement in hole size at low or medium (speed x feed) Figures (105)-(107) is obtained due to the reduction in drilling thrust and the better centring due to the elimination of the chisel edge. The reason for this improvement being limeted to low or medium (speed x feed) is related to the fact that at high (speed x feed) the rate of chip formation in the region where the lip is afterward extended is

higher compared with the rate of chip disposal.

Surface finish obtained by machining depends upon many factors, but the major influencing factors include the geometry of the cutting tool. A reduction in the axial component of the cutting force may reduce chatter in an insufficiently stiff workpiece. This fact could explain the improvement in hole wall surface quality as in Figures (101)-(103) obtained by using the diametral lip drills.

The statistical analysis show no significant improvement in hole out of roundness. As this type of error is mainly due to inaccuracies in drill grinding, the author believes that an accurate control of extension of the two lips would provide improvement on hole roundness.

The shape of the diametral lip drill is a combination of design, manufacturing and point grinding. The different production processes are:

1. The two contradictory conditions, chip disposal and drill rigidity are dealt with using the theoretical analysis in Chapter 3. Accordingly the face-heel corners angle is optimized.

2. The oblique flute is directly obtained using the developed

method by the author in Chapter 5 Figures (71),(72). This developed method facilitates the analysis by predicting the oblique flute form without the necessity of finding the orthogonal flute form.

3. Traditionally, trial and error methods are used to predict the cutter form, especially for special flute shapes. To provide an accurate prediction of the cutter form and to eliminate the interference caused by the helical nature of the flute, a mathematical analysis and numerical investigation handled by a computer program provide the solution. Figure (77) shows the effect of interference on the flute of a cutter where interference is not allowed for . The solid contour represents the required flute, the dashed contour represents the intersection of the cutter with the blank at different planes along cutting direction. The final obtained flute shape is the superimposed dashed contours.

Both sides, face and heel, of the drill flute are affected by the interference action. The effect on the face side will provide convex rather than straight cutting lips. The convex cutting lip sets up a tensile force within the chip in addition to the other metal cutting forces. The interference taking place on the heel side will affect the drill rigidity and the optimization of the two contradictory factors, chip disposal and cross section

area. Using the computer program in Appendix 4, the cutter shapes required to produce the diametral lip drill and the diametral partially curved drill are obtained. Figures(79) and (80) show computer plotted cutter shapes for both drills respectively.

4. To enable the drill designer and drill manufacturer to predict the flute shape which can be obtained using a certain cutter shape, the author developed a mathematical analysis (Chapter 5) and computer program (Appendix 5) to handle the objective. The contribution of this computer program is to avoid an actual cutting operation to find which cutter for which flute, Another practical contribution is to store and sort the available cutters.

9.6 DIAMETRAL DRILL MODIFIED FOR IMPROVED LIFE

The diametral drill provides many advantages over the conventional one, although the tool life improvement is limited to about 10%. However using the special grinding technique in Chapter 4 the cutting edge near the periphery is curved, the chip thickness is decreased, and the stress and heat are more evenly distributed on the cutting edge, accordingly the tool life is increased by 40%. The limitation of curving the periphery rather than the whole cutting lip is attributed to the fact that curving the portion near the drill centre

would increase the point angle in that region. An increase in the point angle on the near to centre portion will increase the thrust force at that region. For insufficiently rigid tools, like twist drills this force causes severe vibration or chatter of both workpiece and cutting tool during the tool commence meet with the workpiece.

A prototype grinding machine designed and built for the work was used for the preparation and grinding of the diametral drill to provide a partially curved diametral point drill. Tool life tests were run to determine the improvement obtained by this point grinding technique. As a matter of economy and because resources were , a hundred holes were drilled after which flank wear was measured at the outer corner and taken as the criterion for drill life. Figures (95) to (98) show the diametral partially curved point has a considerable effect upon wear rate compared with the conventional point. It can also be seen from the above figures that the wear pattern followed the classical wear pattern and that in general uniform wear patterns occured after the first rapid stage.

CHAPTER 10

CONCLUSIONS AND FUTURE WORK

10.1 INTRODUCTION

The work reported in this thesis can be divided into the following parts

(i) Review of the fundamentals of drilling and drill modification (Chapter 1).

(ii) Investigation of an asymmetric drill with the aim of modification to its performance (Chapter 2).

(iii) Analysis of the twist drill rigidity and chip disposal capacity (Chapter 3).

(iv) Design of a new drill flute (Chapter 4).

(v) Design of the cutter shape to mill any required flute shape (Chapter 5).

(vi) Comparative performance tests between a conventional drill and the new flute drill (Chapters 6, 7, and 8).

In the present work, twist drills are dealt with in three stages; manufacturing, point grinding and hole producing. These three stages represent a complete typical function cycle of a twist drill.

10.2 CONCLUSIONS

1. The difficulty of point grinding and balancing the cutting forces over the two lips for an asymmetric drill necessitates the similarity of the two lips (symmetrical approach).

2. For complete definition of the flute profile the flute heel can be mathematically modelled. This model can be based on the proper compromise of the chip disposal capacity and the drill rigidity.

3. The radius of the circle which could be inscribed in the flute space normal to the drill axis is considered to be a good index of flute disposal capacity, because the chip which is formed in a curled-conical shape will only occupy a circular part of the flute space.

4. A study of a range of twist drills indicates that for some cases the inscribed diameter of the circle which could be inscribed in the cross section normal to the drill axis is not an accurate index of the torsional rigidity. The polar moment of area may be counted on as an accurate and reliable index of torsional rigidity.

5. The traditional selection of land width by the drill

manufacturer (land width = flute width) is not entirely correct.

6. The provisional polar moment of area can be estimated theoretically.

7. The shape of the drill flute should be such that the cutting lip will be a straight line. If the lip is concave, a compression force is set up within the chip, and conversely, if convex, a tensile force is set up in addition to the other metal cutting forces.

8. The chisel edge can be eliminated by the design of a flute shape to provide diametral-straight lips as viewed normal to the drill axis.

9. A quadratic spherical model can be used to provide a diametral partially curved lip drill. This distributes the load along the cutting lips and compensates for the variation of the cutting speed along the lips.

10. The oblique flute form (normal to the helix) is of practical importance as it enables the profile of the form milling cutter that should be employed for milling the helical flute from drill blanks to be determined.

11. The interference produced when milling a helical flute with a disc type cutter can critically affect the flute shape, and consequently affect the geometry of the cutting lip and the drill rigidity. Accordingly a proper cutter design should allow for the interference action.

12. To modify the flute form, the lip shape affects drill performance as far as drilling forces, lip wear and hole quality are concerned.

13. Drilling torque and thrust is lower for the new design drill than for the conventional one. The experimental results show that with the new design drill the torque decreased between 10 to 28% as the thrust decreases between 44 to 56%.

14. Analysis of variance on the drilling thrust results has shown the effect of drill type and drilling feed are highly significicant. The effect of the interaction between the drilling speed and drilling feed and the interaction between the three factors (type, speed, and feed) are non-significant.

15. Analysis of variance on the drilling torque results has shown the effect of drill type and drilling feed are highly significant, while the drilling speed and all the

interactions are non-significant.

16. Welded and adhering materials covering the investigated portion of the margin resulted in the abandonment of the attempt to measure and define tool life based on this criterion.

17. Torque, thrust and power measurement show no satisfactory criterion for drill life under the conditions used.

18. Lip wear at flank for both the conventional drill and new design drill show similar wear patterns but different intensities as far as drill type and drilling conditions are concerned. Lip wear is smaller for the new design drill.

19. With a special grinding technique, the straight cutting edge of the new design drill can be converted to curved (Ball) edges which resulted in further improving in tool life by lowering the values of the wear rate.

20. Analysis of variance of the wear rate results show that: the difference between drill types is non-significant for conventional and new design straight-lip drill and significant for conventional and new design diametral, partially curved drills.

21. Analysis of variance has also shown that for both drill types the effect of cutting speed and feed is highly significant. The effect is non-significant for partially curved drills.

22. In certain cutting conditions, it might be possible to use a hole which is produced in one pass of the new design drill which previously would have required a drilled and reamed hole.

10.3 SUGGESTIONS FOR FURTHER WORK

The new flute design based on the conditions of eliminating the chisel edge and providing a diametrally located lip extended to the drill centre when compared to the conventional drill design proved to be an improvement in drilling steel relative to the conventional drill.

The following avenues ahead are suggested for further work:

1. To extend the new drill design for oil-fed deep hole drilling.

2. To apply the new approach to the drilling of ductile materials (copper and aluminium which normally have long ribbon chips) to provide a compact curled chip as was proved from a limited test.

3. To design a point grinder which enables both flank grinding and lip extending at the same time.

4. To introduce a uniform, thicker web since with the new design the web size provides more rigidity without affecting the cutting performance.

5. Such other factors as cutting fluid and machine design can be included in further studies to find the inter-relations among the drill geometry, drill performance and these factors. Different criteria can also be used to find the associated optimum drill geometry and cutting conditions.

6. Other aspects of hole quality, such as hole parallelism and burr formation, and their correlation with other components of the drilling forces such as the horizontal force can also be investigated.

7. To investigate the influence of the diametral and partially curved drill on some other aspects of drilling performance such as forces and hole quality.

8. The performance of the new flute configurations should be studied at a wider range of speeds and feeds as well as sizes and materials.

9 To investigate the influence on drilling performance of a drill with lips located between the conventional and diametral lip locations. It is thought probable that such a lip configuration may provide the advantages of the diametrally located lips reported in this work and the better hole quality at higher metal removal rates (speed x feed).

REFERENCES

[1] **PERA,** Survey of machining requirements in industry, Production Engineering Research Association, Report (1969).

[2] **ERNST H and HAGGERTY A,** The spiral point drill - a new concept in drill point geometry, Transaction of the ASME, June 1958.

[3] **SHEFFIELD TWIST DRILL AND STEEL COMPANY,** Deep hole drilling with HSS twist drills, Brunel University Second International Conference on Deep Hole Drilling and Boring, May 1977.

[4] **BILLAU D.J.,** An investigation relating to double margin drill performance and flank face geometry, PhD Thesis, University of Nottingham 1977.

[5] **WIRIYACOSOL S and ARMAREGO E.J.A.,** Thrust and torque prediction in drilling from a cutting mechanics approach. Annals of the CIRP Vol, 28/1/1979.

[6] **OXFORD C.J.** Some recent research on twist drills and drilling, American Society of Tool Engineering 1955.

[7] **ARMAREGO E.J.A and WRIGHT J.D.,** An analytical study of three point grinding methos for general purpose twist drills, Annals of the CIRP, Vol.29/1/1980.

[8] **OXFORD C.J. Jr.** On the drilling of metals, 1 - basic mechanics of the process, Transaction of the ASME, February 1955.

[9] **OXFORD C.J. Jr.** A review of some recent developments in the design and application of twist drills, Advances in machine Tool Design and Research, MTDR Conference, 1964.

[10] **ARMAREGO E.J.A. and ROTENBERG A.,** An investigation of drill point sharpening by the straight lip conical grinding method, 1 - basic analysis, Int.J. Mech. Tool Des. Res. Vol 13. pp 155-164 Pergamon Press 1973.

[11] **RUSSEL W.R.,** Drill design and drilling conditions for improved efficiency, ASTME paper No 397 Vol 62. Book 1 1962.

[12] **GALLOWAY D.F. and MORTON I.S.,** practical drilling tests, Research Department of the Institution of Production Engineers. 1946.

[13] **TSAI W.D.,** Drill geometry models and dynamics of drilling, PhD Thesis, University of Wisconsin Madison, 1977.

[14] **PAIS M.D.S.,** The influence of flute form on drill design and performance PhD Thesis, Loughborough University of Technology, 1982.

[15] **GALLOWAY D.F.** Some experiments on the influence of various factors on drill performance, Transactions of the ASME, Paper No 56 SA-18, 1957.

[16] **WALLER C.E.,** Some special equipment and techniques developed for the performance testing of twist drills. Annals of the CIRP Vol.8, pp367-373, 1966.

[17] **NATIONAL TWIST DRILL AND TOOL CO.,** Torsional rigidity of twist drill. Metal Cutting. Vol.10, No.3, 1962.

[18] **NATIONAL TWIST DRILL AND TOOL CO.,** Short drills vs long drills, Metal Cutting. Vol.1, No.4, 1954.

[19] **BILLAU, D.J. and HEGINBOTHAM W.B.,** Some aspects of drill performance and testing. 9th International MTDR Conference Proceedings, 1968.

[20] **BILLAU, D.J. and McGOLDRICK P.F.,** An analysis of the geometry of the periphery of the flank face of twist drills ground with cylindrical and conical forms. Int. J. Machine Tool Des. Res., Vol.19, pp69-86, 1979.

[21] **ARMAREGO E.J.A. and ROTENBERG A.,** An investigation of drill point sharpening by the straight lip conical grinding method - II. A criterion for selecting a solution, Int. J. Mach. Tool Des. Res. Vol.13, pp 165-182, 1973.

[22] **ARMAREGO E.J.A. and ROTENBERG A.,** An investigation of drill point sharpening by the straight lip conical grinding method - III drill point grinder design features. Int. J. Mach. Tool Des. Res. Vol 13, pp 233-241, 1973.

[23] **FUJII S, DEVRIES M.F. and WU S.M.,** An analysis of drill geometry for optimum drill design by computer, Part I - Drill geometry analysis. Transactions of the ASME paper No 70 - Prod-5, 1969.

[24] **TSAI W.D. and Wu S.M.,** Computer analysis of drill point geometry. Int. J. Mach. Tool Des. Res., Vol.19, pp 95-108, 1979.

[25] **FUJII S., DEVRIES M.F., and WU S.M.,** Analysis and design of a drill grinder and evaluation of grinding parameters. Transactions of the ASME, Paper No.71 - WA/Prod-5. 1971.

[26] **PERA,** Drilling alloy steel, PERA report No.53, 1957.

[27] **BIRD W.W.,** A twist drill dynamometer, Trans. of the ASME, Vol.26, pp 355, 1905.

[28] **LORENZ G.,** A contribution to the standardization of drill performance tests, Annals of the CIRP, Vol. 25/1/1977.

[29] **KALDOR S.,** Investigation in tool life of twist drills, Annals of the CIRP. Vol. 29/1/1980.

[30] **BHATTACHARYYA A., and HAM I.,** Design of cutting tools. American Society of Tool and Manufacturing Engineers, 1969.

[31] **LORENZ G.,** Helix angle and drill performance, Annals of the CIRP, Vol. 28/1/1979.

[32] SHAW M.C., and OXFORD C.J. Jr., On the drilling of metals, 2 - The torque and thrust in drilling. Transactions of the ASME, 1957.

[33] HATSCHEK R.L., Fundamentals of drilling. American Machinist Special Report 709, 1979.

[34] CRIPS W.H., Fluted cutting tools. U.S. Patent 2,769,355, Nov 6,1956.

[35] BILLAU D.J. McGOLDRICK P.F. and HEGINBOTHAM W.B., The performance of double margin drills with both margins cutting. Proceedings of the 19th International Machine Tool Design and Research Conference, Manchester 1978.

[36] ZHIROV V, Drilling practice. Translated from Russian by Tokmakov, Peace Publishers, Moscow 1964.

[37] BHATTACHARYYA A., and HAM I., Modification of drill point for reducing thrust. Transactions of the ASME, Paper No 71 - Prod-12, 1971.

[38] PERA, An investigation into the effects of point thinning and drill stiffness on drill performance. PERA Report No.89, 1962.

[39] OXFORD C.J. Jr., Self-thinned heavy-duty twist drill structure. U.S. Patent No. 2,778,252. Jan.1957.

[40] GIDDINGS and LEWIS, BICKFORD, Model HC drill point grinder. Catalog No. HC-1-B., 1980.

[41] ERNST H., and MERCHANT M., Chip formation, Friction and high quality machined surfaces: Surface treatment of metals. American Society of Metals, N.Y., Vol.29, p 299, 1941.

[42] MERCHANT M.E., Mechanics of the metal cutting process. J. Appl. Physics, Vol.16, No.5, p 267, May 1945.

[43] PALMER W.B., and OXLEY P.L.B., Mechanics of orthogonal machining. Proc. I.Mech.E., Vol.173, p 623, 1956.

[44] OKUSHIMA K., and HITOMI K., An analysis of the mechanics of orthogonal cutting and its application to discontinuous chip formation. Trans. of the ASME, Series B, J. of Eng. for Ind. Vol.83, p 545, 1961.

[45] BITANS K., and BROWN R.H., An investigation of the deformation in orthogonal cutting. Int. J. Mach. Tool Des.Res. Vol.5, p 155, 1965.

[46] NORMAN et al., SPSS - Statistical Package for Social Sciences.

[47] SPUR G., Drilling with twist drills of different cross section profiles. Annals of the CIRP. Vol. 30/1/1981.

[48] KIRILENKO A.L., Importance of flute helix angle of twist drills. Machines and Tooling. Vol.43, 1972.

[49] TSAI W.D. and WU S.M., Measurement and control of the drill point grinding process. Int.J.Mach. Tool Des. Res. Vol.19, pp 109-120, 1979.

[50] CHITALE A.K., Graphical approach for the determination of flute contour of twist drills. Institute of Engineering (India) Vol.54, January 1974.

[51] SHAW M.C., COOK N.H., and SMITH P.A., The mechanics of three-dimensional cutting operations. Transactions of ASME, Vol.74, p.1055, 1952.

[52] SHAW M.C., Metal cutting principles. The M.I.T. Press, 1952.

[53] SHAW M.C., Discussions of paper no. [8].

[54] LYUBIMOV V.E., New Method of grinding curved lip drills. Machines and Tooling Volume XXXIX No.8, 1968.

[55] TSAI W.D., and WU S.M., A mathematical model for drill point design and grinding. Trans. of ASME Paper No 78-WA/Prod-35, 1978.

[56] RADHAKRISHNAN R.K., KAWLRA R.K, and WU S.M., A mathematical model of the grinding wheel profile required for a specific twist drill flute. Int. J. Mach. Tool Des.Res. Vol.22, No.4 pp 239:-251, 1982.

[57] COMPUTER AIDED DESIGN CENTRE, Gino-F, the general purpose graphics package.

[58] MICHELETTI G.F., and LEVI R., The effect of several parameters of twist drill performance. Advances in Machine Tool Des. and Res. MTDR Conference, 1967.

[59] VENKATARAMAN R., Principles and applications of tool simulation in the metal cutting process. Int. J. Mach. Tool Des. Res., Vol.8 pp.97-106, 1968.

[60] ARSHINOV V., and ALEKSEEV G., Metal cutting theory and cutting tool design. MIR Publishers, Moscow 1970.

[61] RADHAKRISHNAN R.K., Drill point geometry and optimization and on-line monitoring of drill condition. PhD thesis, Univ. of Wisconsin, Madison, U.S.A., 1980.

[62] ARMAREGO E.J.A., Some thoughts on a modified twist drill geometry. Metal Cutting Research Report No. 1968/MC/1.

[63] PAL A.K., BHATTACHARYYA A., and SEN G.C., Investigation of the torque in drilling ductile materials. Int.J Mach Tool Des.Res. Vol.4 pp 205-221, 1965.

[64] PERA, Application of recommended point shape for drilling cast iron. PERA Report No.72.

[65] REZNIKOV A.N., et al., Investigation of stresses in twist drills. Machines & Tooling Vol XXXVI No.9, 1965.

[66] CHAO B.T., and BISACRE G.H., The effect of speed and feed on the mechanics of metal cutting. The Inst of Mech.Eng. Vol.165, 1951.

[67] ROADINGER T.J. and TOWNSEND M.A., Torque and thrust parameters in drilling using dimensional analysis. Trans., of ASME Paper No.79-WA/PROD-4, 1979.

[68] SINGPURWALLA N.D., and KUEBLER A.A., A quantitative evaluation of drill life. Trans. of ASME Paper No.66-WA/PROD-11, 1966.

[69] VARLEY G., Durability of twist drills machining cast iron. The Engineer, August 17, 1934.

[70] WILLIAMS R.A., and McGILCHRIST C.A., An experimental study of drill life. Int. J. Prod. Res. 1972, Vol.10. No.2 175-191.

[71] WILLIAMS R.A., A study of the drilling process. Trans. of the ASME Paper No.73-WA/PROD-6, 1974.

[72] BILLAU D.J., Economic Considerations of drill performance. MSc thesis, University of Nottingham, 1964.

[73] SUBRAMANIAN K., and COOK N.H., Sensing of drill wear and prediction of drill life. Trans. of the ASME Paper No.76-WA/PROD-33, 1976.

[74] LENZ E., MAYER J.E., and LEE D.G., Investigation in drilling. Annals of the CIRP Vol. 27/1/1978.

[75] KANAI M., and KANDA Y., Statistical characteristics of drill wear and drill life for the standardized performance tests. Annals of the CIRP Vol. 27/1/1978.

[76] NATIONAL TWIST DRILL AND TOOL COMPANY, Twist drill life testing. Metal Cuttings Vol.2 No.3, April 1955.

[77] KAHNG C.H., A Study on sequential quality improvement in hole-making processes. Annals of the CIRP Vol.24, 1975.

[78] MORONEY M.J., Facts from figures, Penguin Books, England 1978.

[79] GALLOWAY D.F., Advances in drilling techniques arising from recent research. Microtechnic, Vol.IX, No.3.

[80] SPUR G., Measurement and significance of radial forces in the cutting action of twist drills. Microtechnic, Vol.XV, No.2.

[81] RADHAKRISHNAN T. and WU S.M., On-line hole quality evaluation for drilling composite material using dynamic data. Trans. of the ASME Paper No.80-WA/PROD-16, 1980.

[82] WU S.M., Dynamic data system: A new modeling approach. Trans. of the ASME Paper No. 76-WA/PROD-24, 1976.

[83] SOFRONAS A.S., The formation and control of drilling burrs. PhD Thesis, University of Detroit, U.S.A., 1975.

[84] GRIBKOV YU P., et al., Drill for deep drilling aluminium. Machines and Tooling Vol. XXXVI No.9, 1965.

[85] BRITISH STANDARD 970, 1955.

[86] VAUCLAIN A.C., and WILLE H.V., The Vauclain drill., American Society of Mechanical Engineers, 1912.

APPENDIX 1

SUBPROGRAM REGRESSION

The variable transformation procedures of the SPSS package alllow the regression subprogram to be used for a variety of multivariate analysis, such as polynomial regression, dummy regressions and analysis of variance and covariance. In addition the subprogram allows the user to examine the residual and predicted values for later analyses. Input to the regression subprogram may consist of either raw data cases or a correlation matrix. If the input consists of raw data cases any of the SPSS variable transformation features may be used and several options are available for handling missing data [46].

4.2.2. Printed output subprogram regression

The output from a multiple regression computer 'run' can be varied by selecting from the options available the mannner in which the data is treated and the statistics produced. All the 'runs' made for this part of the work involved the following section:

OPTIONS 1 This option causes the subprogram to include all cases in the calculation of correlation coefficients.

STATISTICS 2 This statistic causes means, standard deviations

and number of valid cases to be printed in a table.

The output is divided into two parts:

(1) Step by step results and

(2) a summary table

The first part provides relevant statistical information for each regression equation calculated, by choice each step involves the addition of one independent variable to the regression equation for ease of analysis and inclusion of only 'significant' variables.

The summary table of the output is printed after the final step in the analysis and provides a brief synopsis of changes occuring at each step. Each step-by-step section is headed with the step number and a list of independent variables entered on the current step. Below it is a list of statistics relevant to the prediction equation. The statistics are:

(1) the multiple correlation coefficient (multiple R)

(2) the value of R^2

(3) the adjusted R^2

(4) the standard error of estimate for the prediction equation.

On the right side is an (ANOVA) table which presents all of

the information relevant to a test for R^2, the overall test for goodness of fit of the equation. Immediately below the foregoing information the step-by-step output is divided into subsections labelled "variables in the equation" and "variables not in the equation". Within the former regression statistics are given for all variables entered into the equation up to and including the current step.

The unstandardized regression coefficients are listed under the column head B. The last value in this column (constant) is the Y intercept. Standardized partial-regression coefficients are listed under the Column (Beta). The column (Std Error B) contains the standard errors for each of the unstandardised regression coefficients, which can be used in a t-test or in establishing confidence limits for the Beta's. The F-ratios in the column (F) are used in tests of significance for the individual Beta's.

Variables that have not been entered into the equation, but that appear in the predictor list, are treated in the "variables not in the equation" segment. The first column, headed "Beta in", is the standardized partial regression coefficient that a variable would have if it alone were entered on the very next step. Under the column head "partial" is the partial-correlation coefficient for each vaariable with the dependent variable, after variables already in the equation have been

partialled out. The remaining two values, "Tolerance" and "F", are used by SPSS when a stepwise mode of analysis is called for. In order to be entered in a stepwise regression, the tolerance and F values must exceed those specified in the parameters section of the regression design statement. From the variables whose tolerance and F values are satisfactory, the variable with the largest partial-correlation coefficent is selected for entry on the next step.

A summary table appears near the end of the print out. It should be noted that the summary table treats variables as if they had been entered one by one, even when variables are entered in blocks or in a single step.

The simple correlation cooefficient between the dependent variable and each of the independent variables appears under the column head "simple R".

APPENDIX II

DERIVATION FOR THE AREA AND POLAR MOMENT OF INERTIA OF THE DRILL CROSS SECTION

Flute Face

The flute face is that portion of the drill flute which yields the cutting edge. Galloway [15] developed a mathematical model for this part of the flute in the plane normal to the drill axis. As shown in Figure 44, any point P' on the straight cutting edge has a corresponding point P_o on the primary flute whose coordinates in the R-ε polar reference system are given by Galloway as:

$$R = \frac{W}{\sin(\varepsilon_1)}$$

$$\varepsilon = \varepsilon_1 + \frac{\tan\theta_o \cot P \,(R^2 - W^2)^{\frac{1}{2}}}{R_o}$$

where $\varepsilon_1 = \sin^{-1}\left(\frac{W}{R}\right)$

Flute Heel

There is no full specification for the heel shape and the heel corner. The heel shape and heel corner position will affect the torsional rigidity of the twist drill and the conveyance of drilling chips. To define the heel side, it is necessary first to define the heel corner position e with respect to the face corner a and secondly the heel side is represented by a second degree polynomial. In terms of the angular difference margin/heel, β, and from the end conditions the portion ce can be defined as:

$$Y = m\,x^2 + W$$

From the end condition

$$m = \frac{\text{Sin } (\beta+\varepsilon_o) - \frac{W}{R_o}}{R_o . \text{Cos}^2 (\beta+\varepsilon_o)^2}$$

From Figure 45, half the cross section area A/2

= (area I + area II) under curve ac

+ (area III) under curve ce

+ (area IV) under curve ex

$$\text{area I} = \int_W^{R_o} R.\varepsilon \, dr$$

$$\text{where} \quad \varepsilon = \text{Sin}^{-1} \frac{W}{R_o} + \frac{\tan \theta_o \text{ Cot P } (R^2 - W^2)^{\frac{1}{2}}}{R_o}$$

$$\text{area I} = \frac{R_o^2}{2} \text{ Sin}^{-1} \frac{W}{R_o} + \frac{W}{2} (R_o^2 - W^2)^{\frac{1}{2}}$$

$$+ \frac{\tan \theta_o \text{ Cot P } (R_o^2 - W^2)^{3/2}}{3} - \frac{\pi W^2}{4}$$

$$\text{area II} = \frac{\pi W^2}{4}$$

$$\text{area III} = \int_{x_e}^{0} y \, dx$$

$$= - \left(\frac{m x_e^3}{3} + W x_e\right)$$

$$\text{area IV} = \int_{-R_o}^{x_e} y \, dx$$

$$= \frac{x_e}{2} (R_o^2 - x_e^2)^{\frac{1}{2}} + \frac{R_o^2}{2} . \text{Sin}^{-1} \frac{x_e}{R_o} + \frac{\pi R_o^2}{4}$$

Half the polar moment of area $J_o/2$

$= M_1$ moment of area I

$+ M_2$ moment of area II

$+ M_3$ moment of area III

$+ M_4$ moment of area IV

$$M_1 = \int_W^{R_o} R^3 \varepsilon \, dR$$

$$= \frac{R_o^4}{4} \cdot \sin^{-1} \frac{W}{R_o} + \frac{W}{4} \left(\frac{F\sqrt{F}}{3} + W^2 \sqrt{F}\right)$$

$$+ \frac{\tan \theta_o \cot P}{R_o} \left(\frac{F^2\sqrt{F}}{5} + \frac{W^2 . F\sqrt{F}}{3}\right) - \frac{\pi W^4}{8}$$

$$M_2 = \frac{\pi W^4}{8}$$

$$M_3 = -\left(\frac{m^3 x_e^7}{28} + \frac{3W m^2 x_e^5}{20} + \frac{m W^2 x_e^3}{4} + \frac{x_e W^3}{4}\right)$$

$$- \left(\frac{m x_e^5}{5} + \frac{W x_e^3}{3}\right)$$

$$M_4 = \frac{x_e F\sqrt{F}}{16} + \frac{3 x_e R_o^2 \sqrt{F}}{32} + \frac{3 R_o^4}{32} \cdot \sin^{-1} \frac{x_e}{R_o} + \frac{3\pi R_o^4}{64}$$

$$- \frac{x_e F\sqrt{F}}{4} + \frac{x_e R_o^2 \sqrt{F}}{8} + \frac{R_o^4}{8} \cdot \sin^{-1} \frac{x_e}{R_o} + \frac{\pi R_o^4}{16}$$

where $x_e = R_o \cos (\varepsilon_o + \beta)$

and $F = R_o^2 - x_e^2$

APPENDIX III

COMPARISON OF SEVERAL EXPRESSIONS FOR THE CALCULATION OF THE RAKE ANGLE

The normal rake angle α_n, as defined by Shaw [51], is the angle measured from a normal to the finished surface in a plane perpendicular to the cutting edges.

From his geometrical observations, Shaw [51-53] has derived the following expression for the calculation at the rake angle:

$$\tan \alpha_n = (\tan \alpha_s \cos C_s + \tan \Theta \sin C_s) \cos i \qquad \text{(III.1)}$$

and

$$\tan \alpha_s = \frac{\tan \Theta}{\tan C_s} - \frac{\tan i}{\sin C_s} \qquad \text{(III.2)}$$

substituting (III.2) into (III.I) we get:

$$\tan \alpha_n = \frac{\cos i}{\sin C_s}(\tan \Theta - \tan i \cos C_s) \qquad \text{(III.3)}$$

where

$$\cos C_s = \frac{\cos P}{\cos i}$$

substituting the value of C_s into III.3

$$\tan \alpha_n = \frac{1}{[\cos^2 i - \cos^2 P]^{\frac{1}{2}}}(\tan\Theta \cos^2 i - \sin i \cos P) \qquad \text{(III.4)}$$

where

i : inclindation angle

P : half the point angle

Θ : helix angle at radius R

Oxford [8] defined the normal rake angle α_n as the angle, measured in a plane normal to the cutting edge, between the cutting face (plane) and a normal to the plane containing both the cutting edge and the drill velocity vector. Accordingly its value was given by:

$$\alpha_n = \alpha_f - \Phi \qquad \text{(III.5)}$$

where

$$\tan \Phi = \tan \beta \ \text{Cos P:}$$

$$\tan \alpha_f = \frac{\tan \Theta \ \text{Cos} \ \beta}{\text{Sin P} - \frac{2\pi W}{H} \text{Cos P}}$$

$$\sin \beta = \frac{W}{R}$$

From (III.5)

$$\tan \alpha_n = \tan (\alpha_f - \Phi) = \frac{\tan \alpha_f - \tan \Phi}{1 + \tan \alpha_f \tan \Phi} \qquad \text{(III.6)}$$

substituting the value of Φ, α_f and β into (III.6) we get:

$$\tan \alpha_n = \frac{\tan\Theta \ \text{Cos}\beta - \tan\beta \ \text{CosP Sin P} + \frac{2\pi W}{H} \text{Cos}^2\text{P} \tan \beta}{\text{SinP} - \frac{2\pi W}{H} \text{CosP} + \tan\Theta \ \text{Sin}\beta \ \text{CosP}} \qquad \text{(III.7)}$$

where

$$\tan \Theta = \frac{2\pi R}{H} \qquad \text{(III.8)}$$

$$\sin \beta = \frac{\text{Sin i}}{\text{Sin P}} = \frac{W}{R} \qquad \text{(III.9)}$$

$$\frac{W}{R} \ \text{sin P} = \text{sin i} \qquad \text{(III.10)}$$

From (III.8) and (III.9) it can be found that

$$\frac{2\pi W}{H} = \tan\Theta \sin\beta \qquad \text{(III.11)}$$

Multiply (III.7) by sin P and substituting the value of $\frac{2\pi W}{H}$ from III.11. we can get

$$\tan \alpha_n = \frac{1}{[\cos^2 i - \cos^2 P]^{\frac{1}{2}}} (\tan\Theta \cos^2 i - \cos P \sin i) \qquad \text{(III.12)}$$

where

α_f : face rake angle

W : half the web thickness

Galloway [15] defined the normal rake angle as the angle between the drill face and the plane which contains the cutting edge and which is perpendicular to the machined surface at the given point on the cutting edge. The following equation was obtained for α_n.

$$\tan\alpha_n = \frac{(p^2 - \tau^2 \sin^2 P)}{(p^2 - \tau^2)^{\frac{1}{2}} \sin P} \tan\Theta_o - \frac{\tau \cos P}{(p^2 - \tau^2)^{\frac{1}{2}}} \qquad \text{(III.13)}$$

where:

$$p = \frac{R}{R_o} \qquad \text{(III.14)}$$

$$\tau = \frac{W}{R_o} = \frac{R}{R_o} \frac{\sin i}{\sin P} \qquad \text{(III.15)}$$

substituting (III.15) into (III.13) we get:

$$\tan\alpha_n = \frac{[(\frac{R^2}{R_o}) - (\frac{R}{R_o}\sin i)^2]\tan\theta_o - \frac{R}{R_o} \cos P \sin P}{\sin P \left(\frac{R^2 - W^2}{R_o^2}\right)^{\frac{1}{2}}} \qquad \text{(III.16)}$$

From (III.9) :

$$\text{Cos } \beta = \frac{(R^2 - W^2)^{\frac{1}{2}}}{R}$$

$$(R^2 - W^2)^{\frac{1}{2}} = R \text{ Cos } \beta \qquad \text{(III.17)}$$

substituting (III.17) into (III.16) we get:

$$\tan \alpha_n = \frac{\tan \Theta \text{ Cos}^2 i - \text{Cos P Sin } i}{\text{Sin P Cos } \beta} \qquad \text{(III.17)}$$

From (III.9)

$$\text{Cos } \beta = \frac{(\text{Sin}^2 P - \text{Sin}^2 i)^{\frac{1}{2}}}{\text{Sin P}}$$

$$= \frac{(\text{Cos}^2 i - \text{Cos}^2 P)^{\frac{1}{2}}}{\text{Sin P}} \qquad \text{(III.18)}$$

substituting (III.18) into (III.17) we get:

$$\tan \alpha_n = \frac{1}{[\text{Cos}^2 i - \text{Cos}^2 P]^{\frac{1}{2}}} (\tan \Theta \text{ Cos}^2 i - \sin i \text{ Cos P}) \qquad \text{(III.19)}$$

Comparing (III.4), (III.12) and (III.19) which come from the expressions presented by Shaw [51-53], Oxford [8] and Galloway [15] respectively shows that although different expressions have been developed by different workers, however it can be proved that each one can be trigonometrically transformed to be the other.

C APPENDIX V
C
C
C
C ***PROGRAM FLUTE***
C TO FIND THE FLUTE SHAPE FROM AKNOWN CUTTER SHAPE
C SETTED AT THE SAME ANGLE AS THAT OF THE HELIX
C
C

```
      DIMENSION XWBAR(800),YWBAR(800),XF(800),YF(800)
      DIMENSION XBAR(800),YBAR(800),X(800),Y(800)
      DIMENSION XWHEEL(200),YWHEEL(200)
      DIMENSION XFLUT(200),YFLUT(200)
      DIMENSION XFSTAN(75),YFSTAN(75)
      READ(1,5)NW,NFSTAN
    5 FORMAT(2I3)
      READ(1,10)(XFSTAN(J),YFSTAN(J),J=1,NFSTAN)
   10 FORMAT(2F8.3)
C     READ THE DRILL PARAMETERS
      READ(1,15)RO,HO,P,RWEB
   15 FORMAT(4F6.3)
      PI=3.1415926
      HO=HO*PI/180.
      P=P*PI/180.
C     READ CIUTTER PARAMETERS
      READ(1,20)RMAX
   20 FORMAT(F6.3)
      N=0
      NP=0
      NPOT=0
      IN=0
C  ***  READ X,Y FROM DATA FILE WHICH DEFINE THE CUTTER SHAPE
      READ(1,25)(XWHEEL(MM),YWHEEL(MM),MM=1,NW)
   25 FORMAT(2F8.3)
C  ***  TAKE THE CUTTER EFFECT ON DIFFERENT SECTIONS STARTING FROM
C  ***  ZBA=0 TO ZBA=16 AND NEGLECT THE NEGATIVE SIDE BECAUSE THERE
C  ***  IS NO INTERFERENCE IN THAT SIDE
      Z=0.0
   30 Z=Z+1.0
      IZ=Z
      ZBA=Z
      IF(IZ.GT.14)GO TO 40
      DO 35 M=1,NW
      XWBAR(M)=XWHEEL(M)
      YWBAR(M)=RMAX+RWEB-SQRT((RMAX+RWEB-YWHEEL(M))**2-ZBA*ZBA)
C  ***  THIS PART IS TO CHECK IF ANY POINT IS OUTSIDE THE DRILL CROSS SECTION
      XX=XWBAR(M)-ZBA*TAN(HO)
      YY=YWBAR(M)
      AA=RO/COS(HO)
      BB=RO
      CC=XX*XX/(AA*AA)
      DD=YY*YY/(BB*BB)
      IF((CC+DD).GT.1)GO TO 35
C  ***
```

```
      IN=IN+1
      N=N+1
      GAMA=ZBA*TAN(HO)/RO
      X1=XWBAR(M)-ZBA*TAN(HO)
      Y1=YWBAR(M)
      XBAR(N)=X1*COS(GAMA)+Y1*SIN(GAMA)
      YBAR(N)=Y1*COS(GAMA)-X1*SIN(GAMA)
   35 CONTINUE
      GO TO 30
   40 NPOT=0
C  ***  THIS PART IS TO FIND THE LOWEST PONT(SMALLEST YBAR) AT AN INTERVALS
C  ***  OF 0.5 mm IN AN ARBITARY RANGE 10.0 : -5.0
      DO 110 IX=100,-100,-4
      XR=FLOAT(IX/10)
      NP=NP+1
      J=1
      DO 100 K=2,IN
      TTT=10*(XBAR(K)-XR)
      KKK=ABS(TTT)
      IF(KKK.GT.2)GO TO 100
      J=J+1
      IY1=YBAR(K)*10.0
      YF(1)=YBAR(1)
      IY2=YF(J-1)*10.0
      IF(IY1.LT.IY2)GO TO 50
      XF(J)=XR
      YF(J)=YF(J-1)
      GO TO 100
   50 XF(J)=XR
      YF(J)=YBAR(K)
  100 CONTINUE
      NPOT=NPOT+1
      X(NPOT)=XF(J)
      Y(NPOT)=YF(J)
      YF(1)=0.0
  110 CONTINUE
      LL=0
      DO 120 L=1,NPOT
      IXX=X(L)
      IYY=Y(L)
C  *** THE COMMING STEP IS TO REJECT THE PONTS AMONG THE ARBITARY RANGE
C  *** WHICH IS OUTSIDE THE FLUTE ZONE
      IF(IXX.EQ.0.AND.IYY.EQ.0)GO TO 120
      LL=LL+1
      XFLUT(LL)=X(L)
      YFLUT(LL)=Y(L)
  120 CONTINUE
      WRITE(11,130)
  130 FORMAT(15X,'FLUTE PRODUCED')
      WRITE(11,140)
  140 FORMAT(//,5X,'X        Y')
      WRITE(11,150)(XFLUT(I),YFLUT(I),I=1,LL)
  150 FORMAT(2F8.3)
C     XFLUT(1)=XFLUT(2)
```

```
C       YFLUT(1)=RO*SQRT(1-XFLUT(1)*XFLUT(1)/((RO/COS(HO))**2))
        LL=LL+1
        XFLUT(LL)=XFLUT(LL-1)
        YFLUT(LL)=SQRT(RO*RO-XFLUT(LL)*XFLUT(LL)*COS(HO)*COS(HO))
        CALL GINO
        CALL UNITS(5.0)
        CALL SHIFT2(19.0,14.0)
        CALL CHASIZ(0.4,0.4)
        CALL AXIPOS(0,0.0,0.0,24.0,1)
        CALL AXIPOS(0,0.0,0.0,12.0,2)
        CALL AXISCA(3,12,-12.0,12.0,1)
        CALL AXISCA(3,6,0.0,12.0,2)
        CALL AXIDRA(1,1,1)
        CALL AXIDRA(-1,-1,2)
        CALL MOVTO2(3.5,-2.8)
        CALL CHAHOL(10HX-A*LXIS*.)
        CALL MOVTO2(-1.0,13.4)
        CALL CHAHOL(10HY-A*LXIS*.)
C       CALL MOVTO2(-14.0,12.0)
C       CALL CHAHOL(13HFLUTE SHAPE*.)
        CALL MOVTO2(-13.0,10.0)
C       CALL CHAHOL(12HSCALE 1:5 *.)
        CALL MOVTO2(8.0,12.0)
C       CALL CHAHOL(19H__FLUTE REQUIRED*.)
        CALL MOVTO2(-5.0,-13.0)
        CALL CHAHOL(34HF*LIGURE(   ) FLUTE PRODUCED      *.)
C       CALL GRACUR(XWHEEL,YWHEEL,NW)
        CALL MOVTO2(XWHEEL(1),YWHEEL(1))
C       CALL LINTO2(XWHEEL(1),10.0)
        CALL MOVTO2(XWHEEL(NW),YWHEEL(NW))
C       CALL LINTO2(XWHEEL(NW),10.0)
        CALL MOVTO2(0.0,0.0)
        CALL DASHED(-1,0.5,0.3,0.0)
        CALL GRACUR(XFLUT,YFLUT,LL)
        XSCAL=1.0/COS(HO)
        CALL SCALE2(XSCAL,1.0)
        CALL MOVTO2(0.0,RO)
        CALL DASHED(0,0.0,0.0,0.0)
C       CALL PENSEL(2,0.0,0)
        CALL ARCTO2(0.0,0.0,0.0,RO,1)
        XSCAL=COS(HO)
        CALL SCALE2(XSCAL,1.0)
C       CALL GRACUR(XFSTAN,YFSTAN,NFSTAN)
        CALL DEVEND
        STOP
        END
£VX
```

C APPENDIX IV

C

C

C COMPUTER PREDICTION OF THE CUTTER SHAPE

C

C

```
      DIMENSION XF(100),YF(100),XW(100),YW(100)
      DIMENSION BAK(100)
      DIMENSION X(100)
      PI=3.1415926
C     READ THE DRILL PARAMETERS
      READ(1,5)RO,HO,P,RWEB
    5 FORMAT(4F6.3)
      HO=HO*PI/180.
      P=P*PI/180.
C     READ THE WHEEL PARAMETERS
      READ(1,10)RMAX,ITOLER,YLOWER,LOW
   10 FORMAT(F6.3,I3,2F6.3)
C     READ THE FLUTE POINT
      READ(1,155)NPFLUT
      DO 15 L=1,NPFLUT
      READ(2,25)XF(L),YF(L)
      IF(YF(L).GT.YLOWER)GO TO 15
      LOW=LOW+1
      XLOWER=XF(L)
      YLOWER=YF(L)
   15 CONTINUE
   25 FORMAT(2F8.3)
      NPF=NPFLUT*60/100
      DO 65 I=1,NPF
      XW(I)=XF(I)
      YW(I)=YF(I)
      DO 55 IZ=0,16,2
      Z=FLOAT(IZ)
      XWBAR=XW(I)
      YWBAR=RMAX+RWEB-SQRT((RMAX+RWEB-YW(I))**2-Z*Z)
      GAMA=Z*TAN(HO)/RO
      X1=XWBAR-Z*TAN(HO)
      Y1=YWBAR
      XBAR=X1*COS(GAMA)+Y1*SIN(GAMA)
      YBAR=Y1*COS(GAMA)-X1*SIN(GAMA)
      XIDEAL=XLOWER-(YBAR-YLOWER)*(XLOWER-XF(NPFLUT))/
     C(YF(NPFLUT)-YLOWER)
      XDIFR=XIDEAL-XBAR
      IXDIFR=XDIFR*10.0
      IF(IXDIFR.GT.ITOLER)GO TO 75
      DO 35 K=2,NPFLUT
      BAK(1)=ABS(XF(1)-XBAR)
      BAK(K)=ABS(XF(K)-XBAR)
      XBAK=BAK(K)-BAK(K-1)
      IBAK=XBAK*10.
      IF(IBAK.LT.0)GO TO 35
      IYBAR=YBAR*100.
      IYF=YF(K-1)*100.0
```

```
      IF(IYBAR.GT.IYF)GO TO 45
      YBAR=YF(K-1)
      GO TO 45
   35 CONTINUE
   45 CALL XWHEEL(XBAR,YBAR,GAMA,Z,HO,RMAX,RWEB,XW(I),YW(I))
   55 CONTINUE
   65 CONTINUE
   75 I=I-1
      IL=I
      ILL=I-1
      DO 105 J=1,ILL
      IT=IL-J
      I=IL+J
      XW(I)=XW(IL)-XW(IT)+XW(IL)
      YW(I)=YW(IT)
      IJ=2
      DO 95 IZ=0,16,2
      Z=FLOAT(IZ)
      X(IJ)=XW(I)
      X(1)=100.0
      IXIJ=X(IJ)*10.0
      IXI=X(IJ-1)*10.0
      IF(IXIJ.GT.IXI)X(IJ)=X(IJ-1)
      XW(I)=X(IJ)
      IJ=IJ+1
      XWBAR=XW(I)
      YWBAR=RMAX+RWEB-SQRT((RMAX+RWEB-YW(I))**2-Z*Z)
      GAMA=Z*TAN(HO)/RO
      X1=XWBAR-Z*TAN(HO)
      Y1=YWBAR
      XBAR=X1*COS(GAMA)+Y1*SIN(GAMA)
      YBAR=Y1*COS(GAMA)-X1*SIN(GAMA)
      LLOW=LOW+1
      DO 85 K=LLOW,NPFLUT
      BAK(K)=ABS(YBAR-YF(K))
      YBAK=BAK(K)-BAK(K-1)
      IYBAK=YBAK*10.0
      IF(IYBAK.LT.0)GO TO 140
      XBAR=XF(K-2)-0.2*ITOLER
      CALL XWHEEL(XBAR,YBAR,GAMA,Z,HO,RMAX,RWEB,XW(I),YW(I))
      IYEND=YW(I)*10.0
      IYSTRT=YW(1)*10.0
      IF(IYEND.GT.IYSTRT)GO TO 125
      GO TO 95
   85 CONTINUE
   95 CONTINUE
  105 CONTINUE
  115 I=I
      WRITE(2,125)
  125 FORMAT(15X,'CUTTER SHAPE')
      WRITE(2,135)
  135 FORMAT(//,5X,'X        Y')
      WRITE(2,145)(XW(MM),YW(MM),MM=1,I)
  145 FORMAT(2F8.3)
```

```
      CALL GINO
      CALL UNITS(10.0)
      CALL SHIFT2(6.0,7.0)
      CALL CHASIZ(0.2,0.25)
      CALL AXIPOS(0,0.0,0.0,10.0,1)
      CALL AXIPOS(0,0.0,0.0,18.0,2)
      CALL AXISCA(3,5,0.0,10.0,1)
      CALL AXISCA(3,9,0.0,18.0,2)
      CALL AXIDRA(1,1,1)
      CALL AXIDRA(-1,-1,2)
      CALL MOVTO2(4.4,-2.0)
      CALL CHAHOL(10HX-A*LXIS*.)
      CALL MOVTO2(-2.0,8.4)
      CALL CHAANG(90.0)
      CALL CHAHOL(10HY-A*LXIS*.)
      CALL MOVTO2(-5.0,-4.0)
      CALL CHAANG(0.0)
      CALL CHAHOL(45HF*LIG     COMPUTER PREDICTION OF THE CUTTER*.)
      CALL MOVTO2(3.5,-4.0)
      CALL CHAHOL(45H*LSHAPE FOR THE PART. CURVED DRILL IN FIG. *.)
      CALL GRACUR(XW,YW,I)
      A=YW(I)
      D=YW(1)
      DO 165 L=1,I
      READ(1,155)EC
  155 FORMAT(F6.3)
      YF(L)=2.0*YW(1)+EC-YW(L)
  165 CONTINUE
      CALL MOVTO2(XW(I),YW(I))
      B=2.0*YW(1)+EC-YW(I)
      CALL LINTO2(XW(I),B)
      CALL GRACUR(XW,YF,I)
      C=2.0*YW(1)+EC-YW(1)
      CALL MOVTO2(XW(1),C)
      CALL LINTO2(XW(1),YW(1))
      CALL DEVEND
      STOP
      END
      SUBROUTINE XWHEEL(XBA,YBA,GAM,ZZ,HOO,RMA,RWE,XWI,YWI)
      Y11=(YBA+XBA*TAN(GAM))/(COS(GAM)+SIN(GAM)*TAN(GAM))
      X11=(XBA-Y11*SIN(GAM))/COS(GAM)
      XBA=X11+ZZ*TAN(HOO)
      YWBA=Y11
      XWI=XBA
      BNN=-2.0*(RMA+RWE)
      CNN=2.0*(RMA+RWE)*YWBA-ZZ*ZZ-YWBA*YWBA
      YWI=-(SQRT(BNN*BNN-4.0*CNN)+BNN)/2.0
      RETURN
      END
£VX
```

TABLE 1

THE EXPERIMENTALLY OBTAINED THRUST FORCE X 10^3 N

Type of drill \ Speed rpm / Feed X 10^{-3} mm/rev	690				1060				1500			
	81	96	114	137	52	62	74	89	38	43	51	64
as received (asymmetric)	2.0	2.4	2.55	2.8	0.8	0.9	1.4	1.45	0.8	1.0	1.05	1.4
with lip modified	2.0	2.2	2.5	2.7	0.75	0.8	1.0	1.6	0.7	0.9	1.0	1.2
conventional	2.2	2.6	2.8	3.0	2.4	2.6	2.6	3.0	1.6	2.4	2.5	2.6

TABLE 2

THE EXPERIMENTALLY OBTAINED TORQUE, 10^3 N cm

Type of drill \ Speed rpm / Feed $\times 10^{-3}$ $\frac{mm}{rev}$	690				1060				1500			
	81	96	114	137	52	62	74	89	38	43	51	64
as received (asymmetric)	1.0	1.2	1.5	1.6	0.8	1.0	1.1	1.4	0.5	0.8	0.8	0.85
with lip modified	1.2	1.3	1.6	1.8	0.7	0.9	1.2	1.5	0.6	0.7	0.75	0.8
conventional	1.1	1.4	1.6	1.9	1.1	1.1	1.2	1.4	0.7	0.7	0.7	0.8

TABLE 3

THE EXPERIMENTALLY OBTAINED RADIAL FORCE X 10^3 N

Type of drill \ Speed rpm / Feed X 10^{-3} $\frac{mm}{rev}$	690				1060				1500			
	81	96	114	137	52	62	74	89	38	43	51	64
as received (asymmetric)	1.0	1.1	1.2	1.2	0.9	1.2	1.1	1.4	0.7	1.0	1.1	1.2
with lip modified	0.4	0.6	0.8	0.9	0.4	0.45	0.5	0.8	0.38	0.38	0.42	0.48
conventional	0.0	0.0	0.0	0.0	0.05	0.05	0.05	0.05	0.1	0.1	0.1	0.1

TABLE 4

THE EXPERIMENTALLY OBTAINED OUT-OF-ROUNDNESS X 10^{-3} MM

Type of drill \ Speed rpm / Feed X 10^{-3} $\frac{mm}{rev}$	690				1060				1500			
	81	96	114	137	52	62	74	89	38	43	51	64
as received (asymmetric)	89	107	97	79	38	54.8	80	120	125	125	140	160
with lip modified	31.75	44	67	70	20	21	14.7	33	19	13	18	18
conventional	12.7	15	15	18	19	22.8	29.4	22.8	18	12	14	15

TABLE 5

THE EXPERIMENATALLY OBTAINED HOLE OVERSIZE X 10^{-3} MM

Type of drill \ Speed rpm / Feed X 10^{-3} $\frac{mm}{rev}$	690				1060				1500			
	81	96	114	137	52	62	74	89	38	43	51	64
as received (asymmetric)	2362	1160	1193	1346	650	764	863	721	406	564	686	711
with lip modified	584	584	590	610	350	348	180	175	102	127	127	170
conventional	45.7	60	107	62	26.5	18.3	47	46	38.9	37.6	36	47

TABLE 6

COMPARISON BETWEEN POLAR MOMENT OF AREA
AND OXFORD'S INSCRIBED CIRCLE RADIUS

Drill Parameters					Inscribed Circle radius	polar moment of area
Diameter mm	Land mm	Web mm	Helix degree	Point degree	mm	mm^4
19	8.0	1.78	32	118	2.7	3882
14	9.0	2.8	32	118	2.9	1938
14	9.3	1.78	32	118	3.0	4500
19	8.0	4.0	32	118	3.1	4346
16	9.6	3.2	32	118	3.1	3010
19	9.3	3.3	32	118	3.25	4770
16	10.4	3.2	32	118	3.35	3306
19	12.4	3.3	32	118	3.95	6572
20	12.0	4.0	32	118	3.95	7350

TABLE 7

RANGE OF VARIABLES USED FOR REGRESSION ANALYSIS

Diameter mm	3 - 50
Web (% of Diameter)	10, 15, 20
Helix angle degrees	27.5, 32
Point angle degrees	90, 118
Land width (% of Diameter)	40 - 70

TABLE 8

COMPARISON OF ACTUAL AND PREDICTED
CROSS SECTION AREA, MM^2

Drill diameter = $\frac{3}{4}$ inch Point angle = 118 degrees

Helix angle (degrees)		27.5		32	
Land mm	Web % diameter	Actual	Predicted	Actual	Predicted
9	10	95.54	92.84	98.96	96.78
	15	105.10	98.28	108.5	102.46
	20	114.92	102.34	118.28	106.7
11	10	120.86	120.16	126.26	125.28
	15	128.42	127.20	133.66	132.62
	20	136.38	132.48	141.44	138.10
13	10	154.8	148.96	164.12	155.3
	15	159.92	157.70	168.84	164.4
	20	165.46	164.22	173.98	171.2

TABLE 9

COMPARISON OF CALCULATED AND PREDICTED
POLAR MOMENT OF AREA, MM^4

Drill diameter = ¾ inch

Point angle = 118 degrees

Helix angle (degrees)		27.5		32	
Land mm	Web % diameter	Calculated	Predicted	Calculated	Predicted
9	10	4188.8	4210	4379.26	4426.2
	15	4358.14	4318	4548.26	4539.4
	20	4546.78	4396	4736.1	4621.8
11	10	5246.3	5350	5515.12	5624.52
	15	5382.28	5487	5648.72	5768.4
	20	5534.74	5586.6	5798.02	5873.1
13	10	6445.3	6531.2	6831.98	6866
	15	6559.54	6698.28	6943.02	7041.78
	20	6684.4	6819.8	7063.52	7169.56

Table 10: Variation of chip disposal capacity and polar moment of area with face-heel spacing angle

Face-heel spacing angle, β	Land Width L (mm)	Chip disposal capacity $2R_c$ (mm)	Polar moment of area J (mm^4)
70.0	13.22	6.94	7316.46
80.0	12.37	7.45	6758
83.6	12.04	7.62	6543.6
90.0	11.42	7.62	6143.3
100.0	10.38	7.62	5481.37

TABLE 11: Comparison of grinding parameters and drill angles for ellipsoidal and sphe rical grinding models

Type of Drill	Grinding parameters					included angle (deg) at point	included angle (deg) at periphery	clearance angle (deg) at point	clearance angle (deg) at pheriphery	Chisel edge angle (deg.)
	a in.	d in.	s in.	ø (deg)	c in.					
ellipsoidal	0.7	1.11	0.18	35	1.56	46.14	30.27	12.28	9.65	118
spherical	1.2	1.41	0.3	15	-	57.7	27.4	11.53	11.53	118

Table 12: Drilling Factors Combinations used with the Drilling Forces Tests

Conventional		Diametral	
Speed r.p.m	Feed mm/rev	Speed r.p.m	Feed mm/rev
345	0.0762 0.1524 0.2286	345	0.0762 0.1524 0.2286
490	0.0762 0.1524 0.2286	490	0.0762 0.1524 0.2286
690	0.0762 0.1524 0.2286	690	0.0762 0.1524 0.2286

Table 13: Thrust obtained for the conventional and diametral drills(N)

Speed r.p.m	Feed mm/rev	Conventional			Diametral		
		Run 1	Run 2	Average	Run 1	Run 2	Average
345	.0762	2400	2600	2500	1200	1400	1300
	.1524	4400	4000	4200	1900	2200	2050
	.2286	5400	5100	5250	3000	2800	2900
490	.0762	2600	2700	2650	1400	1300	1350
	.1524	4400	4200	4300	2000	2100	2050
	.2286	5600	5800	5700	3000	3400	3200
690	.0762	3000	2800	2900	1400	1300	1350
	.1524	5200	3800	4500	2200	2200	2200
	.2286	6300	6300	6300	2700	2800	2750

Table 14: Torque obtained for the conventional and diametral drills(N·cm)

Speed r.p.m	Feed mm/rev	Conventional			Diametral		
		Run 1	Run 2	Average	Run 1	Run 2	Average
345	.0762	1200	1350	1275	1100	1200	1150
	.1524	2800	2100	2450	1800	1900	1850
	.2286	2800	3200	3000	2800	2600	2700
490	.0762	1500	1400	1450	1000	1100	1050
	.1524	2400	2350	2375	1900	1800	1850
	.2286	3300	3000	3150	2500	2600	2550
690	.0762	1500	1200	1350	1100	1000	1050
	.1524	2200	2000	2100	1900	1800	1850
	.2286	3200	2800	3000	2600	2600	2600

Table 15: Comparative drilling Thrust

Type / Speed r.p.m / Feed mm/rev	Conventional			Diametral		
	345	490	690	345	490	690
.0762	100	106	116	52	54	54
.1524	100	102	107	49	49	52
.2286	100	109	120	55	61	52

Table 16: Comparative drilling Torque

Type / Speed r.p.m / Feed mm/rev	Conventional			Diametral		
	345	490	690	345	490	690
.0762	100	114	106	90	82	82
.1524	100	97	86	75	75	75
.2286	100	105	100	90	85	87

Table 17: Thrust related value

Type / Speed / Feed	D1			D2			Total
	S1	S2	S3	S1	S2	S3	
F1	2.5	2.65	2.9	1.3	1.35	1.35	12.05
F2	4.2	4.3	4.5	2.05	2.05	2.2	19.3
F3	5.25	5.7	6.3	2.9	3.2	2.75	26.1
Totals	11.95	12.65	13.7	6.25	6.6	6.3	57.45
	38.3			19.15			

Table 18: Analysis of Variance for drilling thrust

Effect	Sum of squares	Degree of freedom	Variance Estimate	Variance ratio
drill type	10.1867	1	10.1867	533.4
speed	0.13625	2	0.06812	3.567
feed	8.2279	2	4.1139	215.4
type x speed	0.13434	2	0.06717	3.5172
type x feed	0.801	2	0.4005	20.971
speed x feed	0.03335	4	0.00833	0.4361
type x speed x feed	0.09858	4	0.03298	1.72695
Error	0.34375	18	0.0190972	
Total	19.96187	35		

Table 19: Torque related value

Type / Speed / Feed	d1			d2			
	S1	S2	S3	S1	S2	S3	Totals
F1	1.275	1.45	1.35	1.15	1.05	1.05	7.325
F2	2.45	2.375	2.1	1.85	1.85	1.85	12.475
F3	3.0	3.15	3.0	2.7	2.55	2.6	17.0
Totals	6.725	6.975	6.45	5.7	5.45	5.5	36.8

Table 20: Analysis of variance for Drilling Torque

Effect	Sum of Squares	Degree of Freedom	Variance Estimate	Variance Ratio
Drill type	0.34027	1	0.34027	41.7017
Speed	0.01253	2	0.006265	0.7678
Feed	3.90056	2	1.9528	239.32
Type x speed	0.01629	2	.008145	0.9982
Type x feed	0.01489	2	.007445	0.9124
Speed x feed	0.007529	4	.001882	0.2306
Typexspeedxfeed	0.021988	4	.00549	0.6736
Errors	0.14687	18	0.008159	
Totals	4.46597	35		

Table 21: Wear loss after 100 holes (x 10^{-3} inch)

Type / Speed r.p.m. / Feed in/rev x 10^{-3}	Conventional		Diametral	
	355	480	355	480
8.3	8.1	9.3	7.0	9.8
12	8.5	17	7.6	14.0

Table 22: Symbols for Factor Levels

Level / Factor	Low	High
speed (S)	1	S
feed (F)	1	F

Table 23: Combination of Factors Levels for Wear Testing

Symbol	Factors	
	S (r.p.m.)	F (I PR)
1	355	8.3
S	480	8.3
F	355	12
SF	480	12

Table 24 : Wear Rate

Type / Treatment (drilling condition)	Yield (Wear Rate)	
	Conventional	Diametral
(1)	5.4	4.66
S	6.2	6.533
F	5.66	5.066
SF	11.33	9.33
Total	28.59	25.589

Total sum

54.179

Table 25: Sum of squares (ref to Table 24)

Type / Treatment (drilling condition)	Yield (sum of squares)	
	Conventional	Diametral
(1)	29.16	21.7156
S	38.44	42.68
F	32.035	25.664
SF	128.368	87.048
Total	228	177.1

Table 26 : Analysis of Variance

Source	Sum of Squares	Degree of Freedom
Between Blocks	1.1257	1
Within Blocks	37.0529	6
Total	38.1790	7

Table 27: Treatment sum of squares (refer to Table 24)

Treatment	Yield Conv + Yield Dia.	(Yield Conv + Yield Diam)^2
(1)	10.06	101.2036
S	12.733	162.12928
F	10.726	115.04707
SF	20.66	426.8356
Total	54.179	805.21555

Table 28: Sum of squares relative to residual treatments

Source	Sum of Squares	Degrees of Freedom
Between Blocks	1.1257	1
Treatments	35.682	3
Residual	1.3713	3
Total	38.179	7

Table 29: Treatment Effect

Effect of	SF	S	F	(1)	Total	Square	Sum of Square
S	+20.66	+12.733	-10.726	-10.06	12.607	158.9364	19.867
F	+20.66	-12.733	+10.726	-10.06	8.593	73.839	9.229
SF	+20.66	-12.733	-10.726	+10.06	7.261	52.722	6.5902

Total : 35.6862

Table 30: Analysis of Variance for all factors and their interaction

Source	Sum of Squares	Degree of Freedom	Variance Estimate Mean Square	Variance Ratio	
Between Blocks	1.1257	1	1.1257	2.462	not significant
Treatments	35.6862	3			
S	19.867	1	19.867	43.463	highly significant
F	9.229	1	9.229	20.190	highly significant
SF	6.5902	1	6.5902	14.417	significant
Residual	1.3713	3	0.4571		
Total	38.179	7			

Table 31: Wear loss after 100 holes (x 10-3 inch)

Drill Type	Feed in/rev	Speed r.p.m. 355	480
Conventional	8.3	8.1	9.3
	12	8.5	17.0
Diametral &	8.3	3.9	7.6
partially curved	12	4.5	9.25

Table 32: Analysis of Variance

Source	Sum of Squares	Degree of Freedom	Variance Estimate Mean Square	Variance Ratio	
Between Blocks	17.4936	1	17.4936	10.242	significant
Treatments	27.01	3			
S	8.06	1	8.06	4.718	not significant
F	14.987	1	14.987	8.774	not significant
SF	3.962	1	3.962	2.319	not significant
Residual	5.1241	3	1.708		
Total	49.6277	7			

Table 33: Surface Roughness C.L.A.(x 10^{-3}mm) - mean of 3 readings.

Drill Type	Conventional			Diametral		
Speed r.p.m. / Feed mm/rev	345	490	690	345	490	690
.0762	0.77	1.40	2.20	0.74	0.75	0.65
.1525	0.75	0.83	1.93	0.65	0.583	1.766
.2286	1.20	1.43	2.30	1.166	0.633	1.25

Table 34: Hole out of Roundness (x 10^{-3} mm)

Type of Drill		Conventional			Diametral		
speed rpm / Feed mm/rev		345	490	690	345	490	690
0.762	Top	2.5	1.0	0.75	2.0	1.0	2.0
	Middle	1.5	0.75	1.0	0.75	0.5	1.0
	Bottom	1.0	0.25	0.75	1.0	0.25	1.0
0.1524	Top	1.25	1.5	1.0	1.25	0.75	1.25
	Middle	1.25	0.75	0.5	0.75	0.5	0.75
	Bottom	0.5	0.75	2.0	0.25	0.5	1.0
0.2286	Top	2.0	1.25	1.25	1.25	1.0	2.0
	Middle	1.5	1.0	0.75	0.75	1.0	2.0
	Bottom	0.75	0.75	1.25	0.25	0.5	1.25

Table 35: Hole oversize (x 10^{-3} inch) - mean of 5 readings

Type of Drill		Conventional			Diametral		
speed rpm / Feed mm/rev		345	490	690	345	490	690
.0.762	Top	1.79	2.25	2.4	0.3	0.1	0.35
	Middle	1.15	1.66	3.33	0.27	0.47	0.43
	Bottom	0.17	0.42	3.20	0.67	0.71	1.56
0.1524	Top	2.35	2.44	3.68	0.54	0.20	2.45
	Middle	1.88	2.29	2.97	0.64	0.64	3.20
	Bottom	0.41	0.82	1.09	0.69	1.52	3.82
0.2286	Top	2.44	2.18	2.83	0.98	1.56	2.8
	Middle	2.08	2.50	2.74	0.89	1.28	2.1
	Bottom	0.84	0.89	1.29	2.30	2.39	3.0

Table 36: Maximum Hole oversize (x 10^{-3} inch)

Type of Drill	Conventional			Diametral		
speed rpm / Feed mm/rev	345	490	690	345	490	690
.0762	1.79	2.25	3.33	0.67	0.71	1.56
.1524	2.35	2.44	3.68	0.69	1.52	3.82
.2286	2.44	2.50	2.83	2.30	2.39	3.00

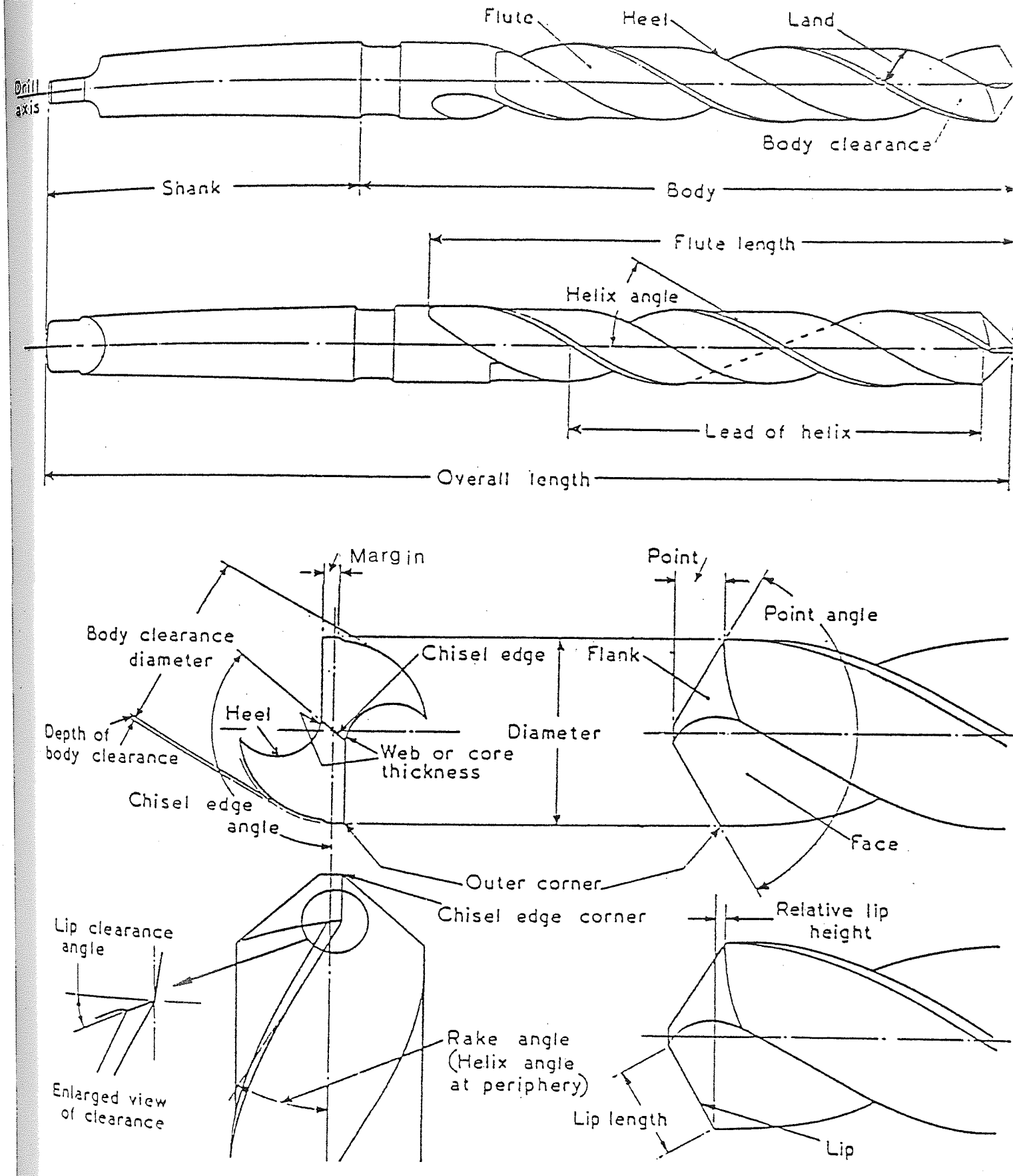

Fig. 1 Twist drill

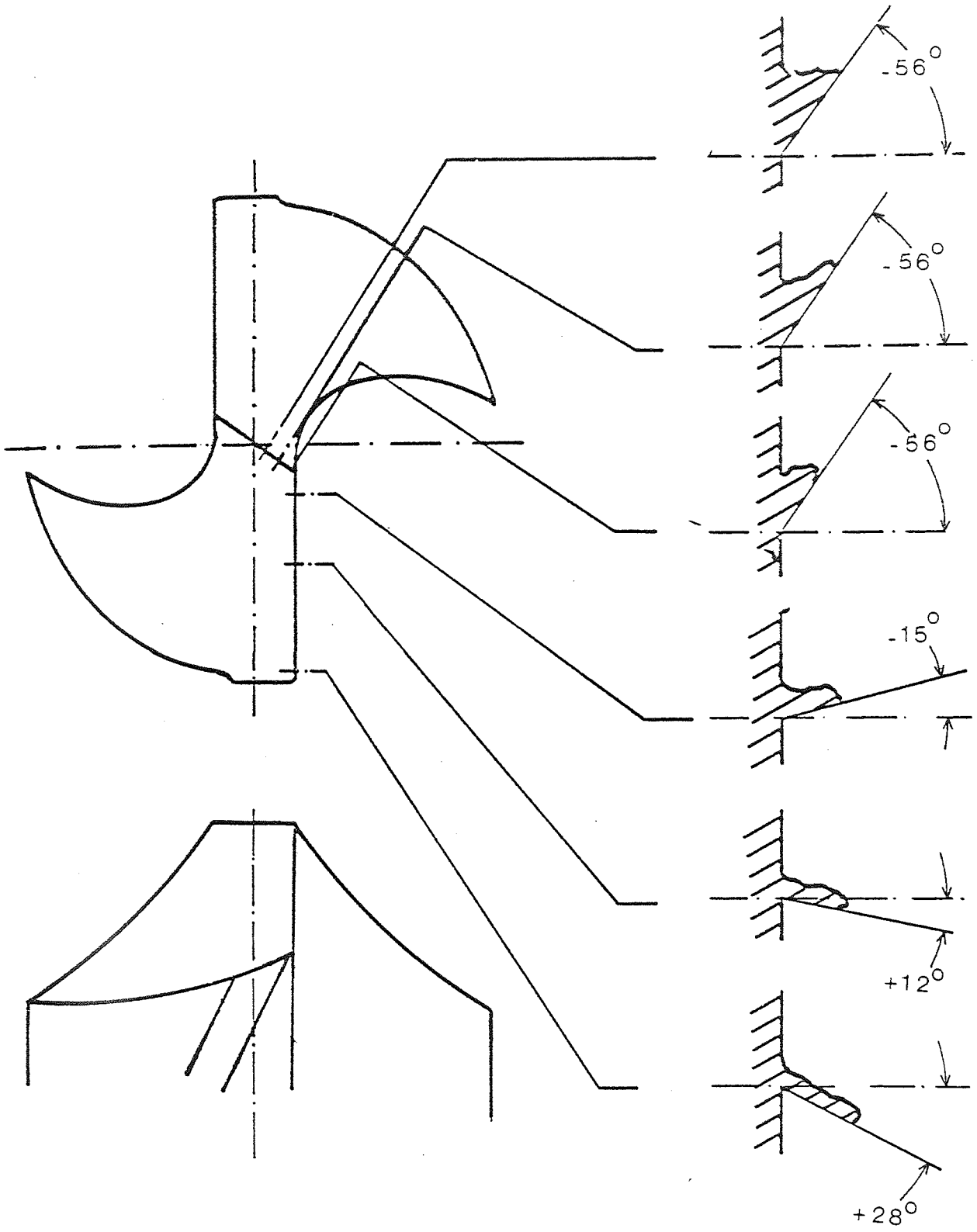

Fig 2 Rake angle variation along the cutting edge (conventional drill)

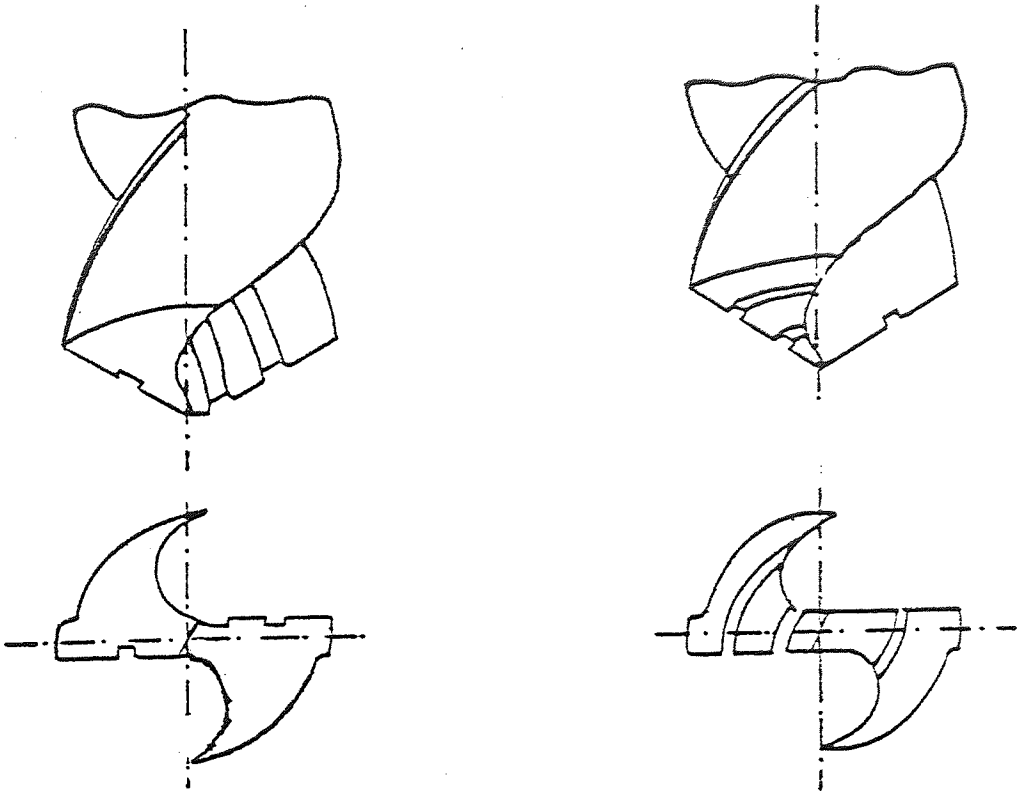

(a) On the face (b) On the flank

Fig 3 Chipbreaker grooves

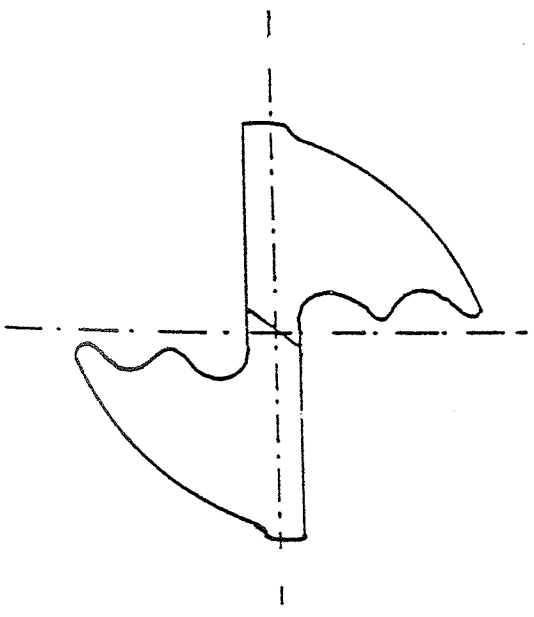

Fig 4 Chipbreaker rib

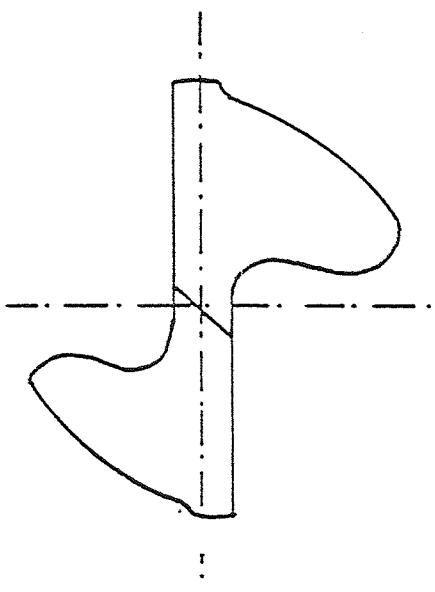

Fig 5 Radiused chipbreaker

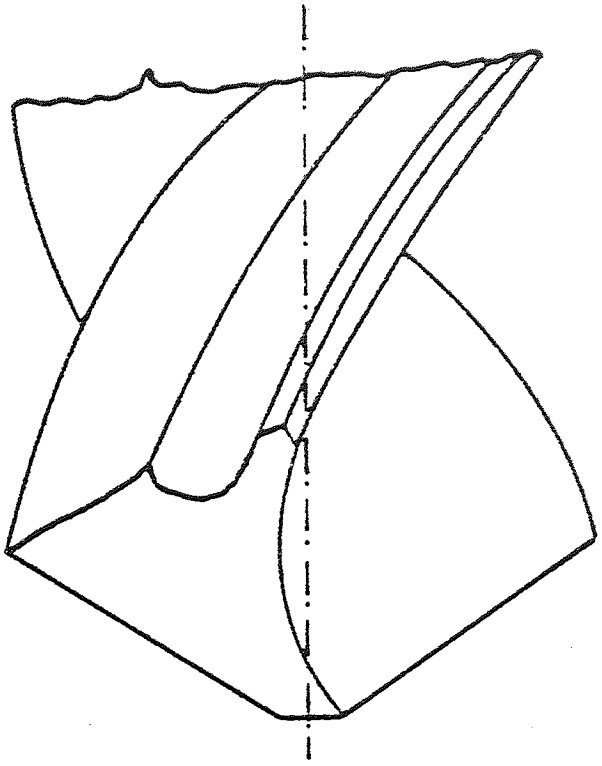

Fig 6 Double margin drill

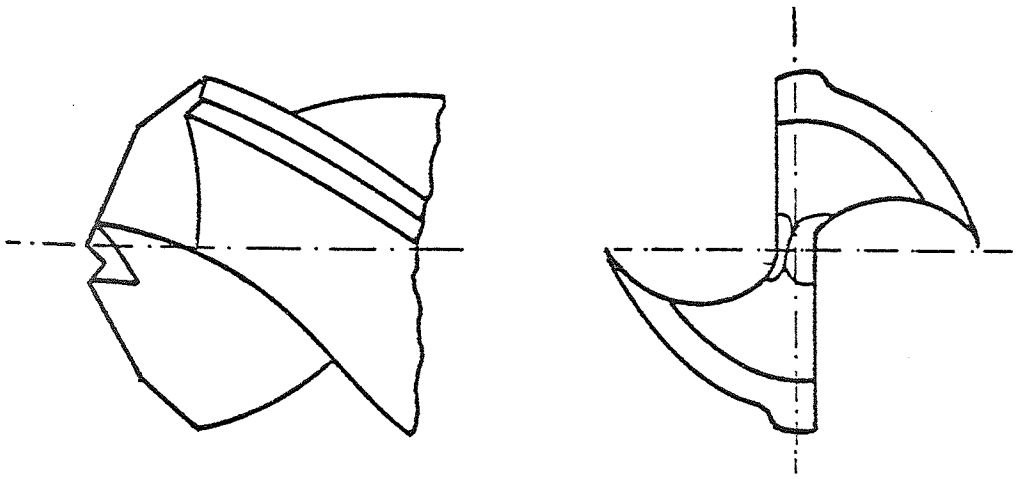

Fig 7 Zhirov point drill

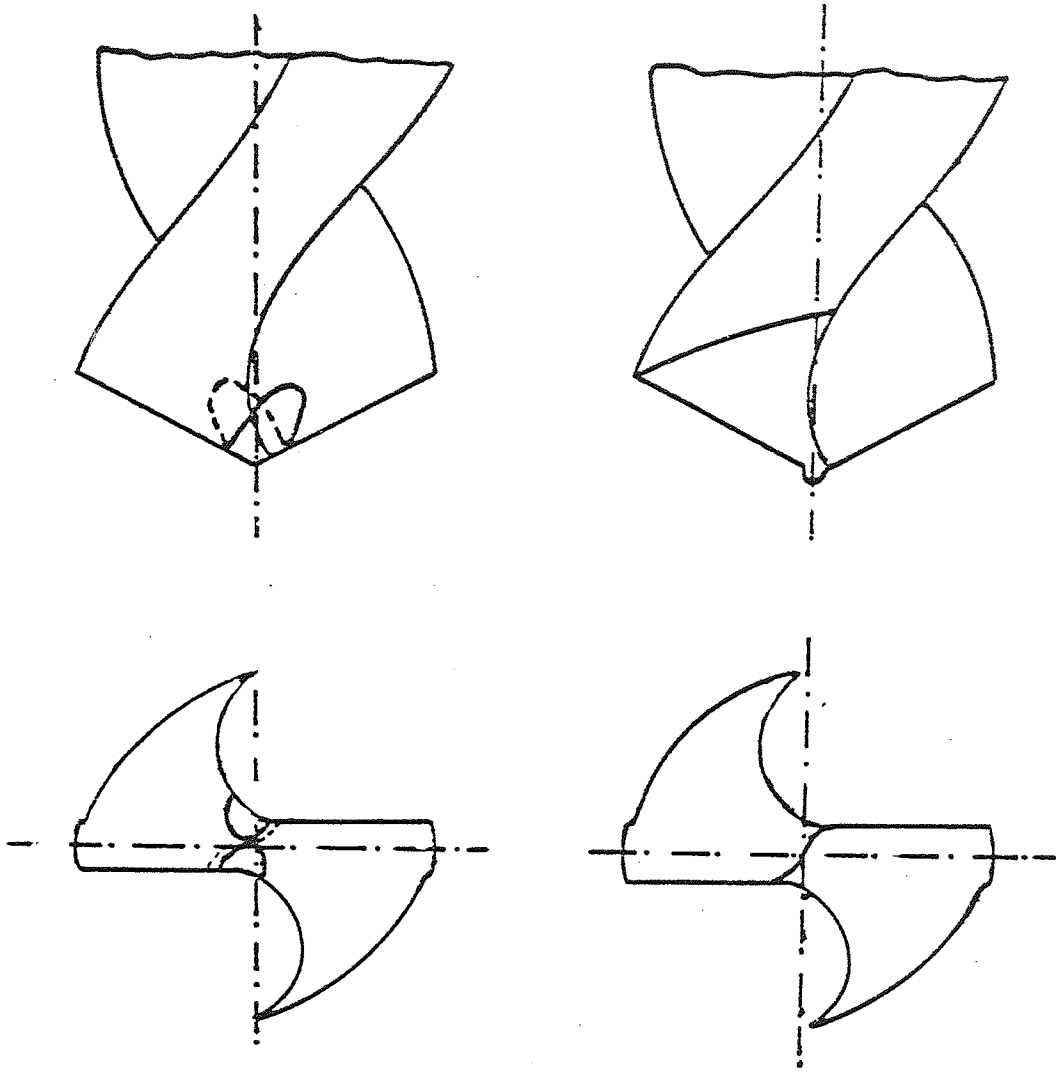

Fig 8 Thinned web Fig 9 Spiral point drill

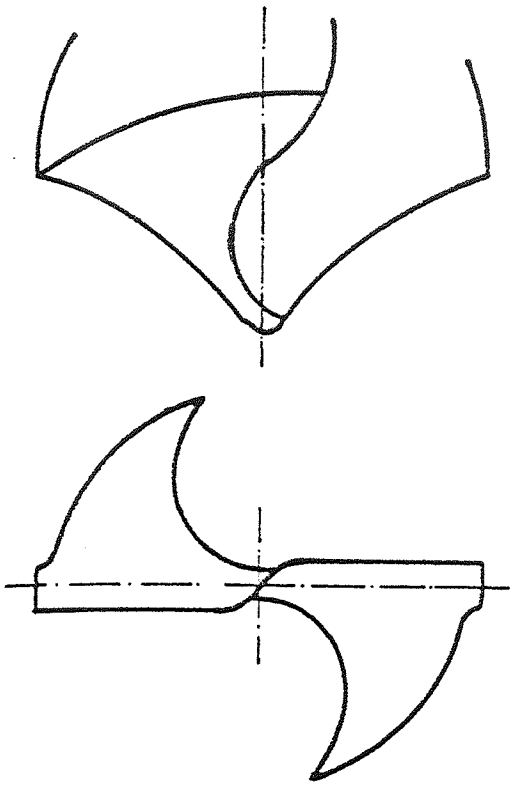

Fig 10 Helical drill

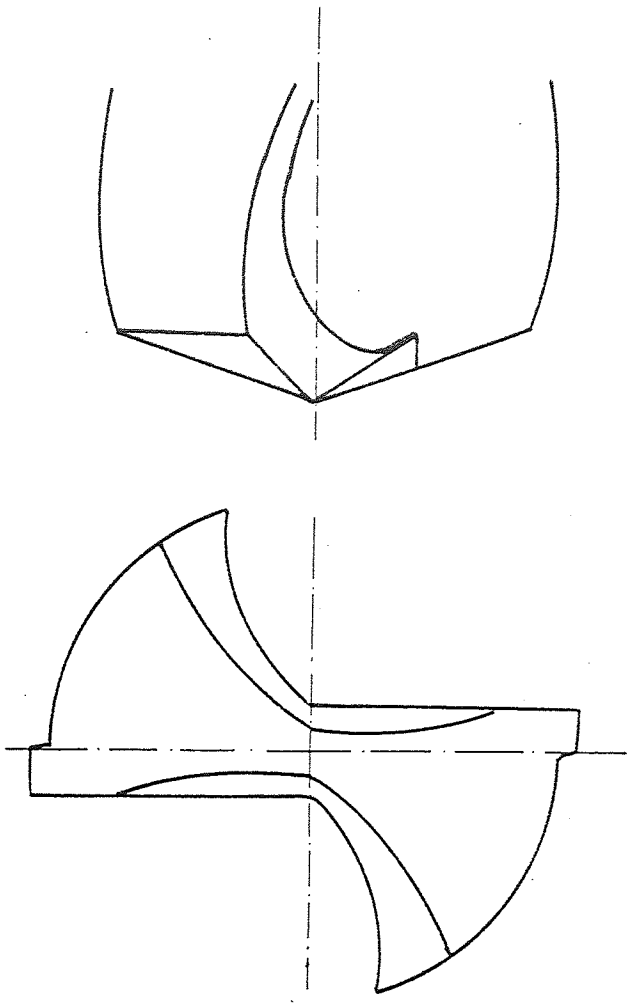

Fig 11 Split point drill

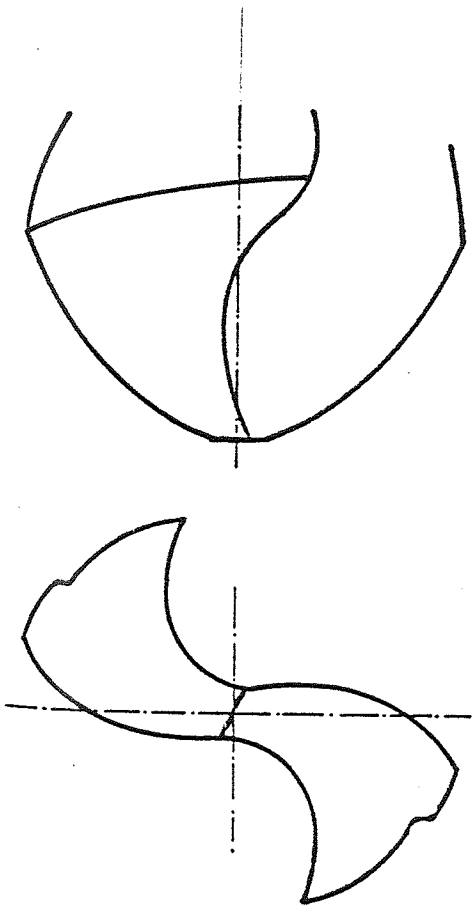

Fig 12 Racon drill

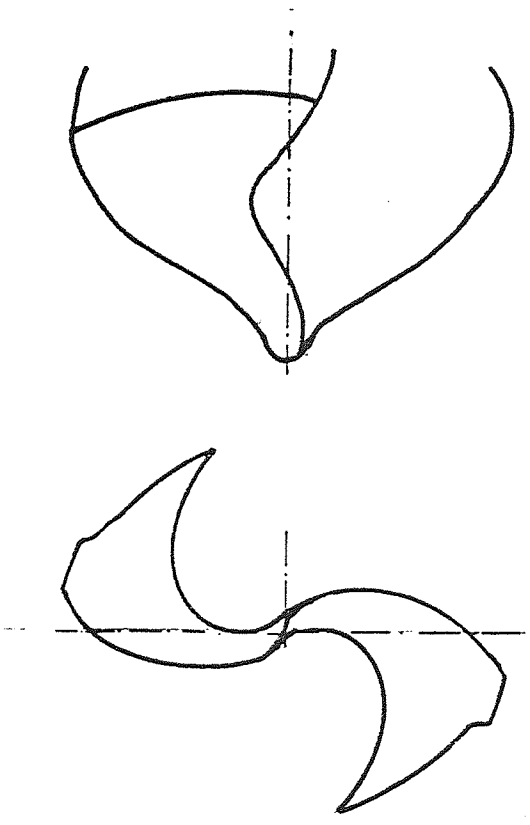

Fig 13 Helicon drill

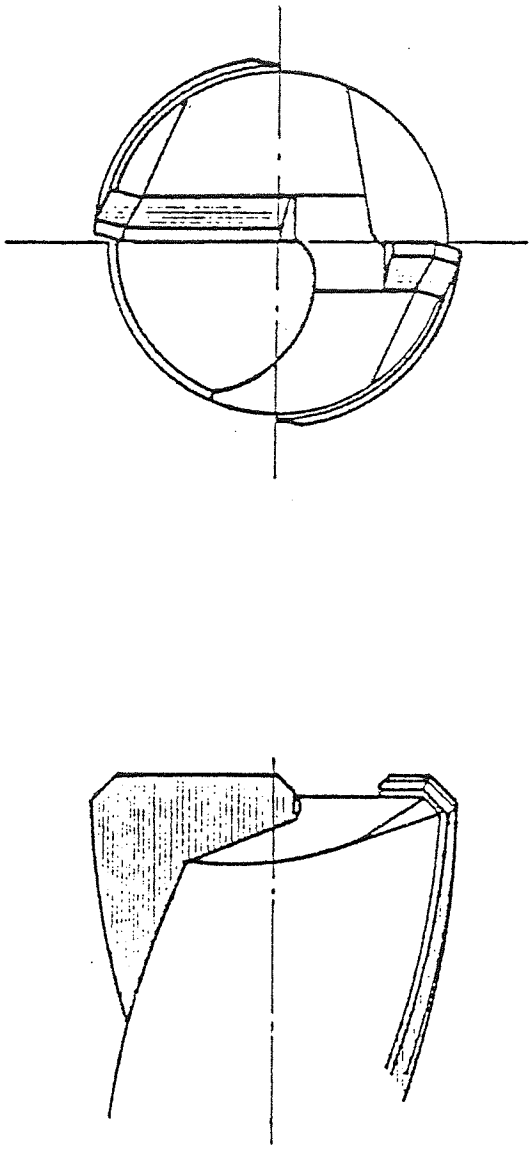

Fig 14 Drill configuration by drill manufacturer

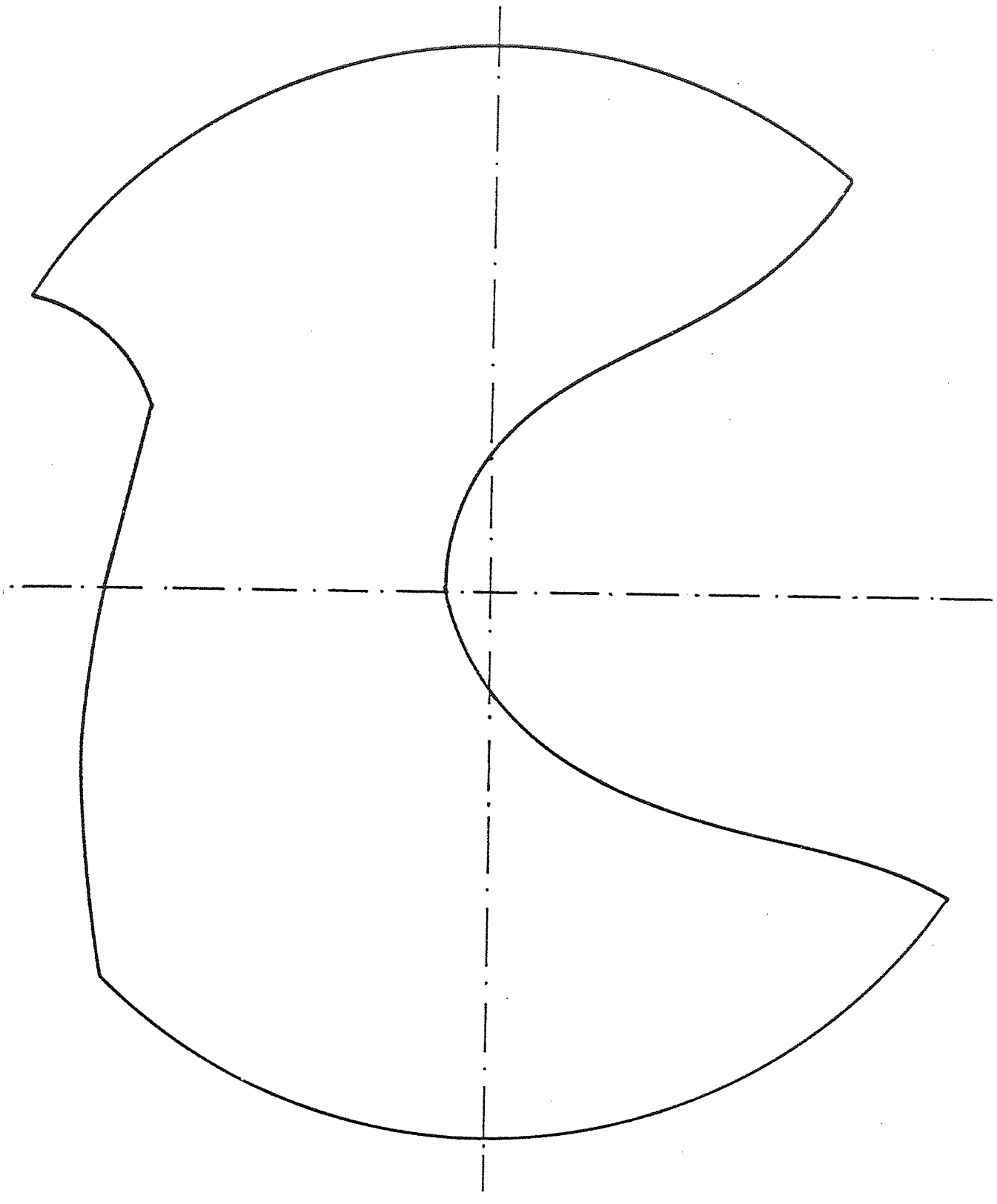

Fig 15 Transverse section through flute

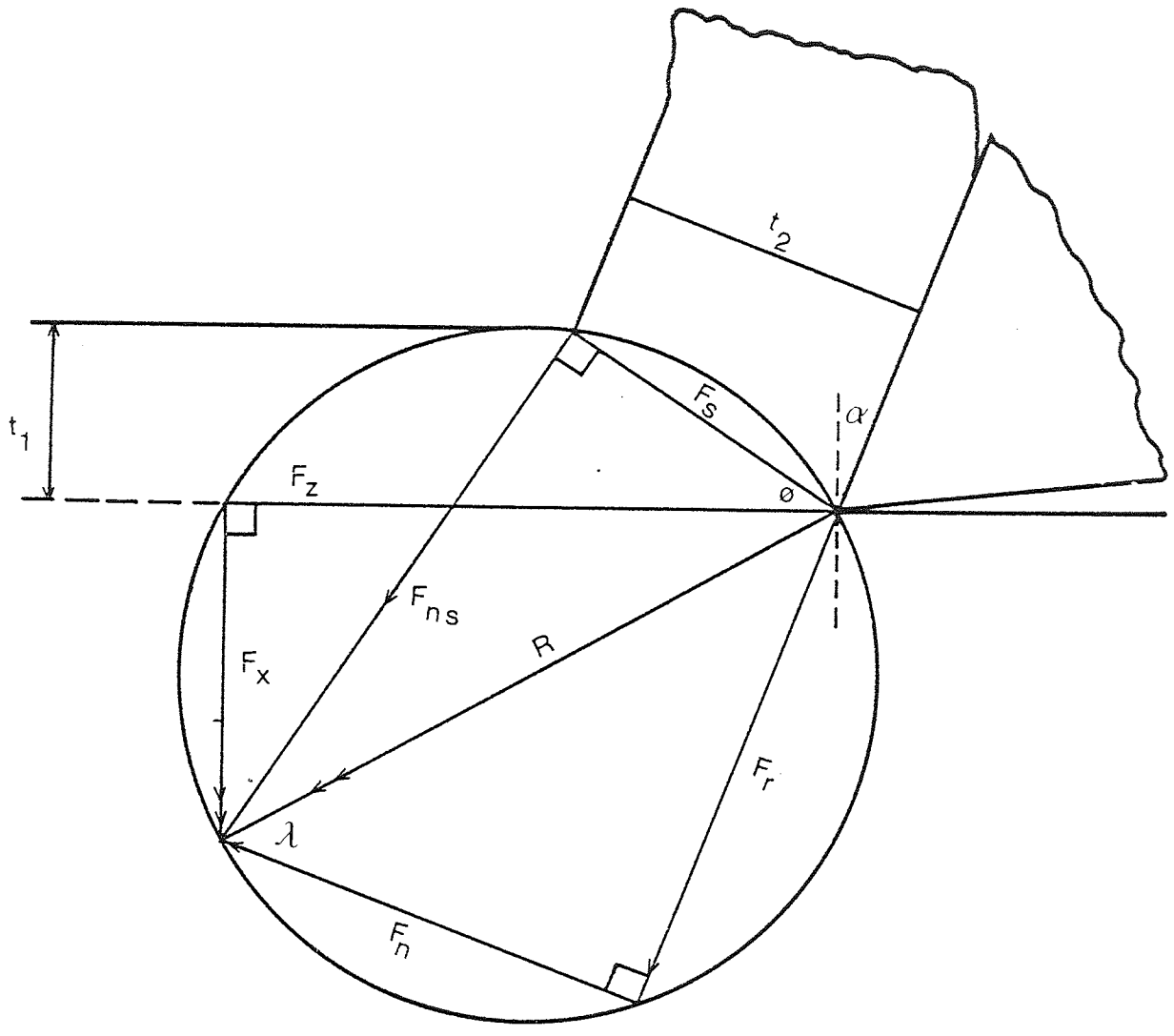

Fig 16 System of forces on orthogonal cutting

as proposed by

Oxley and Palmer

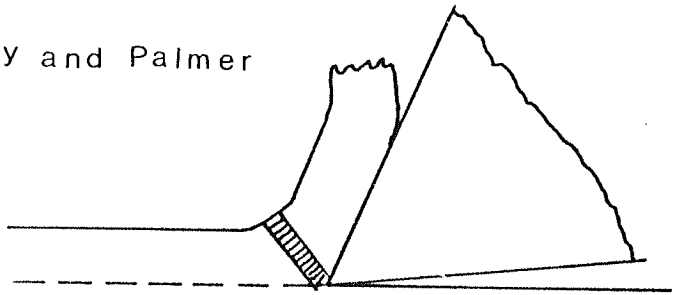

as proposed by

Okushima and

Hitomi

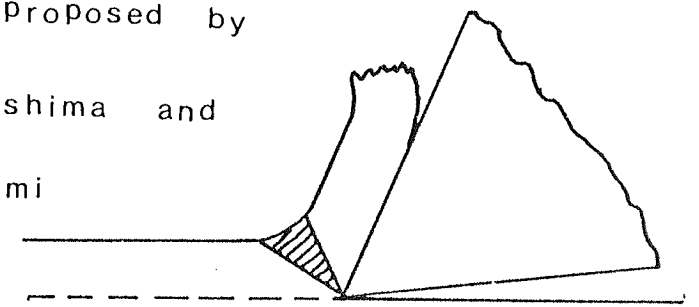

Fig 17 Thick shear zone models

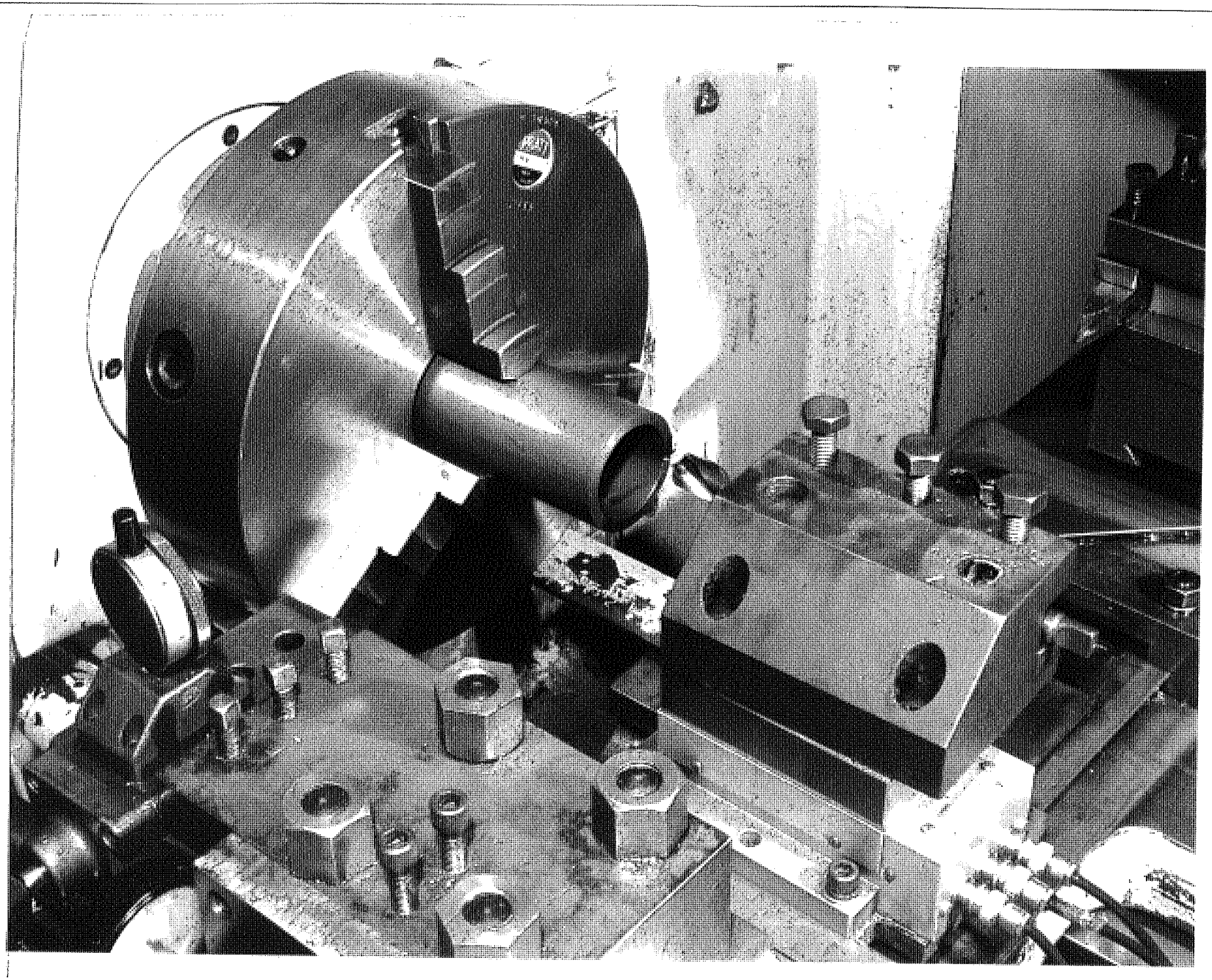

Fig 18 Turning set-up for the prediction of the basic cutting data

Drill Configuration as received

(Manufacturer Configuration)

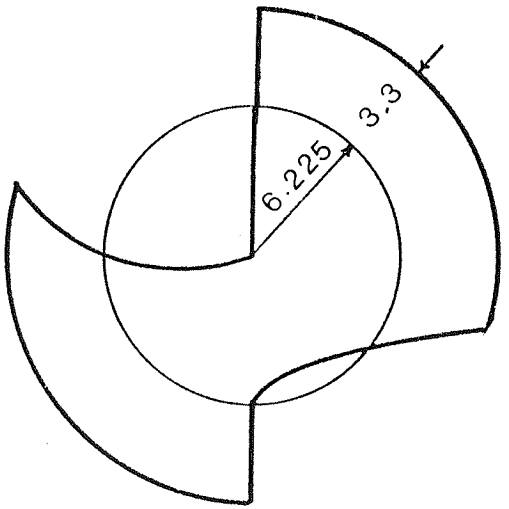

Optimum Modification

based on Force balance
(annular portion left)

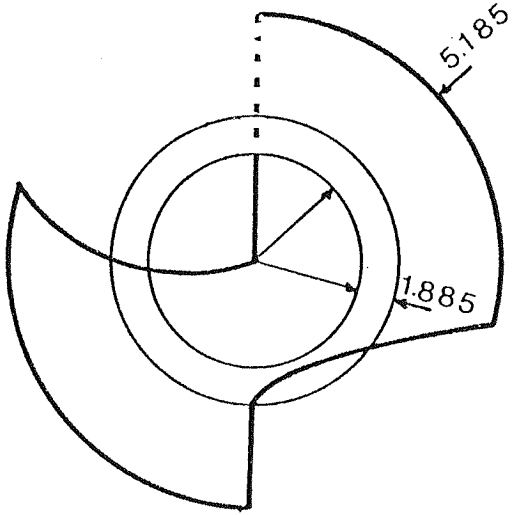

Partial Modification

Due to the constraint of the existing lip lengths and the need for a web.

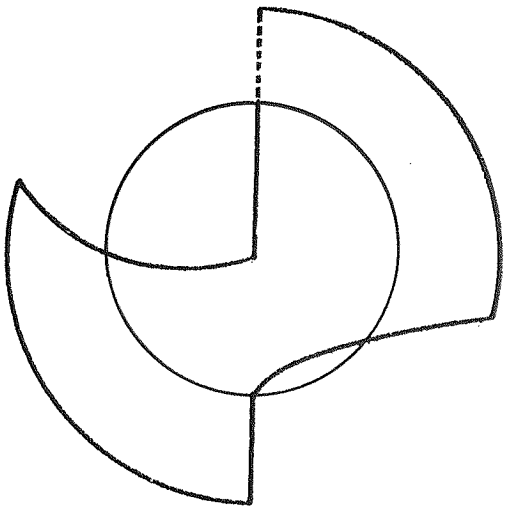

Fig 19 Cutting lips modifications for eliminating the rotary unbalance force

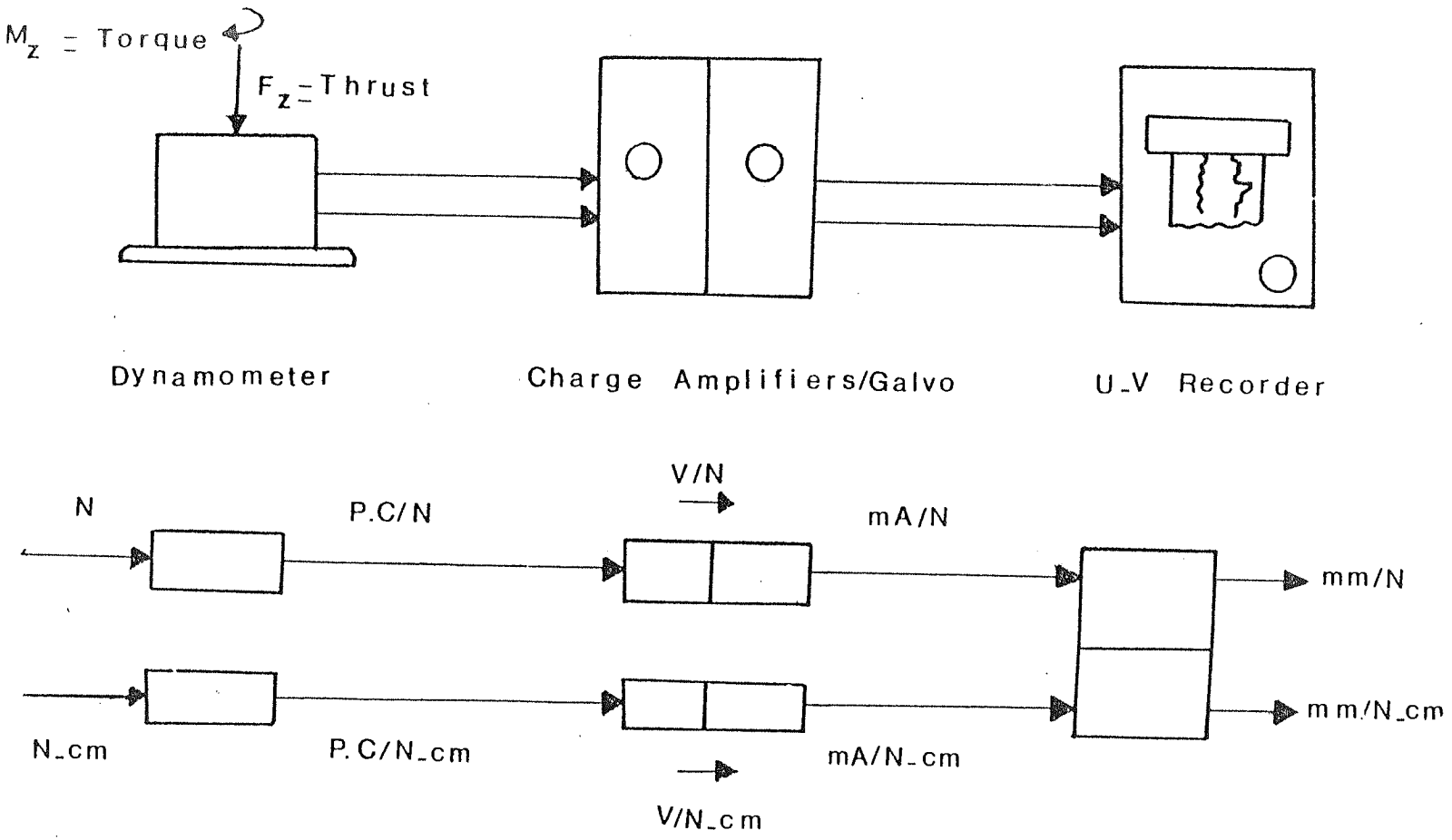

Fig 20 Force measurement recording set-up

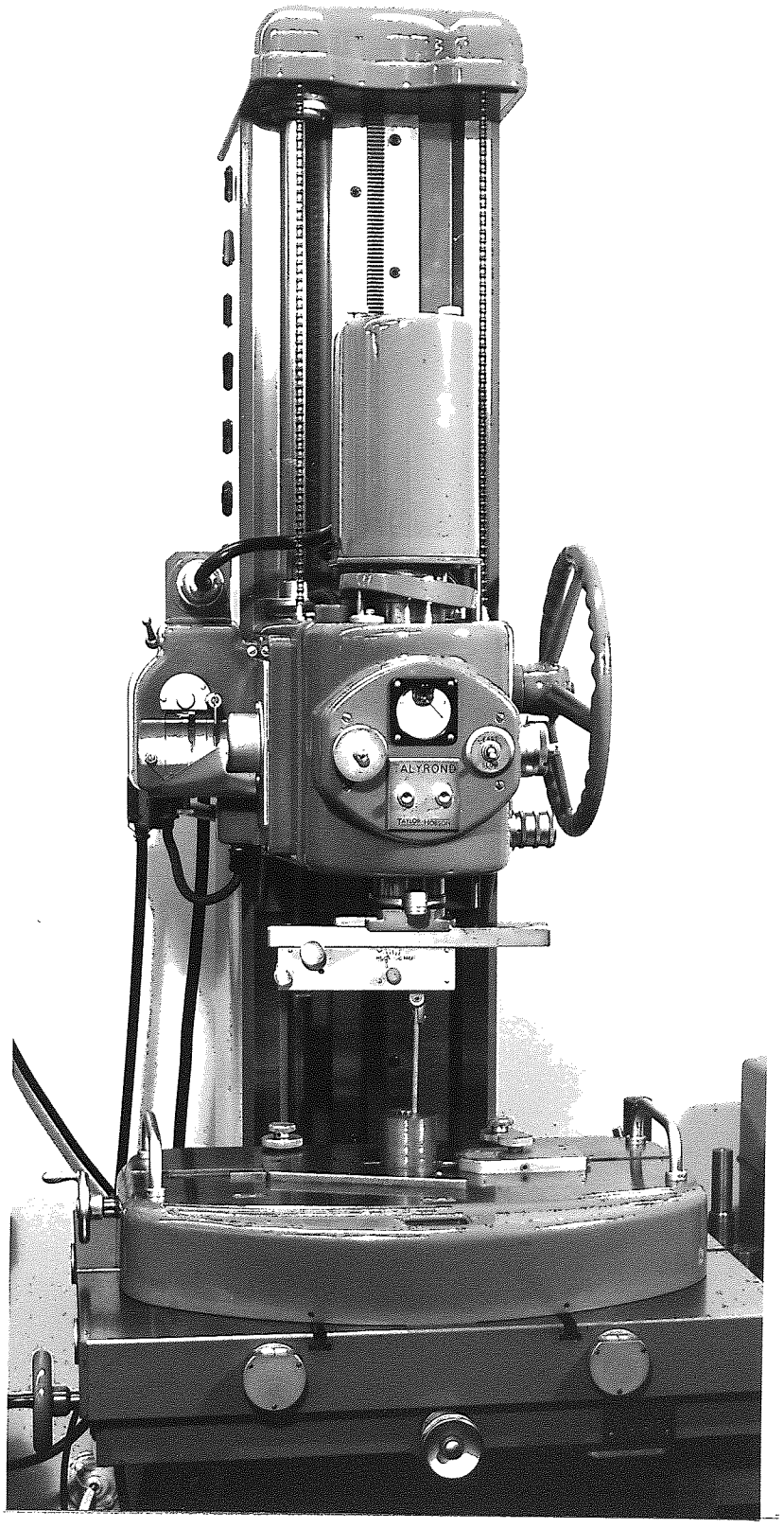

Fig 21 Roundness measurement (Talyrond)

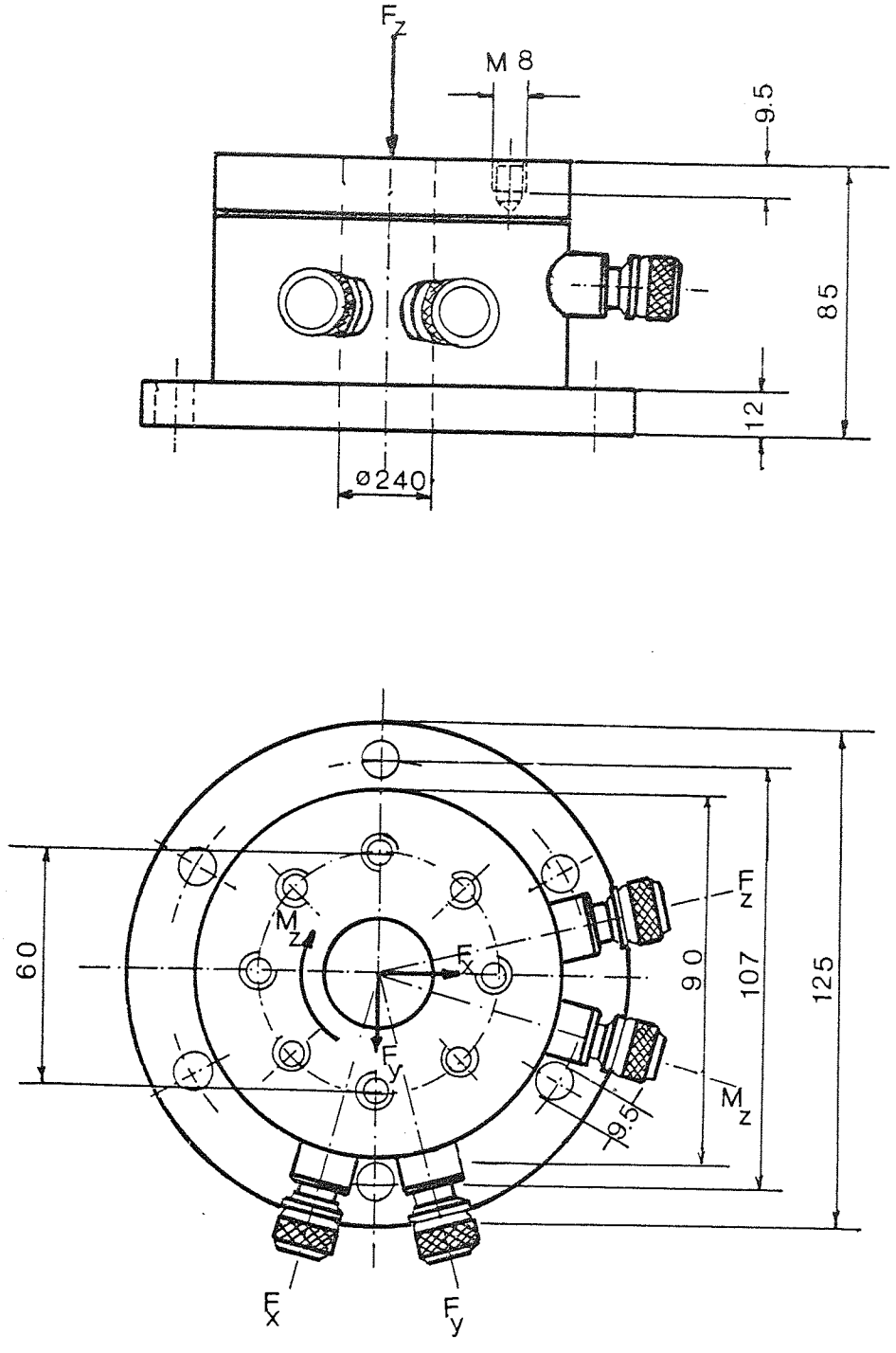

Fig 22 Drilling forces measurement (Dynamometer)

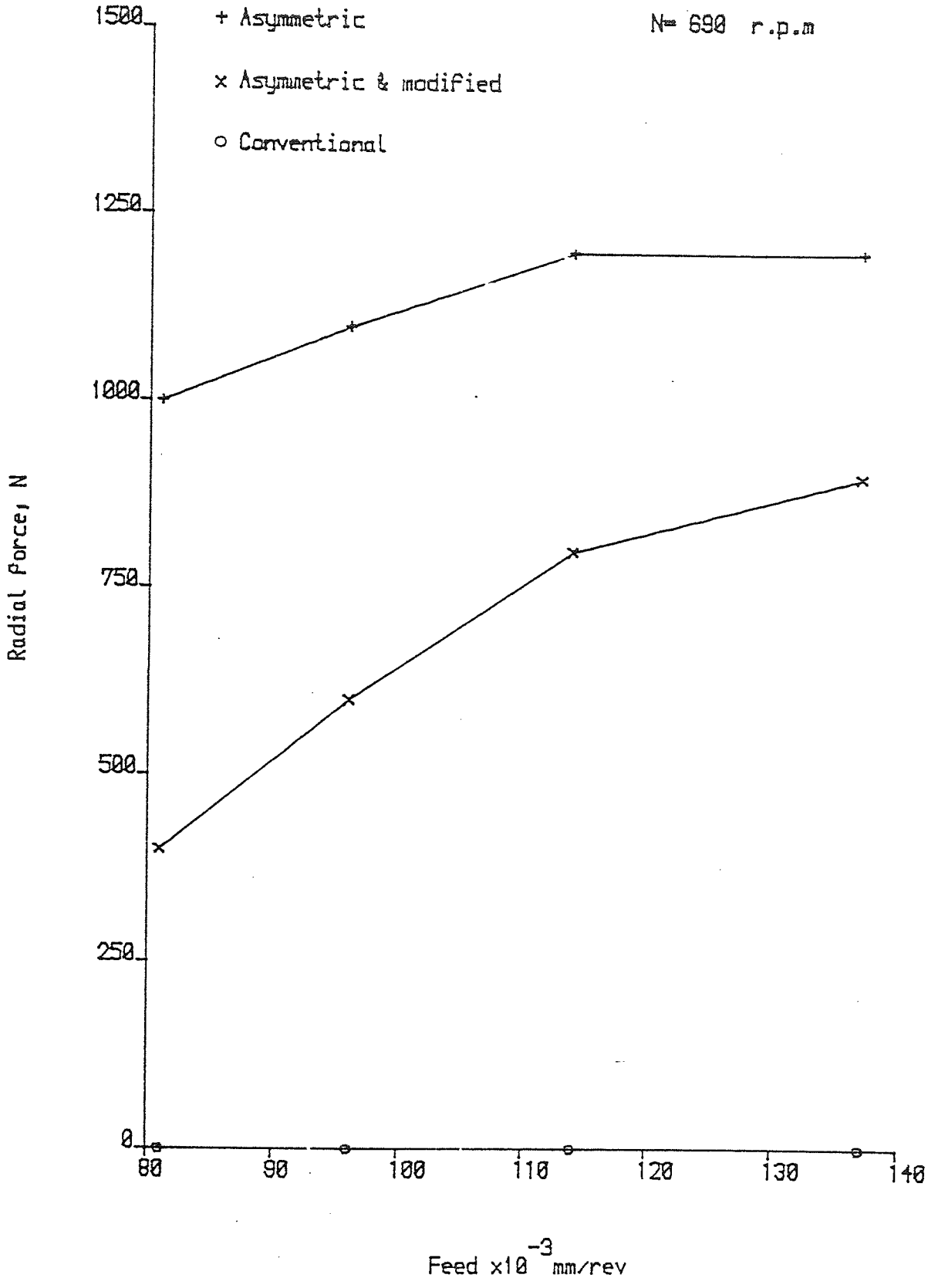

Figure 23 radial force comparison

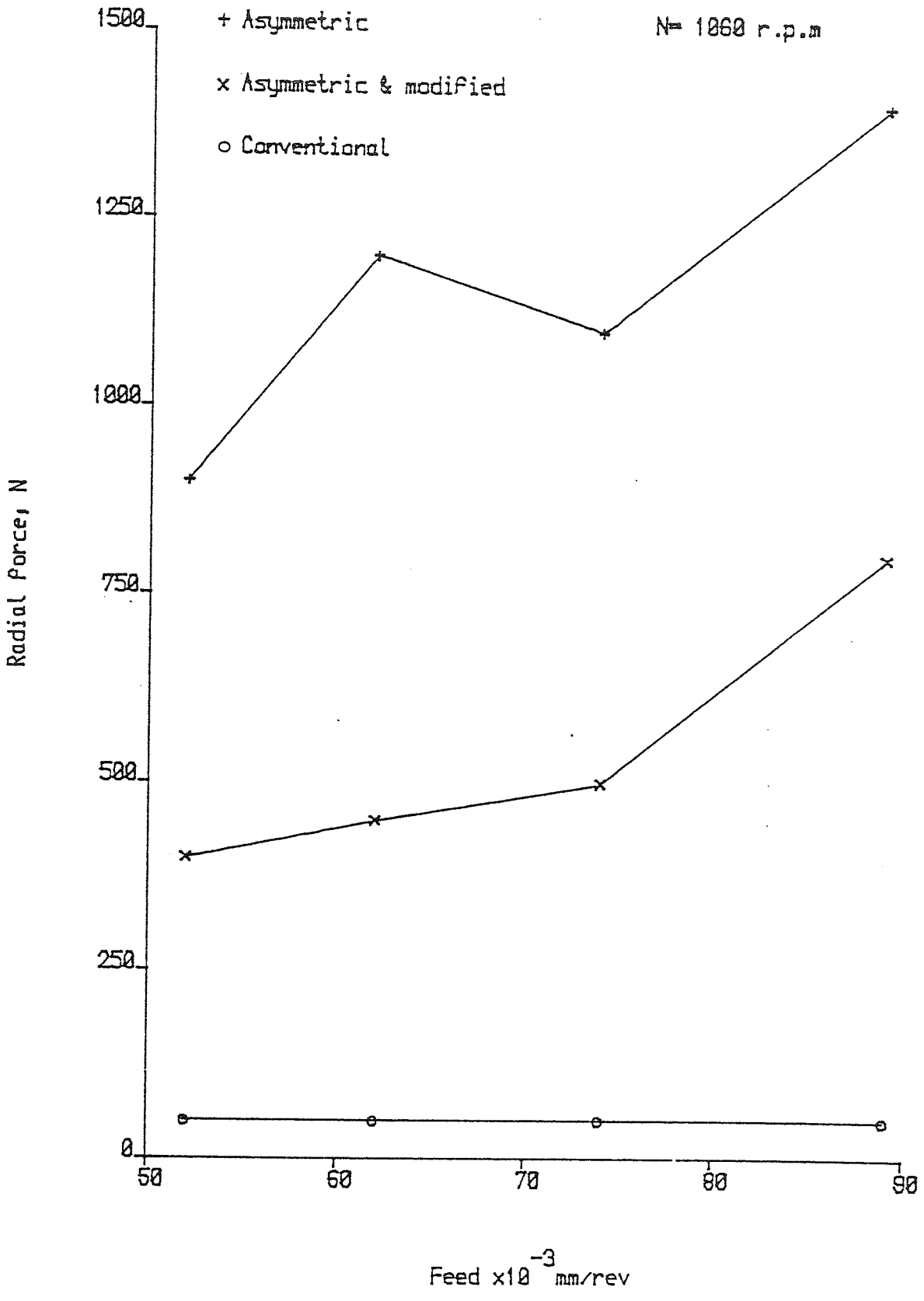

Figure 24 radial force comparison

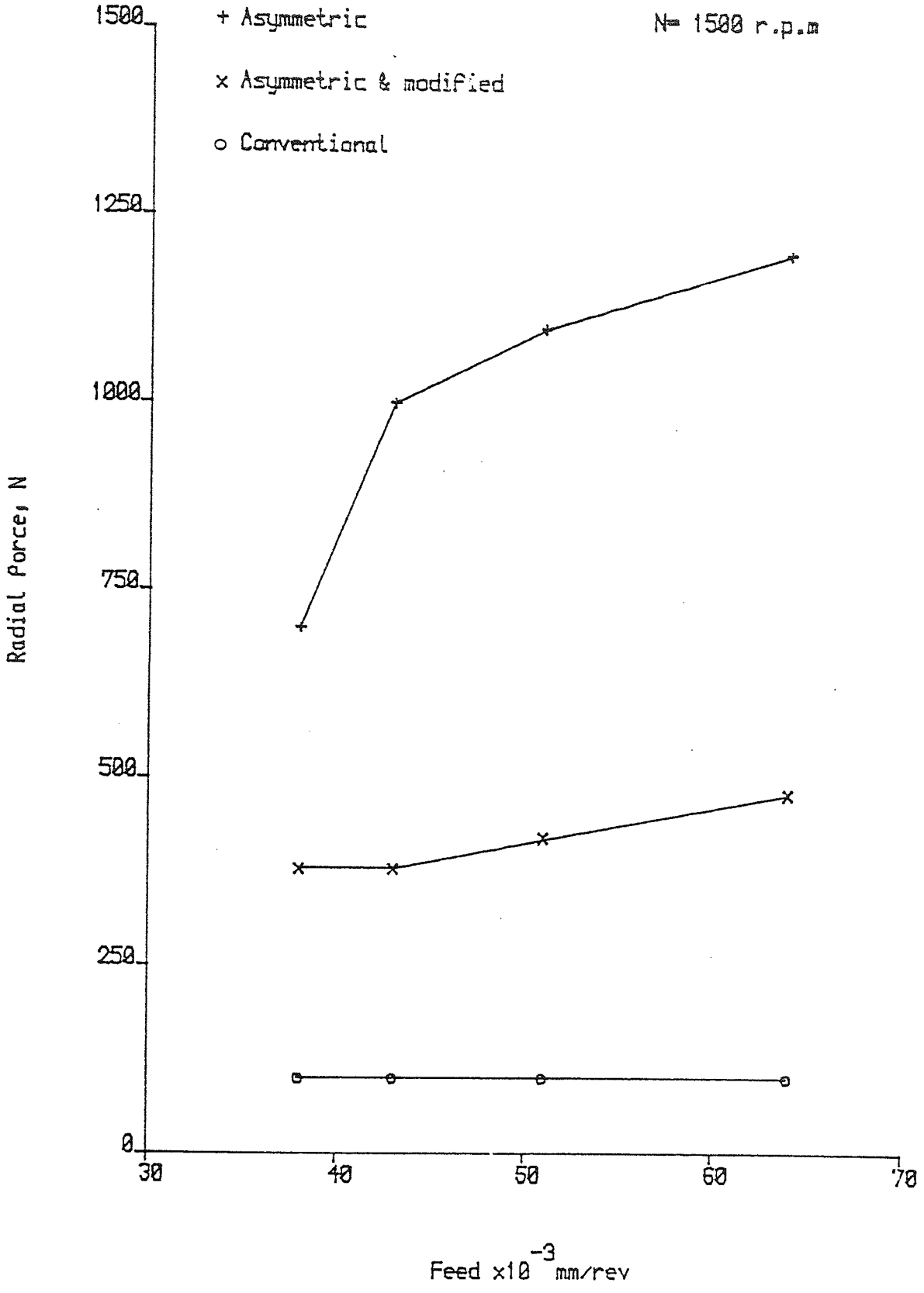

Figure 25 radial force comparison

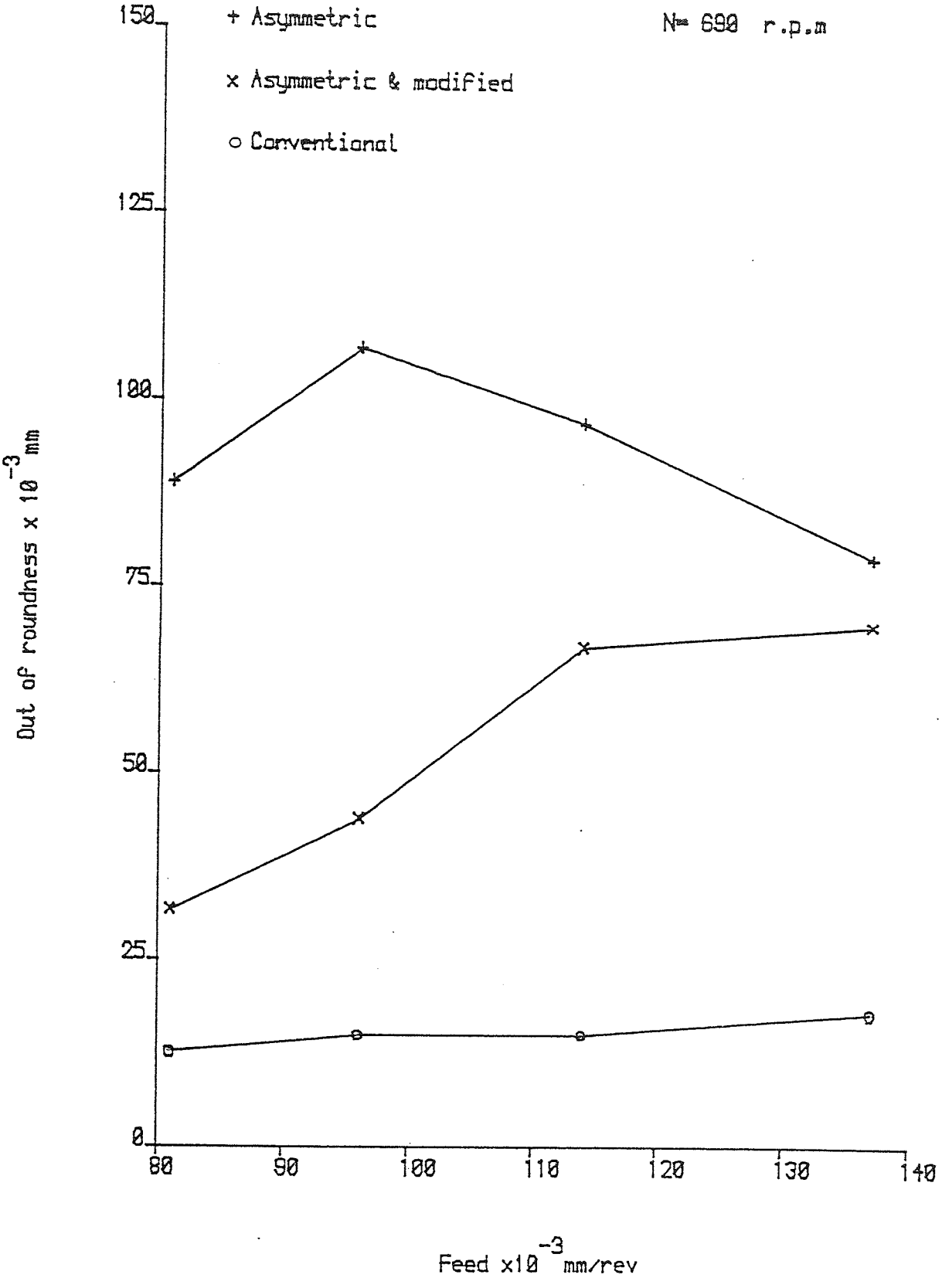

Figure 26 out of roundness comparison

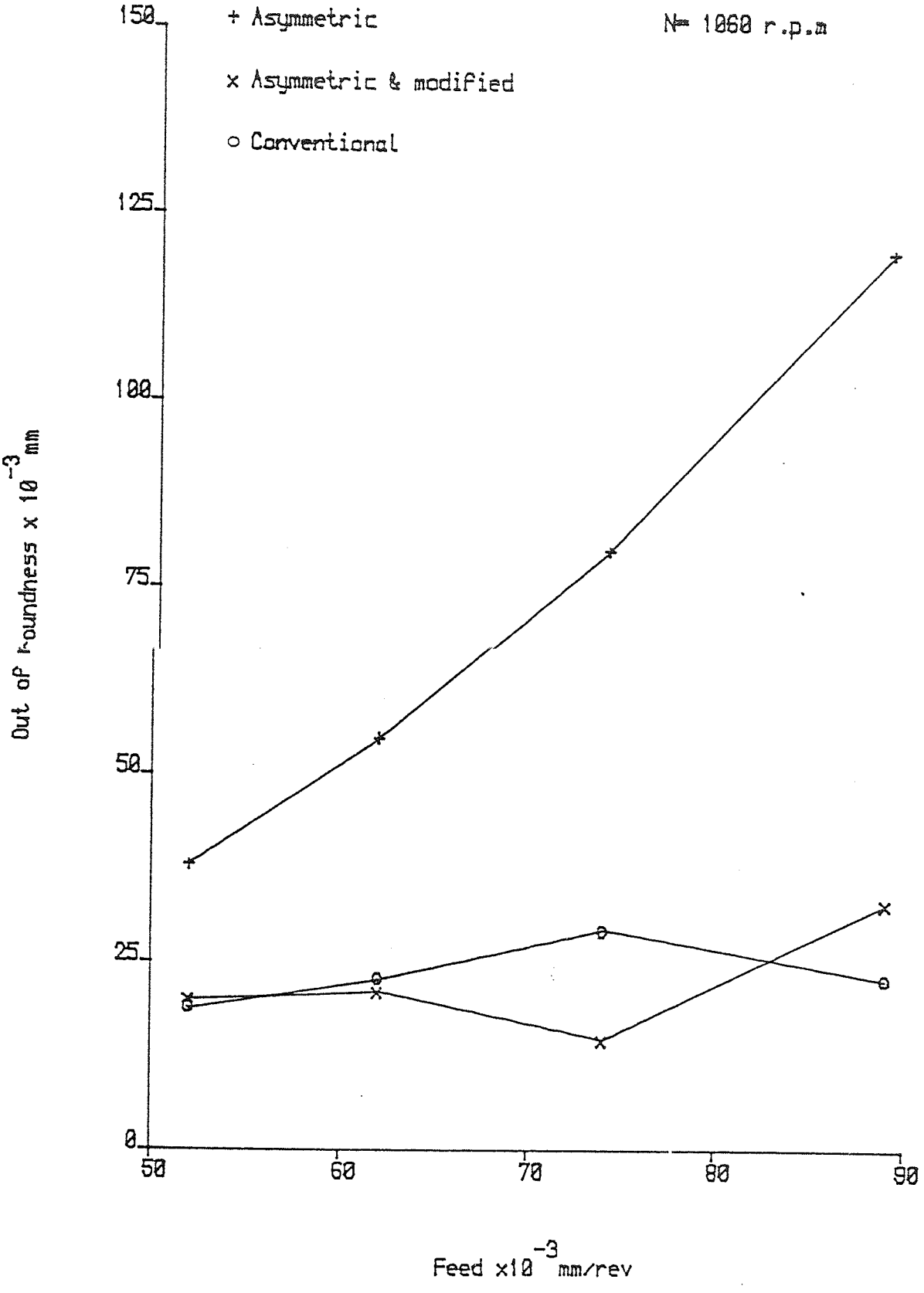

Figure 27 out of roundness comparison

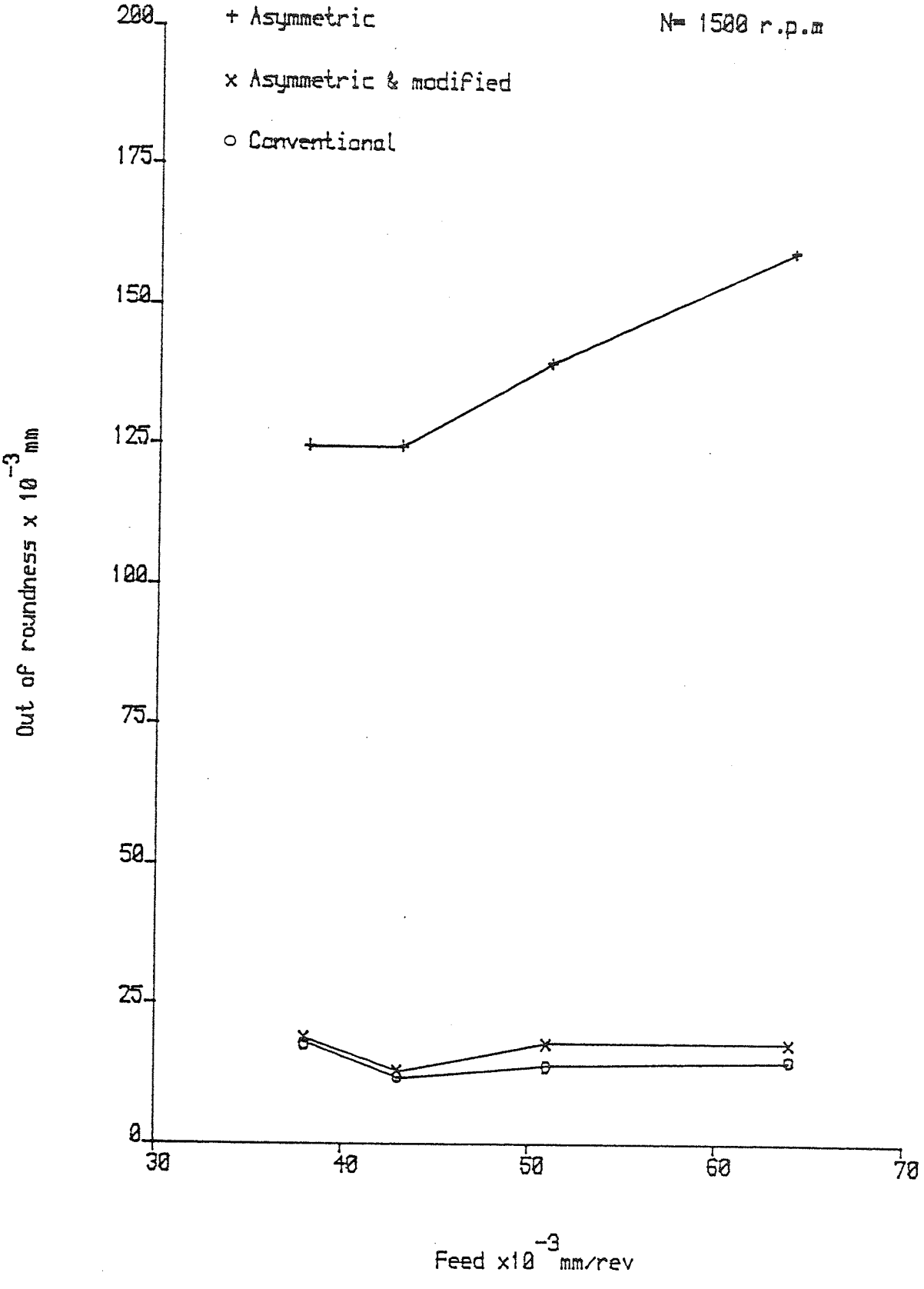

Figure 28 out of roundness comparison

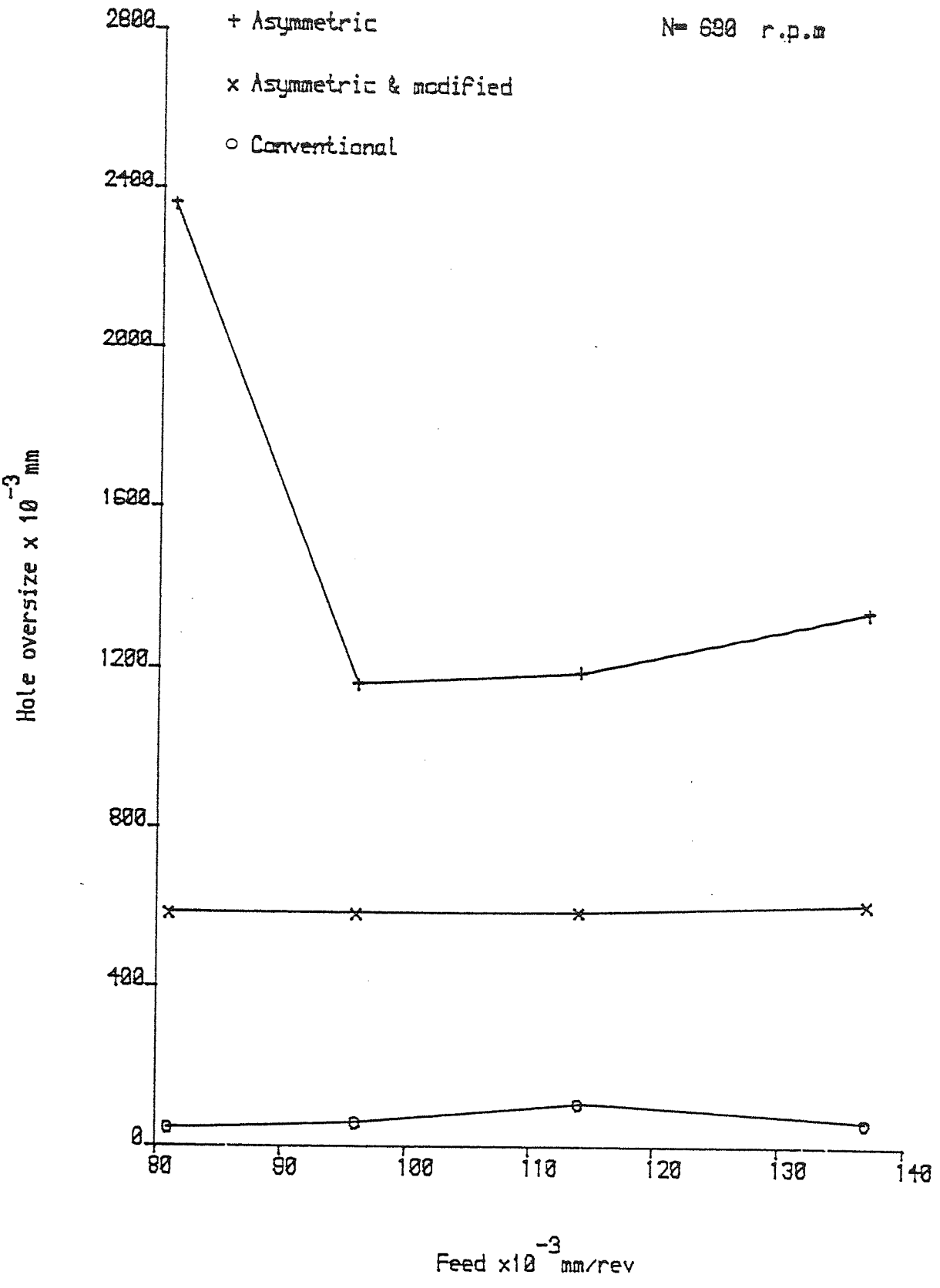

Figure 29 hole oversize comparison

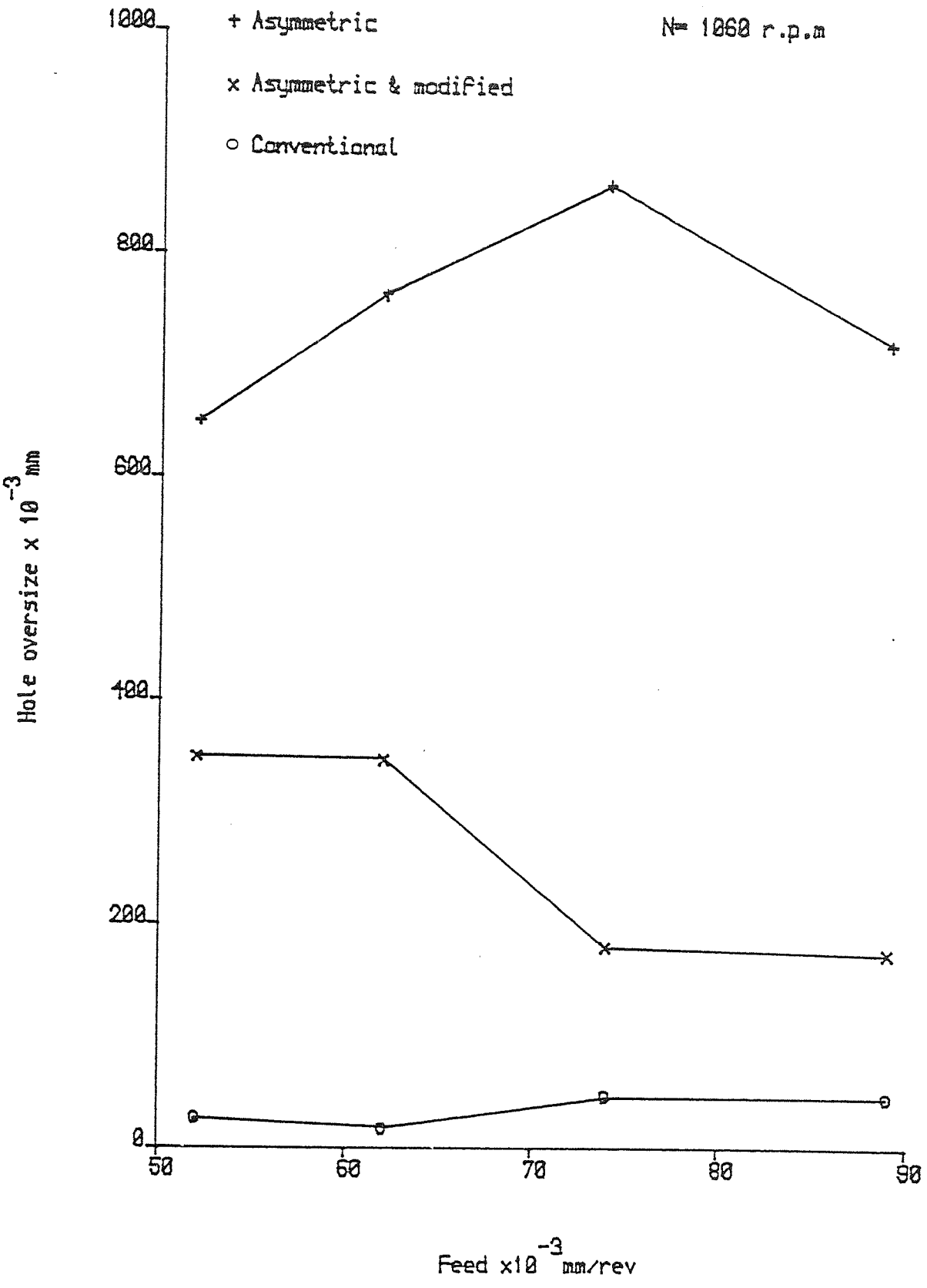

Figure 30 hole oversize comparison

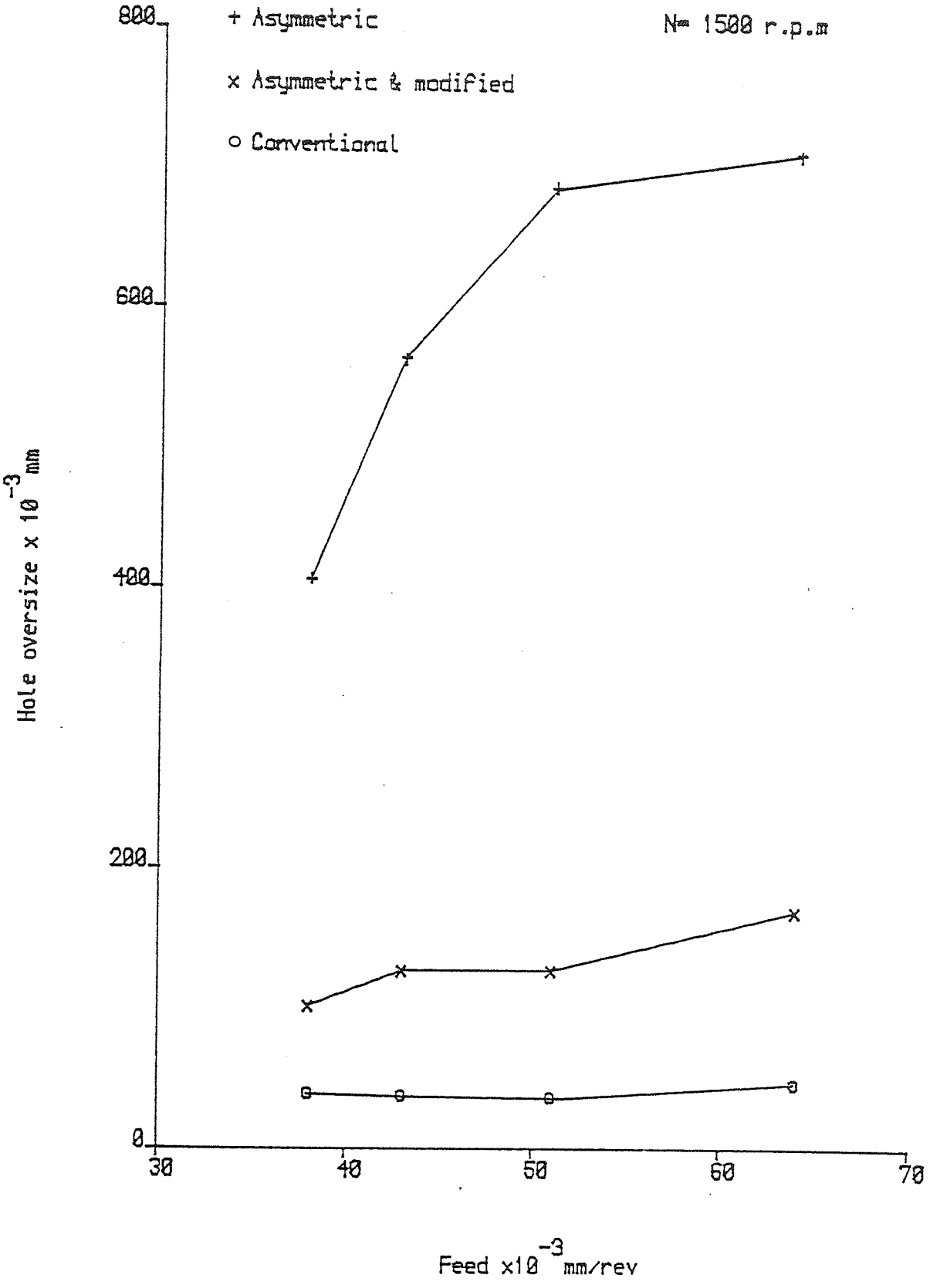

Figure 31 hole oversize comparison

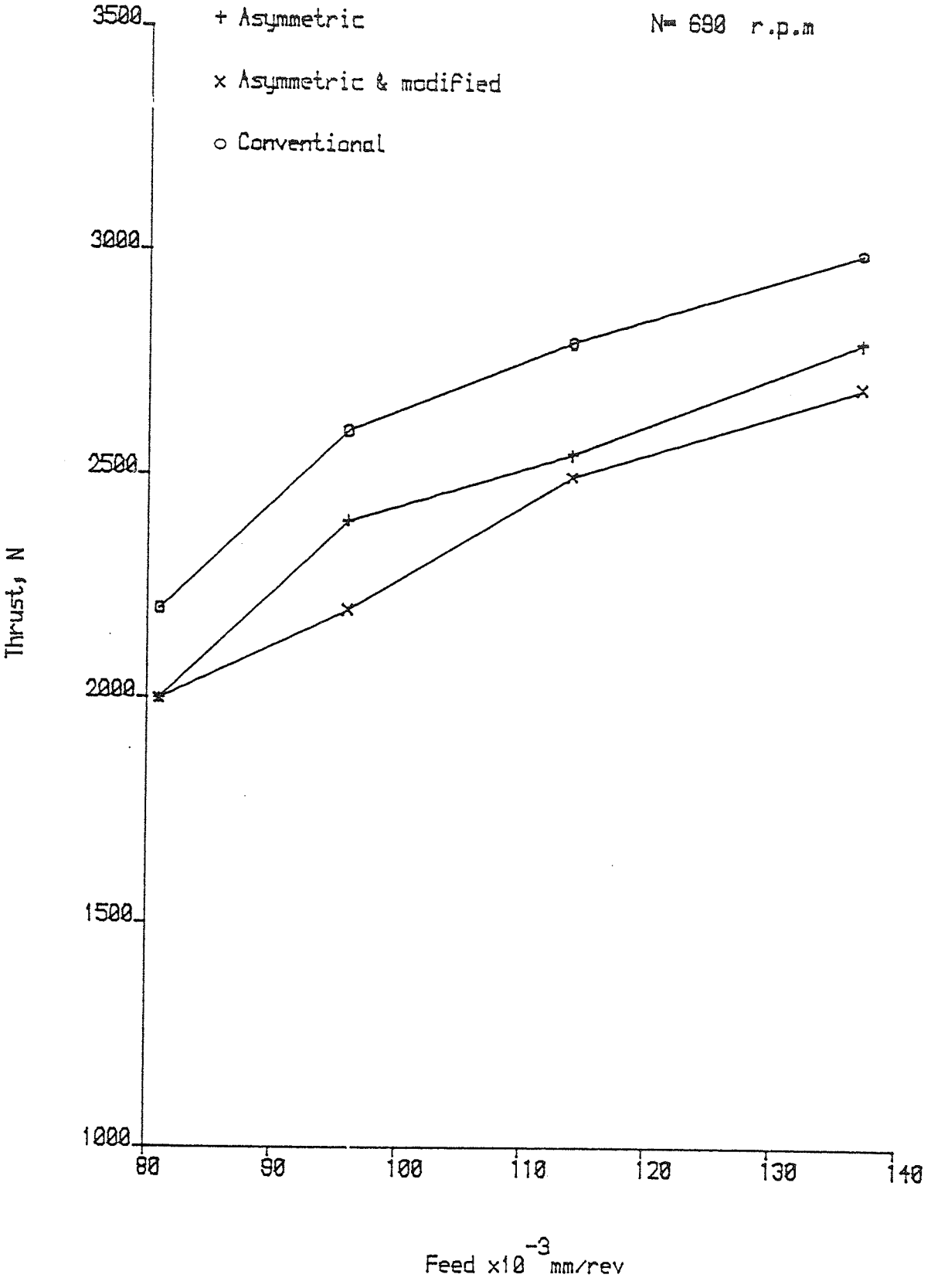

Figure 32 drilling thrust comparison

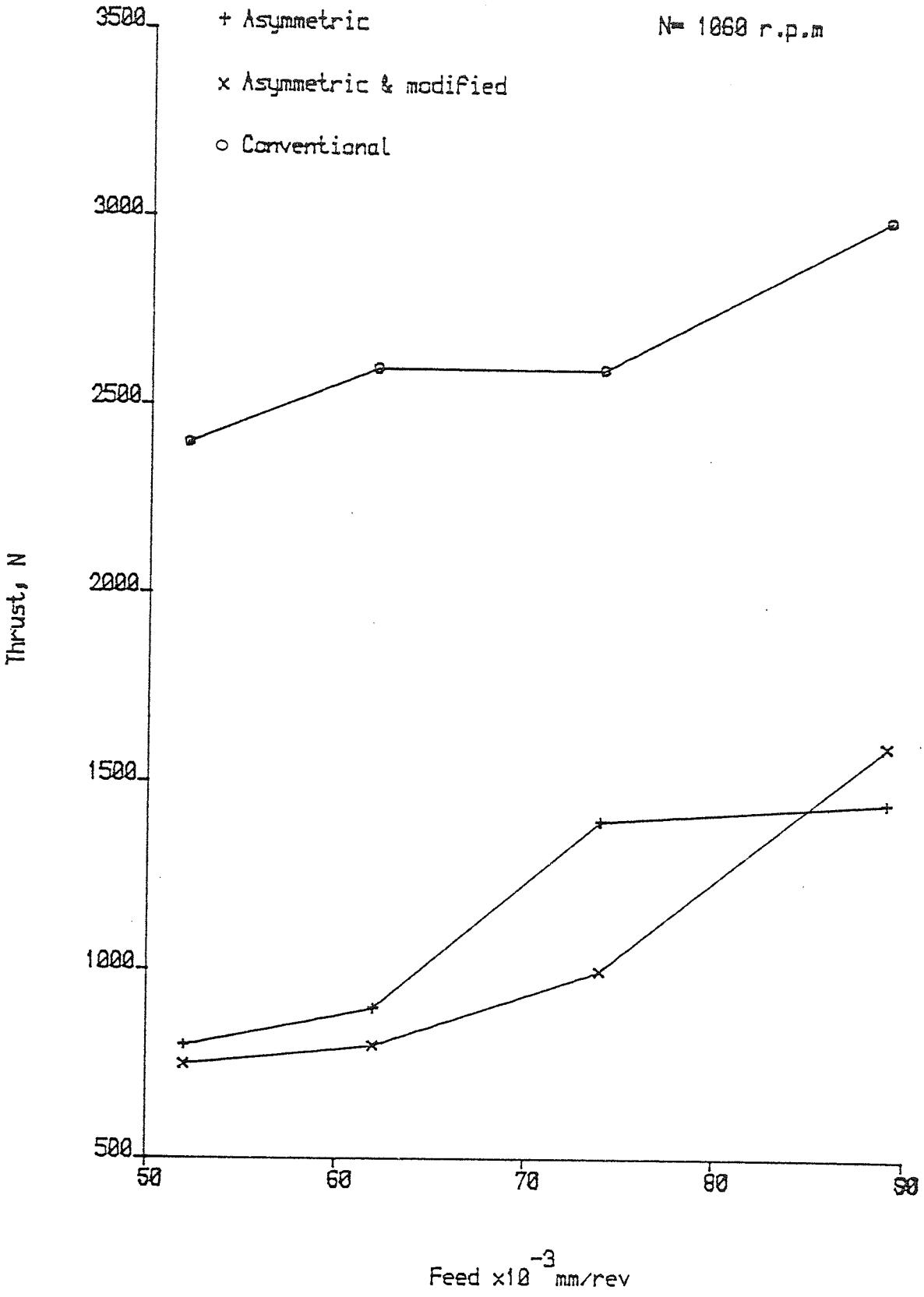

Figure 33 drilling thrust comparison

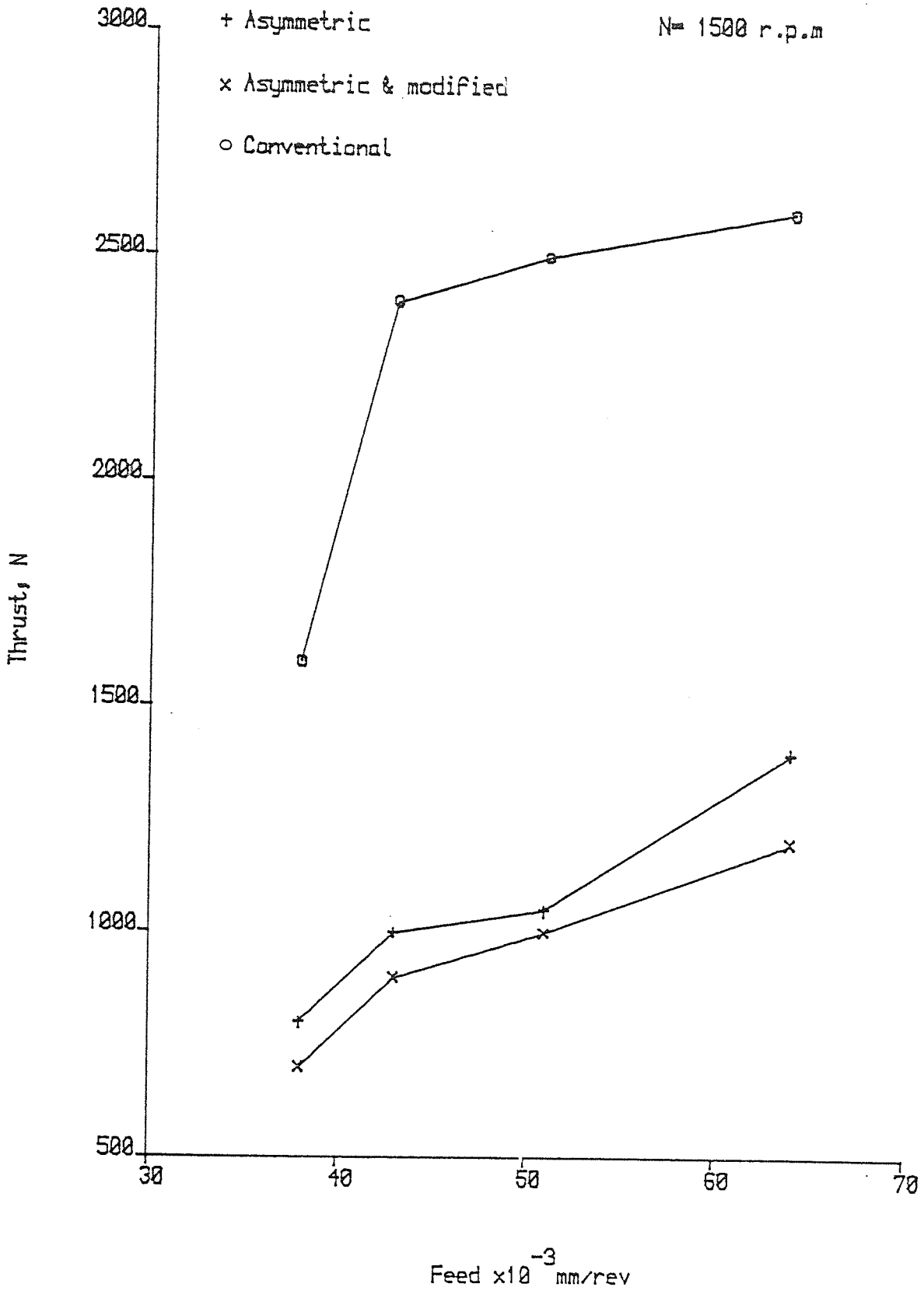

Figure 34 drilling thrust comparison

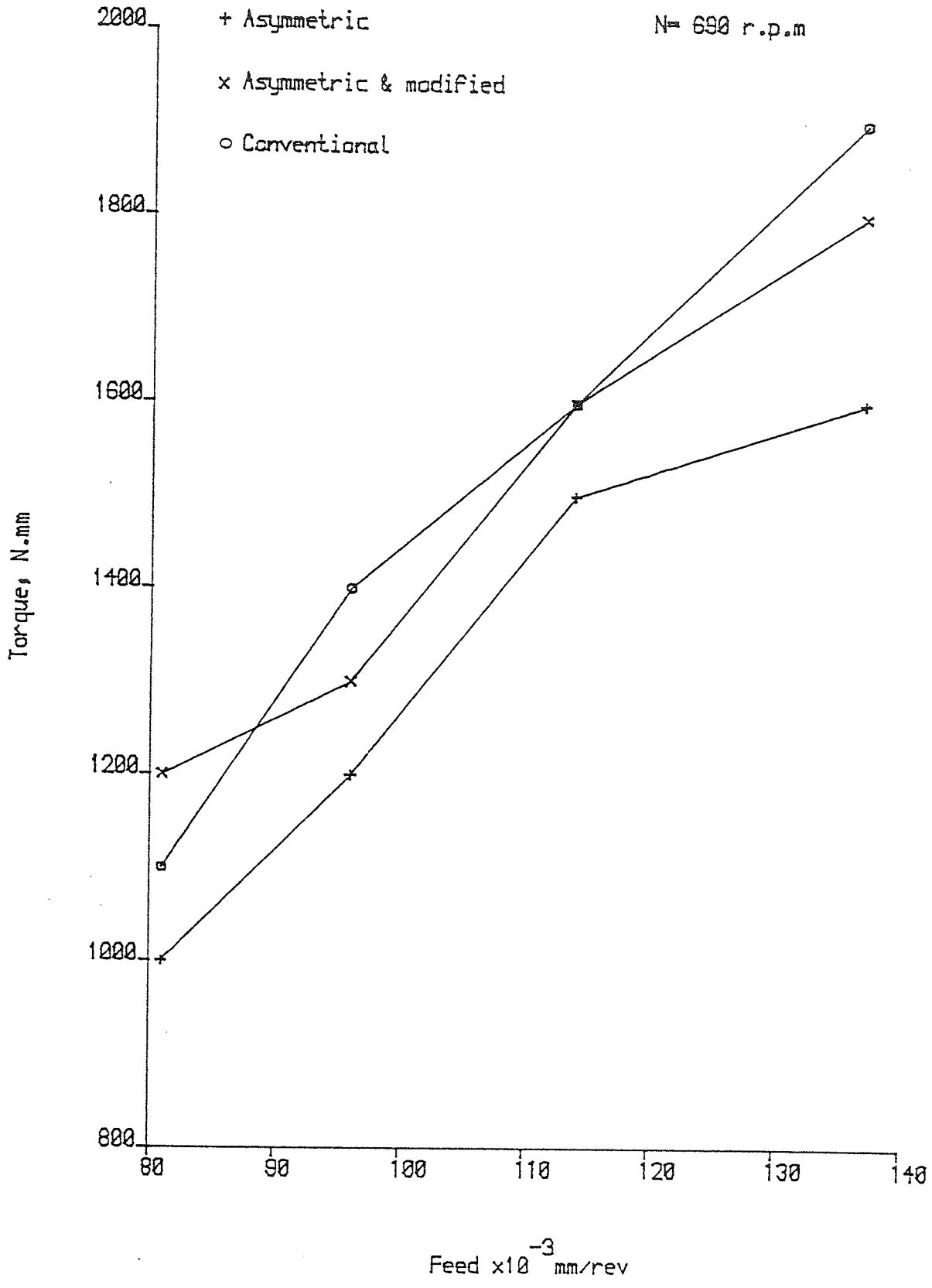

Figure 35 drilling torque comparison

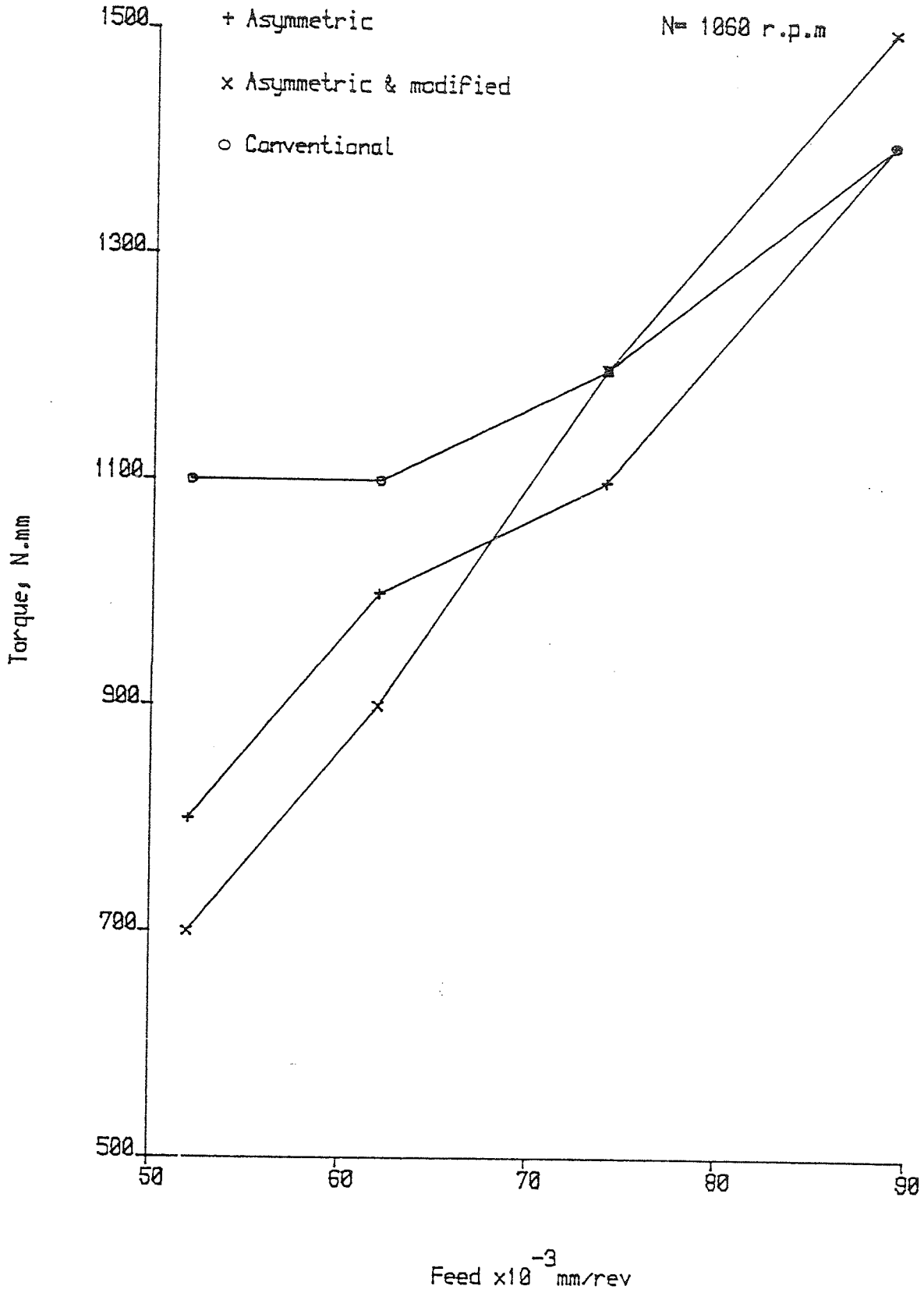

Figure 36 drilling torque comparison

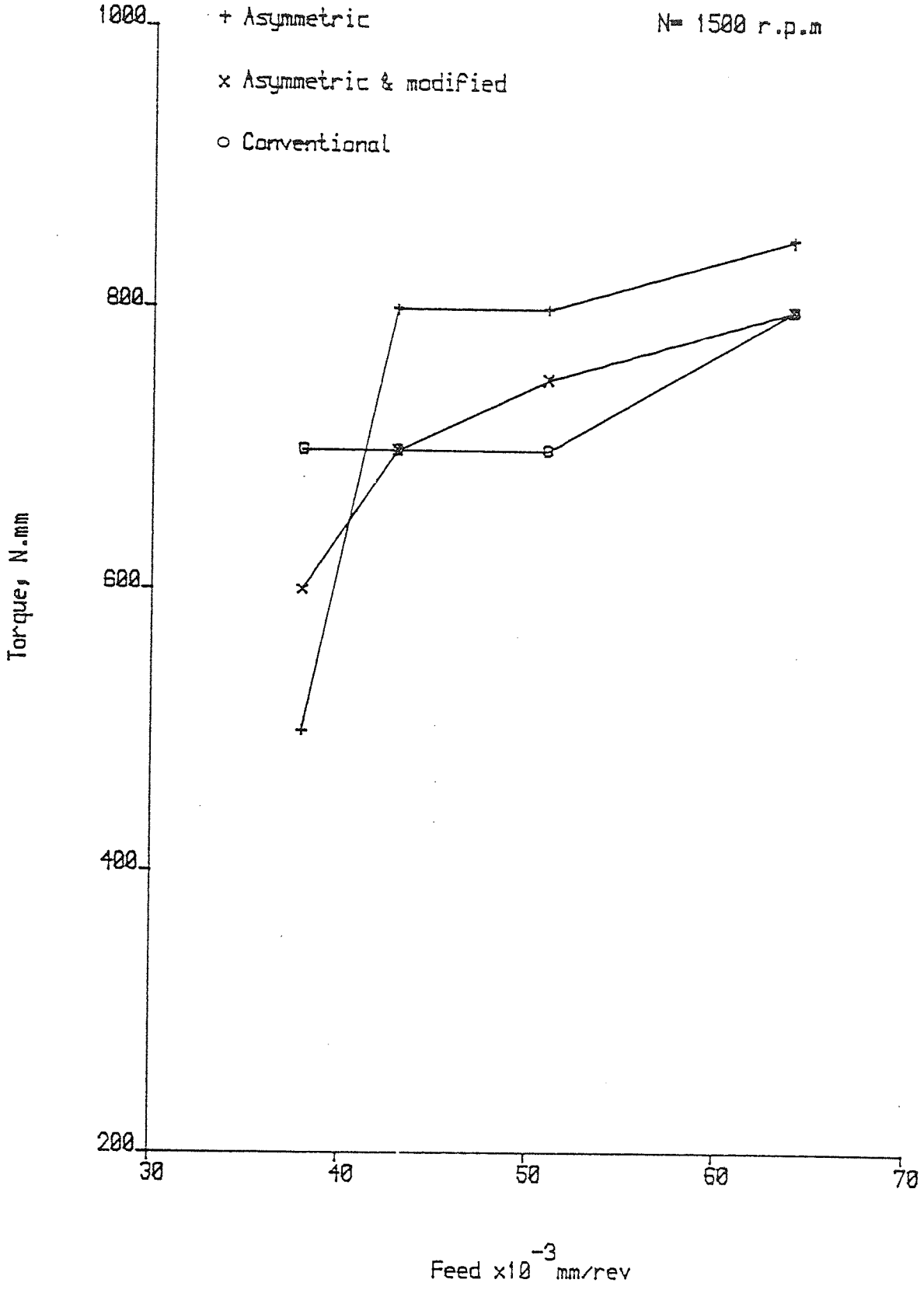

Figure 37 drilling torque comparison

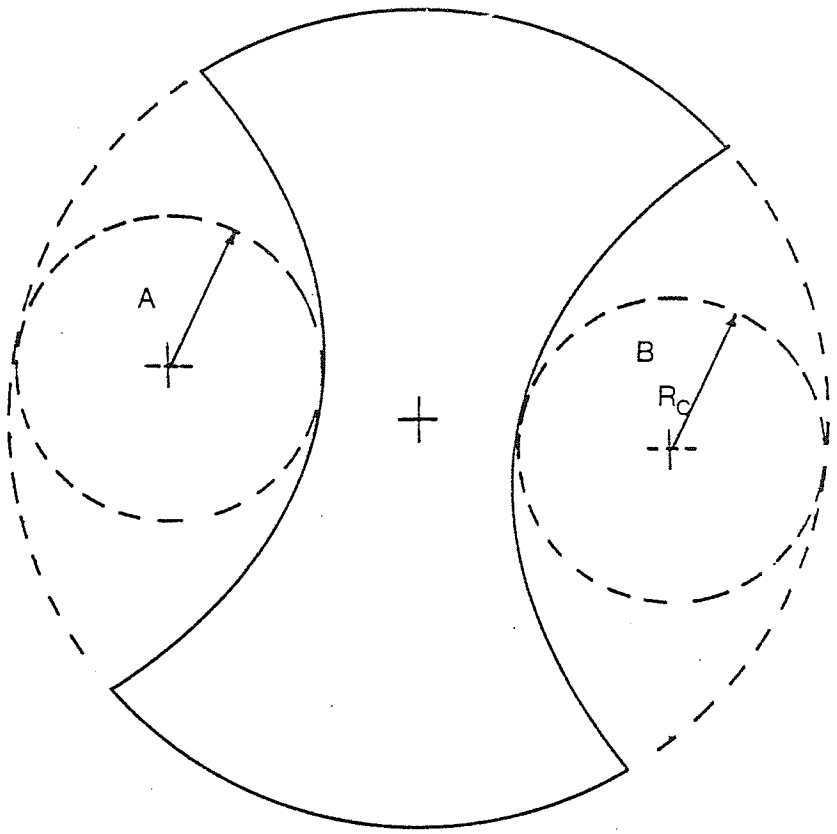

Fig 38 Inscribed circle in the flute space

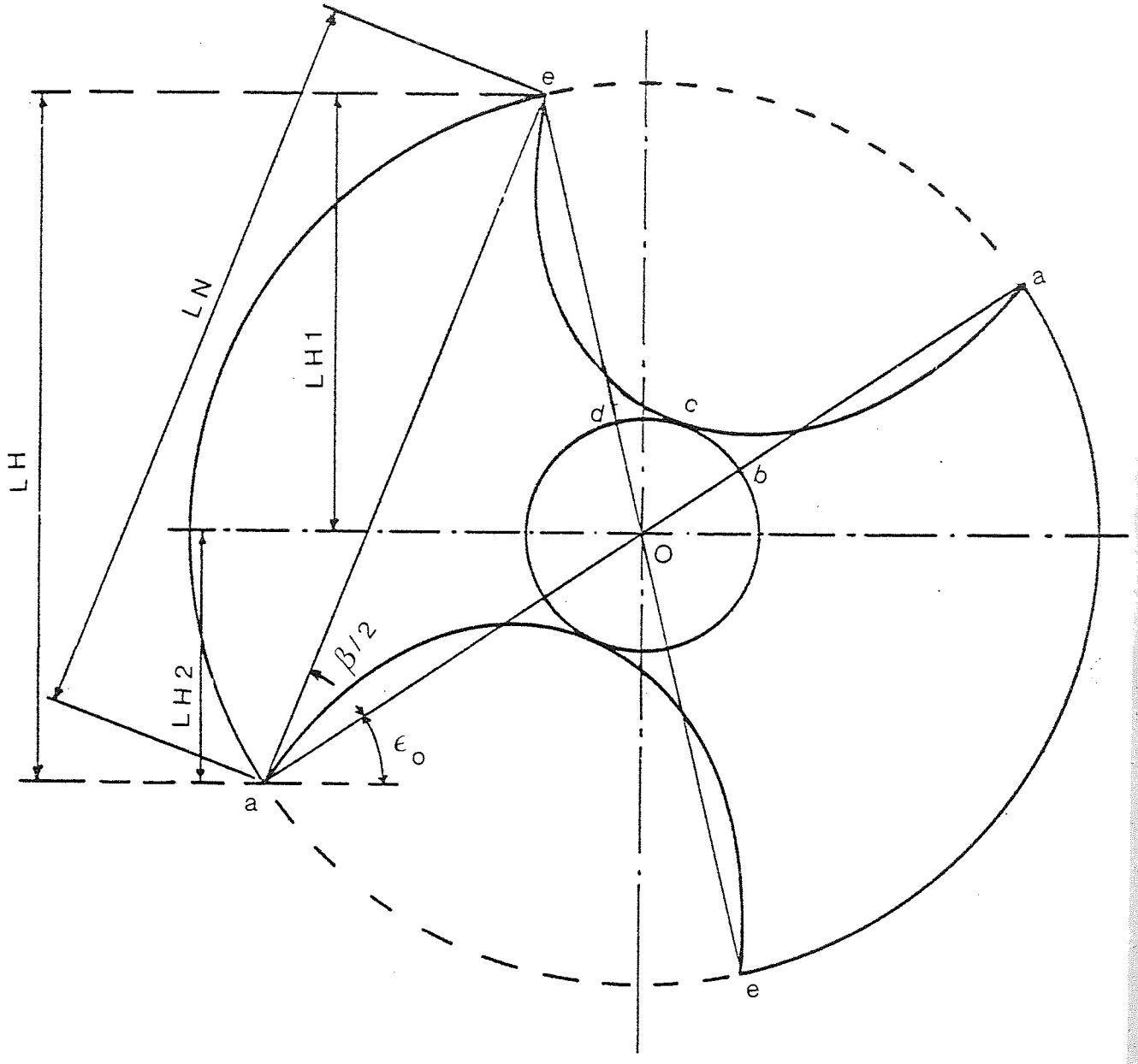

Fig 39 Equivalance of flute space

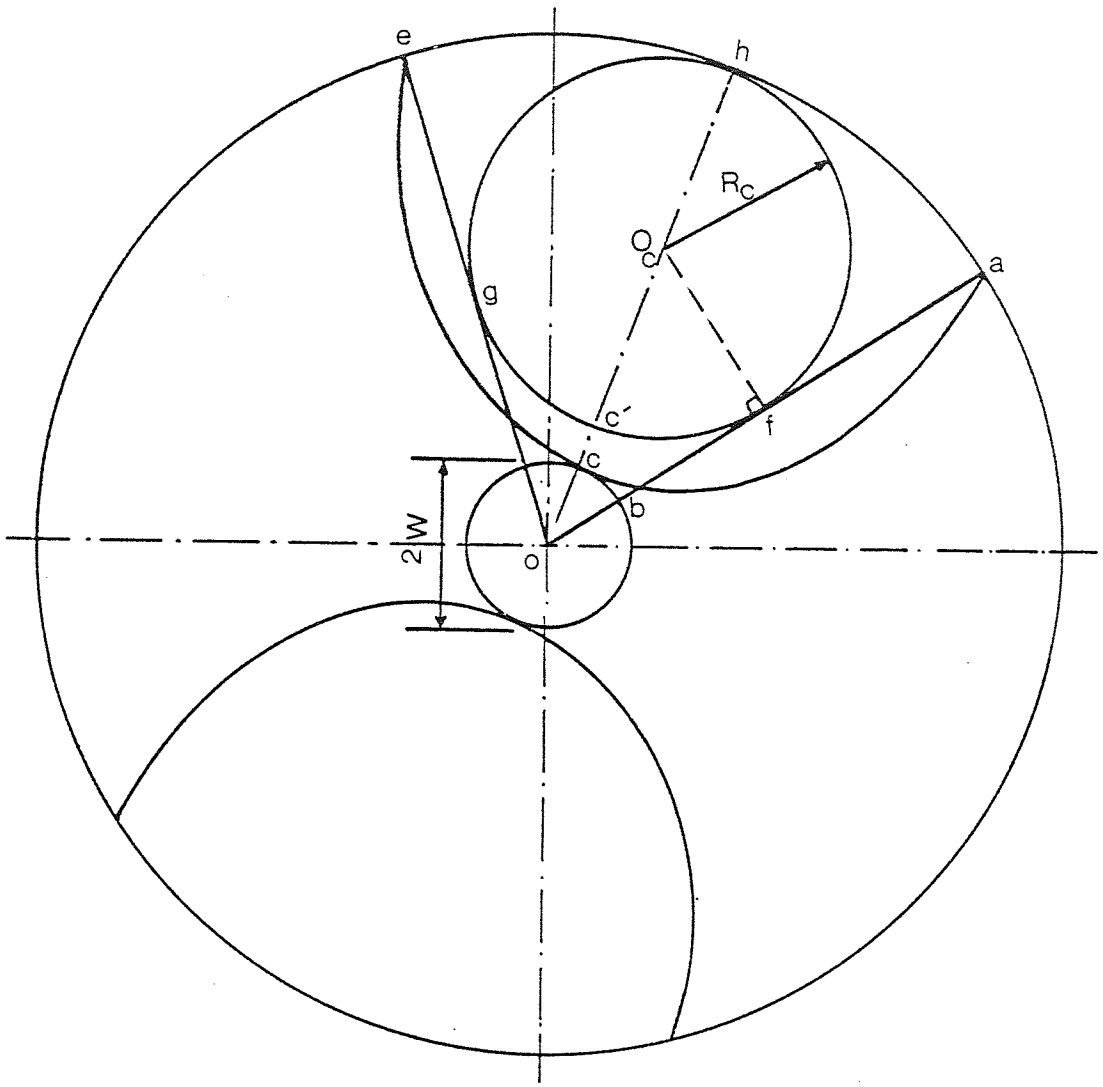

Fig 40 Mathematical representation of R_c

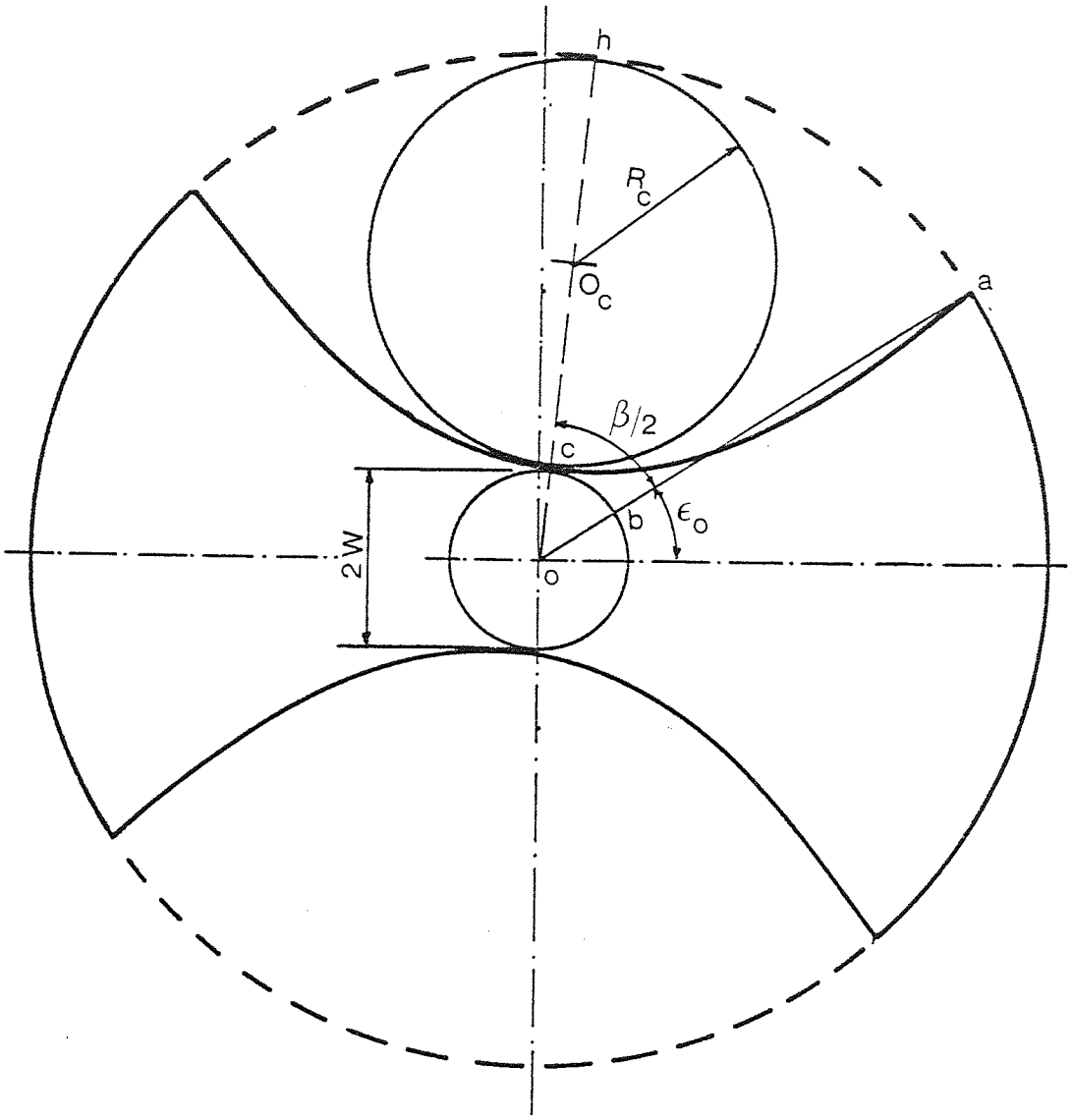

Fig 41 Chip disposal capacity ($L < L_o$)

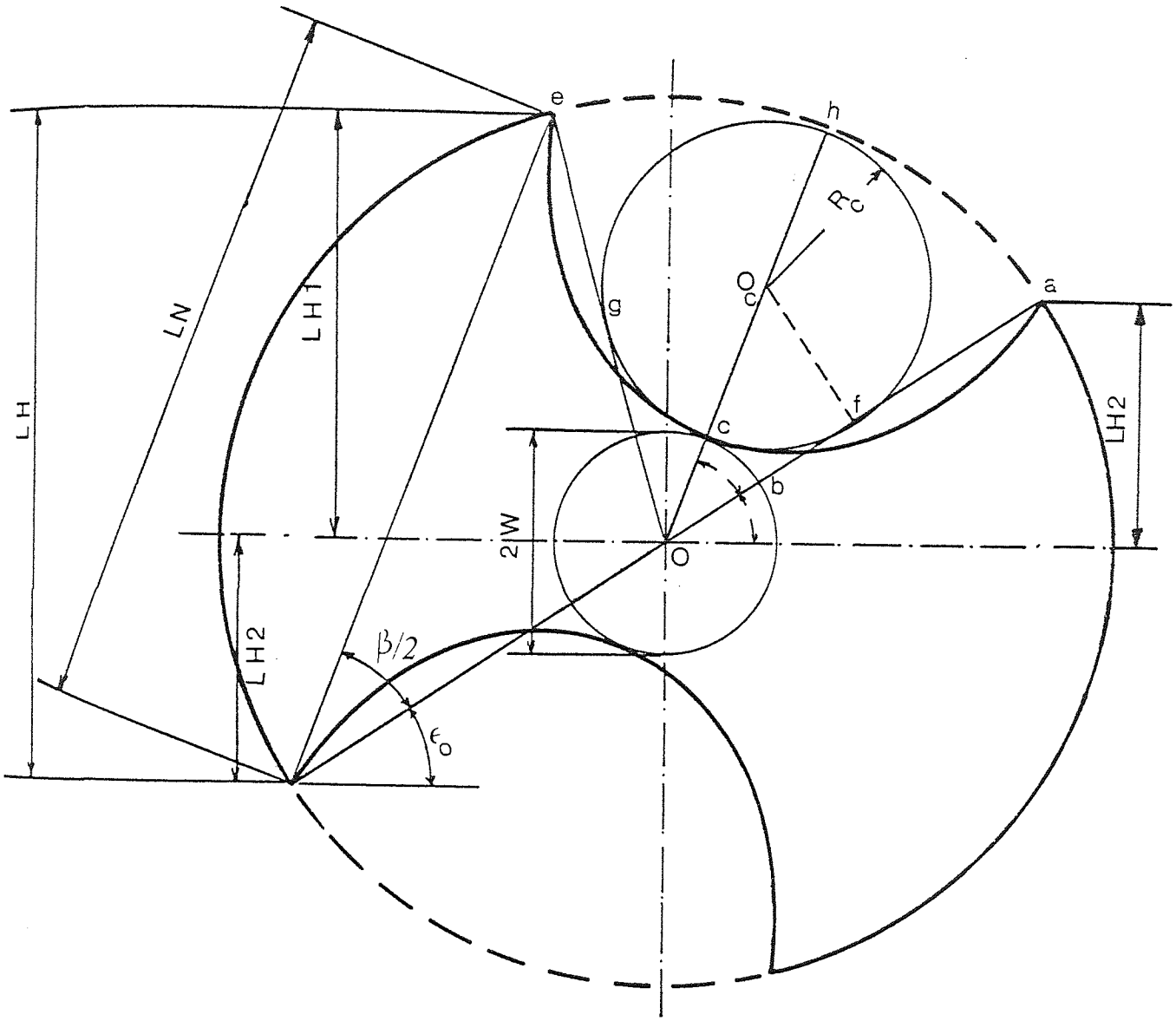

Fig 42 Chip disposal capacity ($L = L_o$ & $W = W_o$)

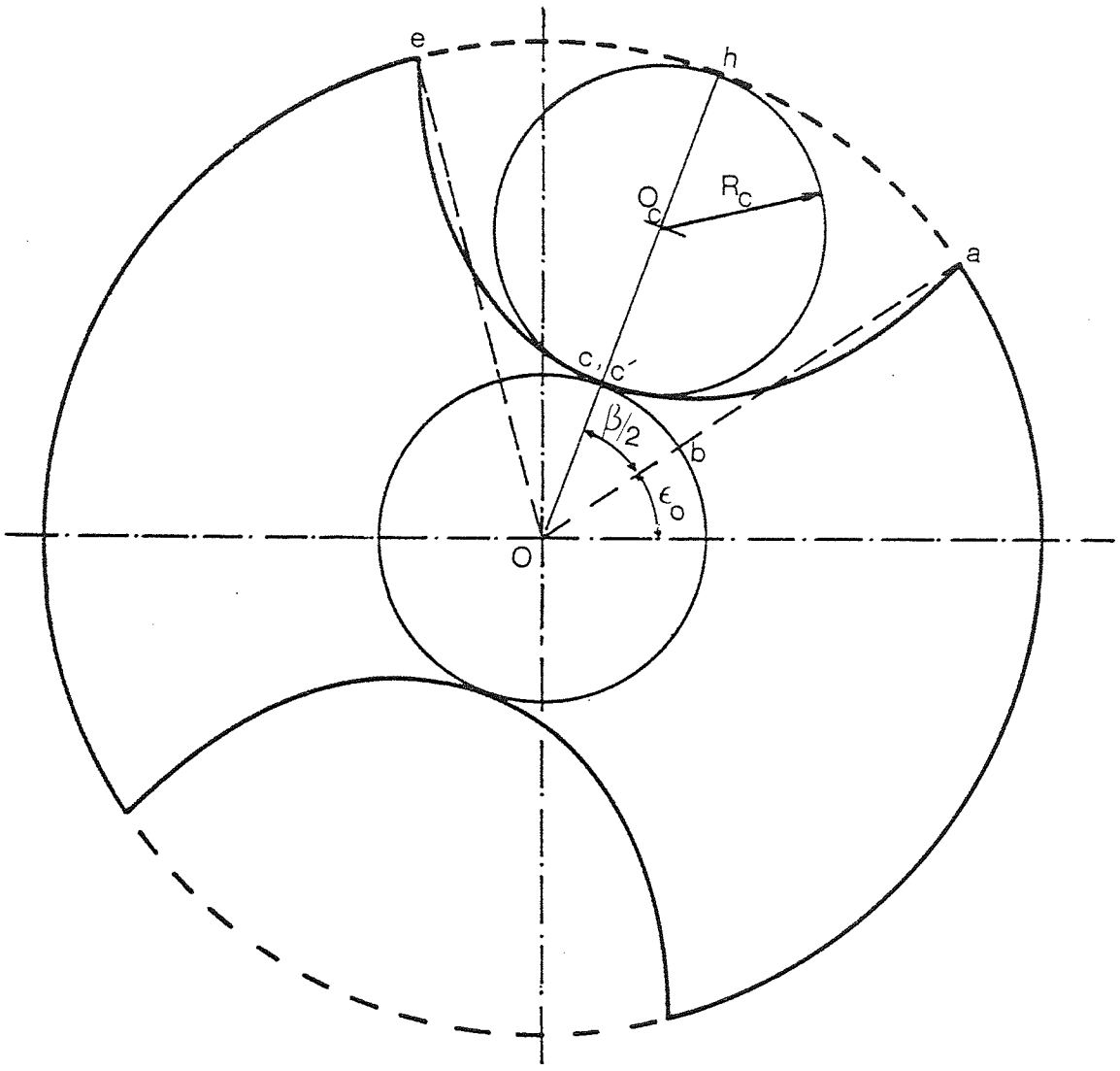

Fig 43 Chip disposal capacity ($W > W_o$)

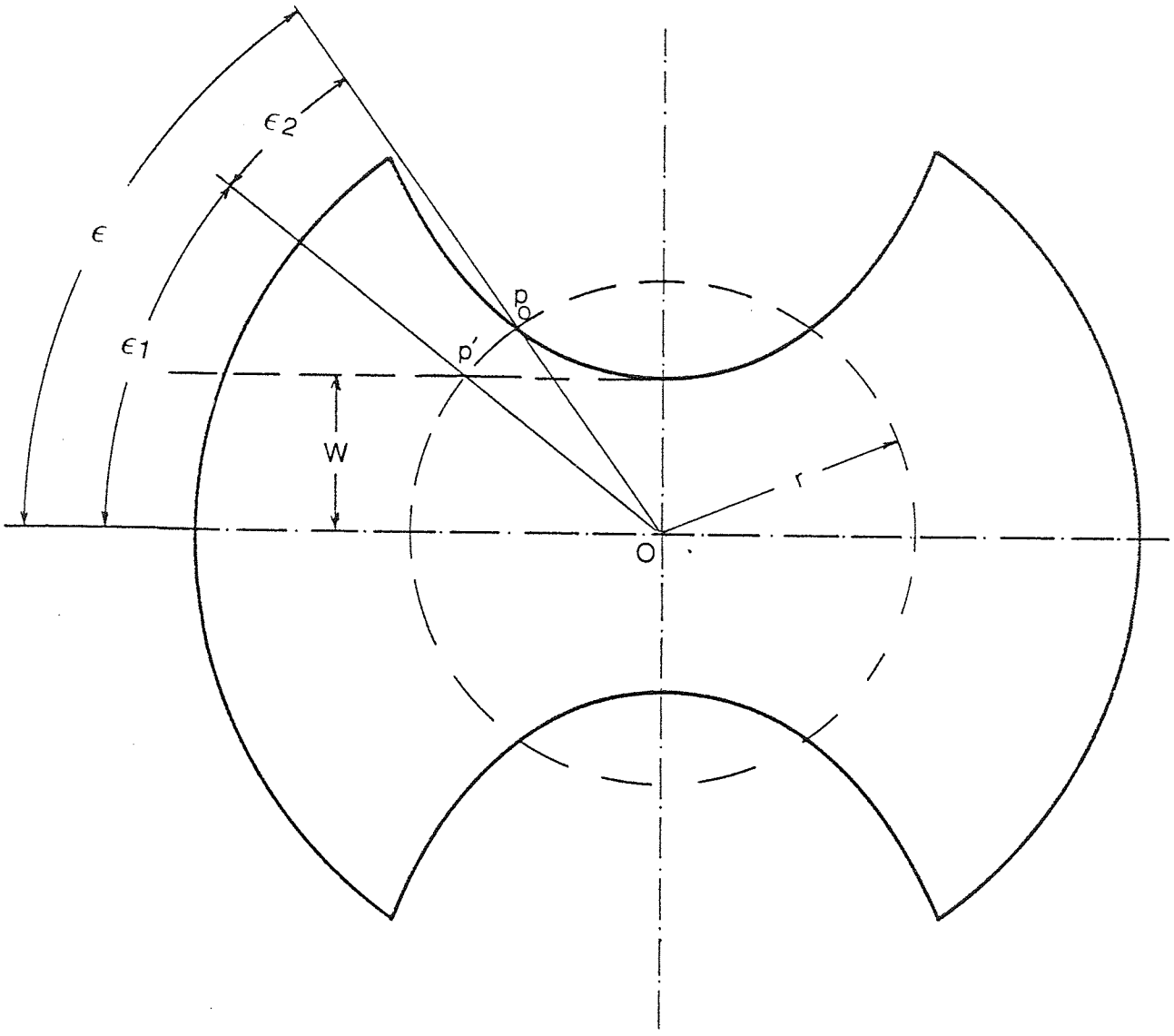

Fig 44 Conventional flute shape

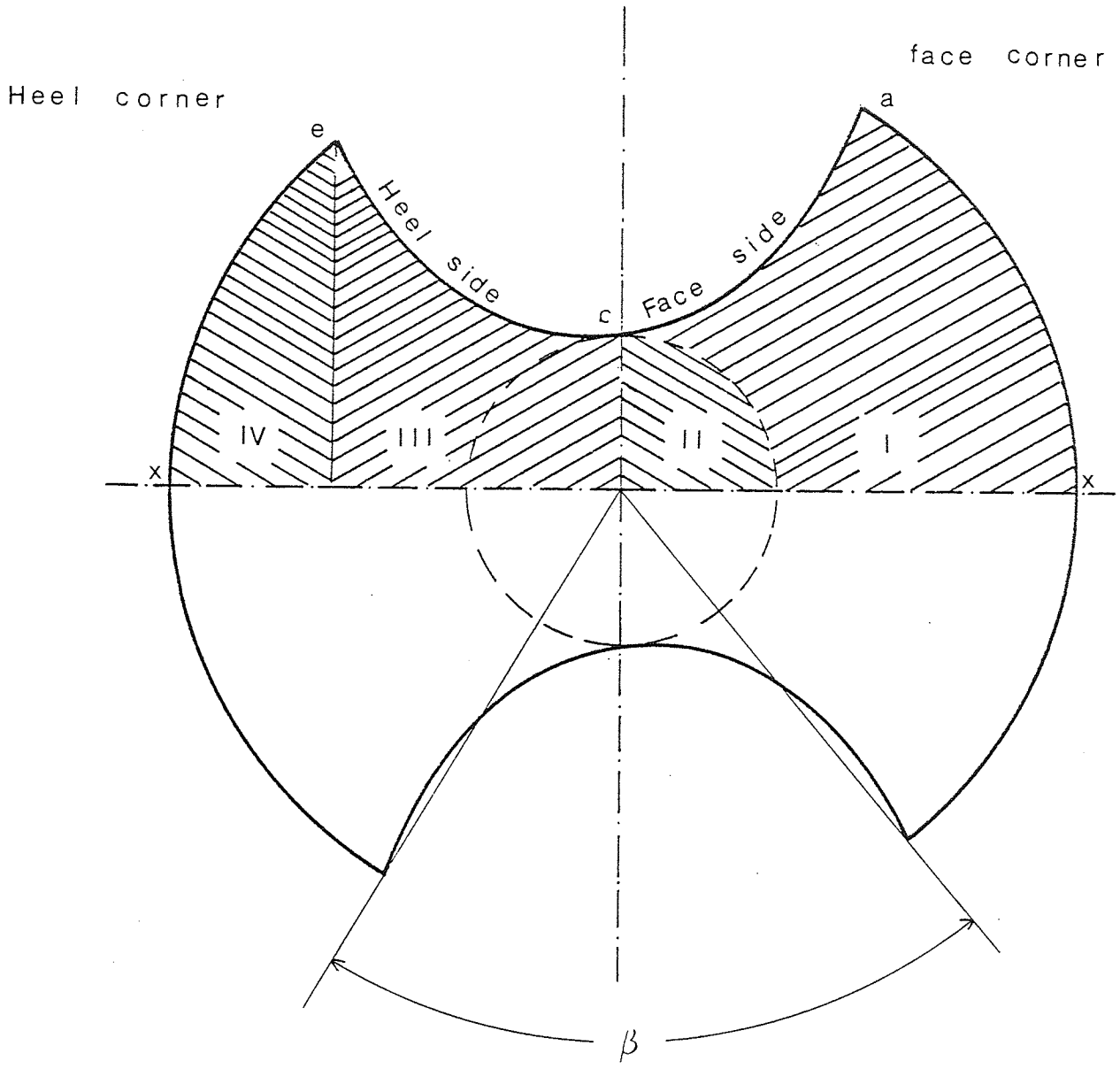

Fig 45 Cross section normal to the drill axis

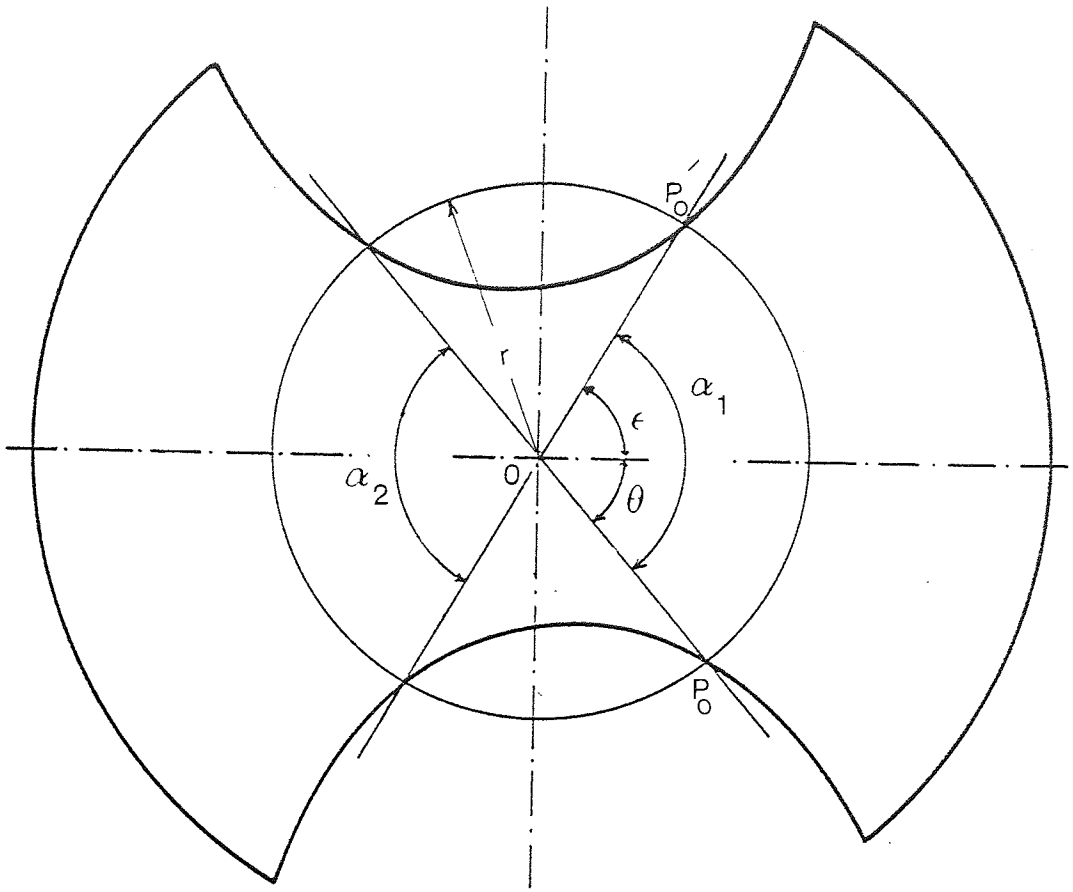

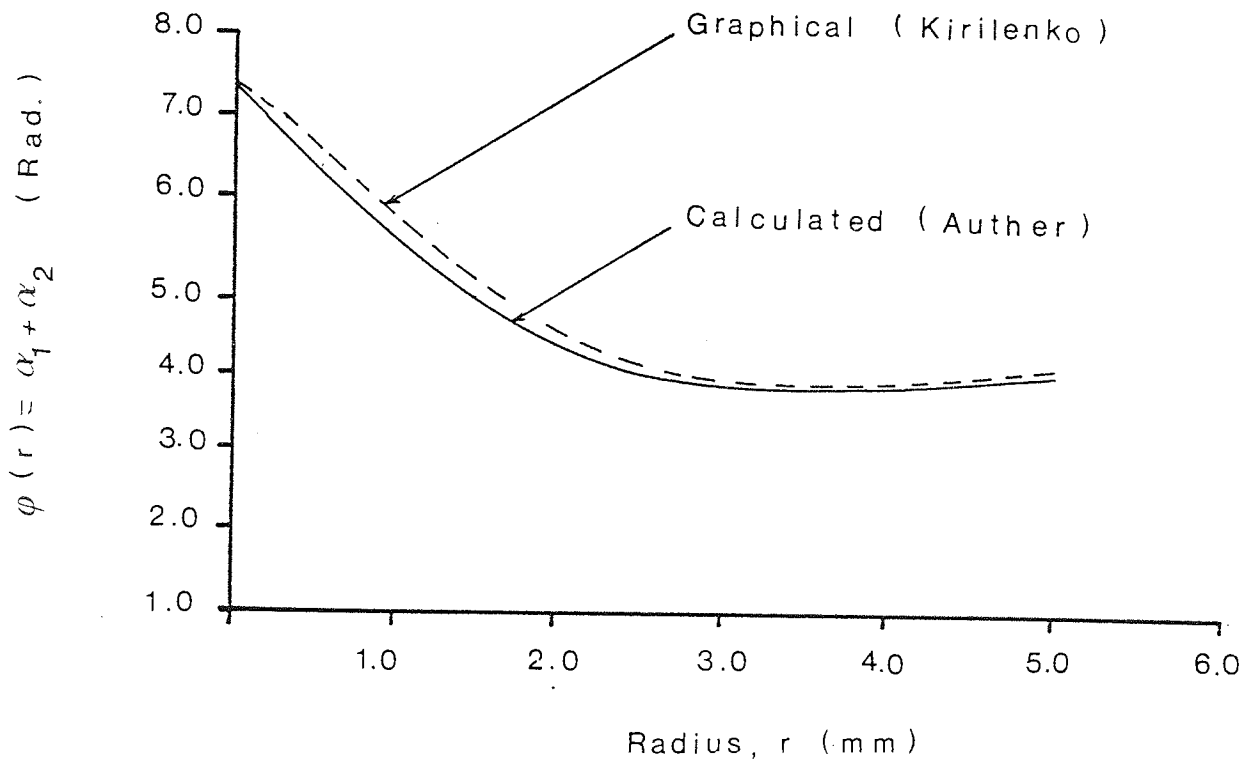

Fig 46 The value of function $\varphi(r)$

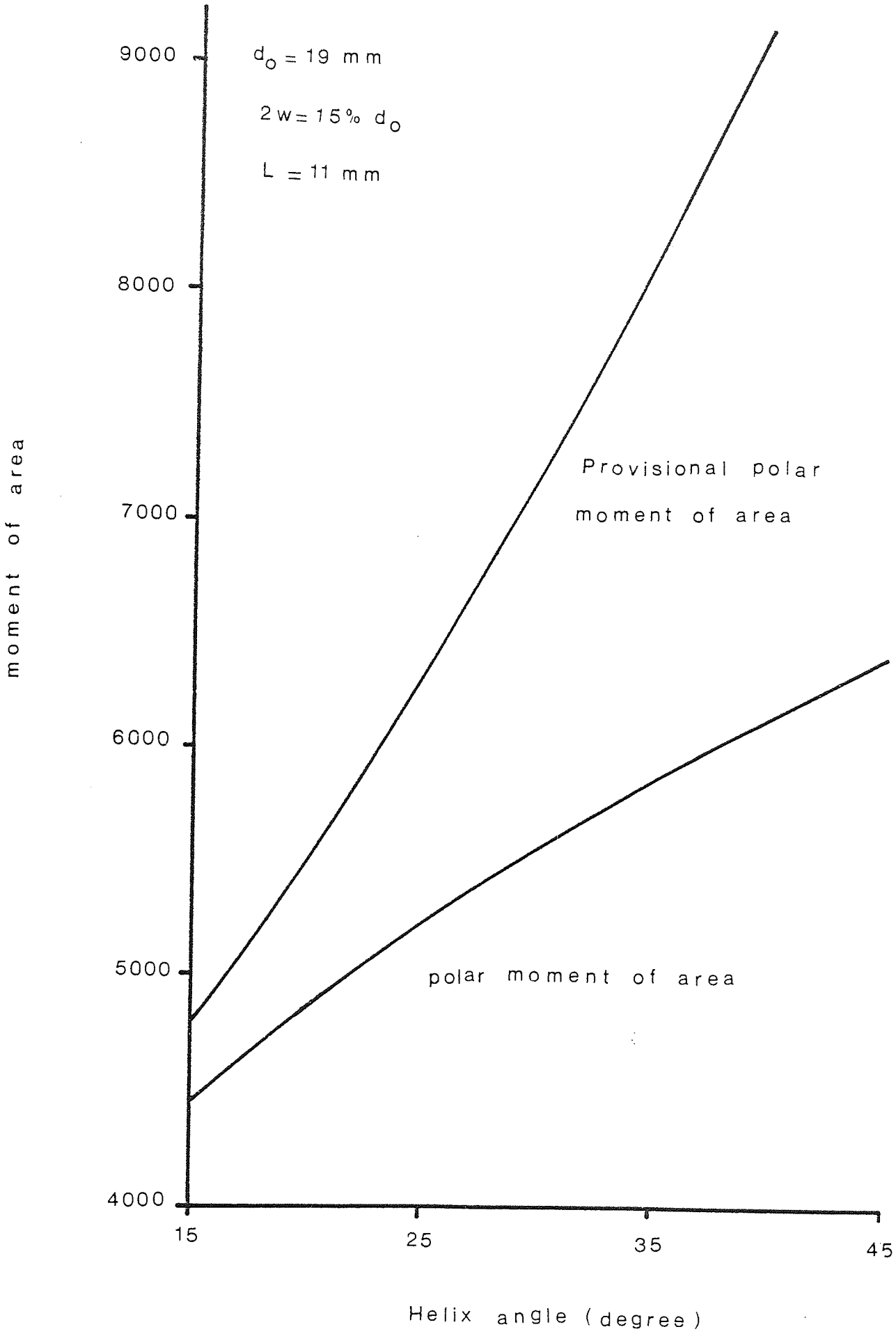

Fig 47 The effect of the helix angle on polar moment of area

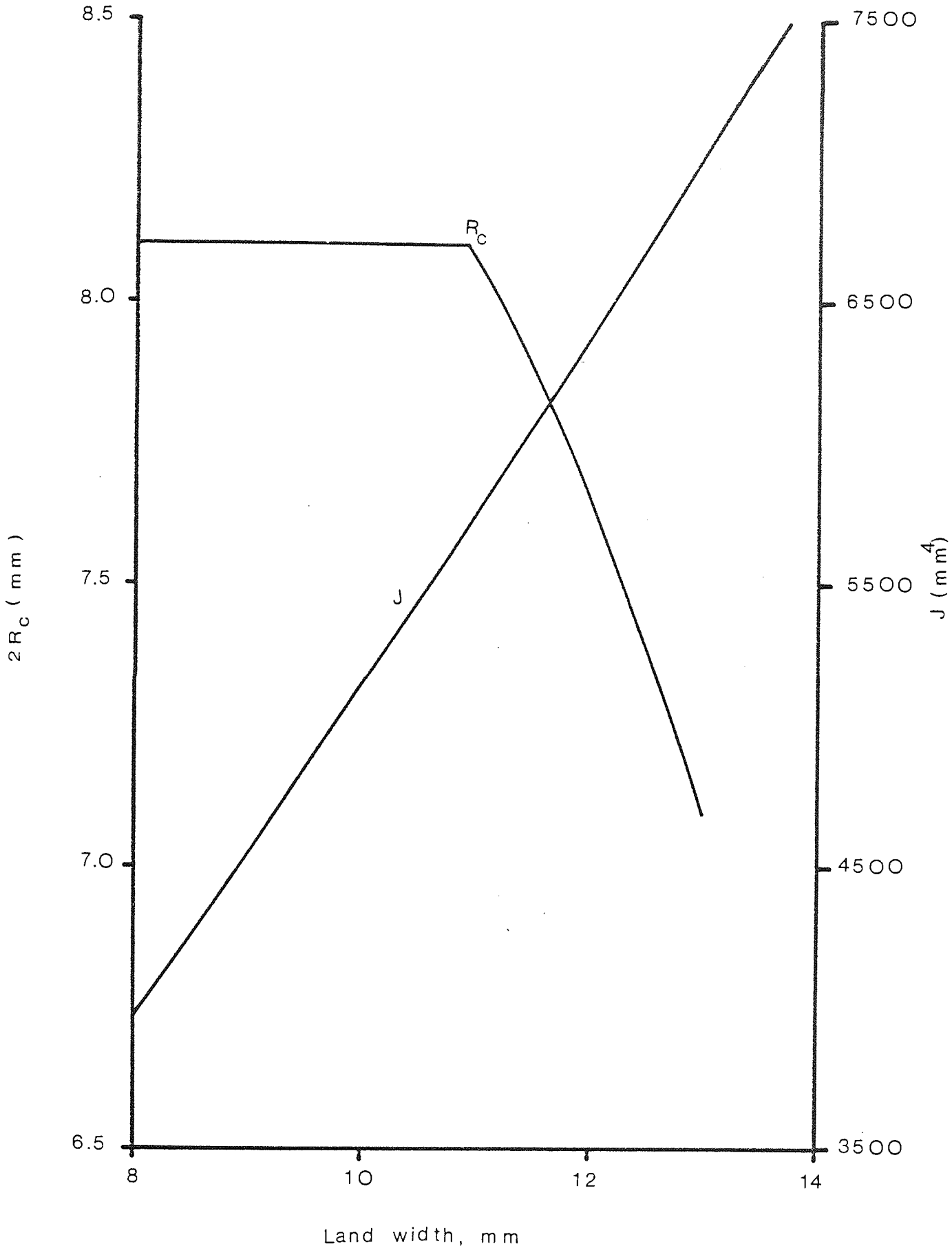

Fig 48 The influence of land width on J & R_c

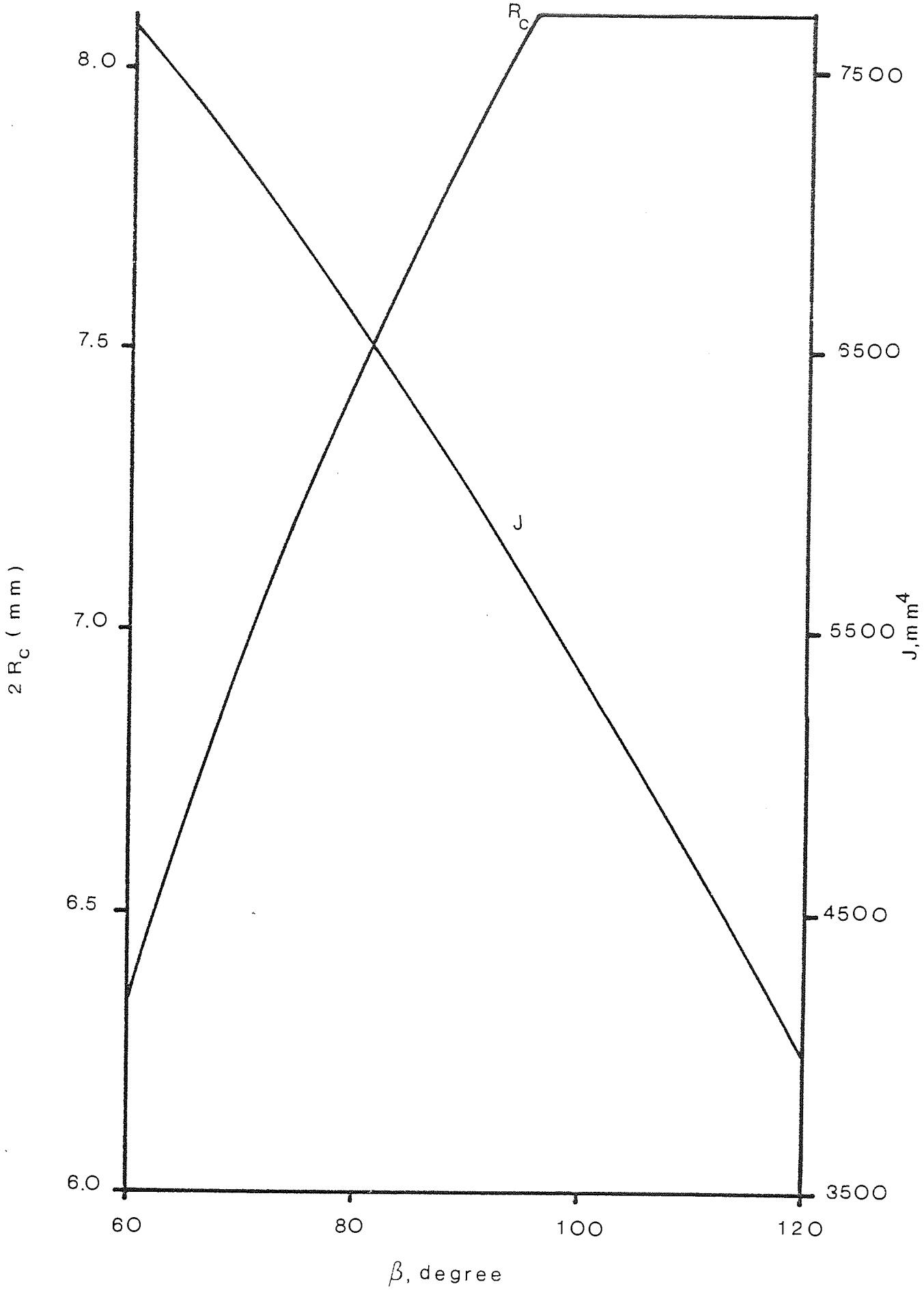

Fig 49 The influence of angular difference margin/heel on J & R_c

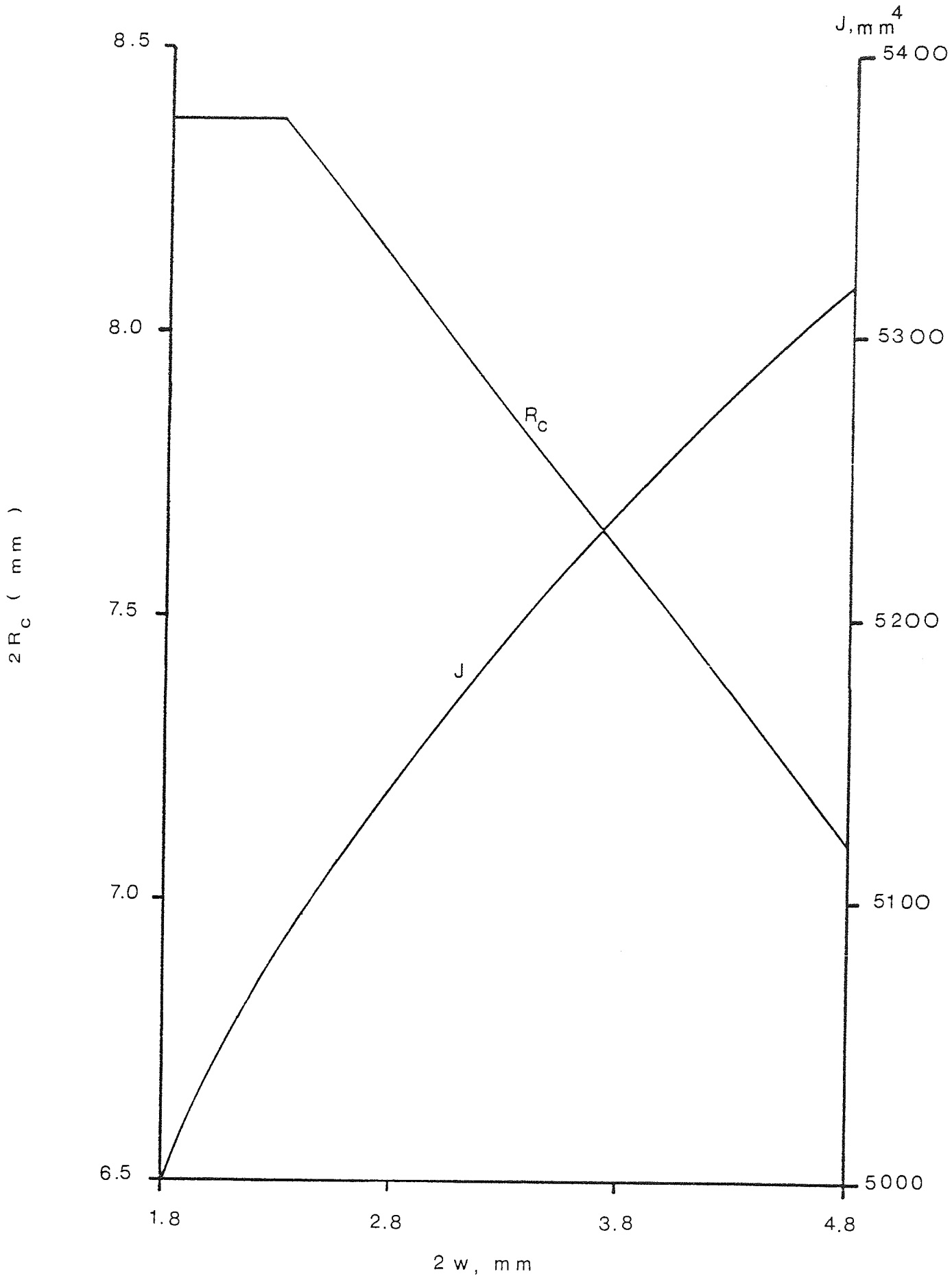

Fig 50 The influence of web thickness on J & R_c

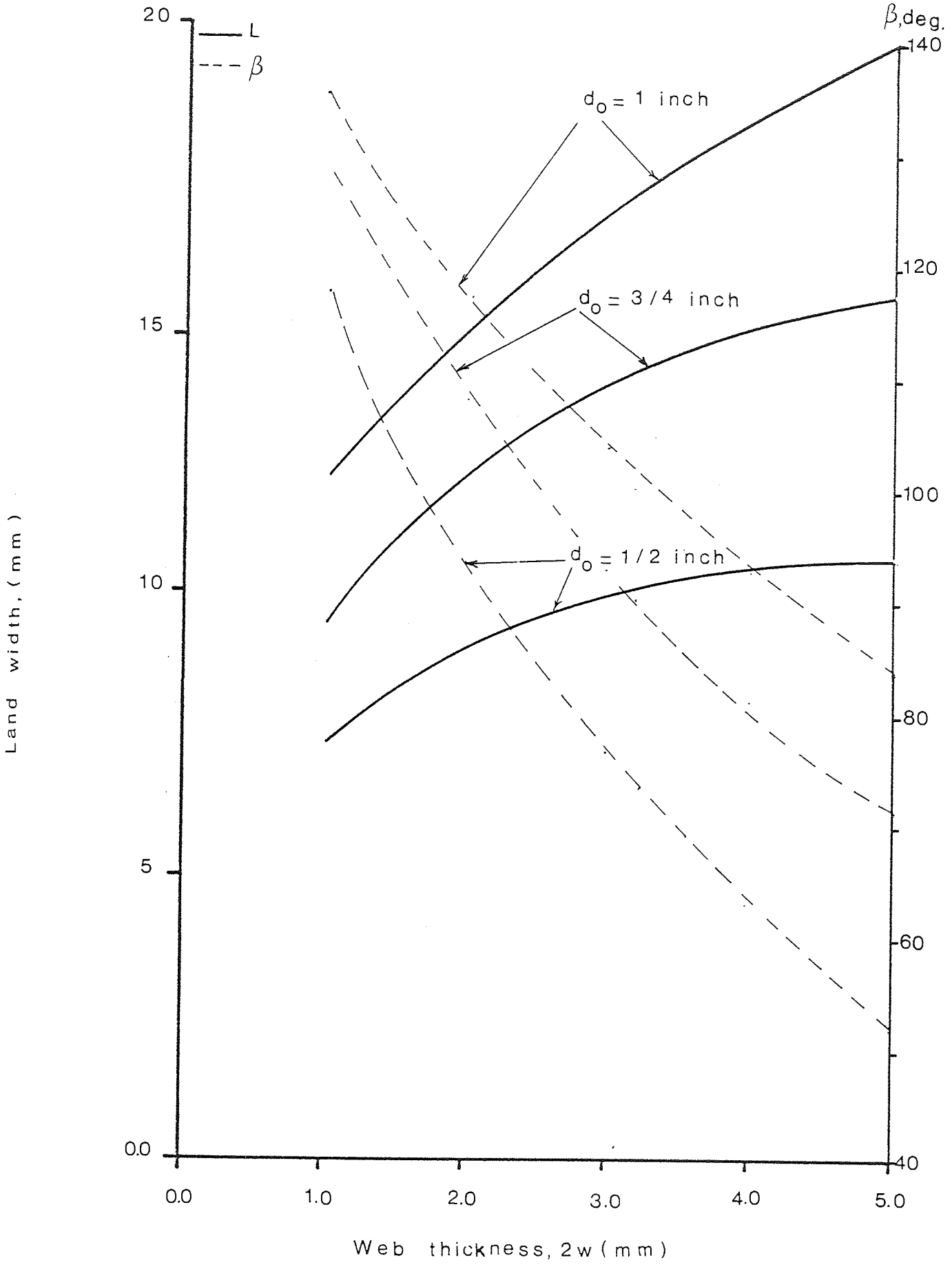

Fig 51 Minimum optimum land width and maximum optimum β

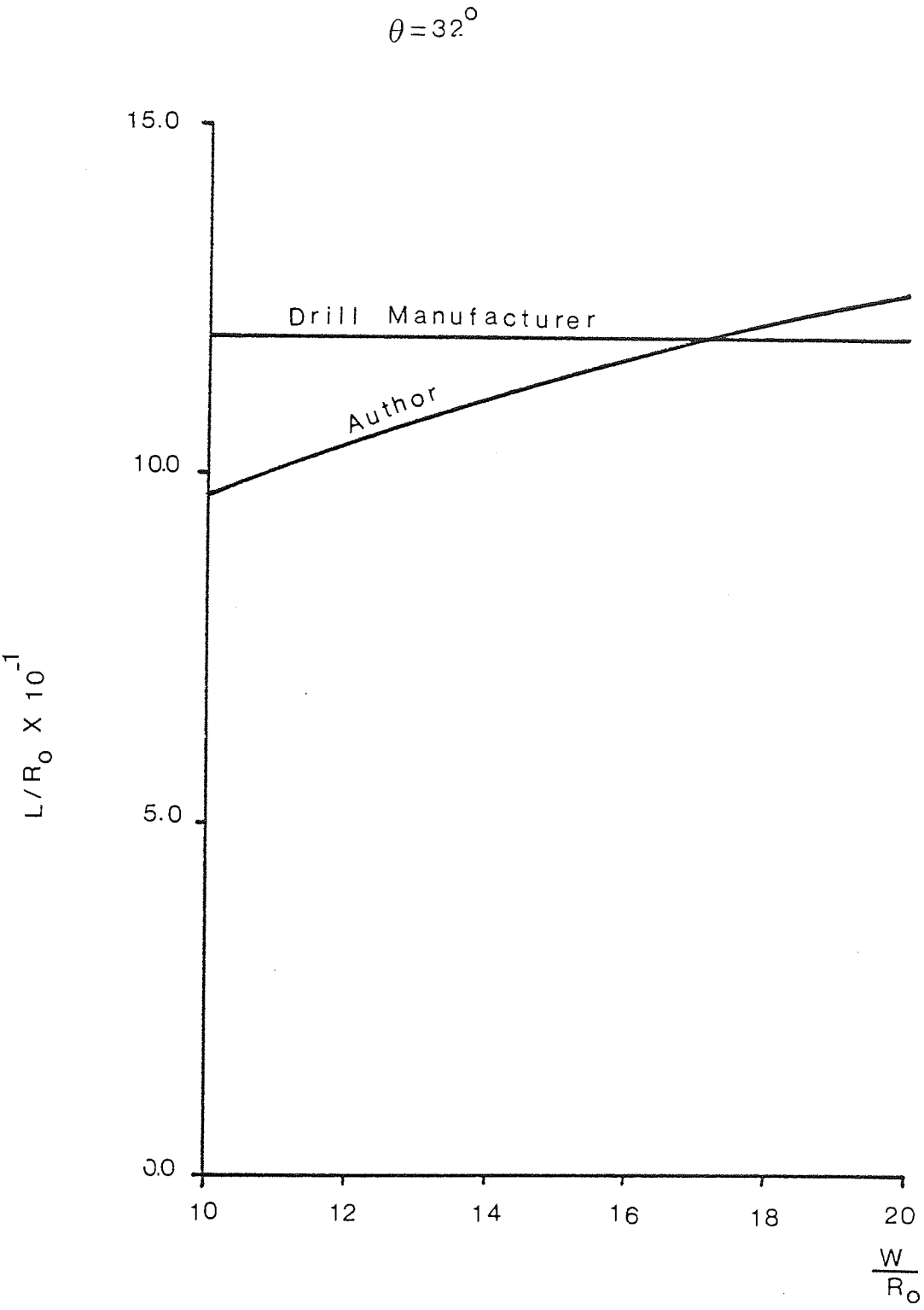

Fig 52 Comparison of land width selection

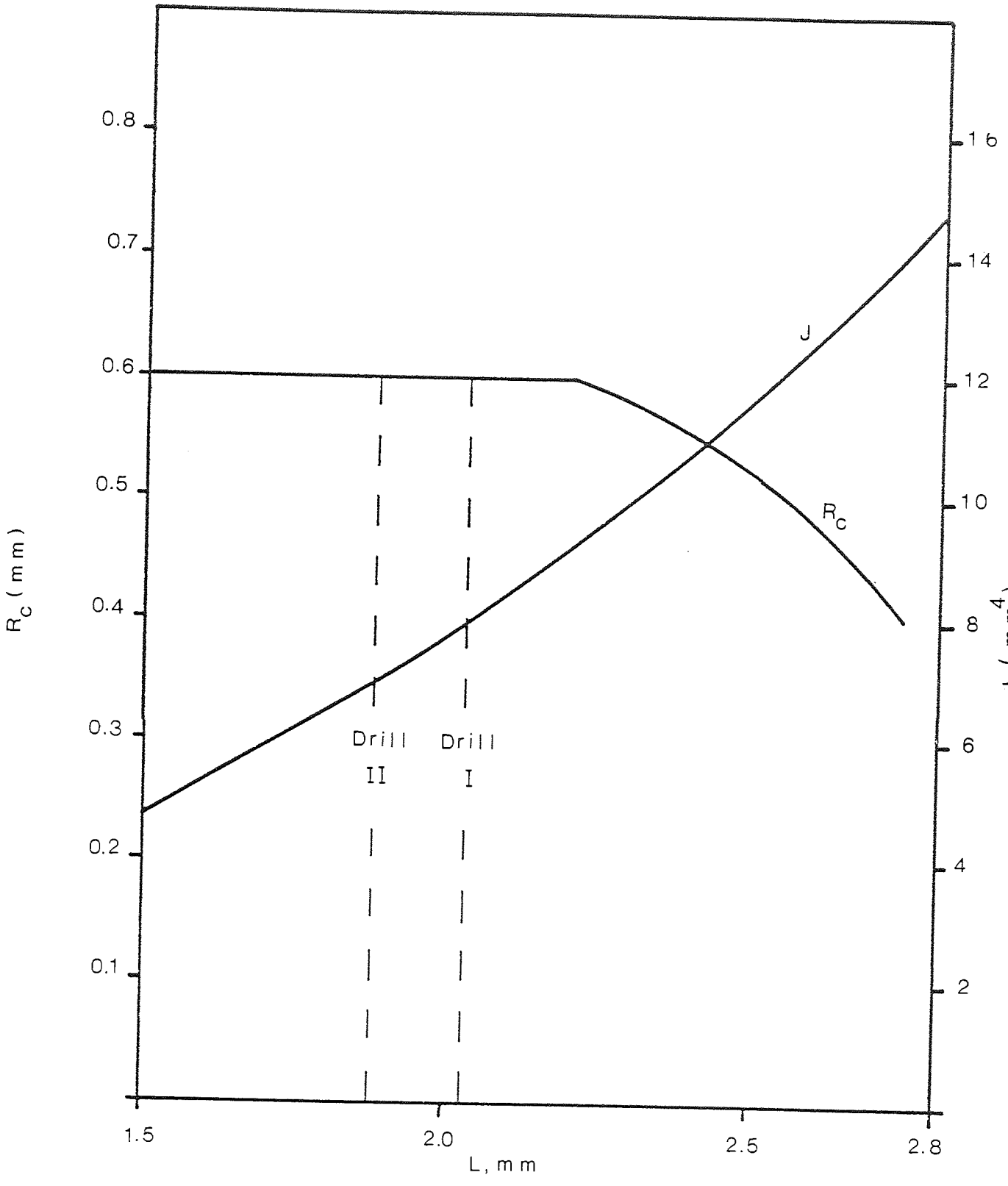

Fig 53 Typical drill features used for clogging test

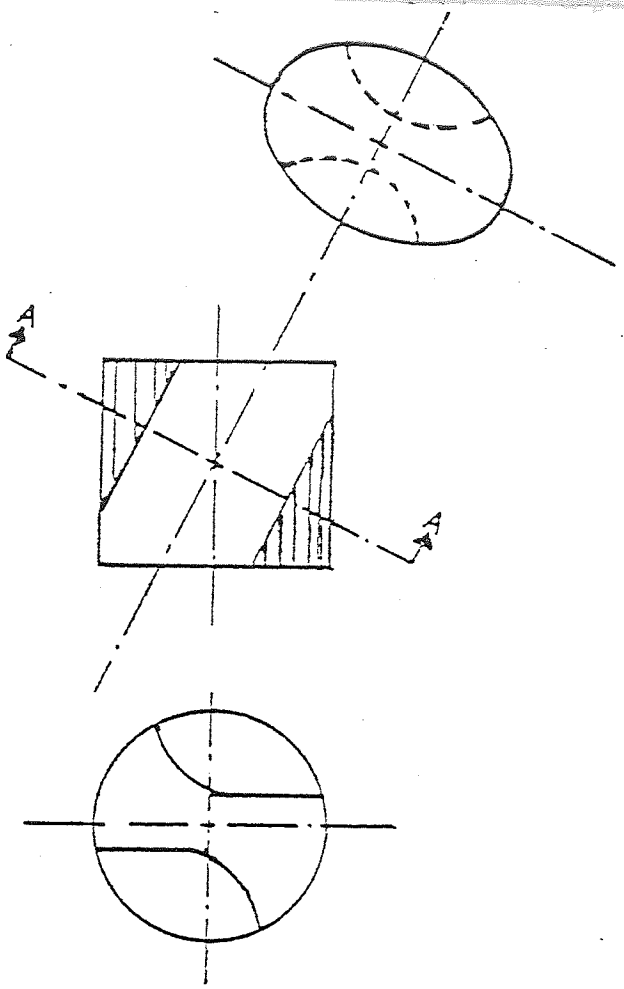

Fig 54 Oblique flute

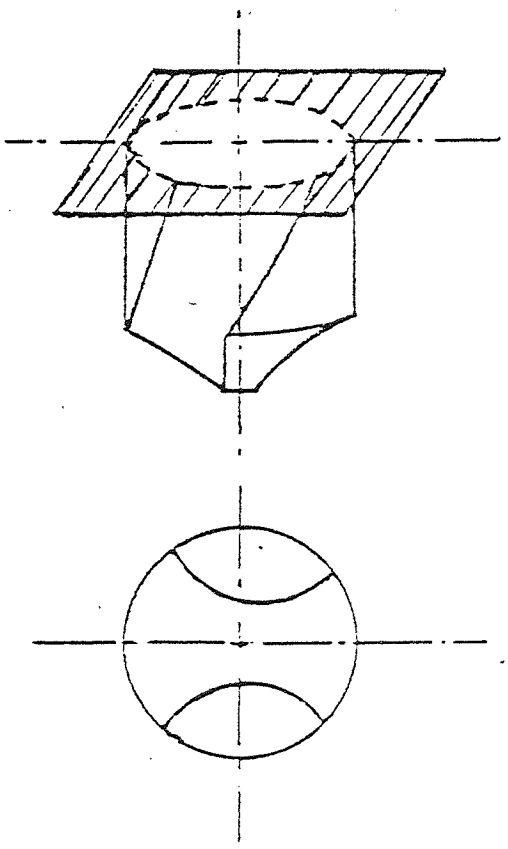

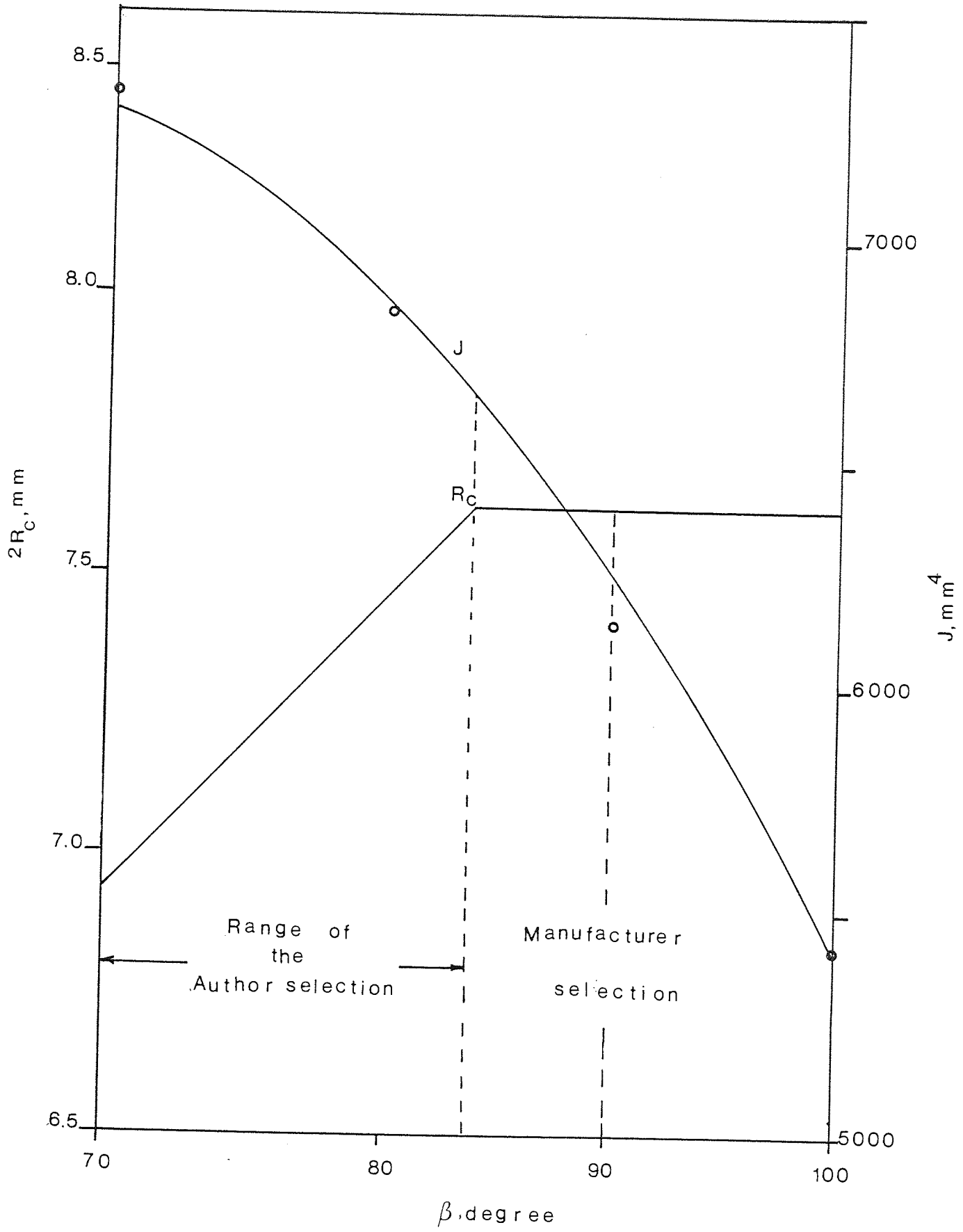

Fig 56 Comparison of Author & Manufacturer selection

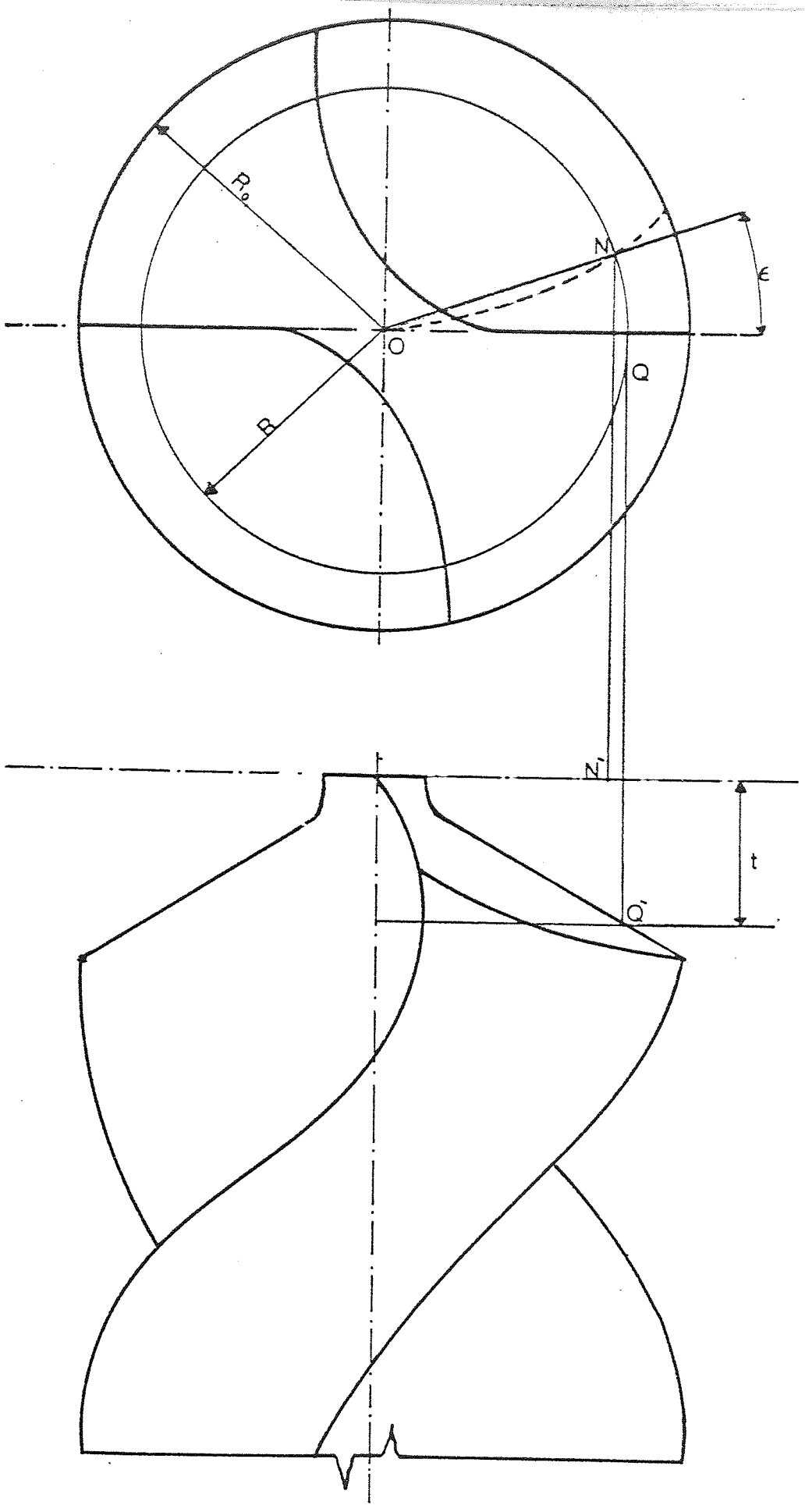

Fig 57 Flute face prediction for diametral lip drill.

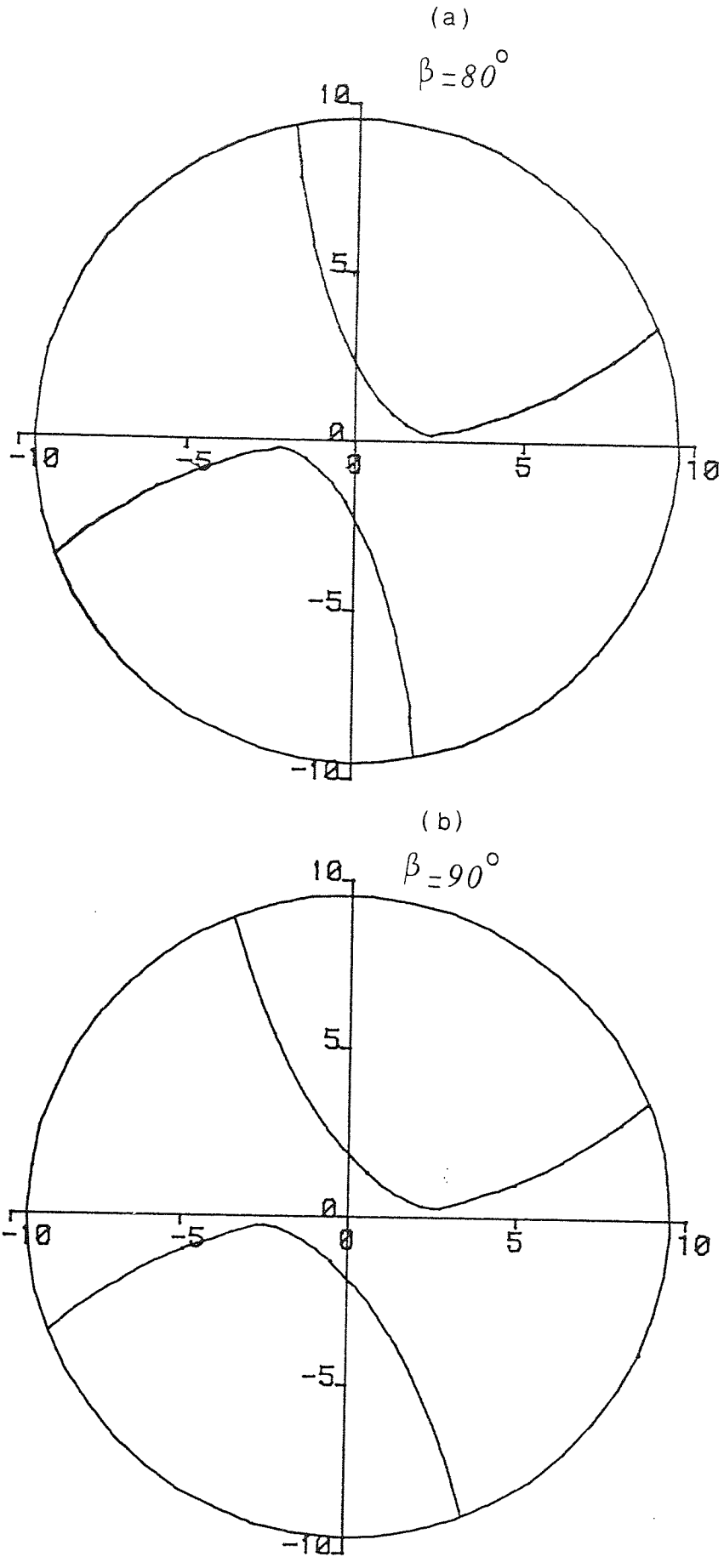

Fig 58 Computer plot of the orthogonal flute (diametral drill)

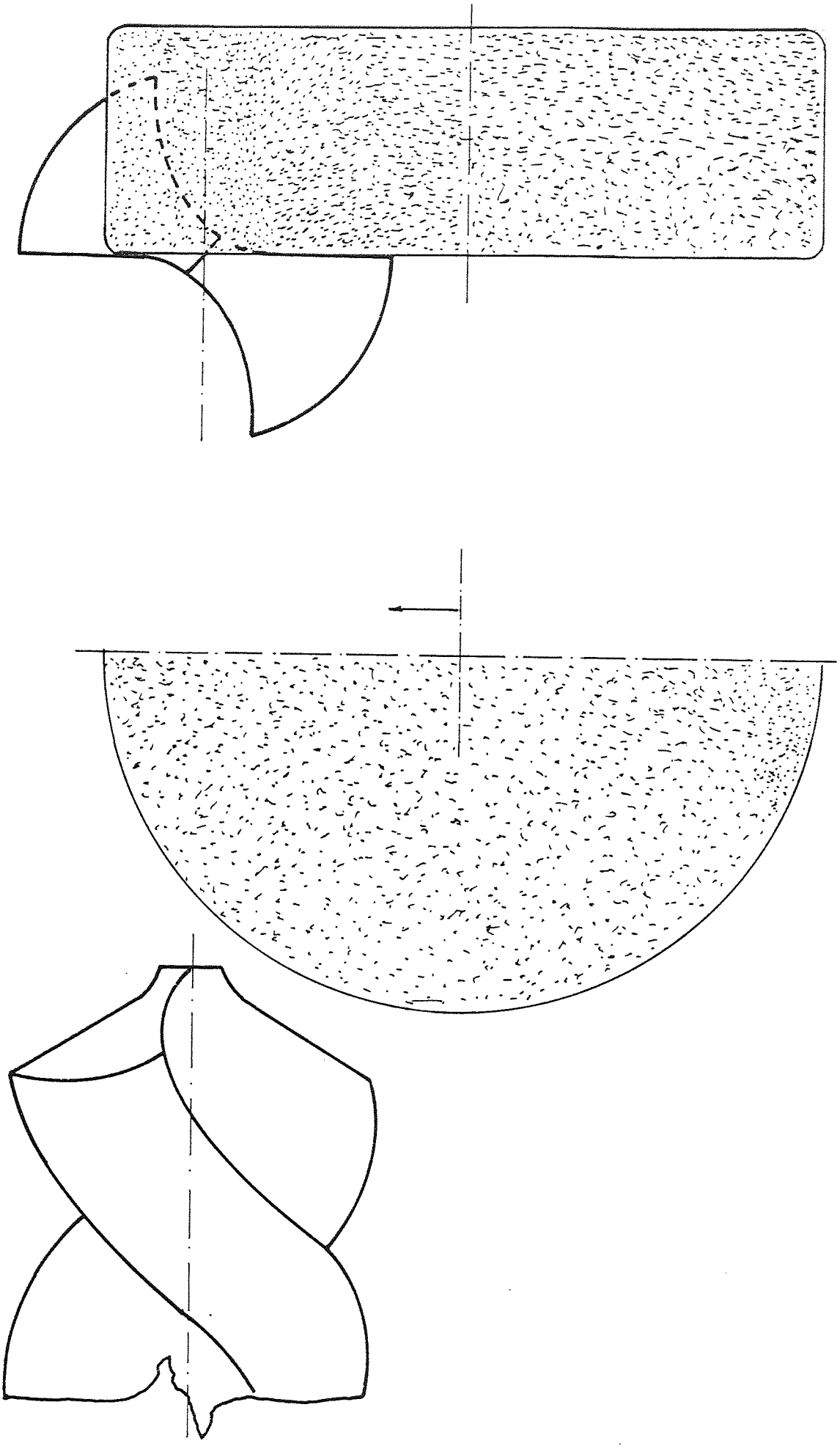

Fig 59 Grinding wheel setting for the extension of the diametral lips

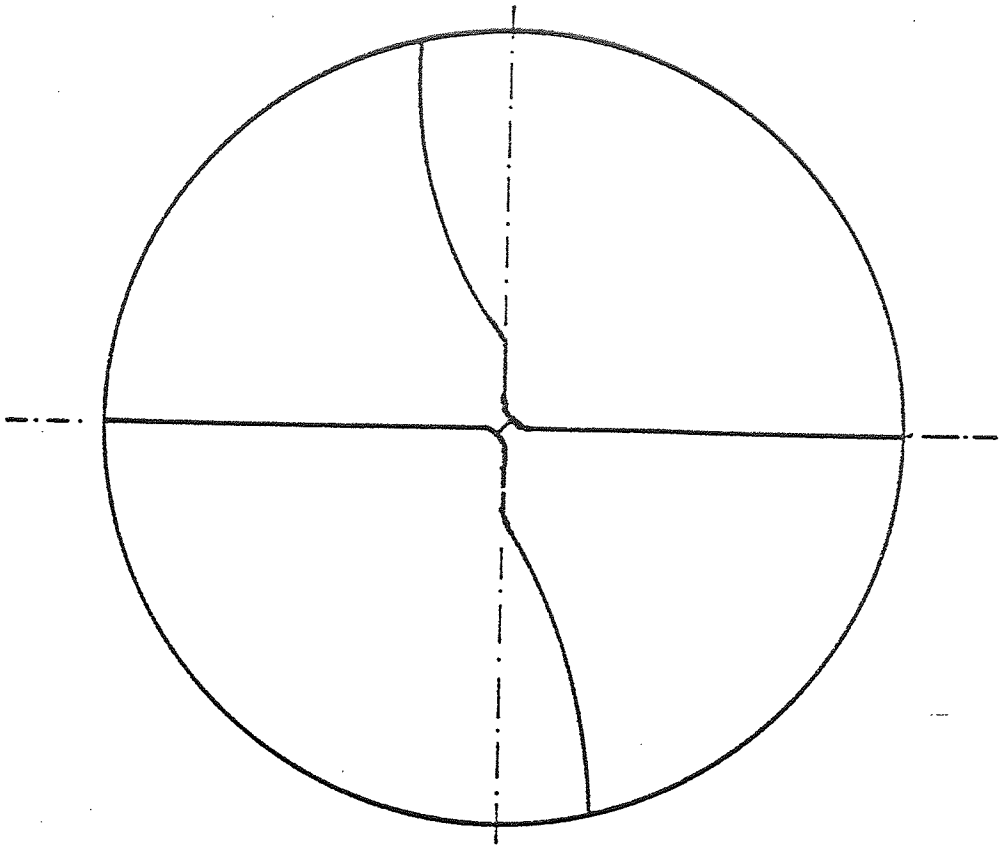

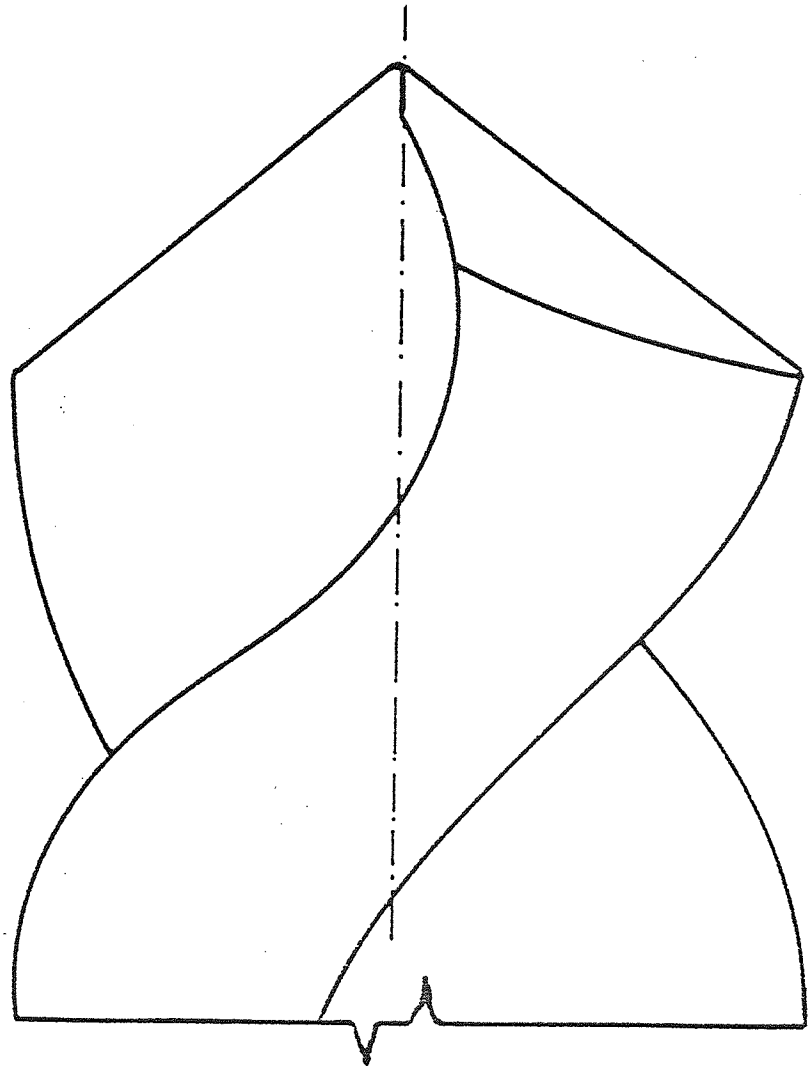

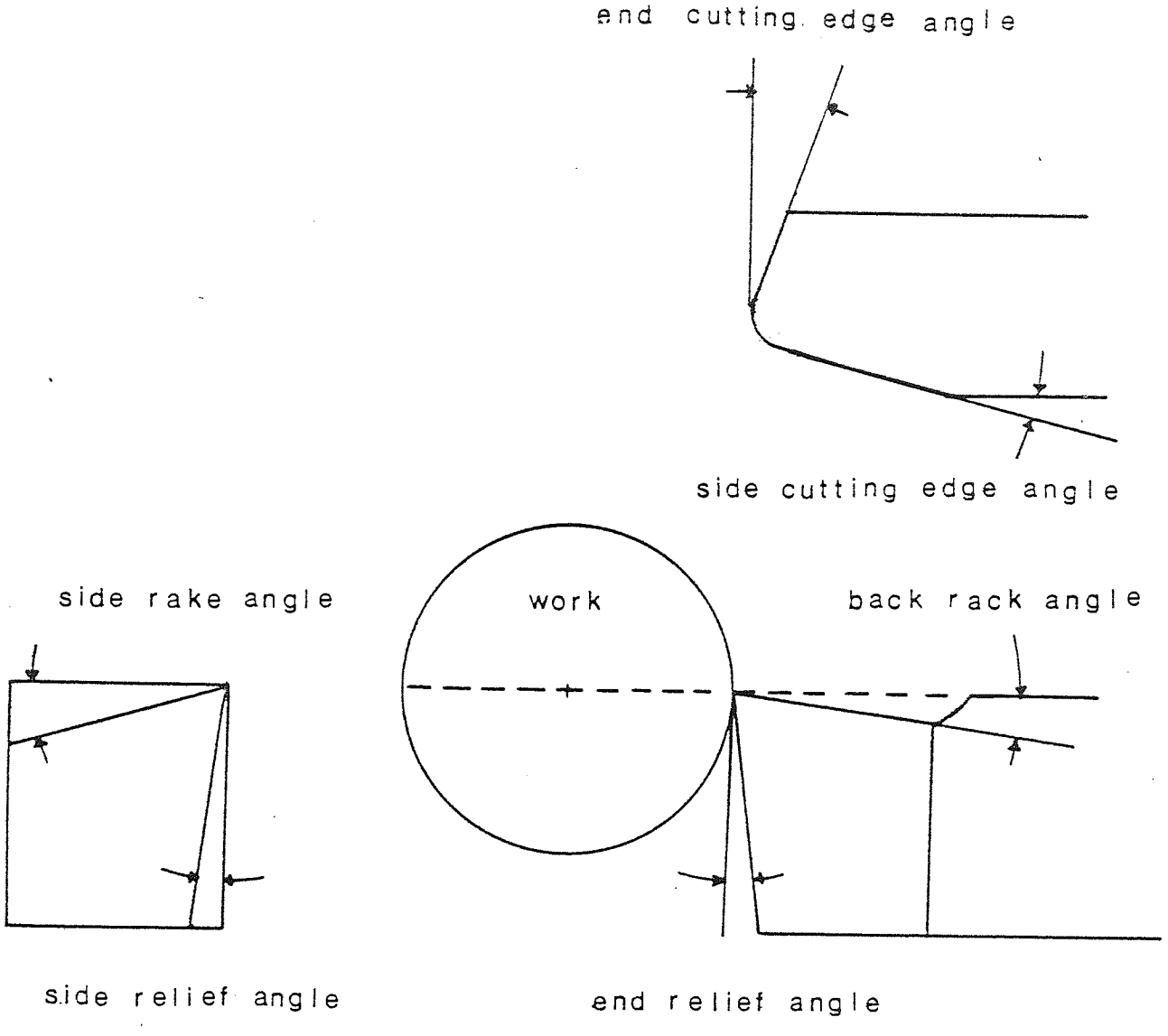

Fig 61 Representive tool angles

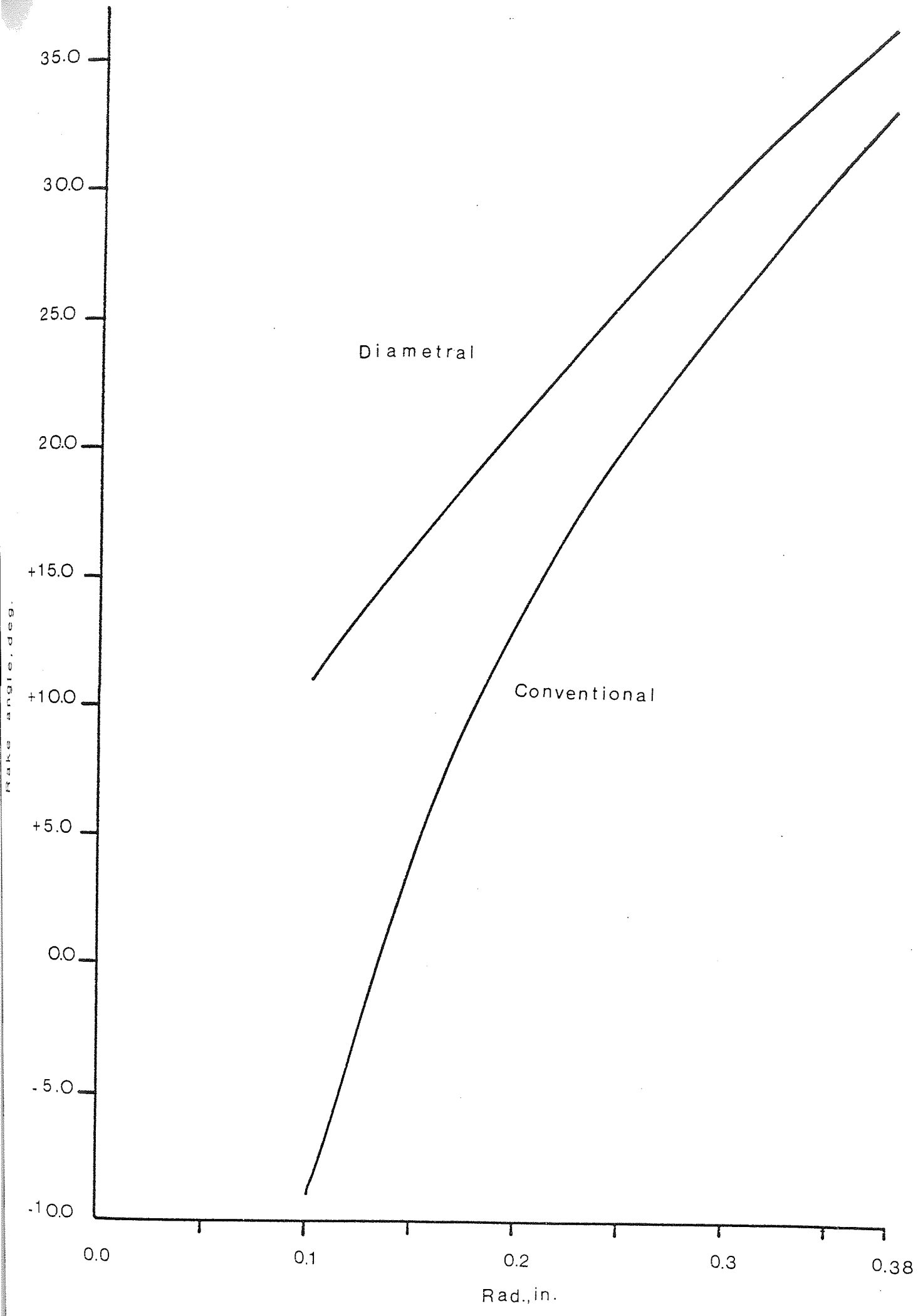

Fig. 62 Normal rake angle for conventional and diametral hi

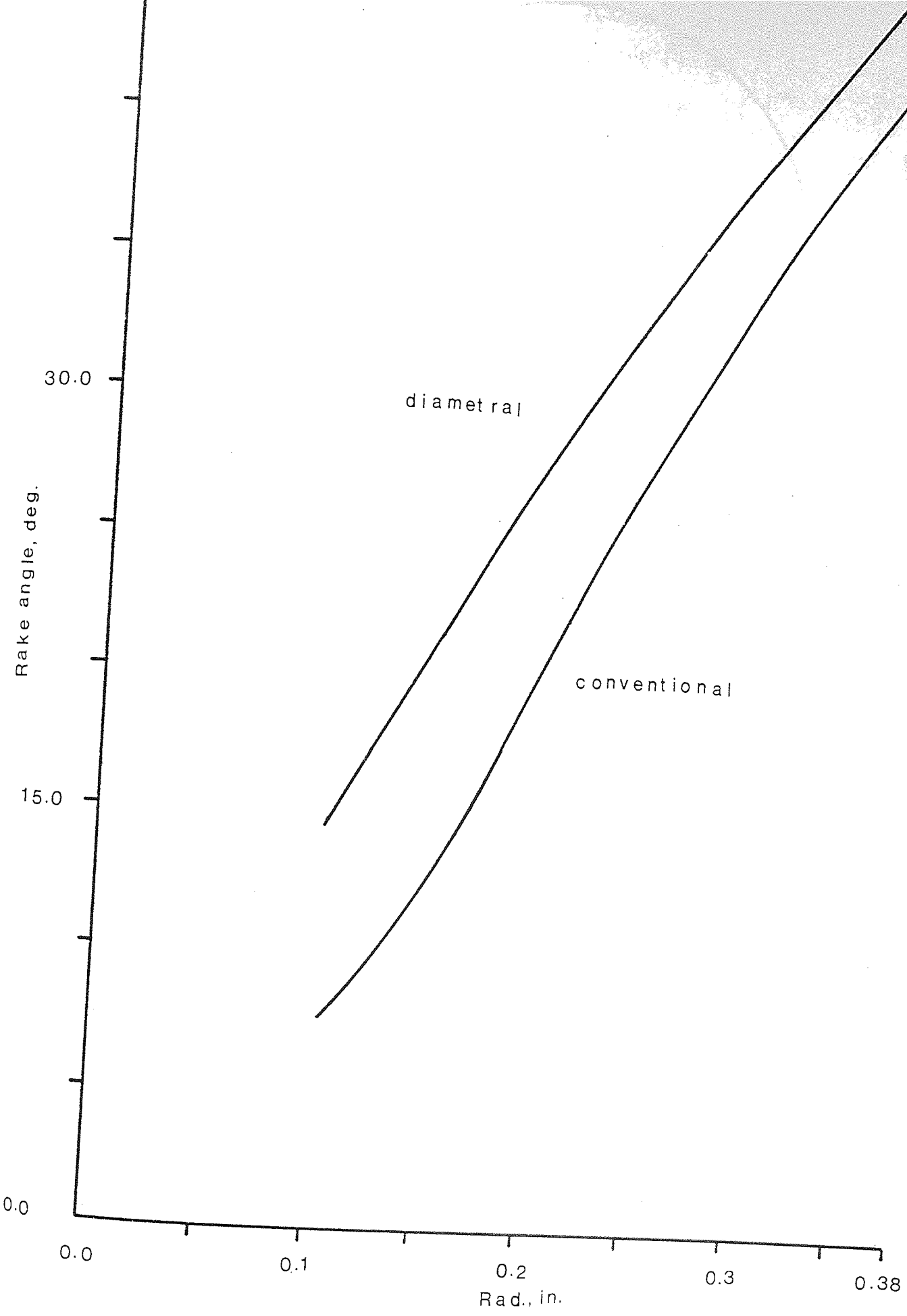

Fig 63 Effective rake angle for conventional and diametral drill

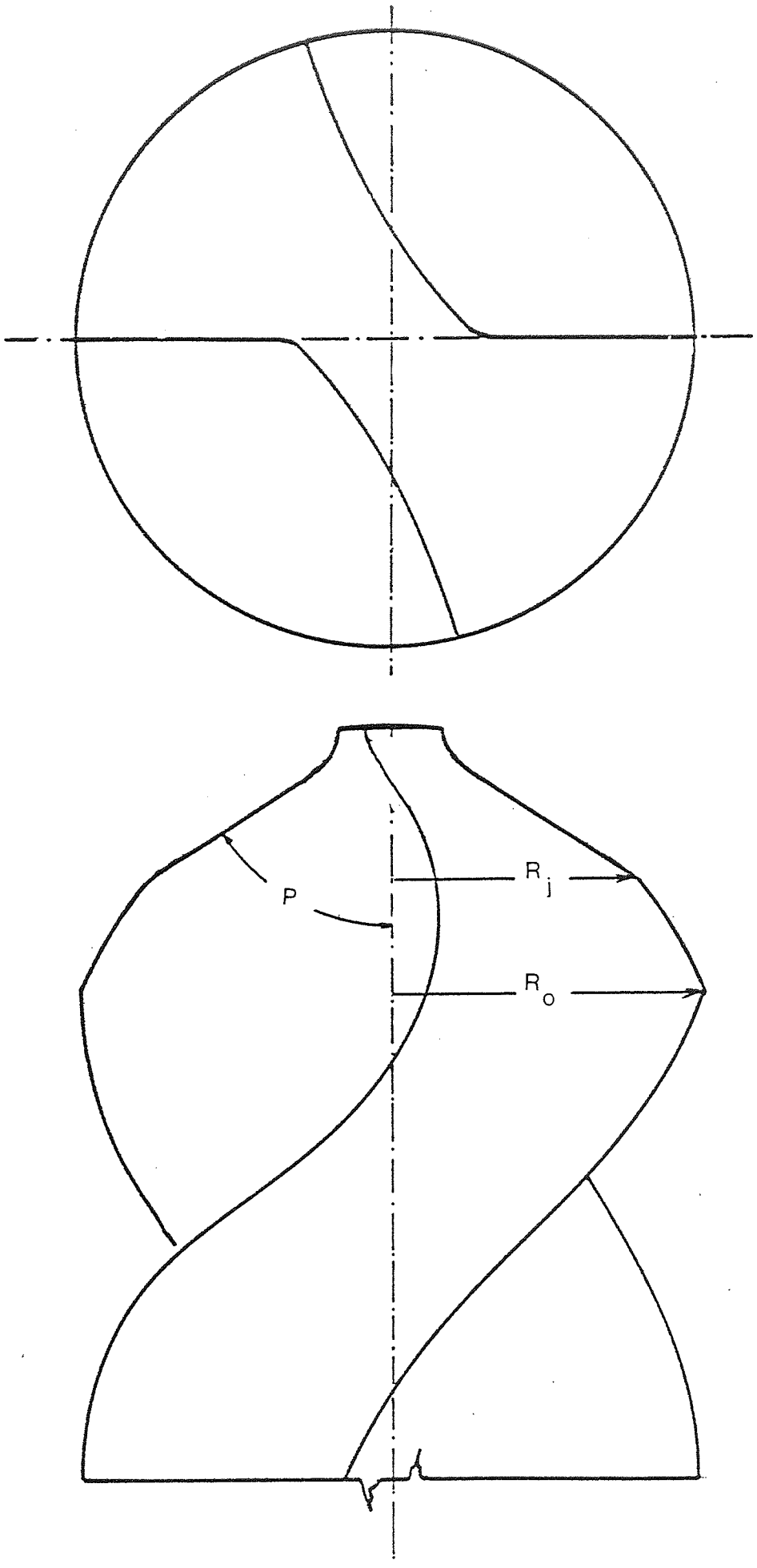

Fig 64 Diametral & partial curved drill

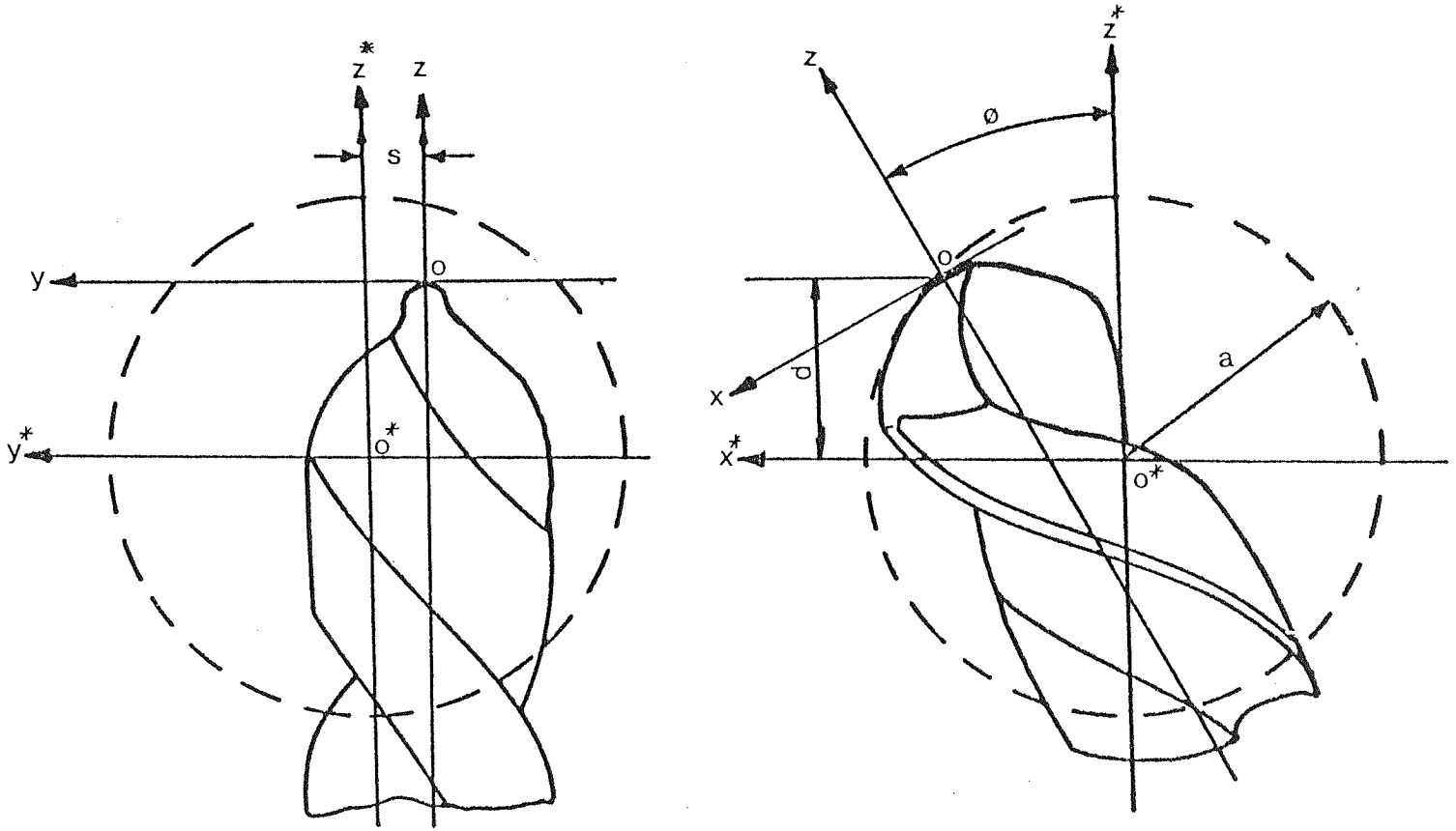

Fig 65 Model for the spherical drill point

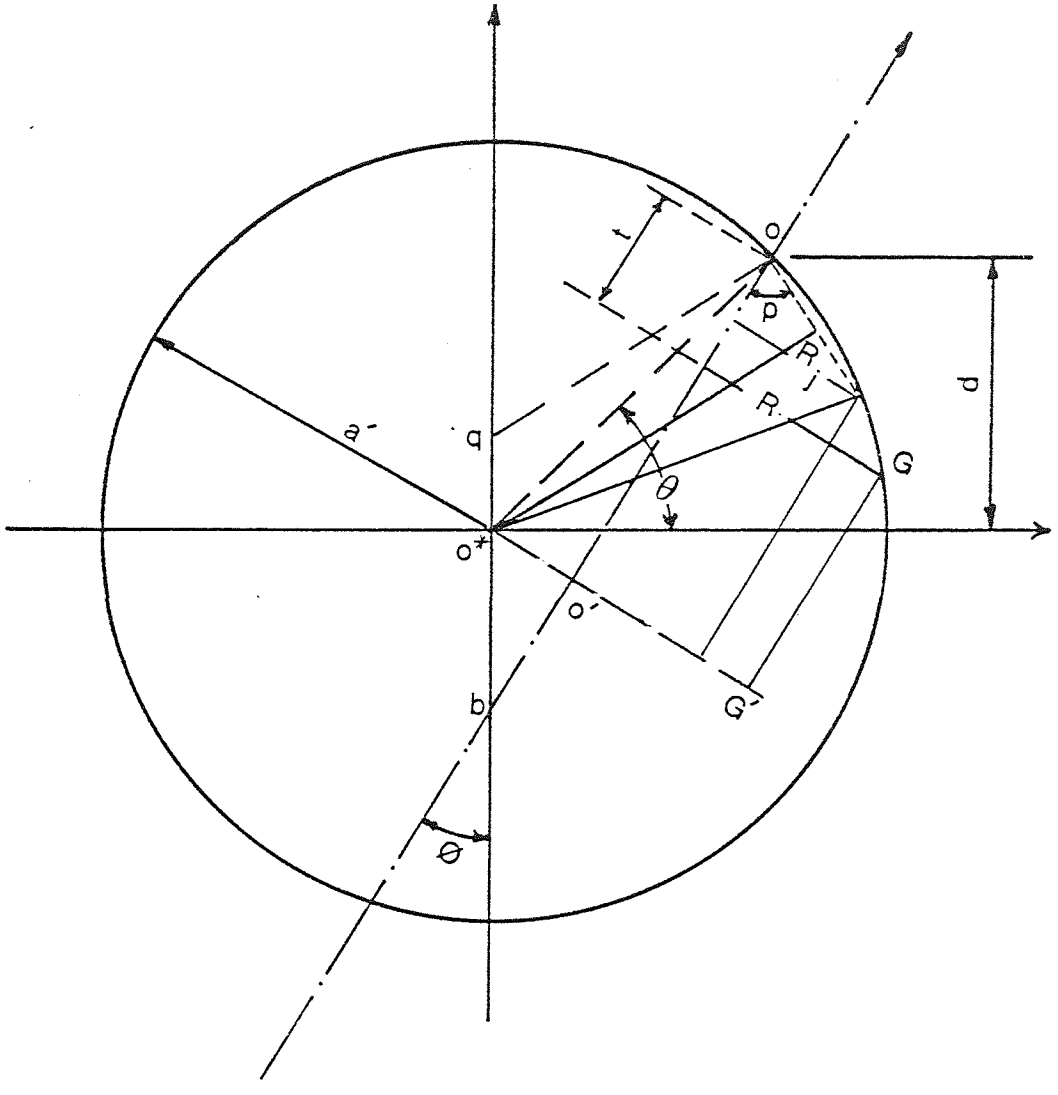

Fig 66 Drill orientation on the grinding surface

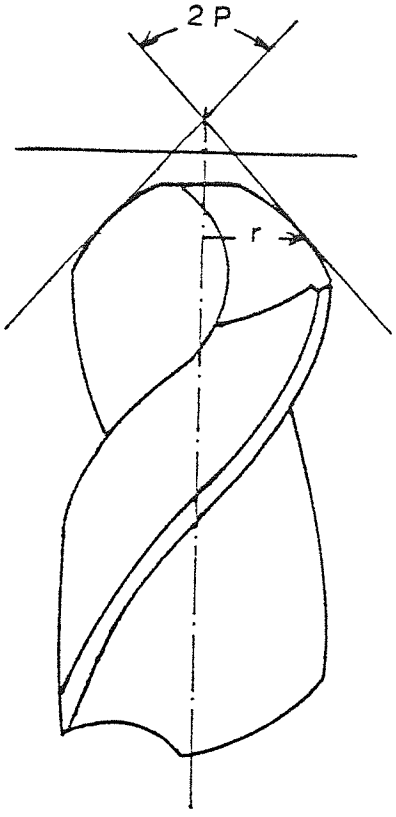

Fig 67.a Included angle

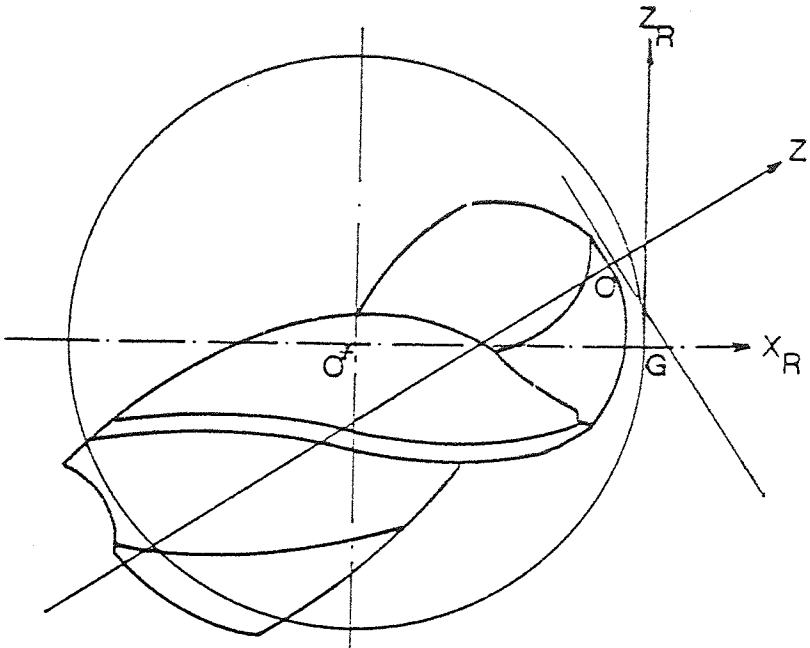

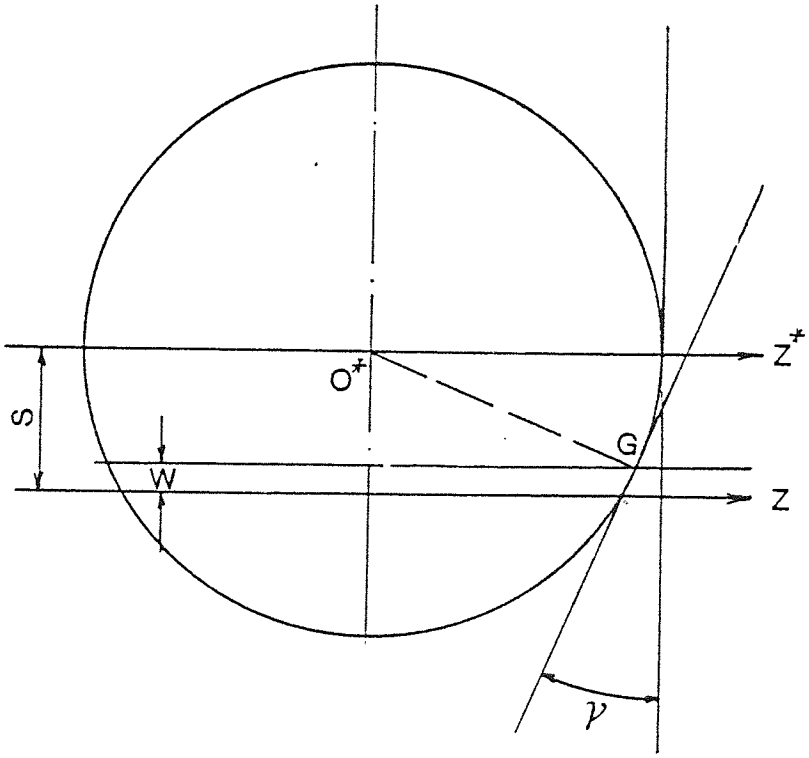

Fig 67.c Clearance angle

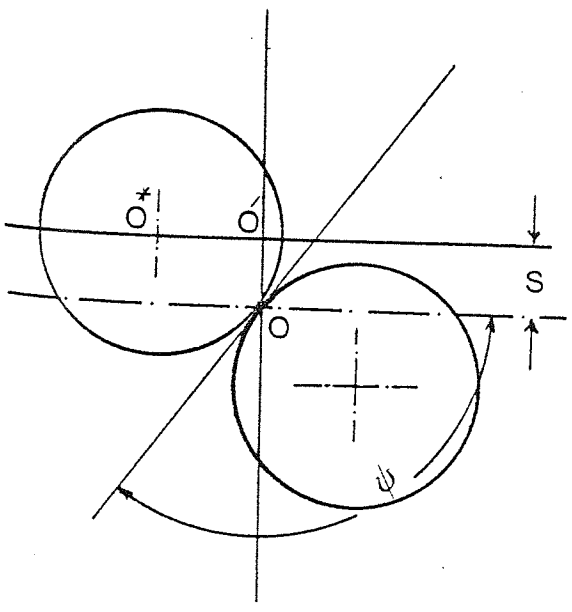

Fig 67.b Chisel edge angle

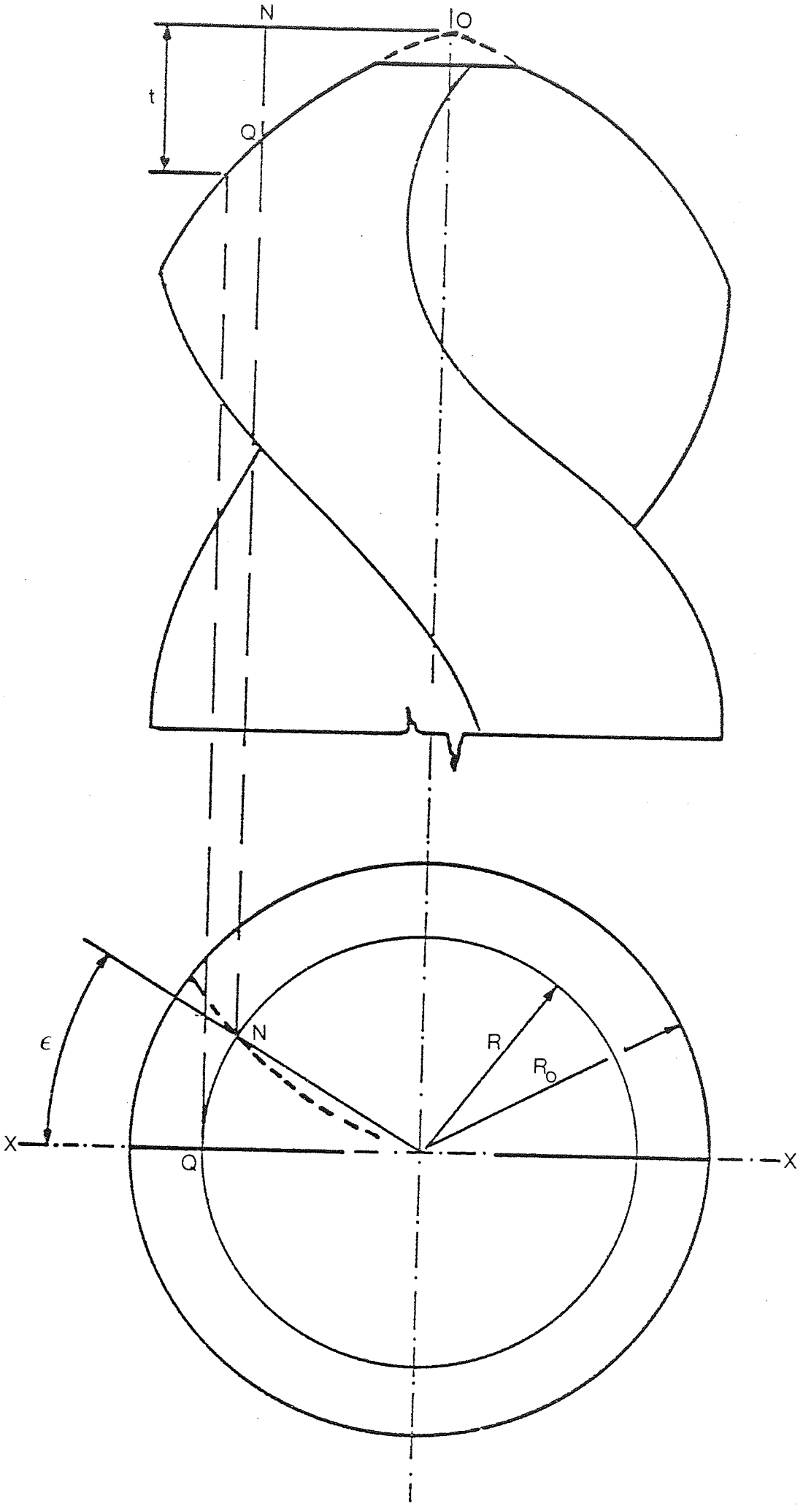

Fig 68 Flute shape for diametrally-curved lip drill

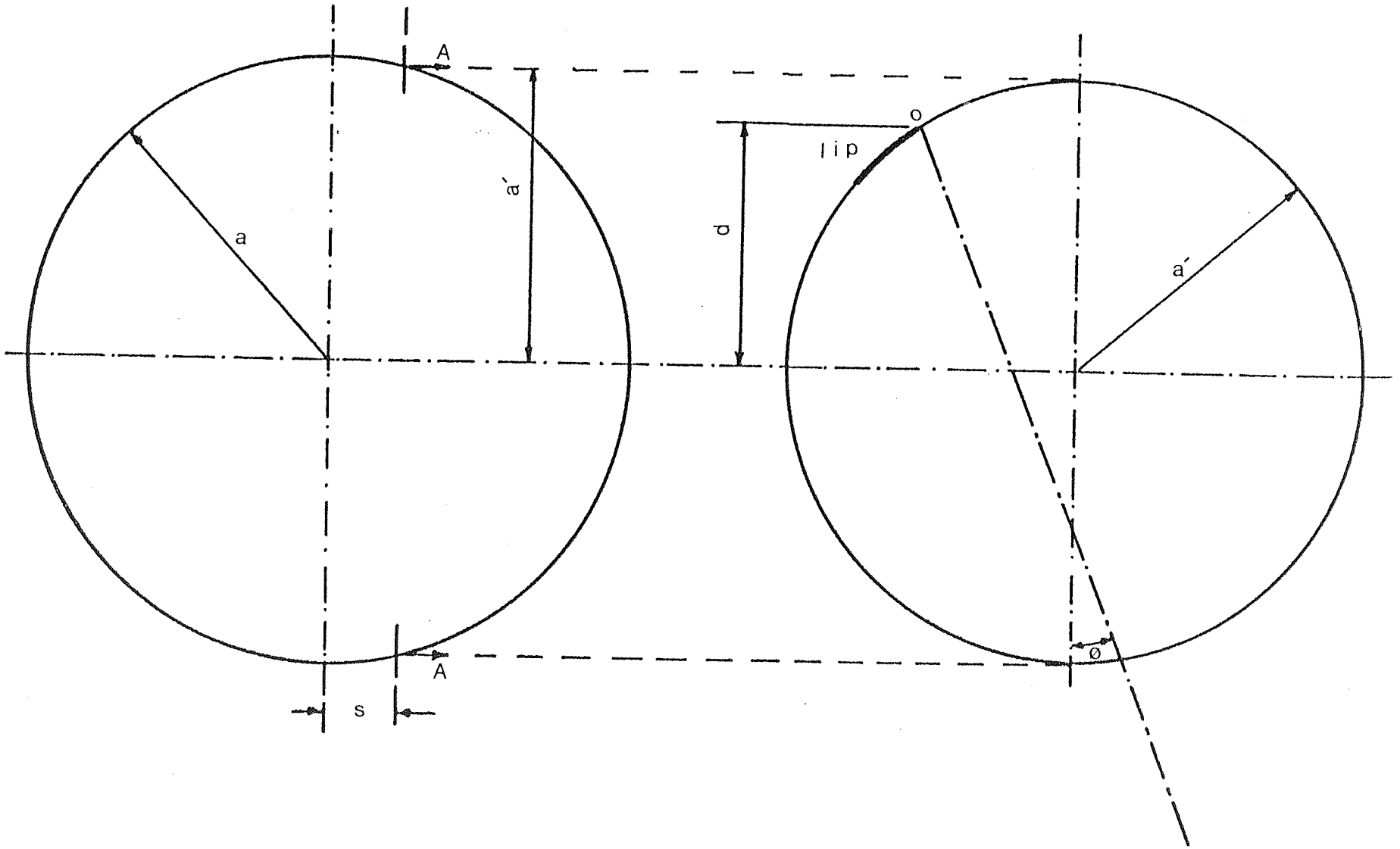

Fig 69 Lip location on the sphere

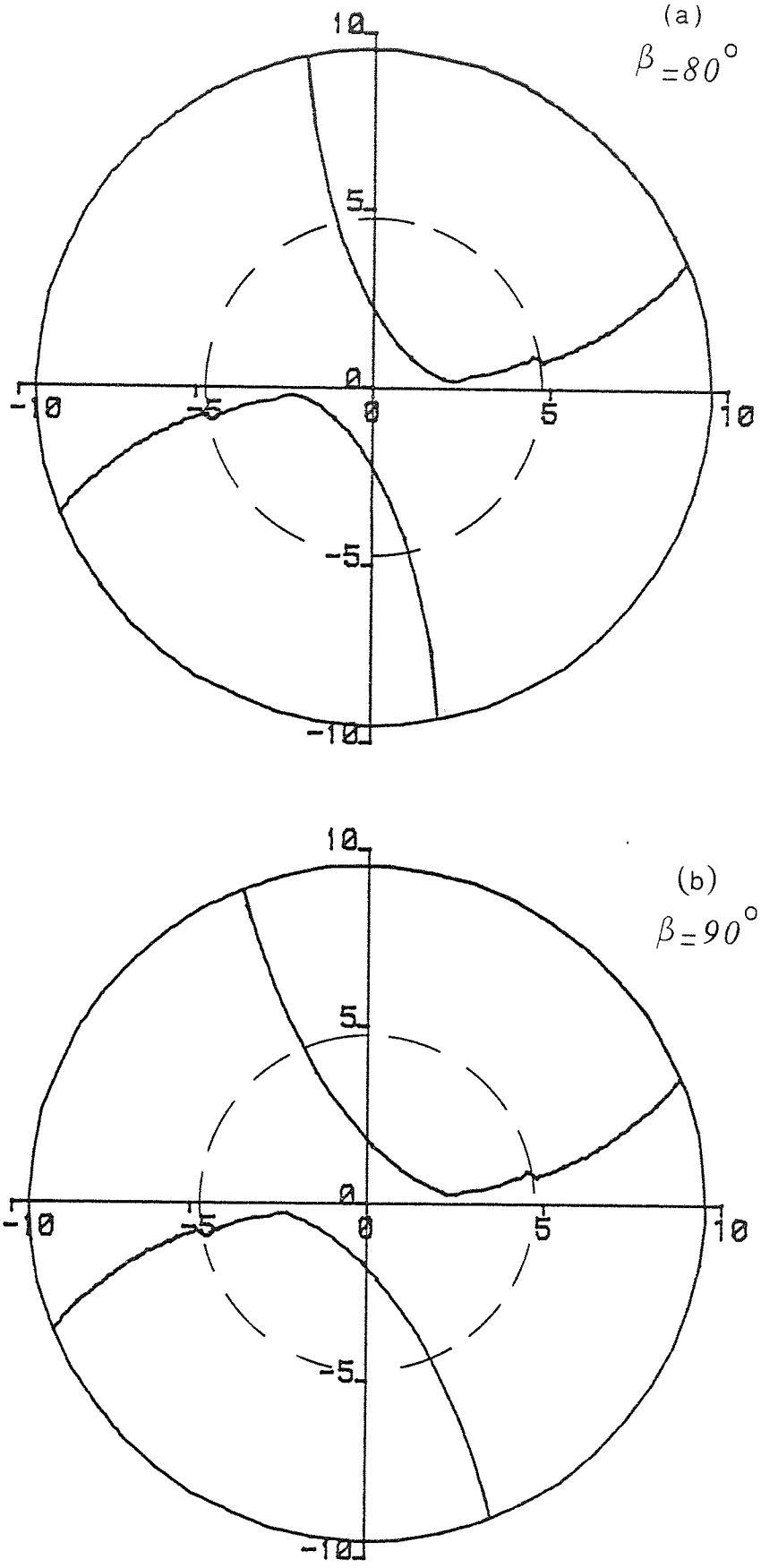

Fig 70 Computer plot of the orthog. Flute (partial curved drill)

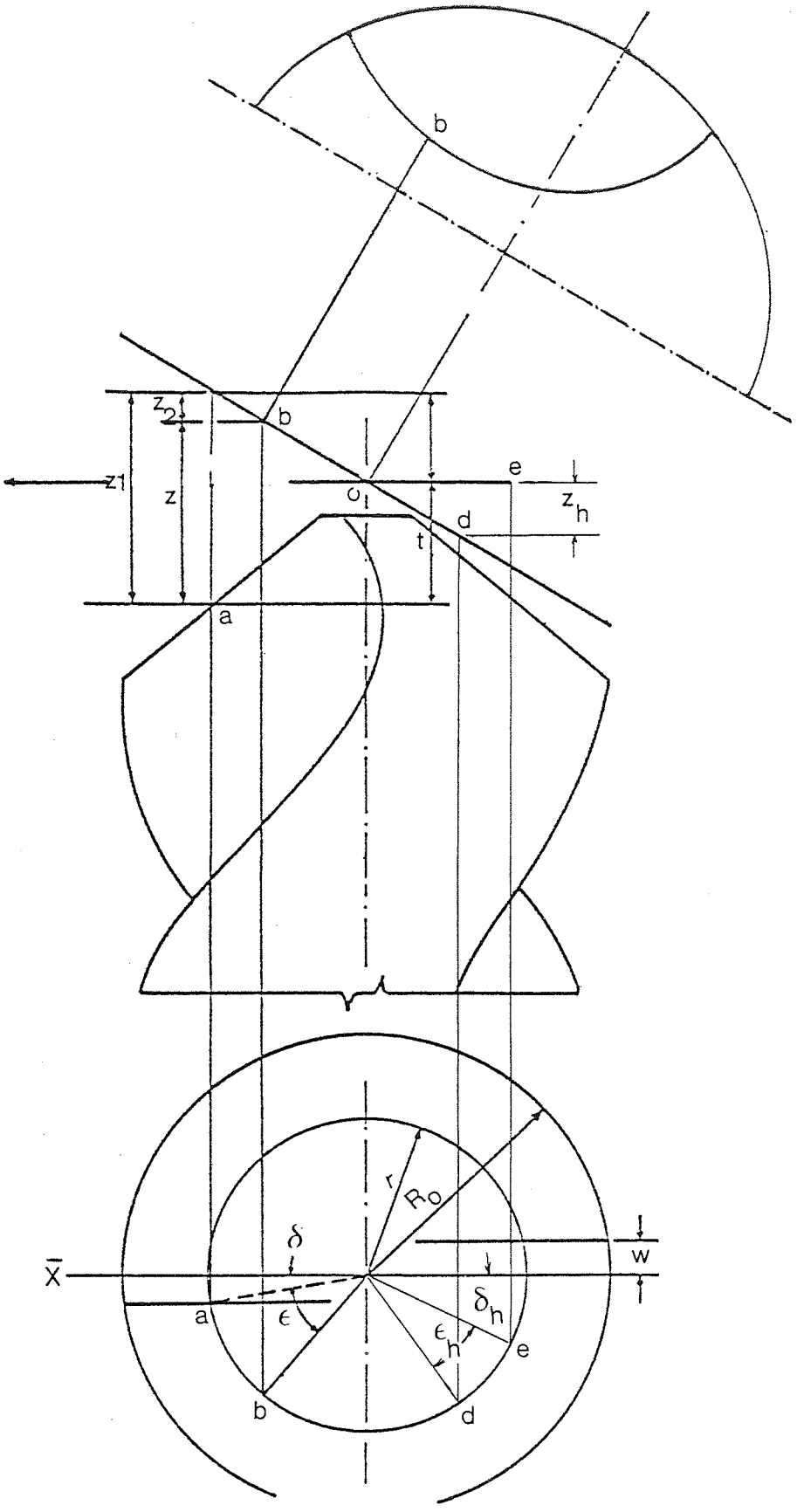

Fig 71 Model for the oblique flute of the conventional drill

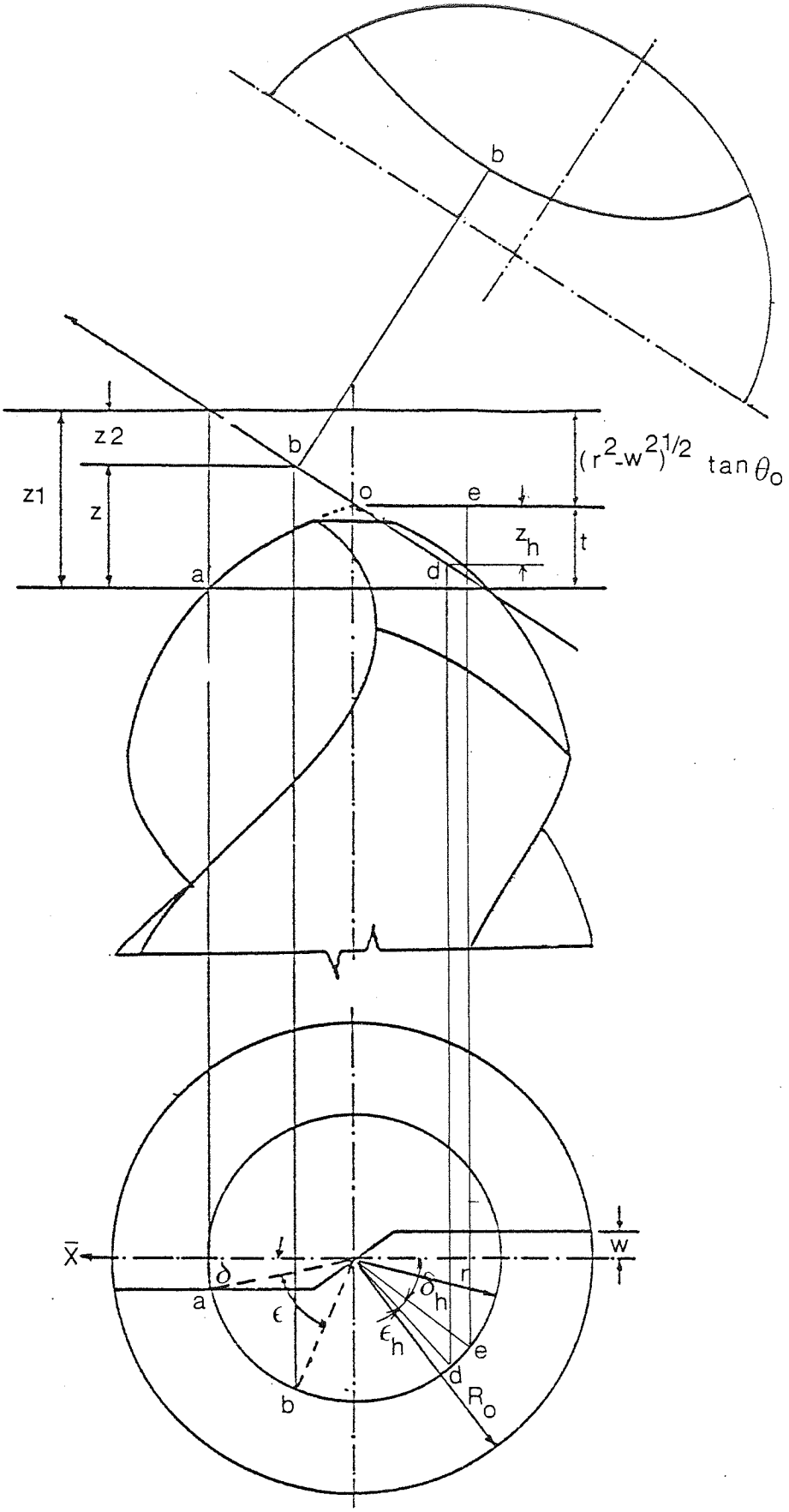

Fig 72 Model for the oblique flute of curved lip drill

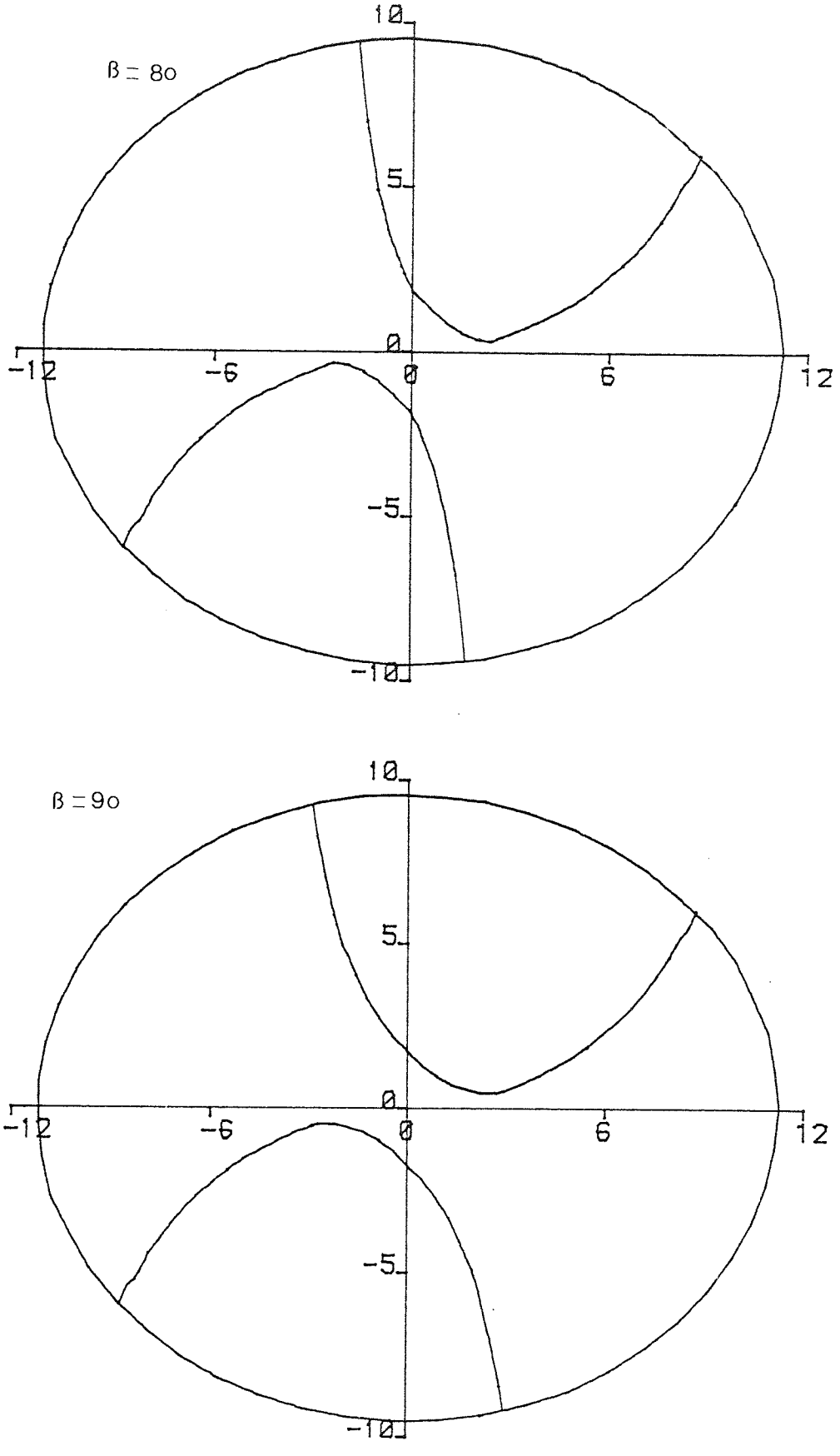

Fig 73 Computer plot of the oblique flute (diametral drill)

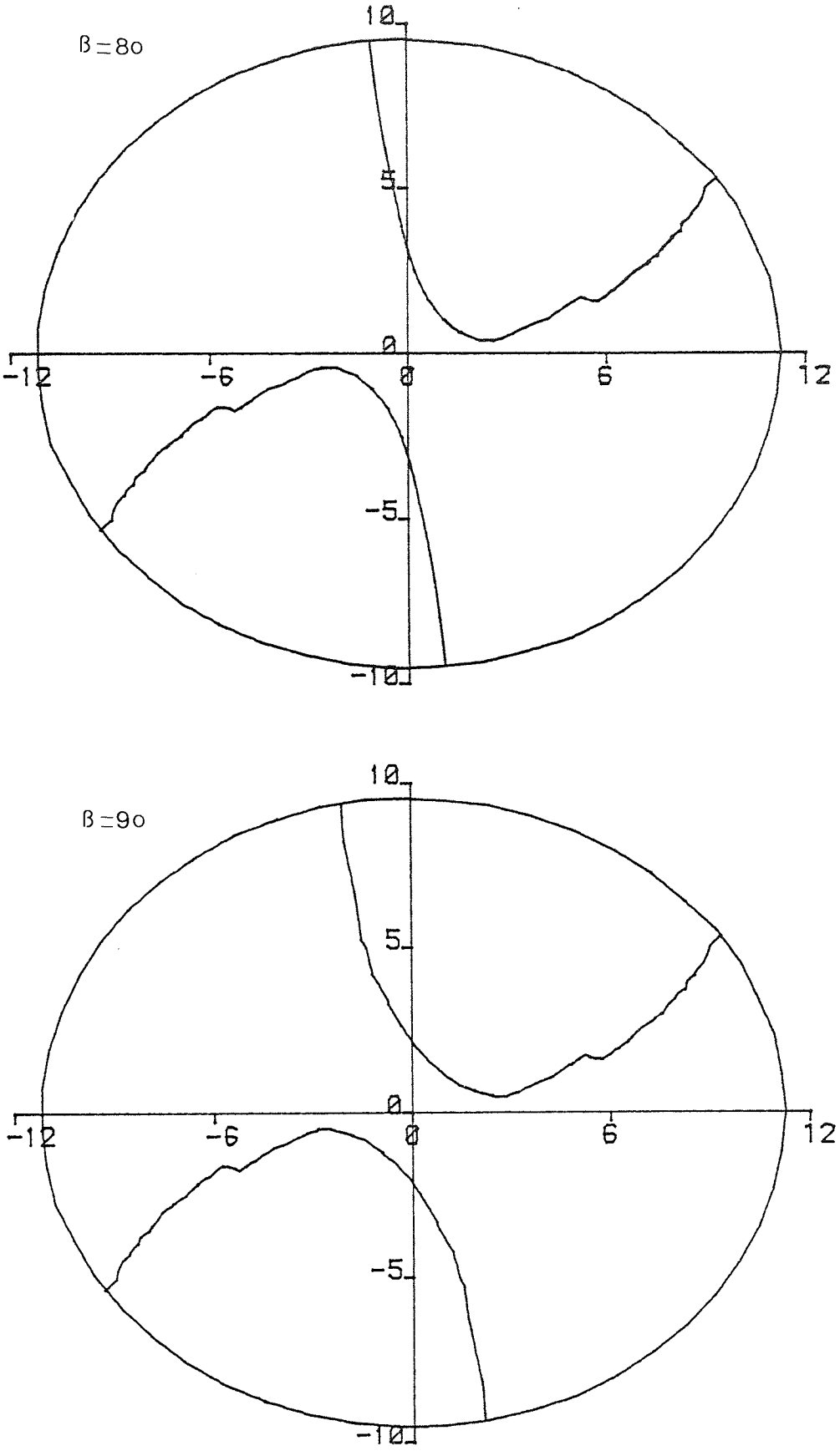

Fig 74 Computer plot of the oblique flute (partial curved drill)

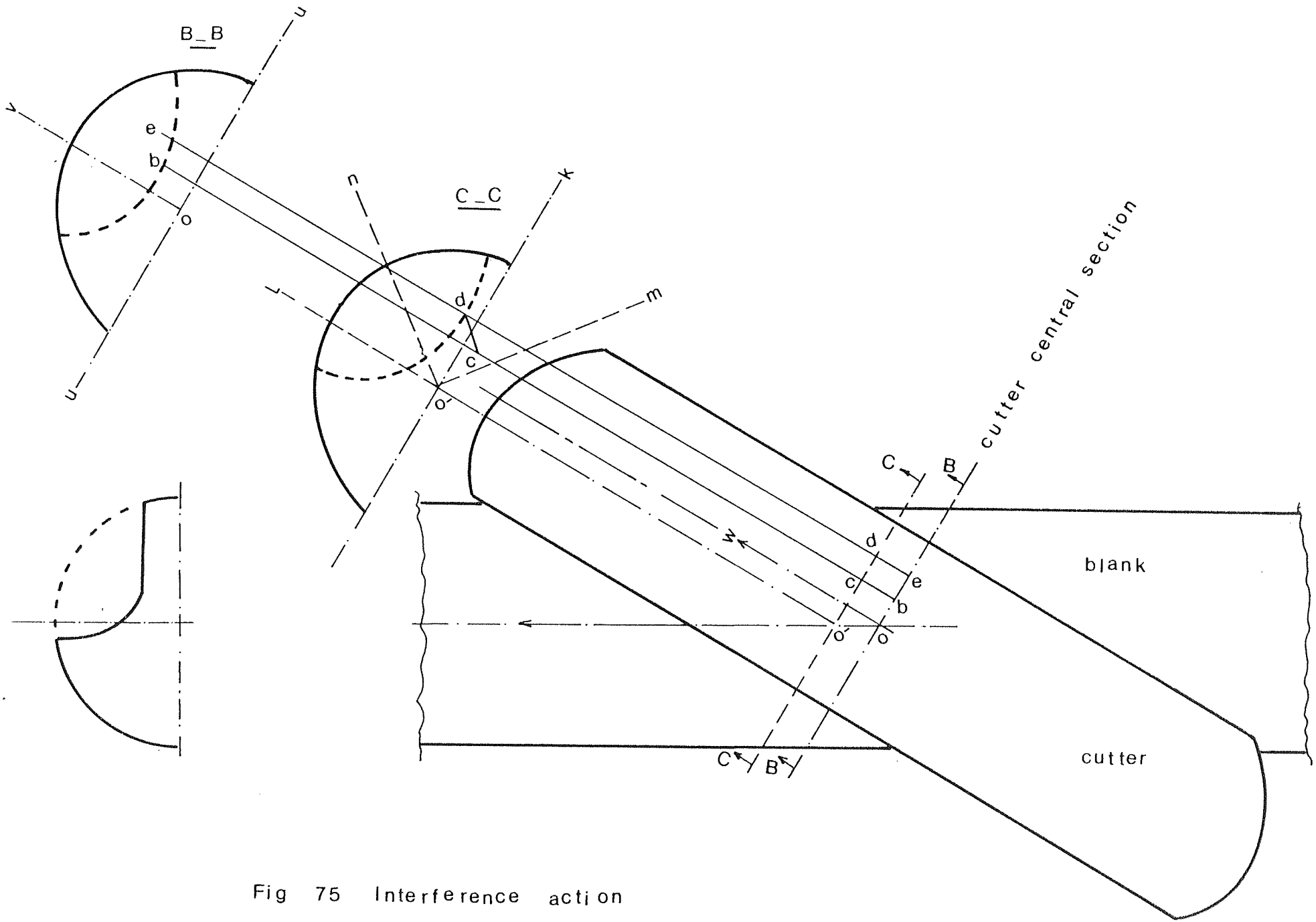

Fig 75 Interference action

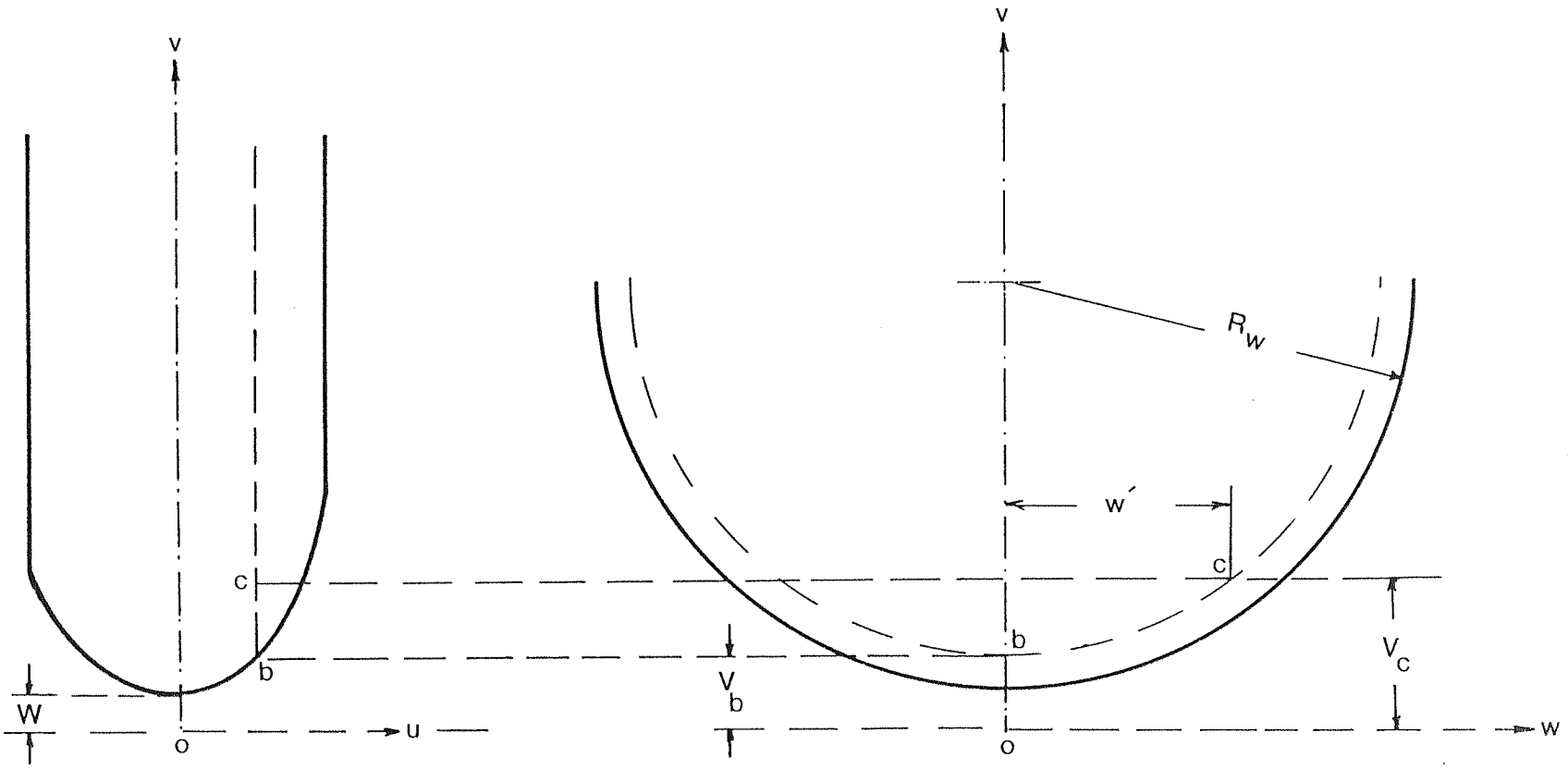

Fig 76 Cutter shape presentation

- - - Cutter at plane $w' = -4.8$

—— Theoretical flute profile

2Ro = 3/4 Inch

Web = 2.46 mm

Helix = 32 deg

Point = 118 deg

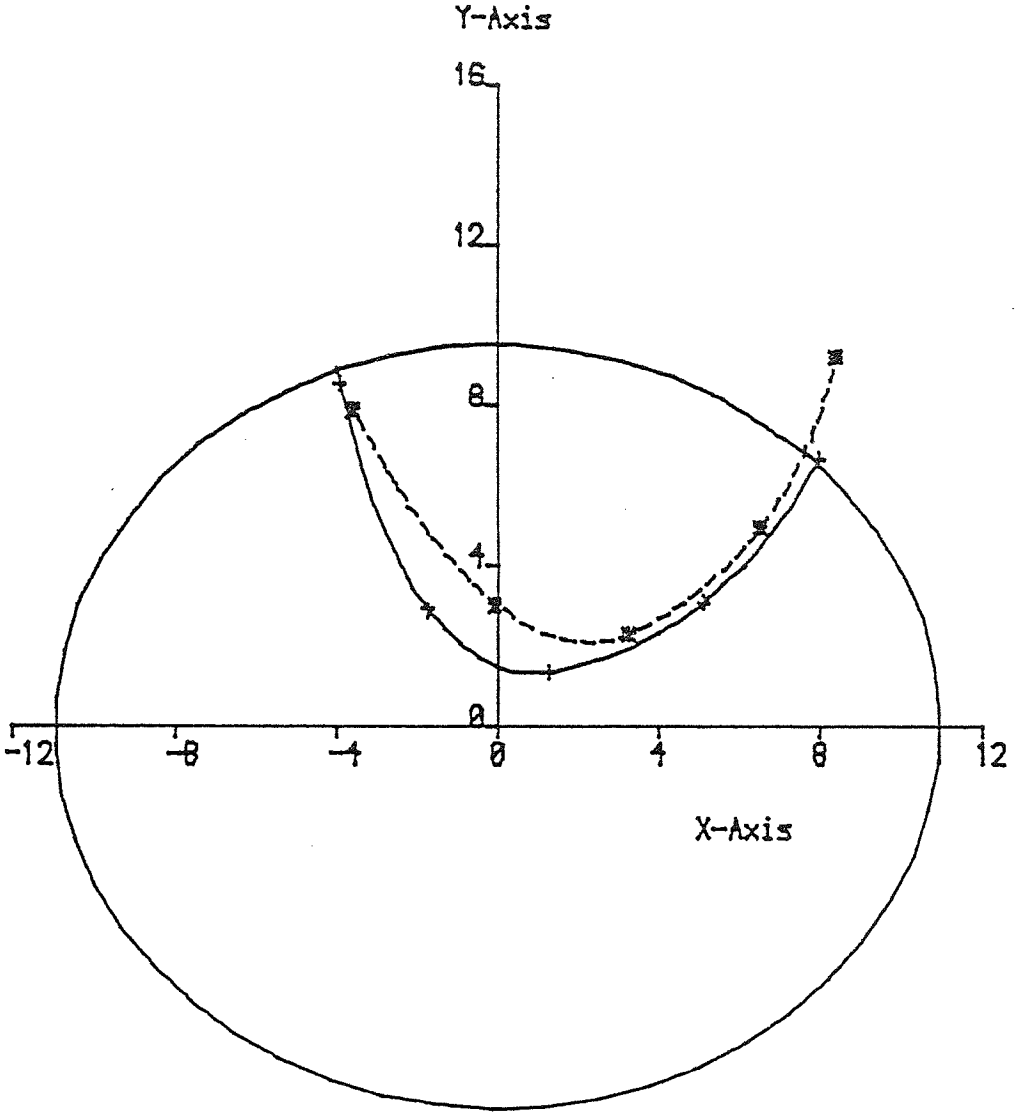

Figure(77.a)intersection of cutter and flute profile

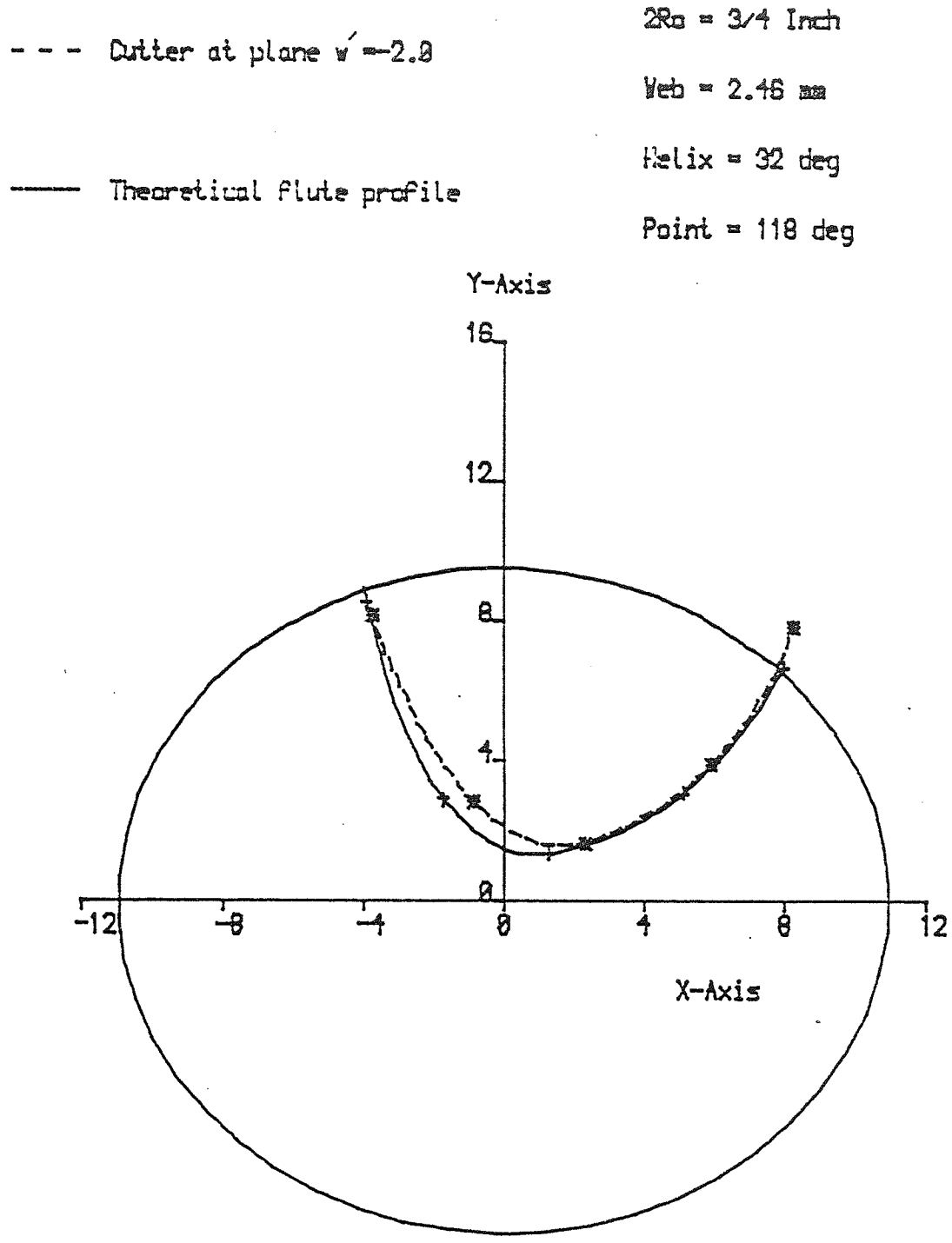

Figure(77.b) intersection of cutter and flute profile

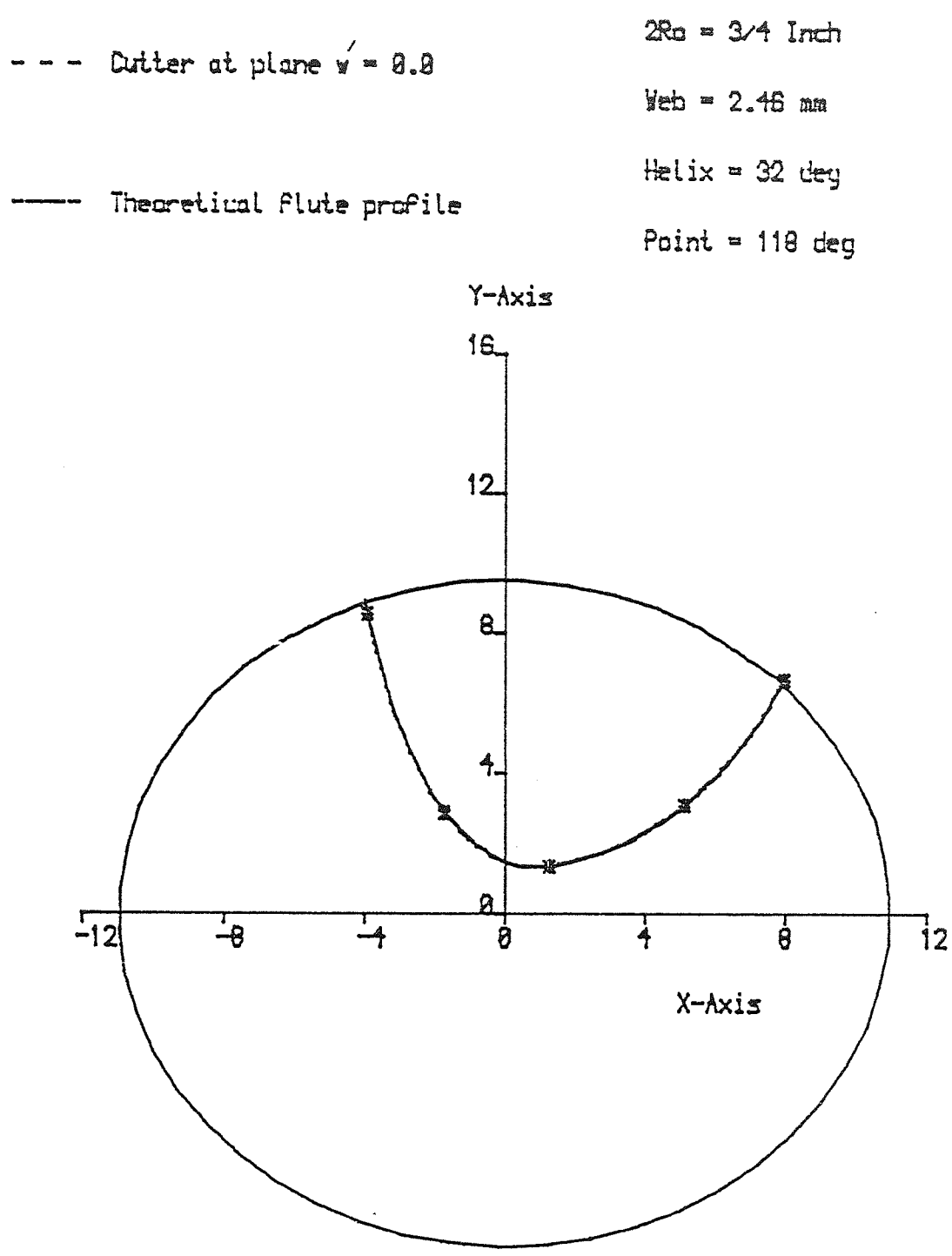

Figure (7.7.c) intersection of cutter and flute profile

- - - Cutter at plane w' = 2.8

——— Theoretical flute profile

2Ro = 3/4 Inch

Web = 2.46 mm

Helix = 32 deg

Point = 118 deg

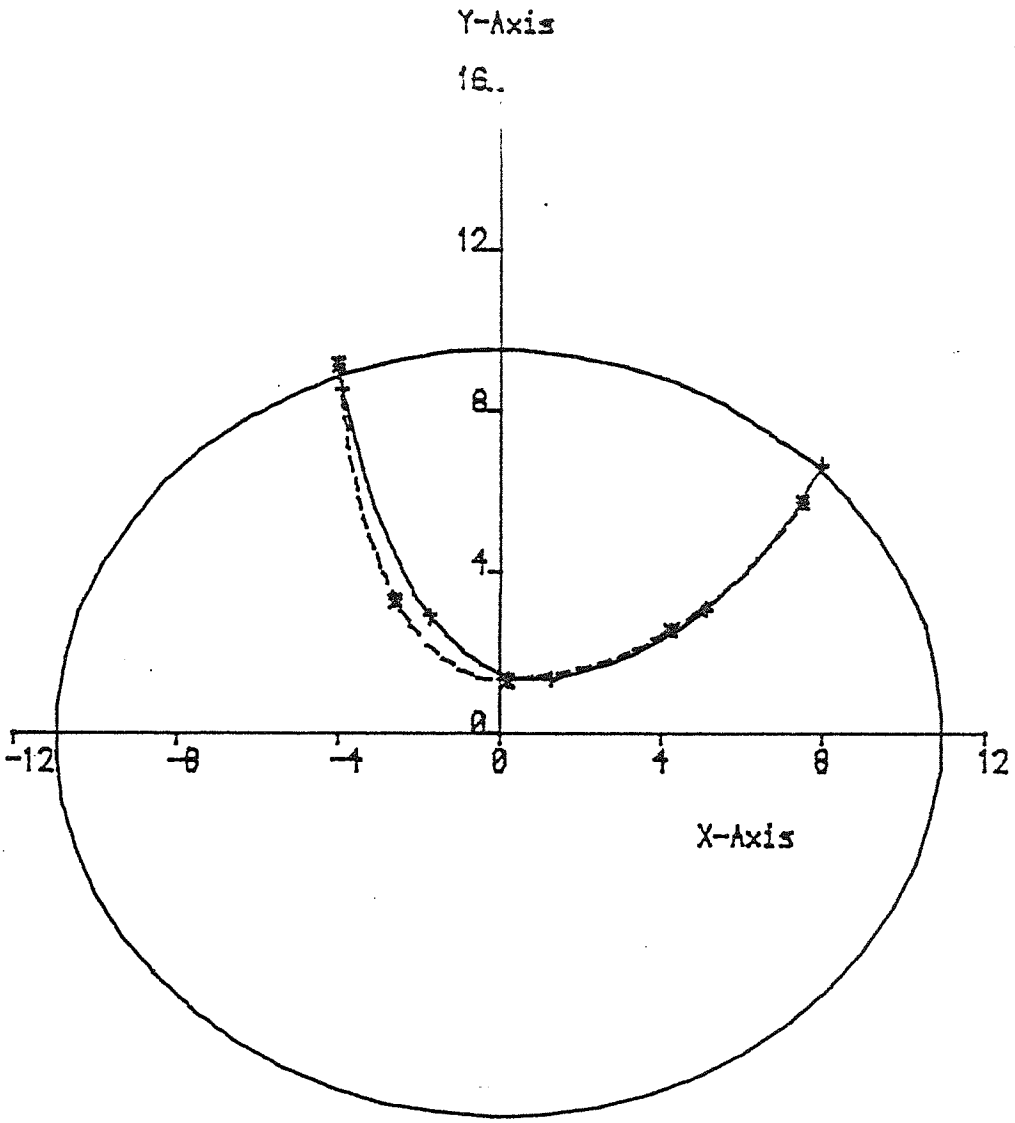

Figure(77.d)intersection of cutter and flute profile

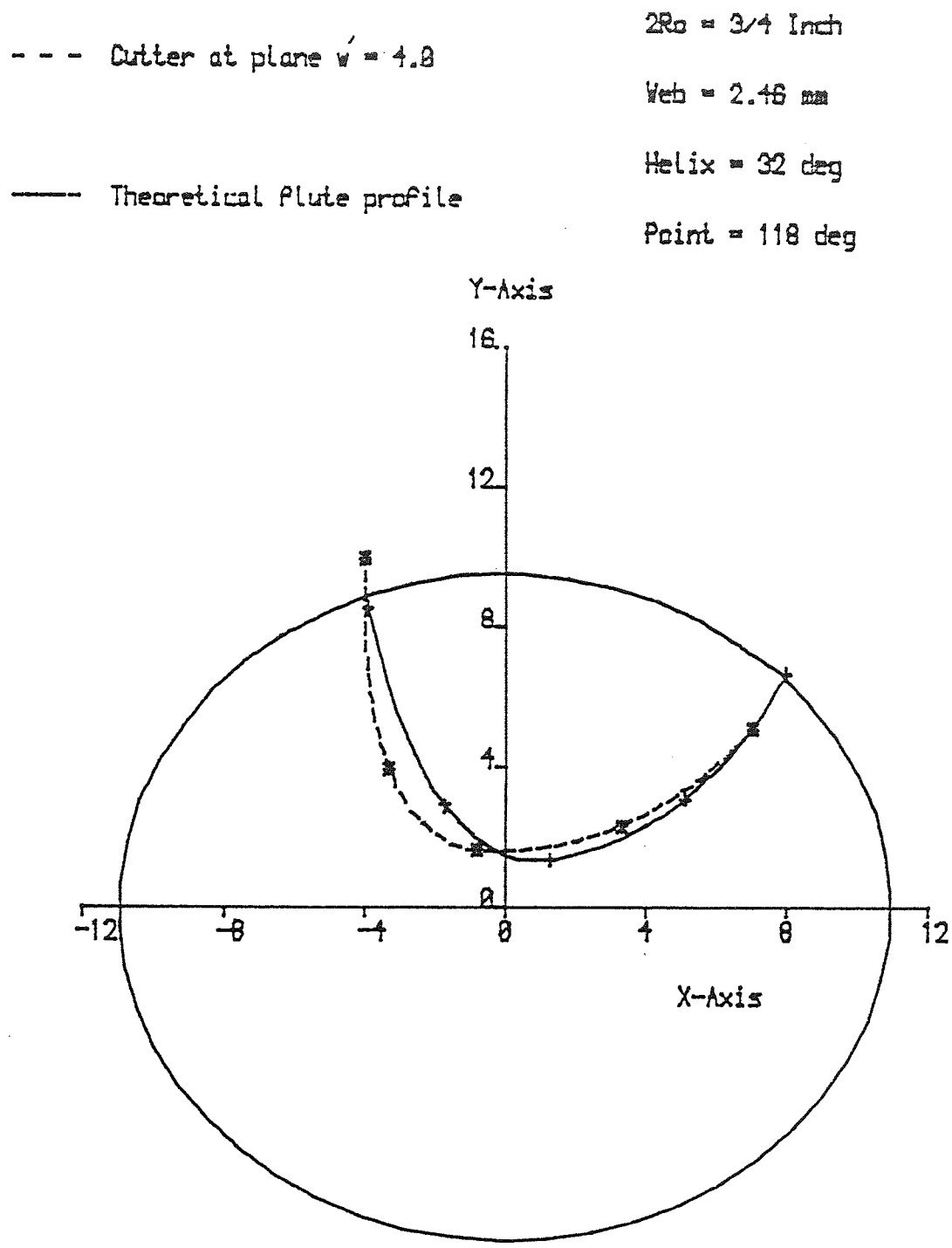

Figure(7 7. e) intersection of cutter and flute profile

- - - Cutter at plane $w' = 6.8$

——— Theoretical flute profile

2Ro = 3/4 Inch

Web = 2.46 mm

Helix = 32 deg

Point = 118 deg

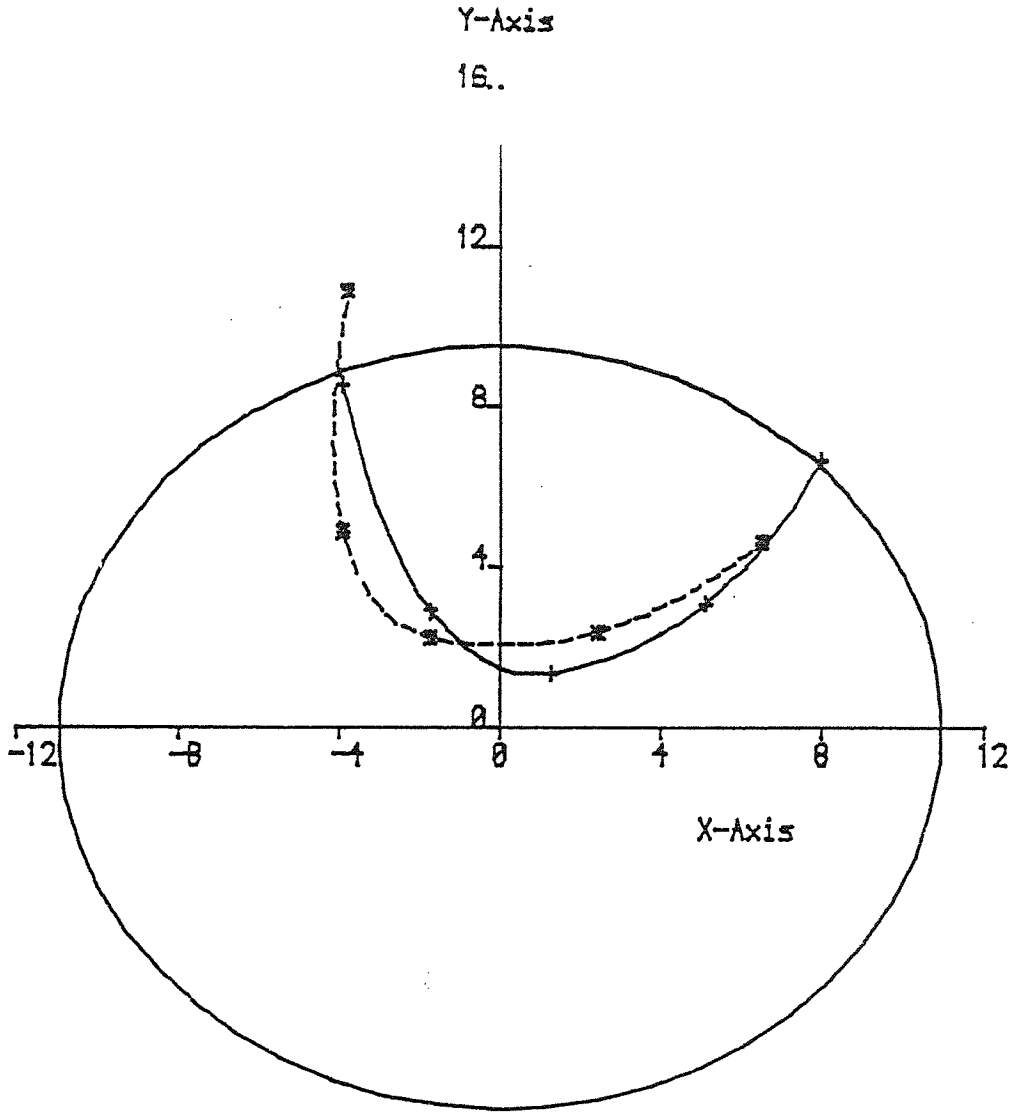

Figure(7.7.f) intersection of cutter and flute profile

- - - Cutter at plane w = 8.0

——— Theoretical flute profile

2Ro = 3/4 Inch

Web = 2.46 mm

Helix = 32 deg

Point = 118 deg

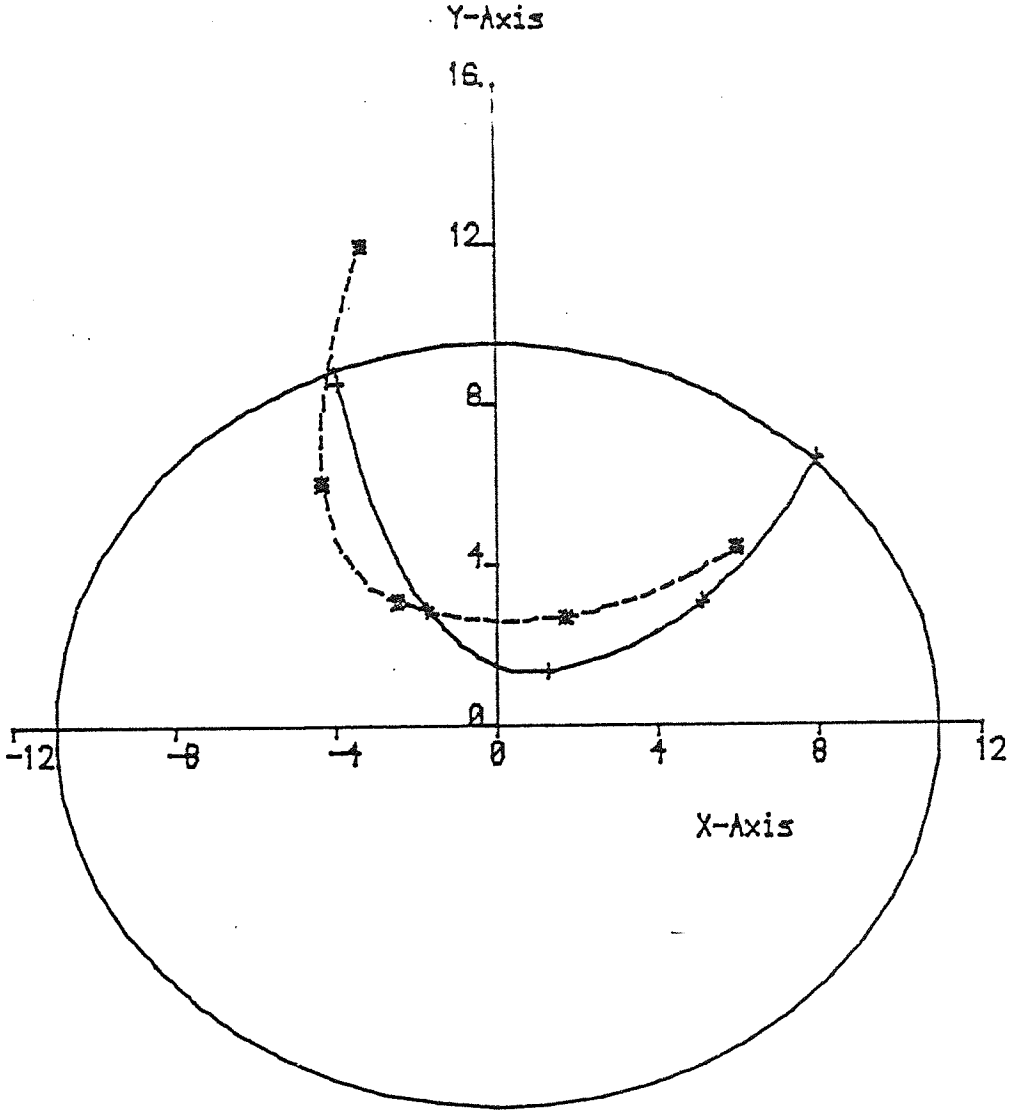

Figure (7.9) intersection of cutter and flute profile

2Ro = 3/4 Inch

- - - Cutter at plane w = 10.0

Web = 2.46 mm

Helix = 32 deg

——— Theoretical flute profile

Point = 118 deg

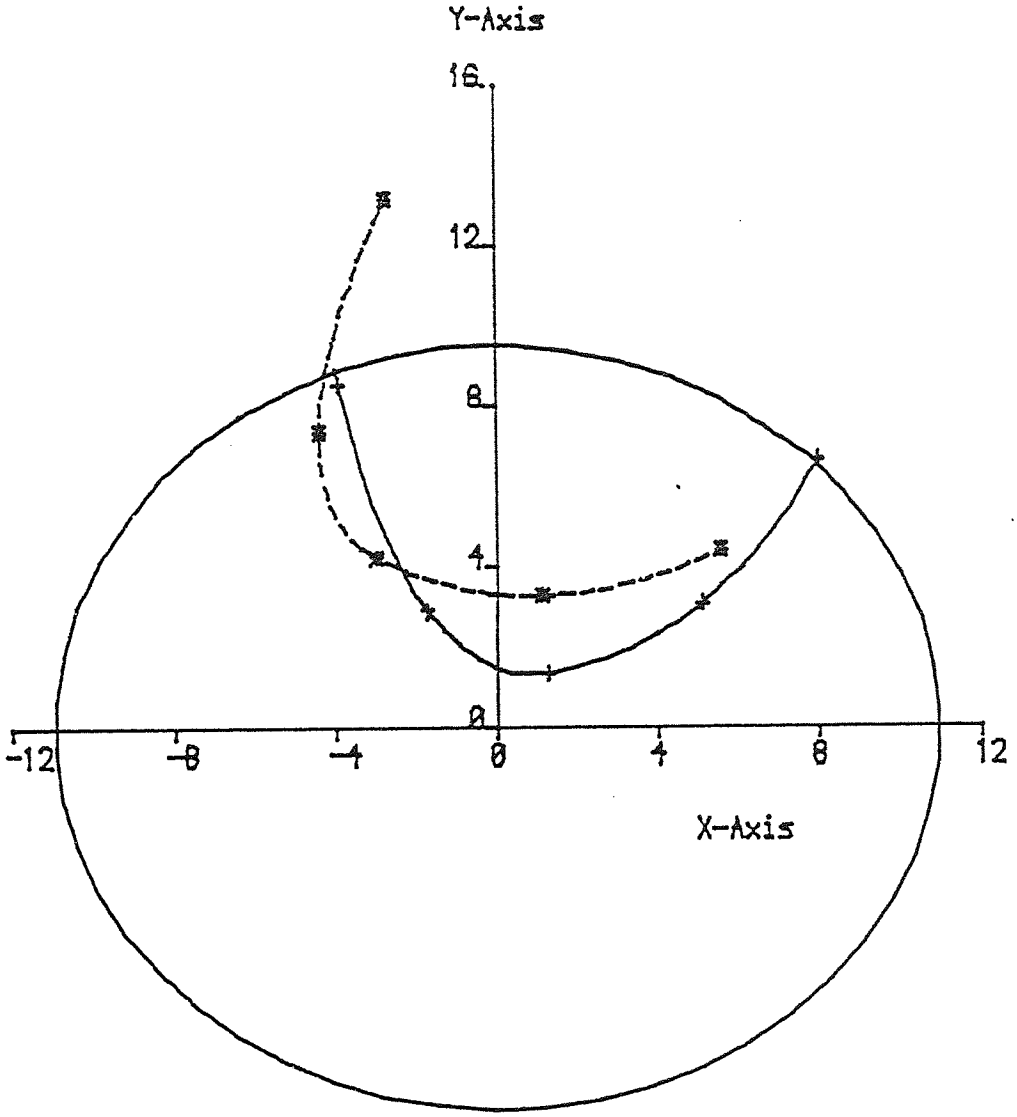

Figure(77.h) intersection of cutter and flute profile

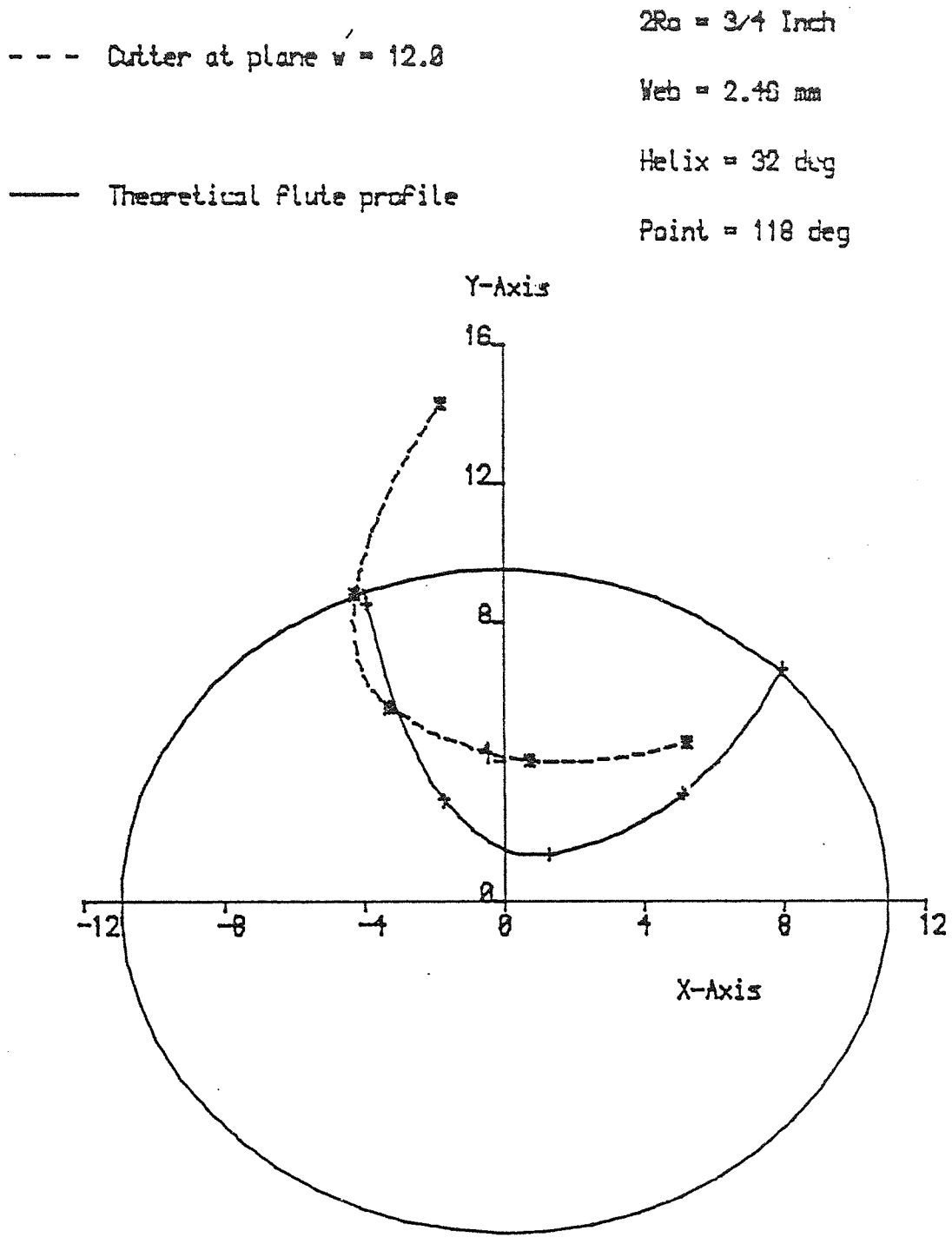

Figure(7.7.1) intersection of cutter and flute profile

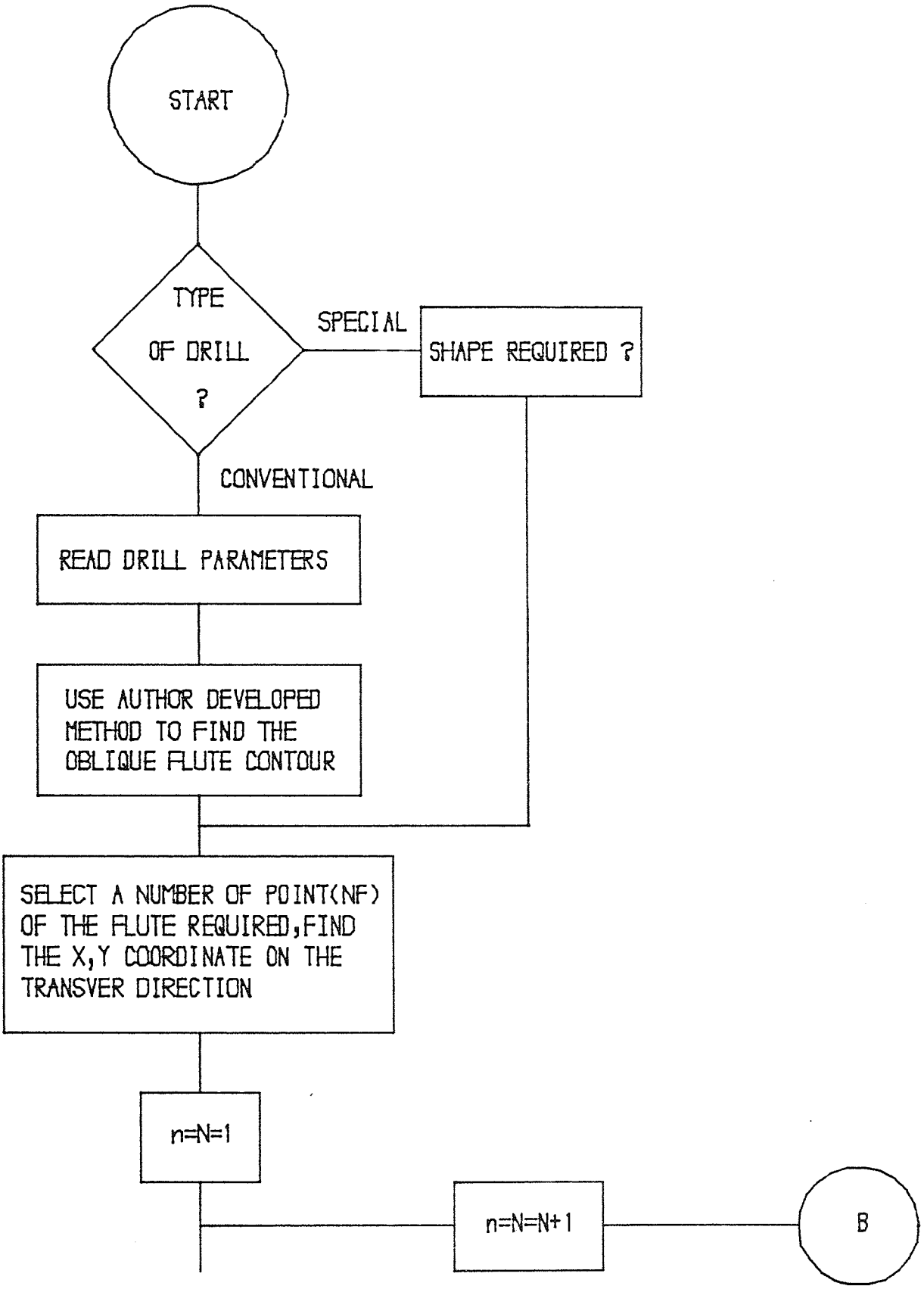

FIGURE 78 (CONTINUED)

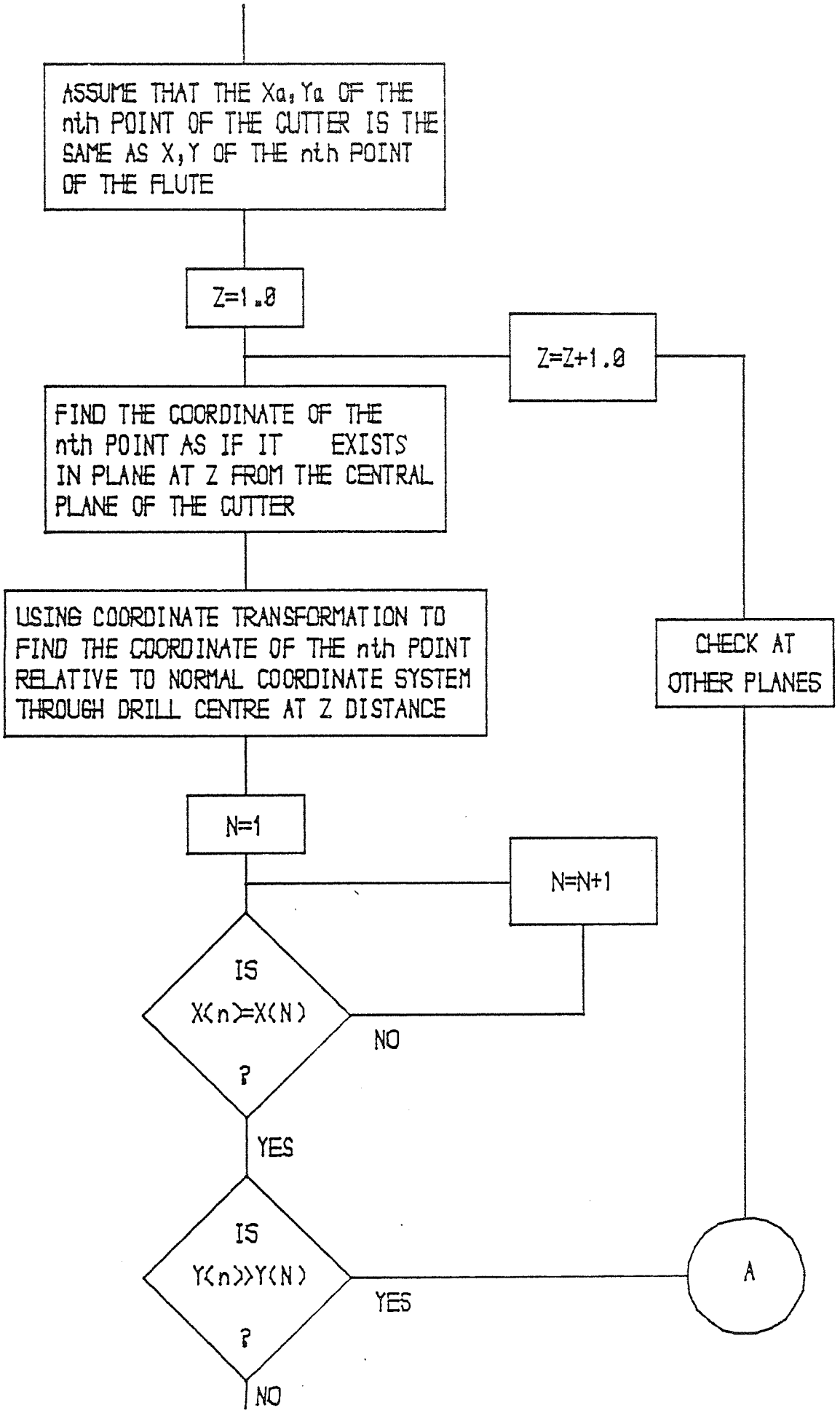

FIGURE 78 (CONTINUED)

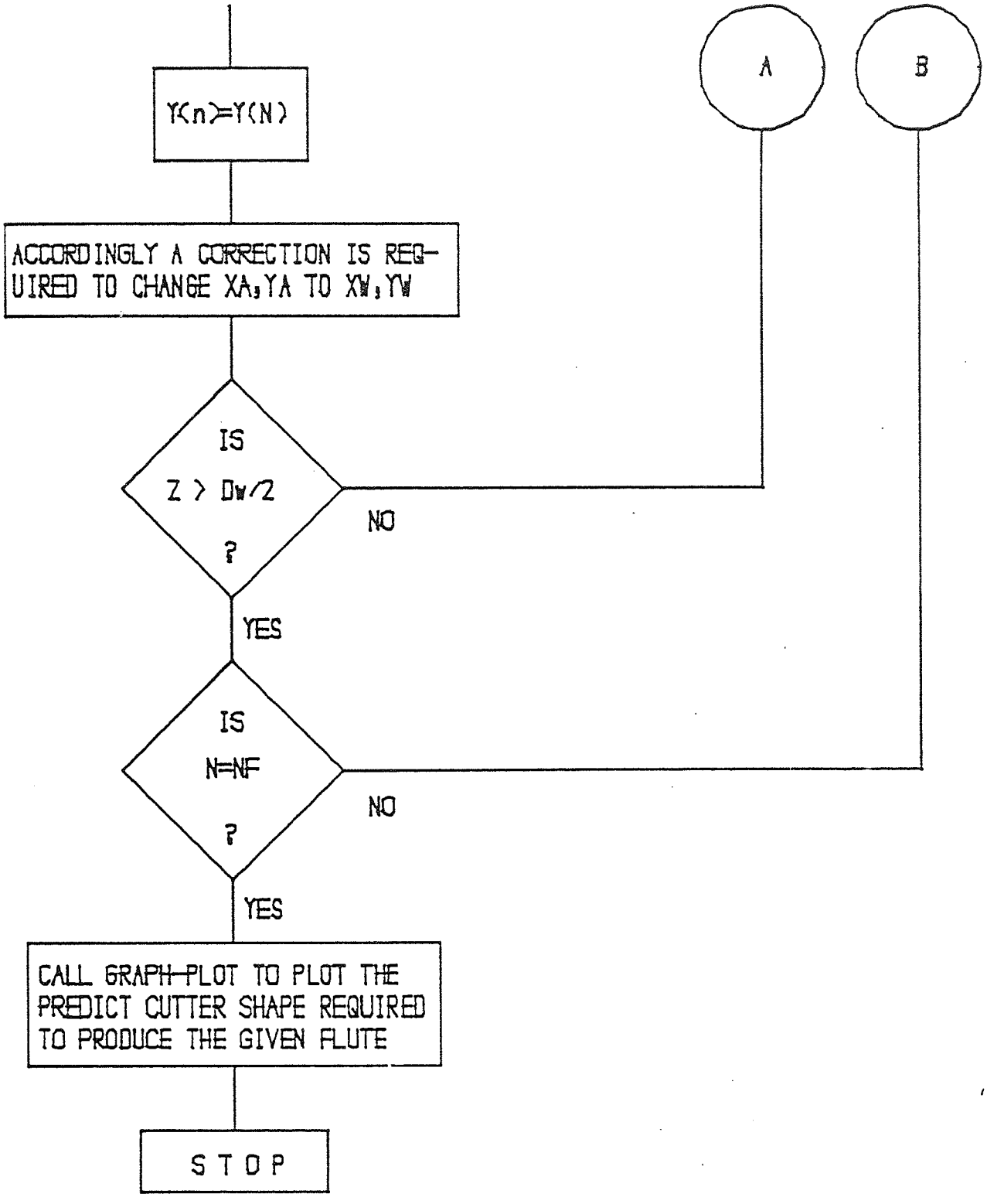

Figure 78 Flow diagram For the computer program for cutter prediction

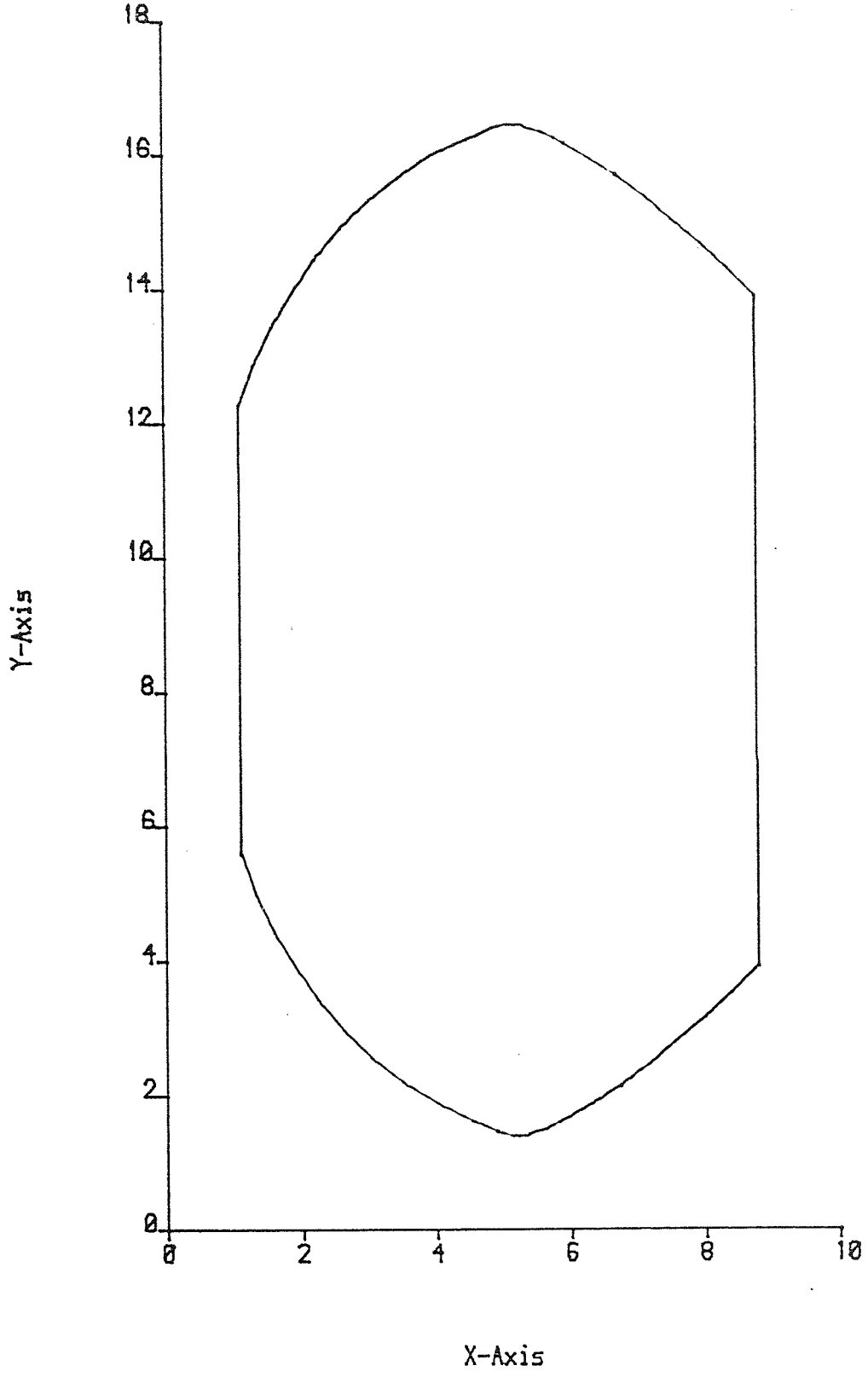

Figure 79.a computer prediction of the cutter shape for the diam. drill in fig.58. a

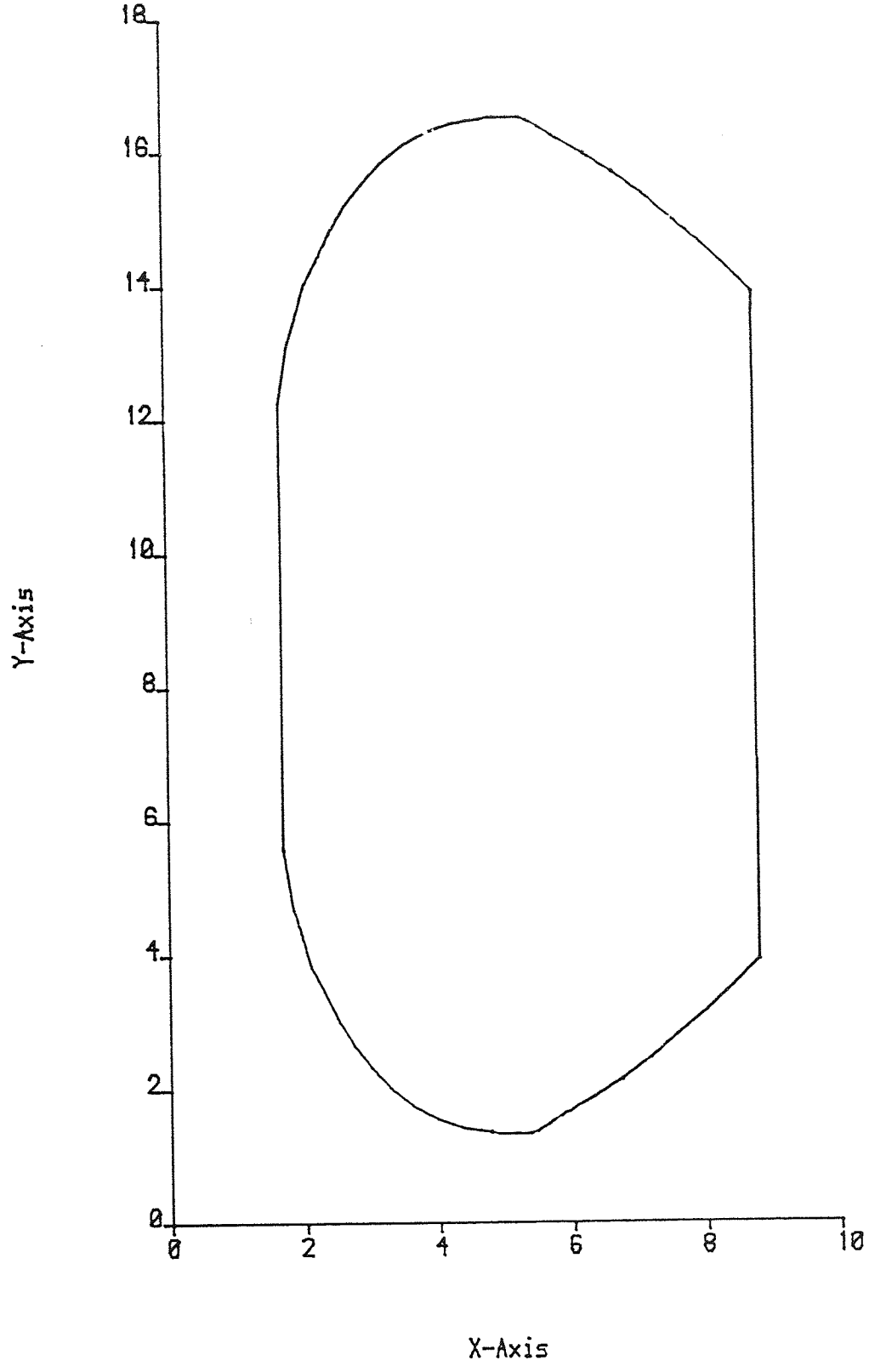

Figure 79.b computer prediction of the cutter shape for the diam. drill in fig. 58.b

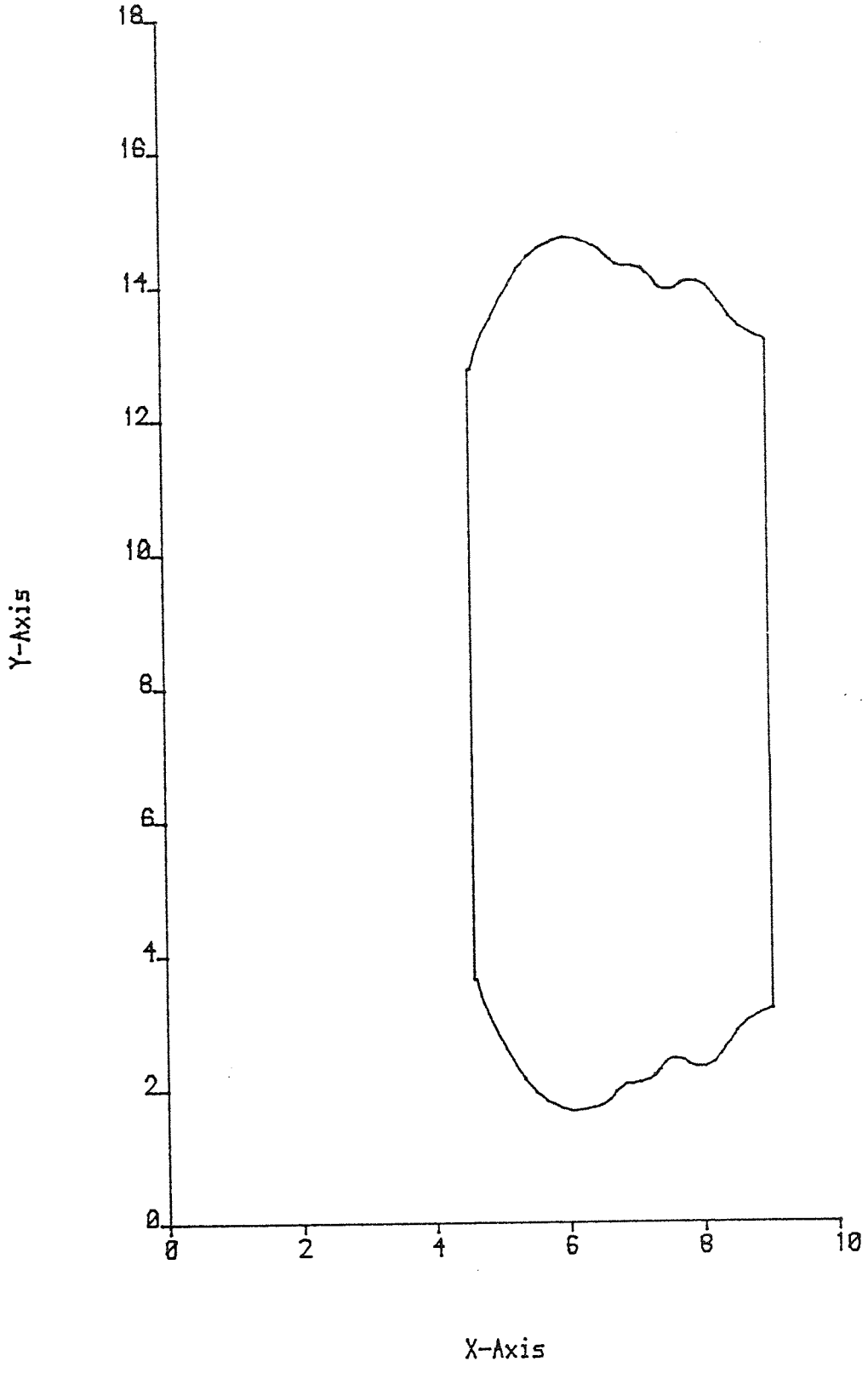

Fig(80.a)computer prediction of the cutter shape for the part. curved drill in fig.70.a

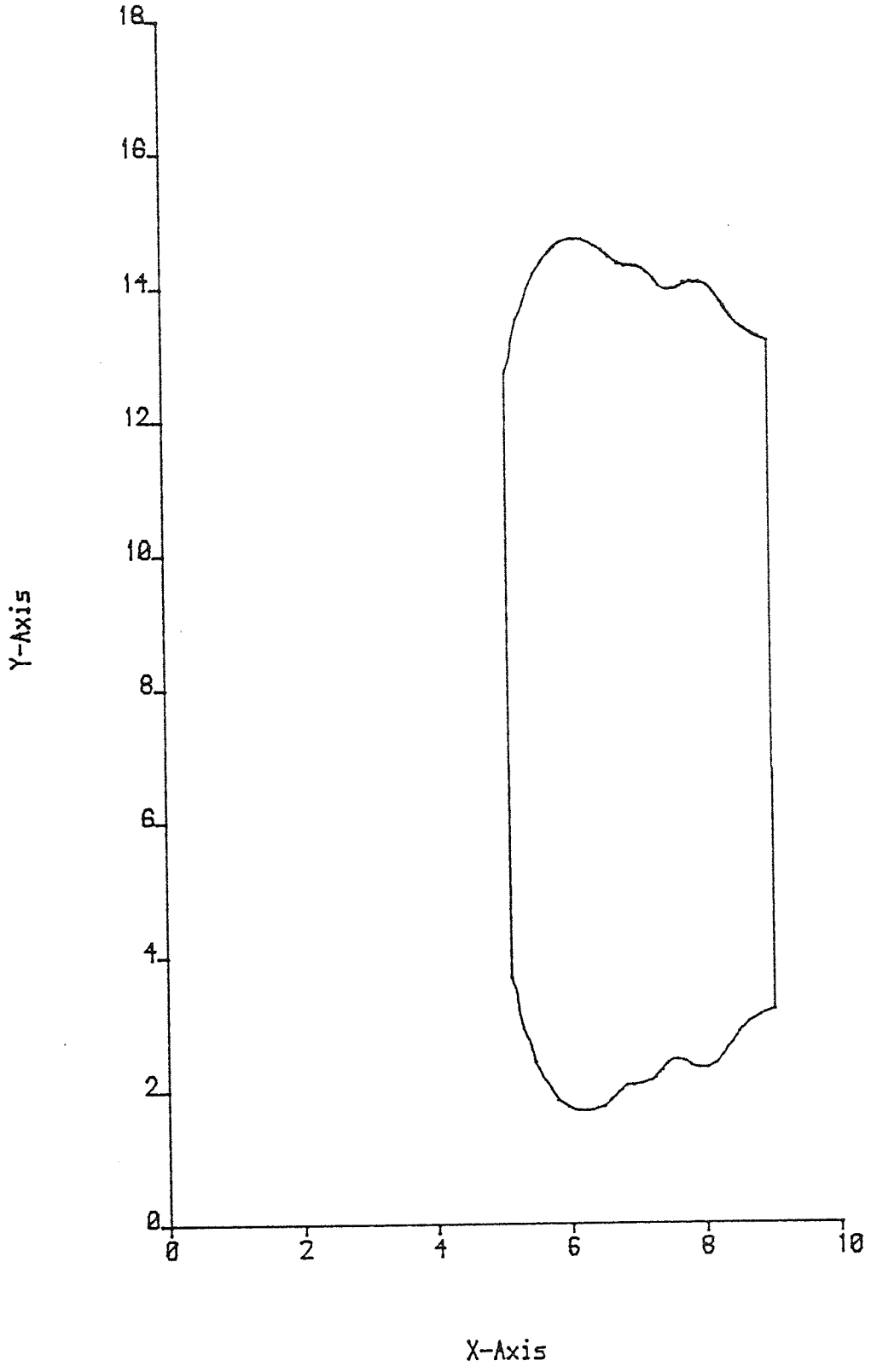

Fig(80.b)computer prediction of the cutter shape for the part. curved drill in Fig.70.b

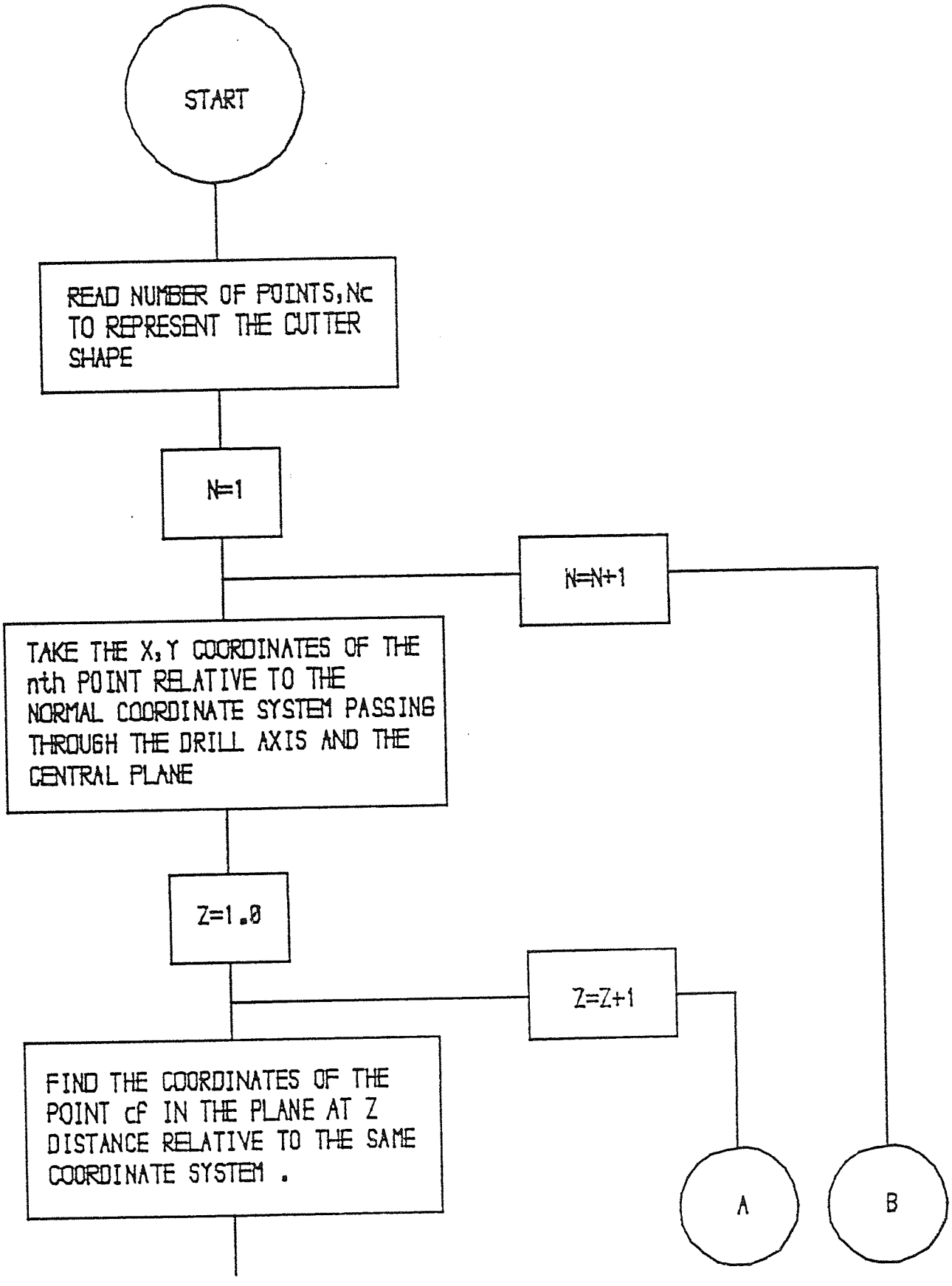

Figure 81 (continued)

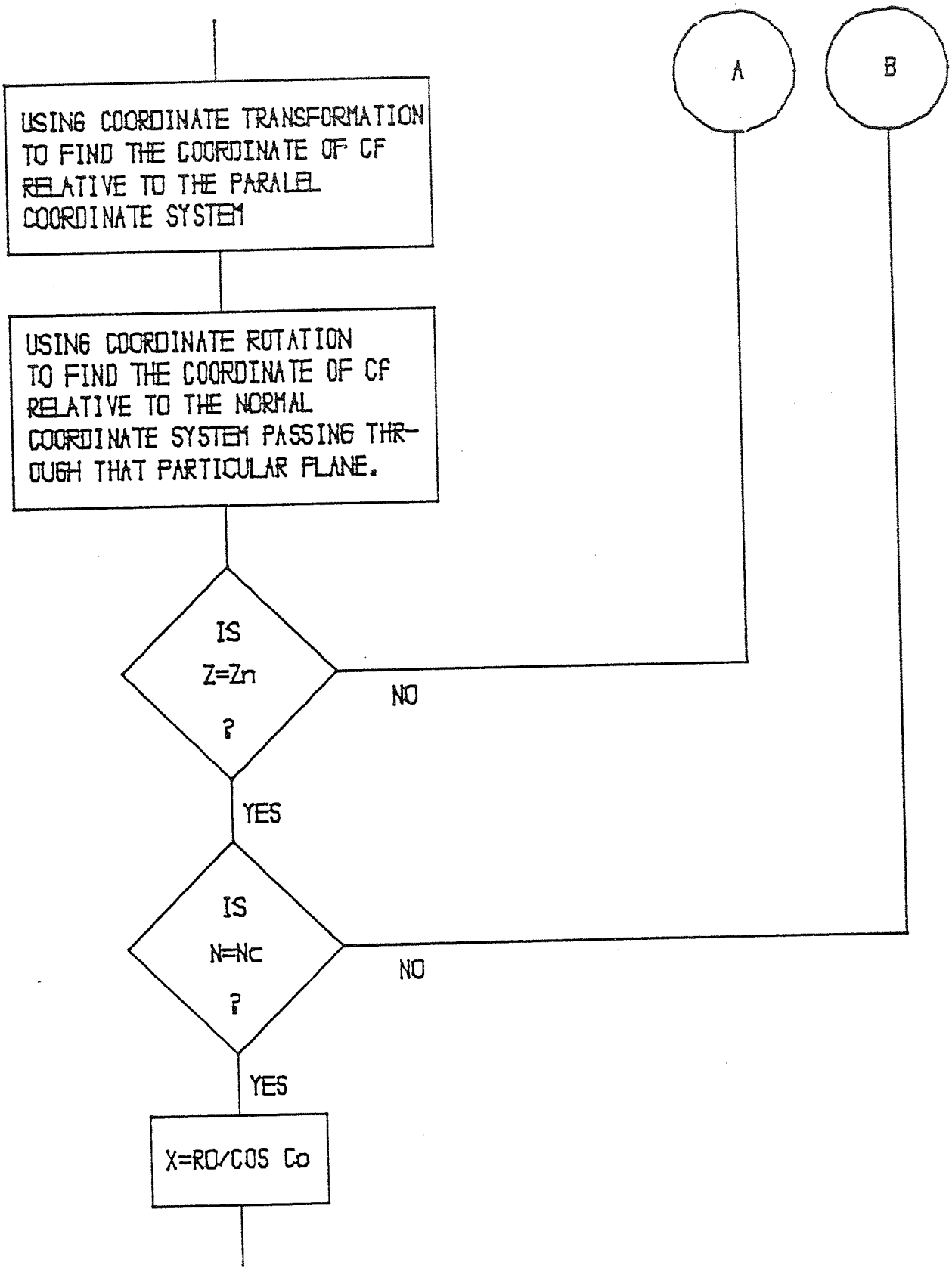

Figure 21 (continued)

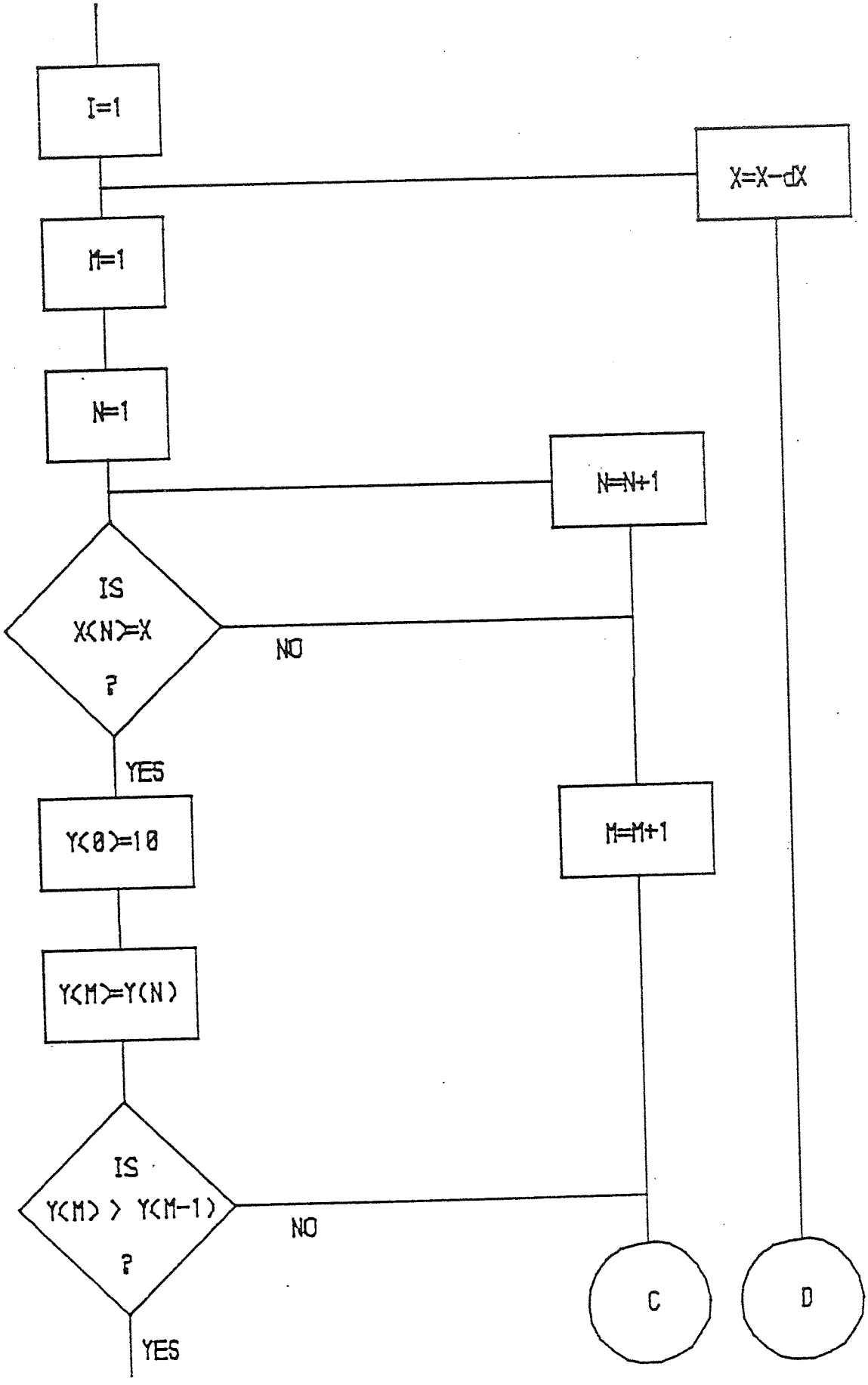

Figure 81 (continued)

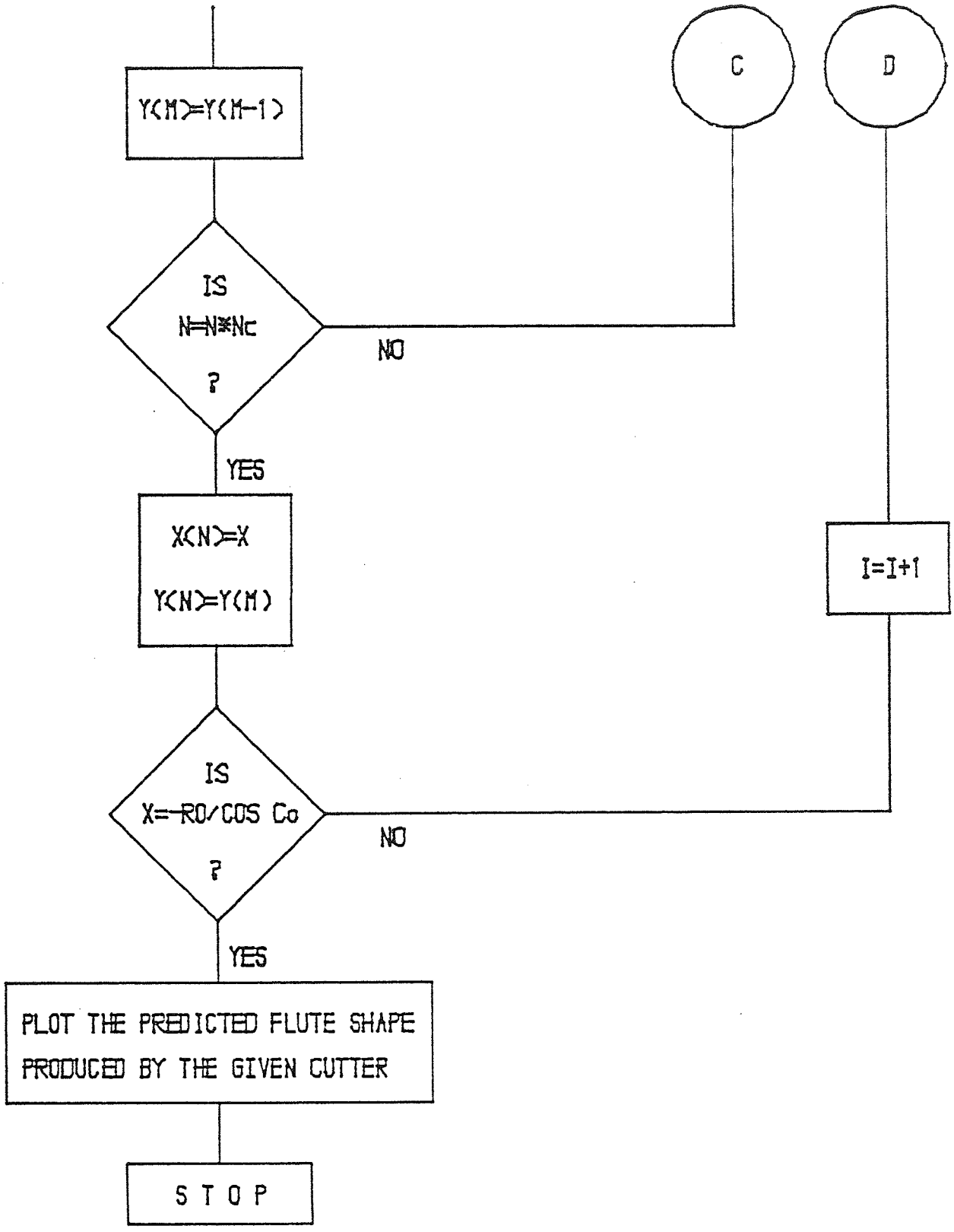

Figure 81 Flow diagram For the computer program For flute prediction

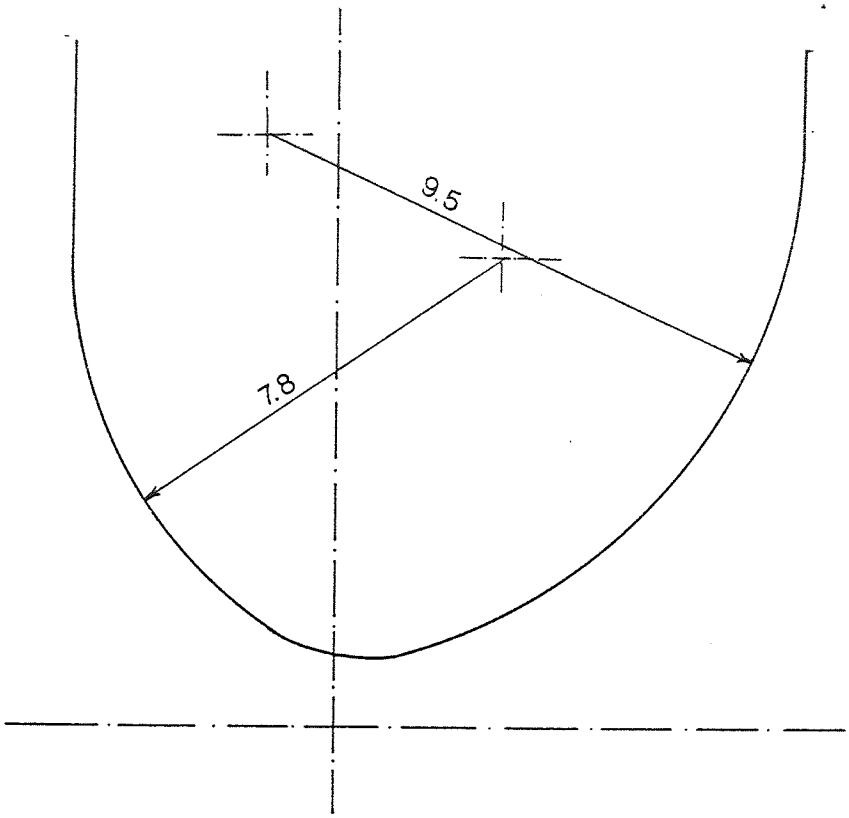

Fig 82 Typical cutter profile

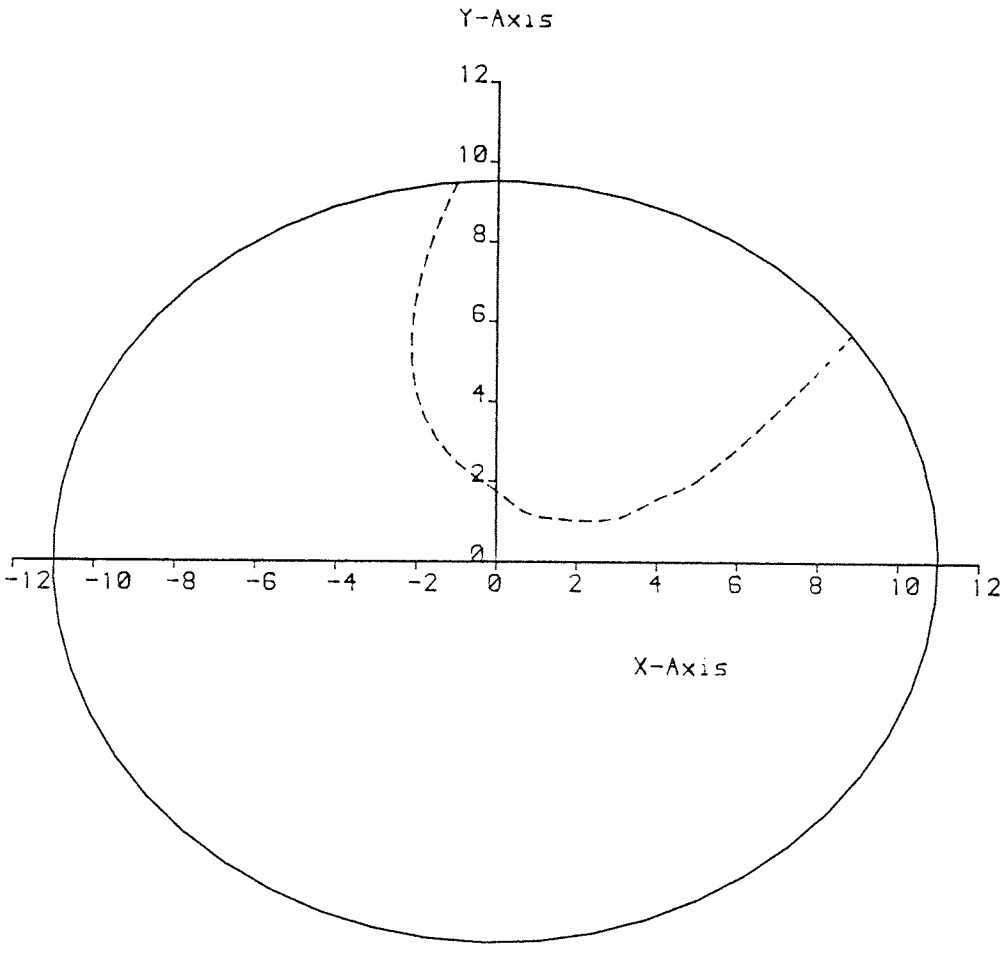

Fig 83 Computer prediction of the flute produced

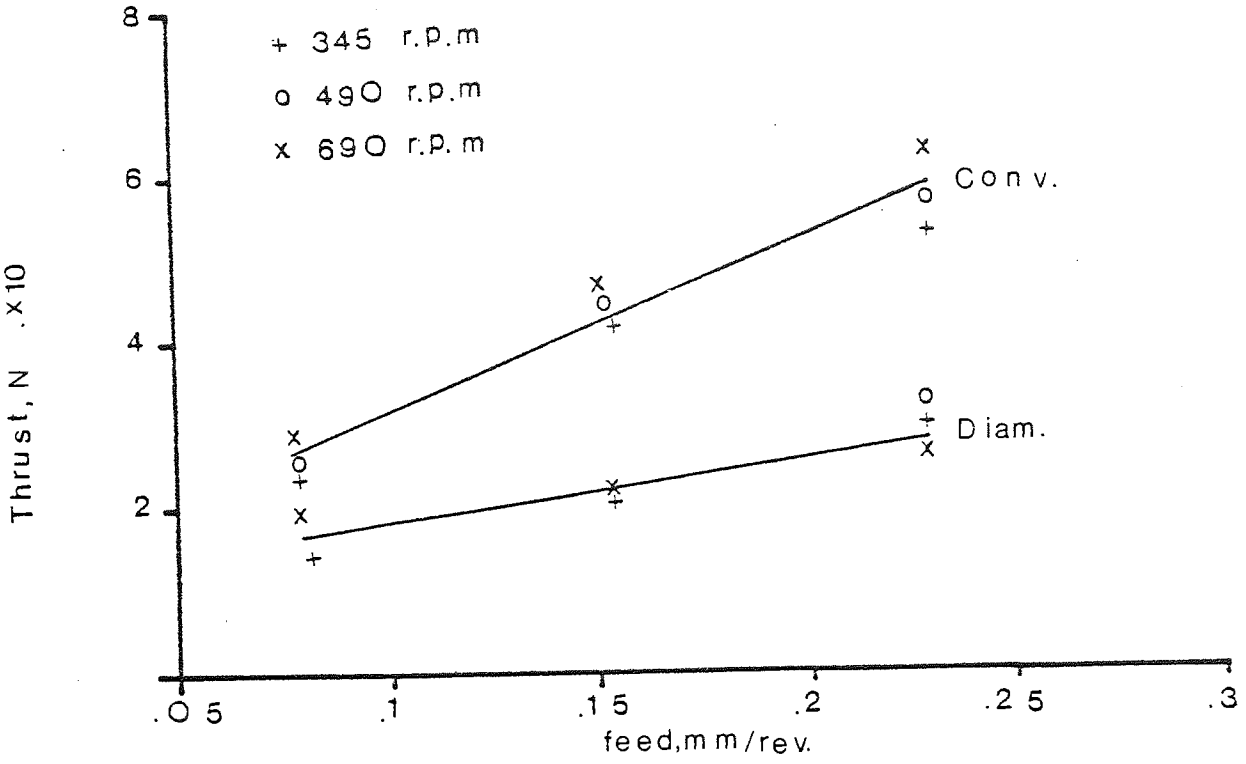

Fig 84 Drilling thrust for conventional and diametral drills

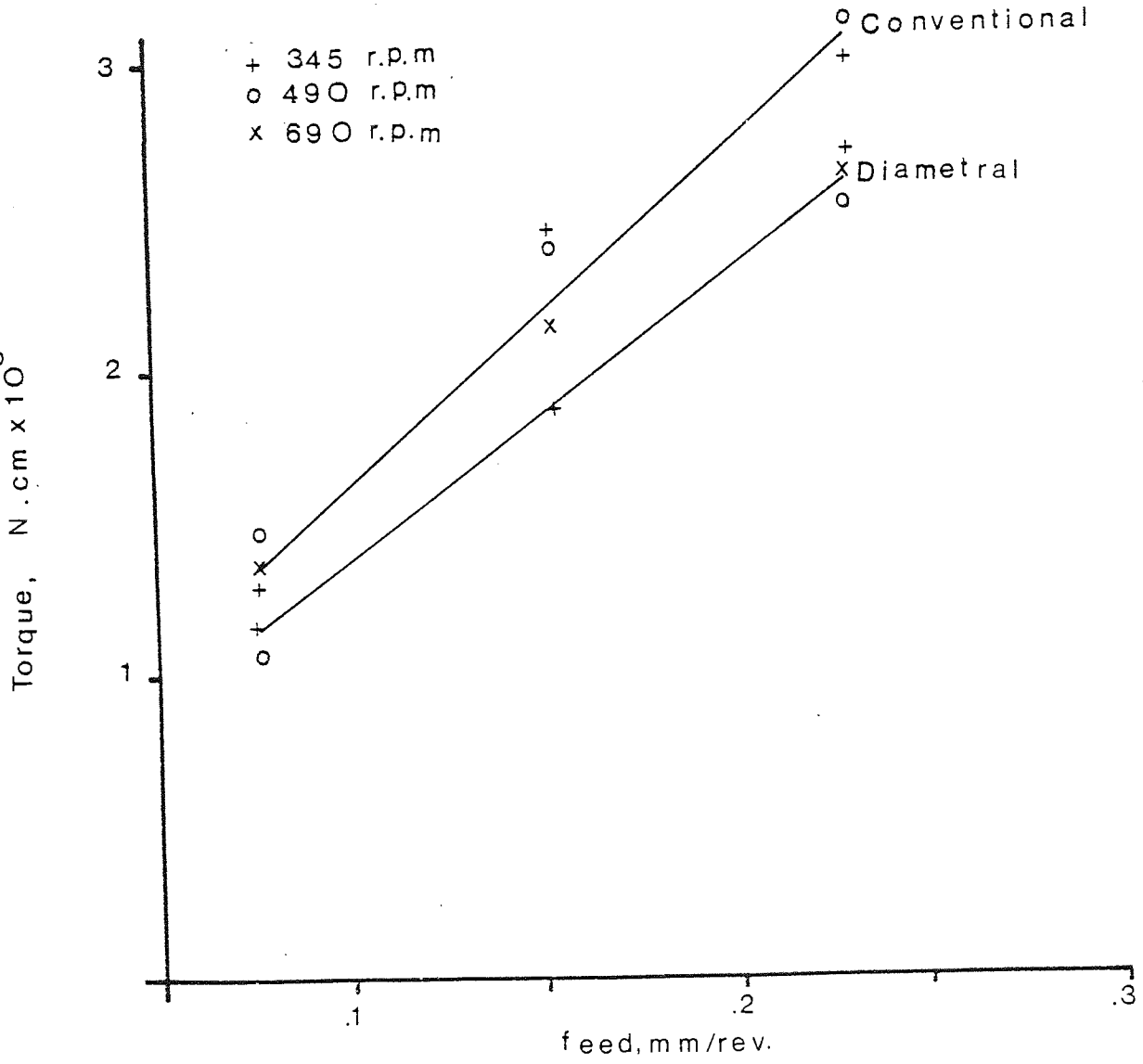

Fig 85 Drilling torque for conventional and diametral drills

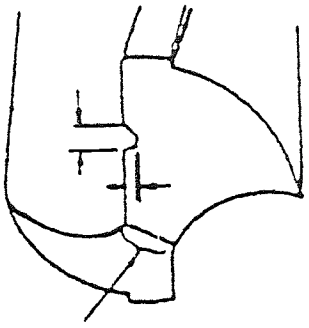

(a) Chipping at lip

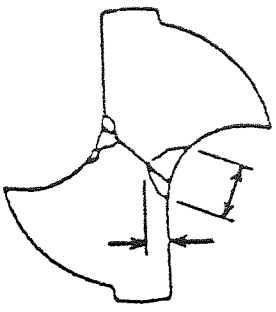

(b) Chisel edge wear

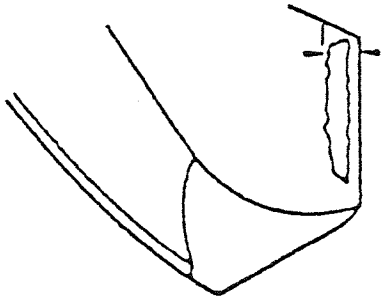

(c) Crater wear

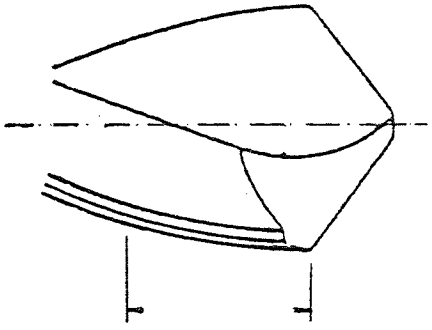

(d) Margin wear

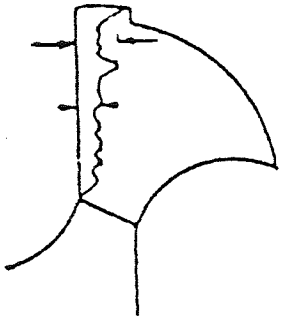

(e) Flank wear

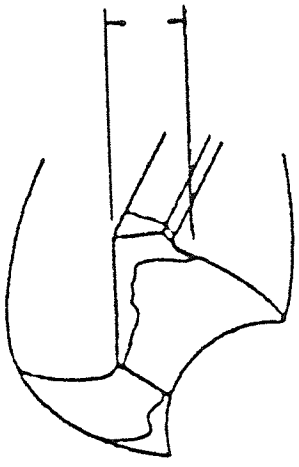

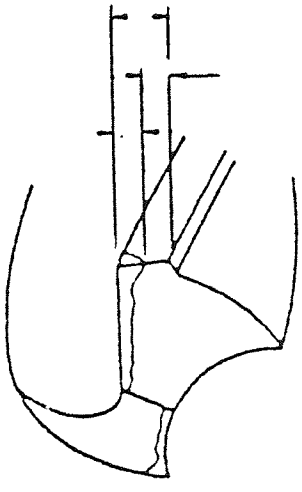

(f) Outer corner wear

Fig 86 Various types of drill wear

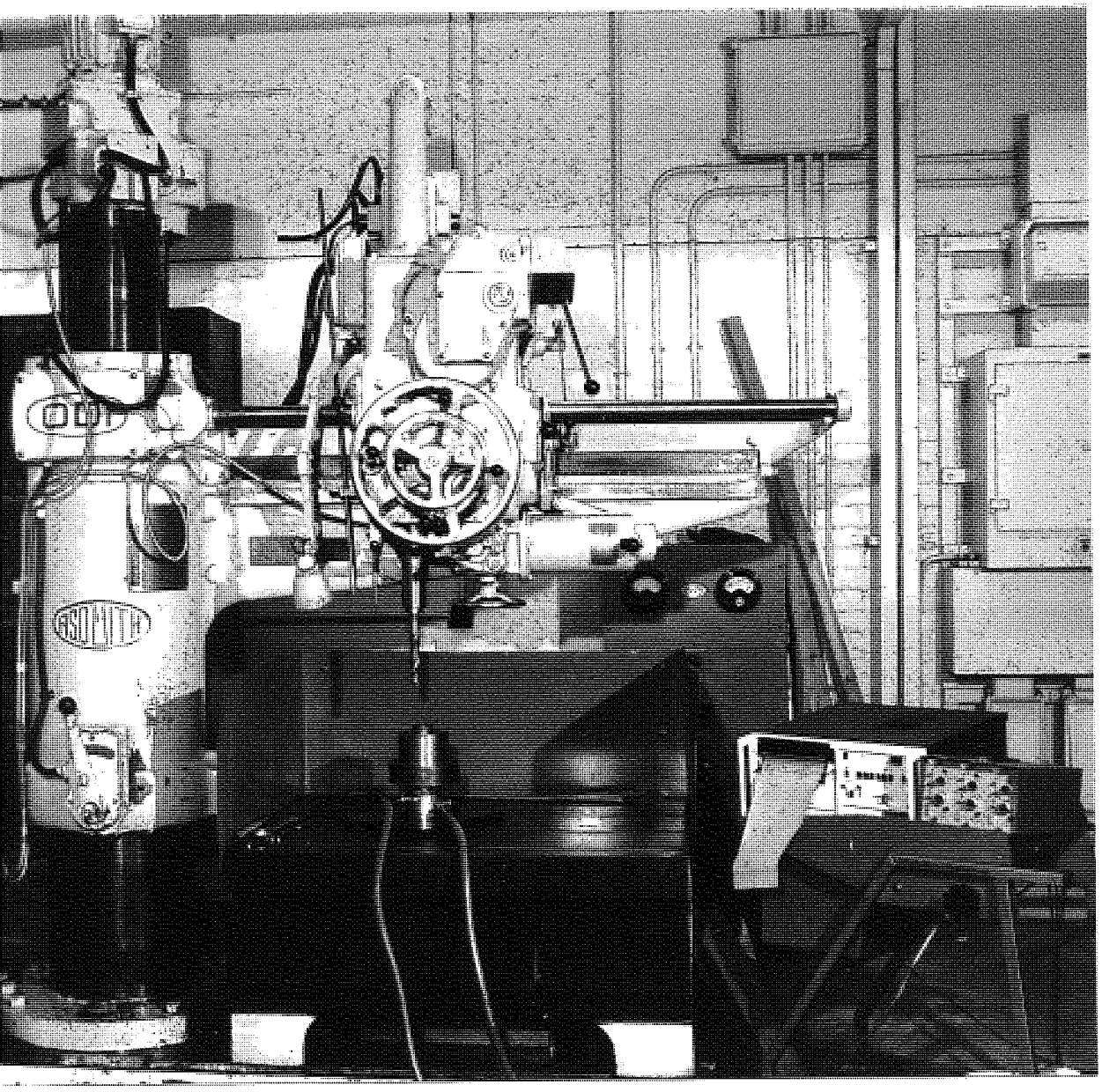

Fig 87 Radial drilling machine

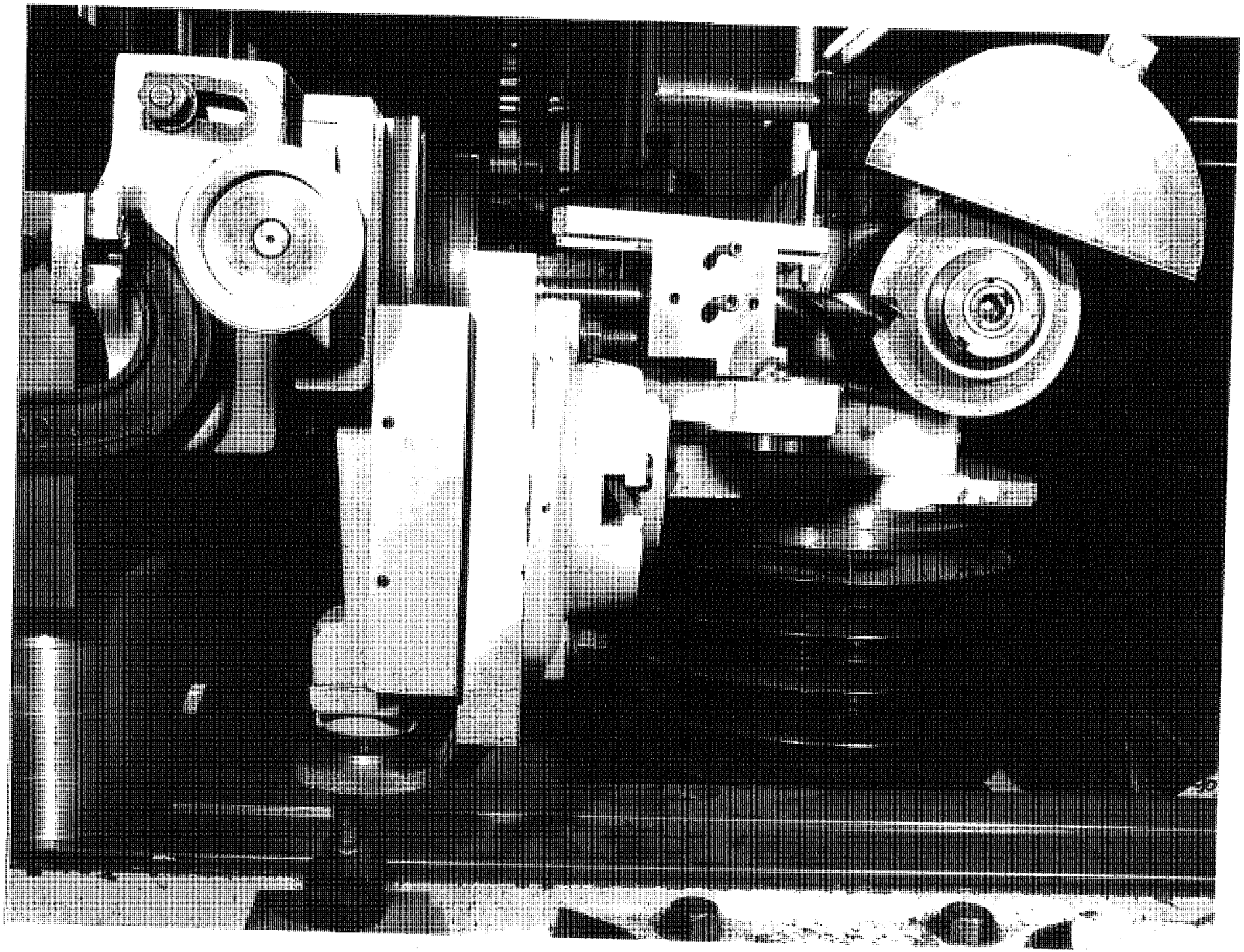

Fig 88 prototype drill grinder

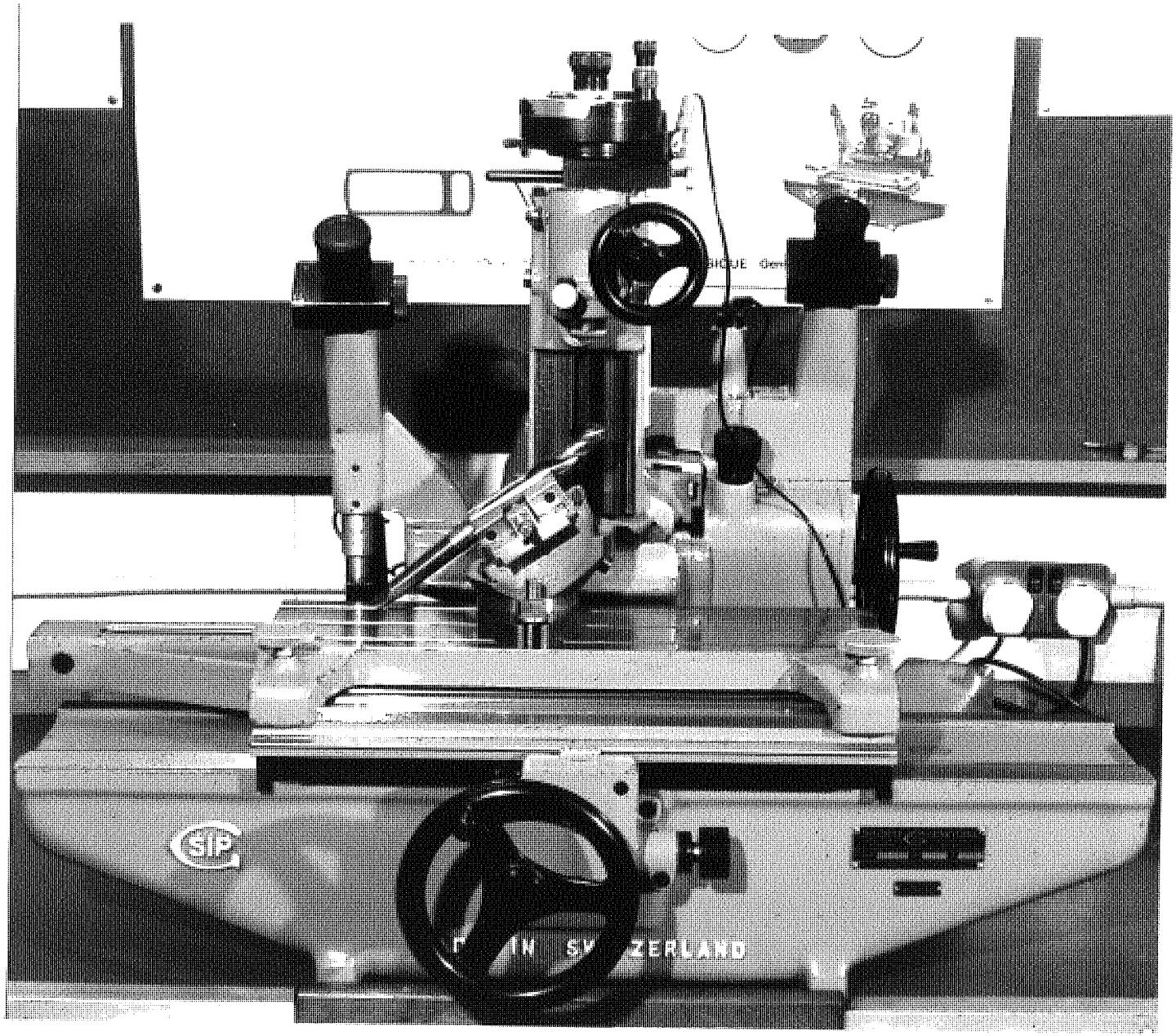

Fig 89 Wear measurement (U·M·M)

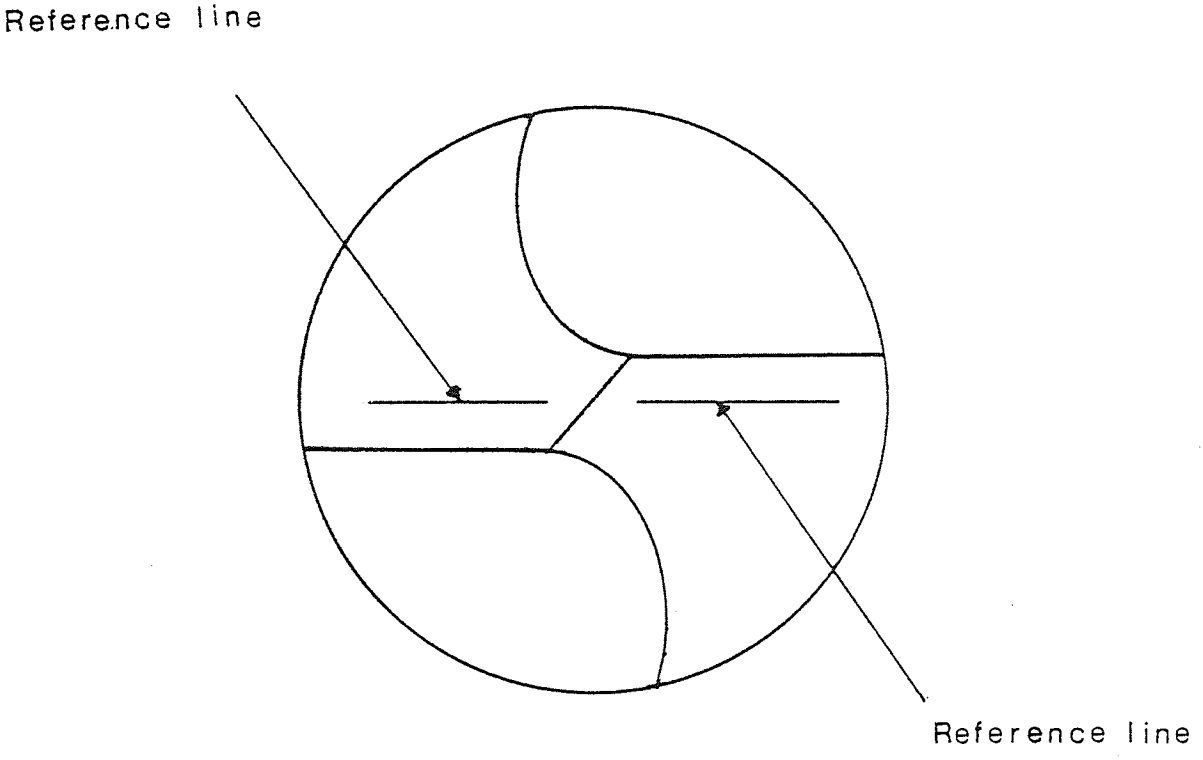

Fig 90 Etched line on the drill flank surface for wear measurement reference.

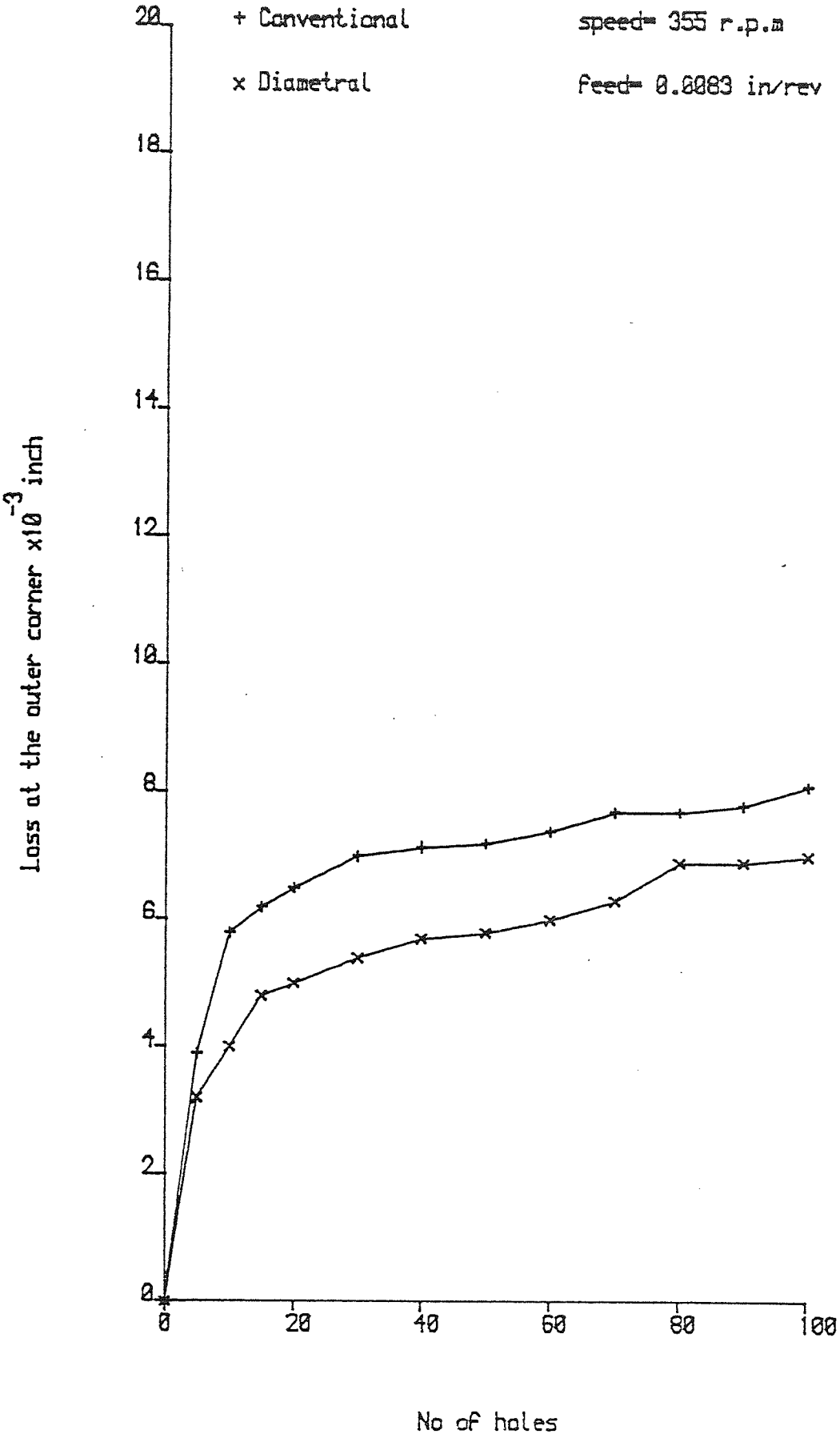

Figure 91 wear loss at the outer corner

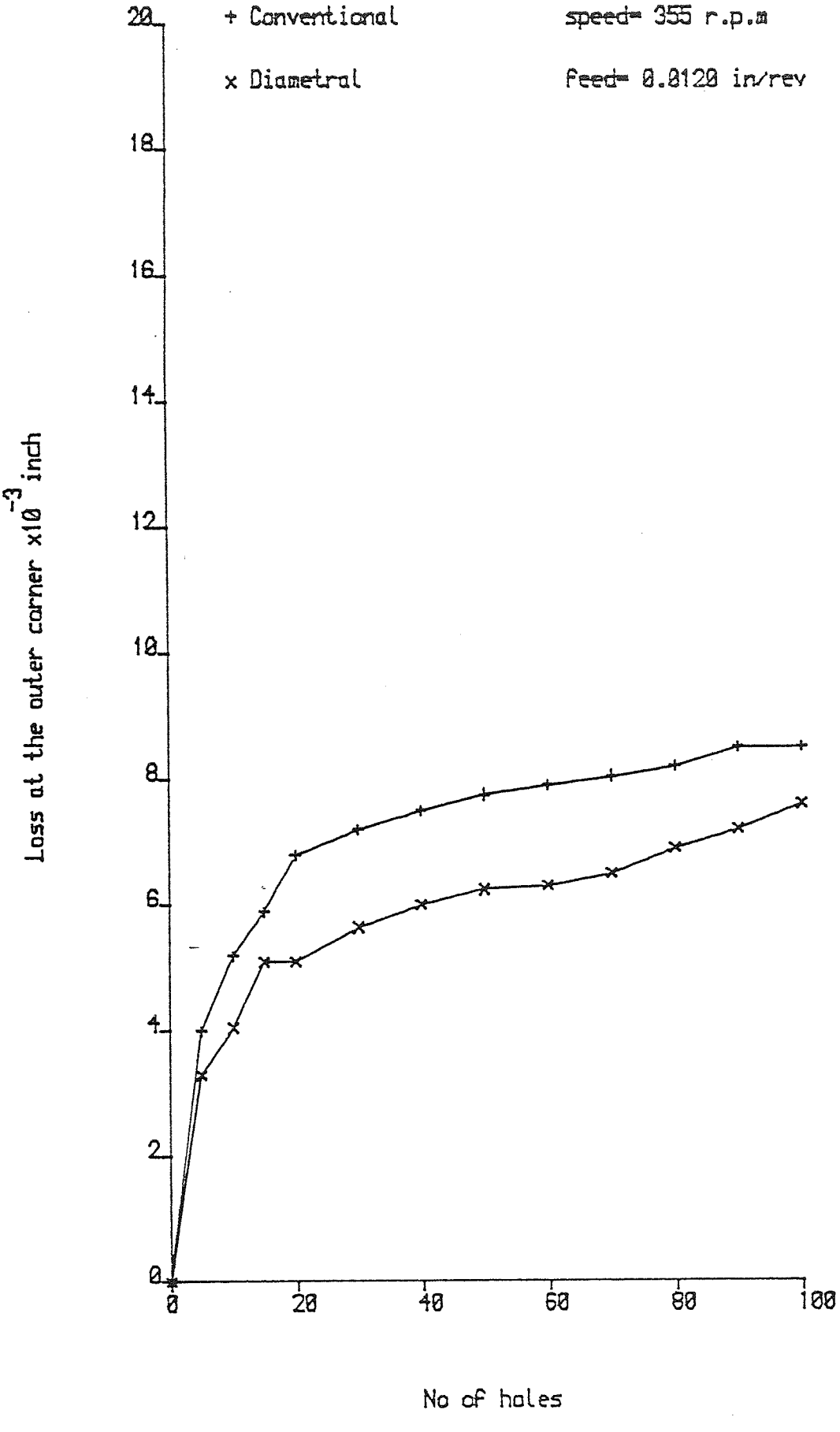

Figure 92 wear loss at the outer corner

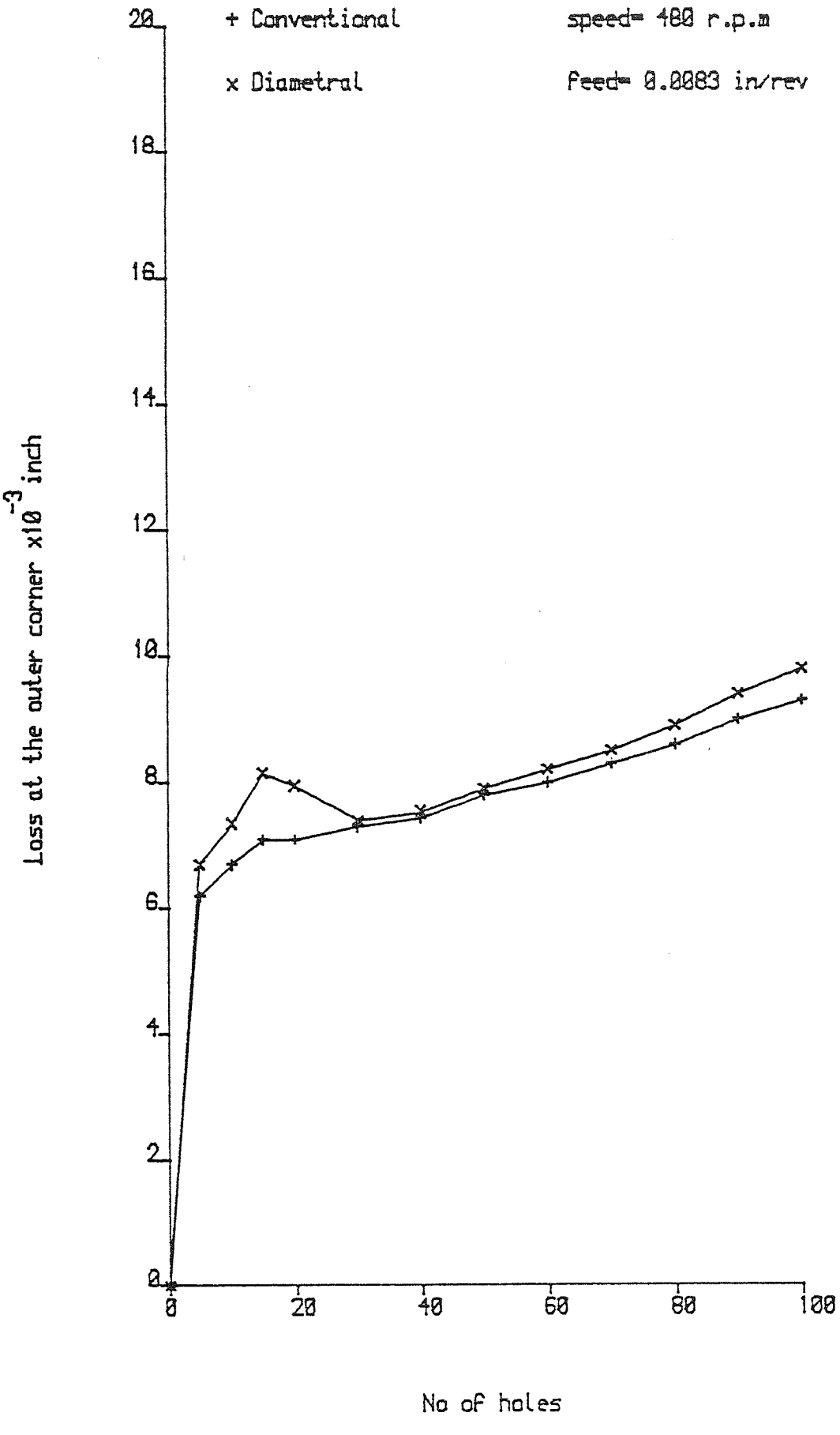

Figure 93 wear loss at the outer corner

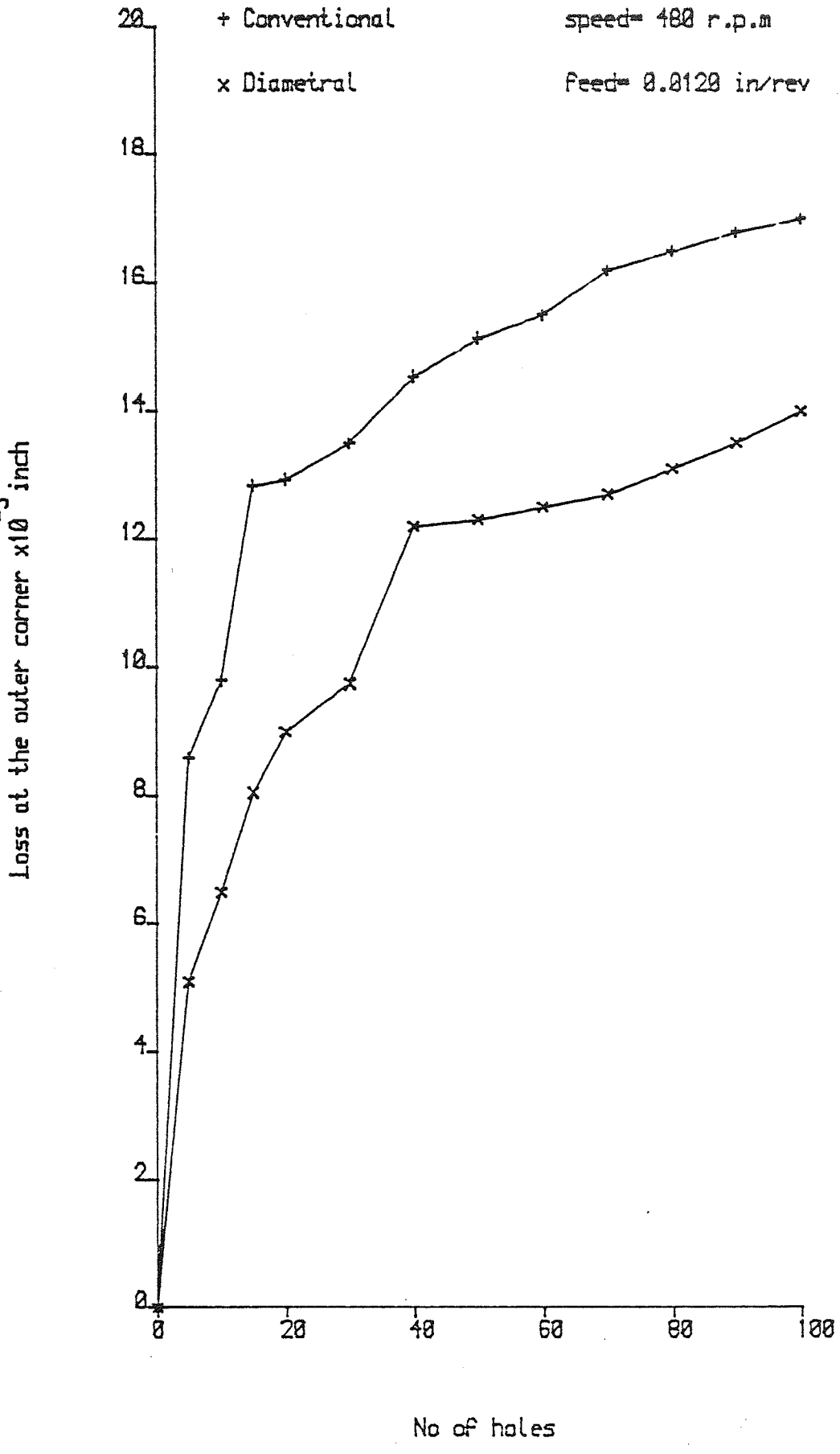

Figure 94 wear loss at the outer corner

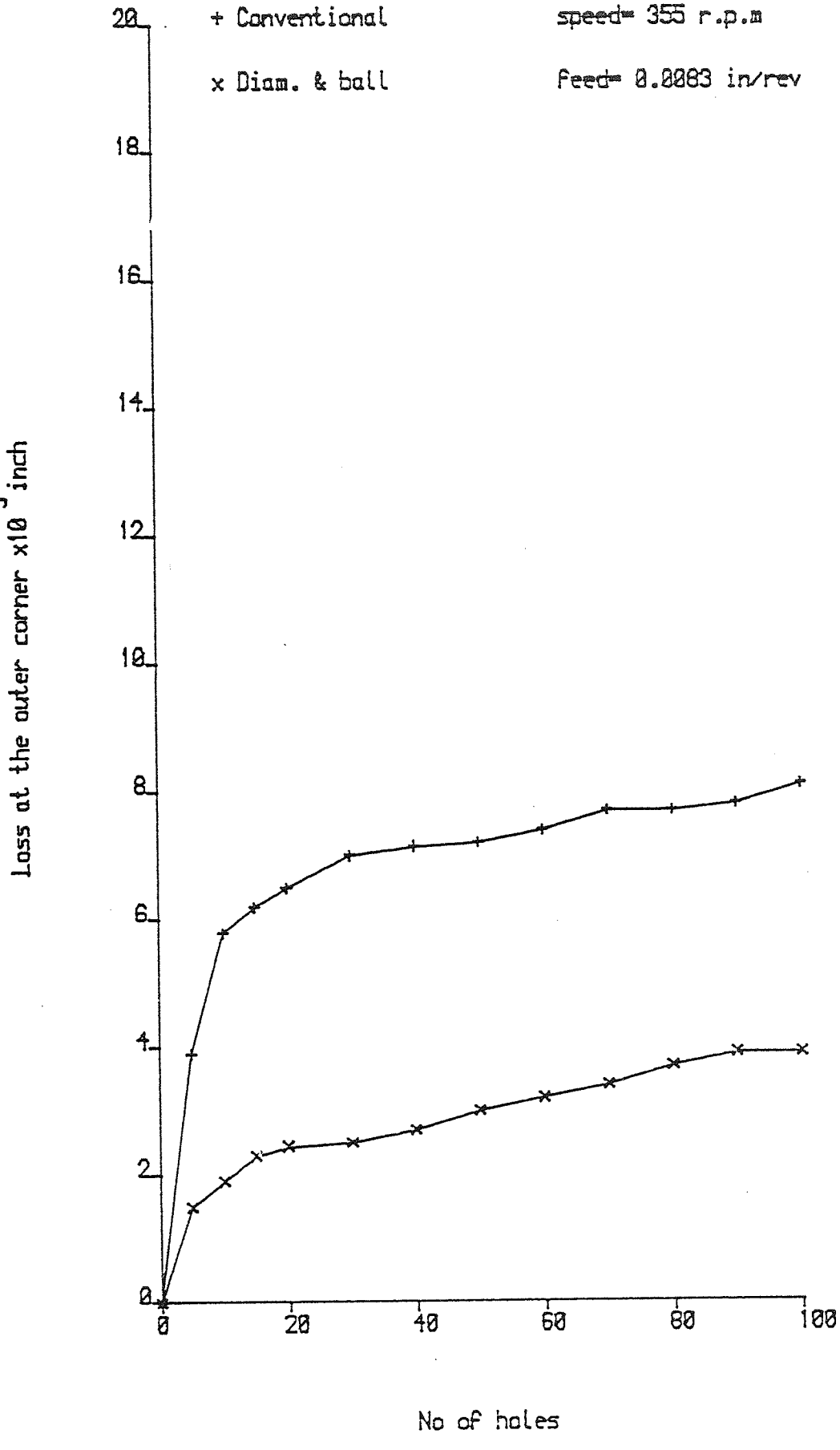

Figure 95 wear loss at the outer corner

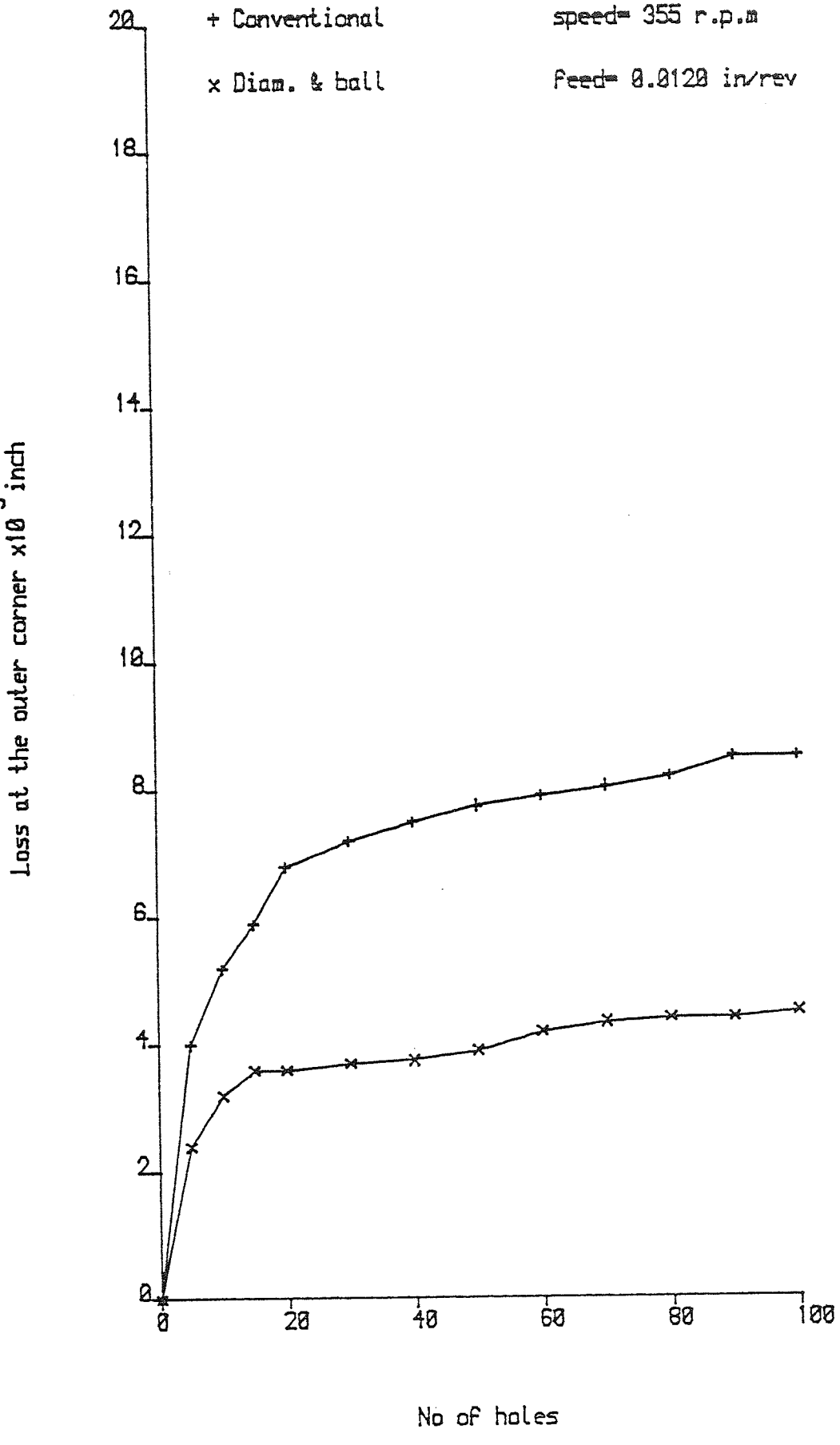

Figure 96 wear loss at the outer corner

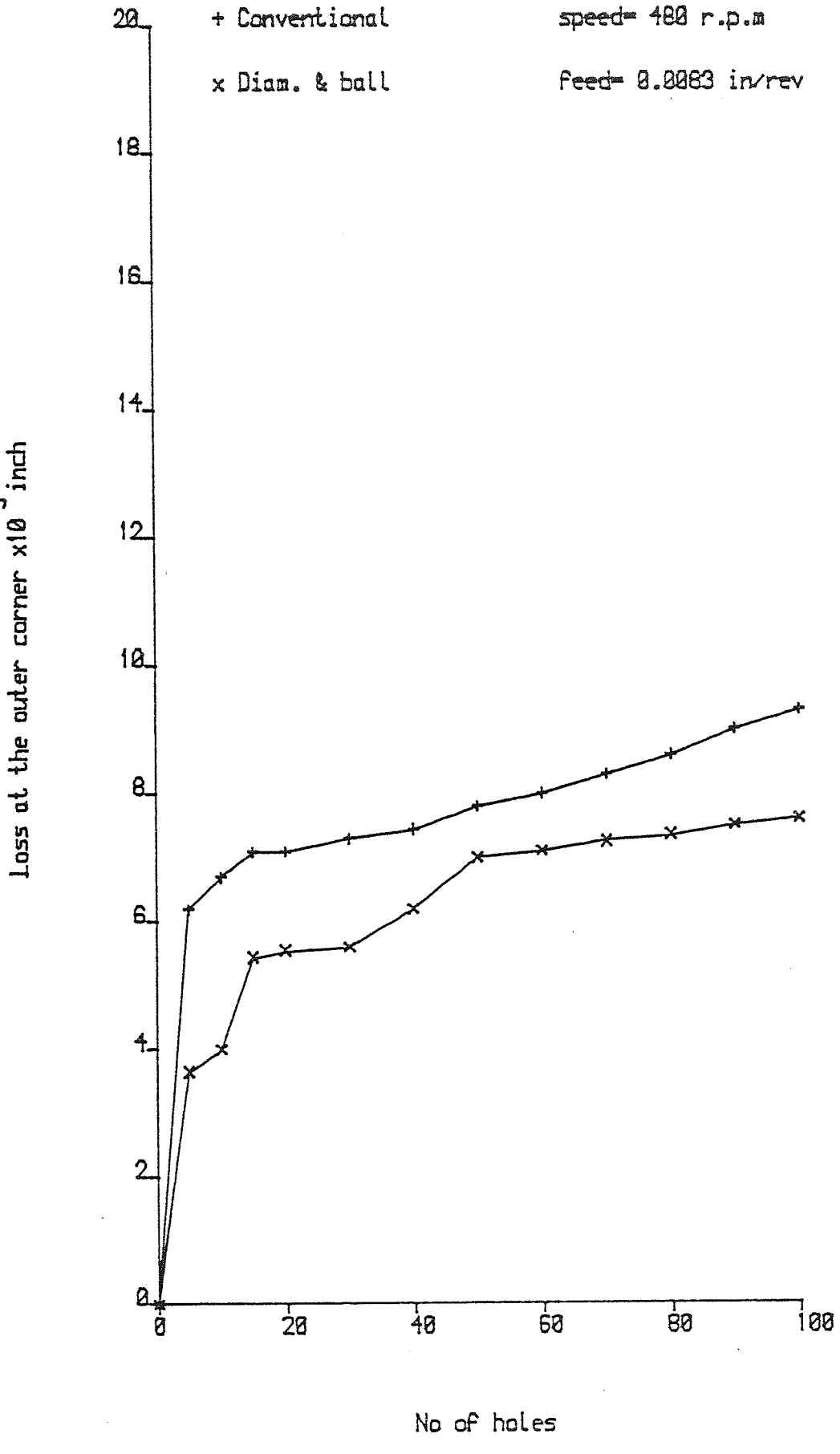

Figure 97 wear loss at the outer corner

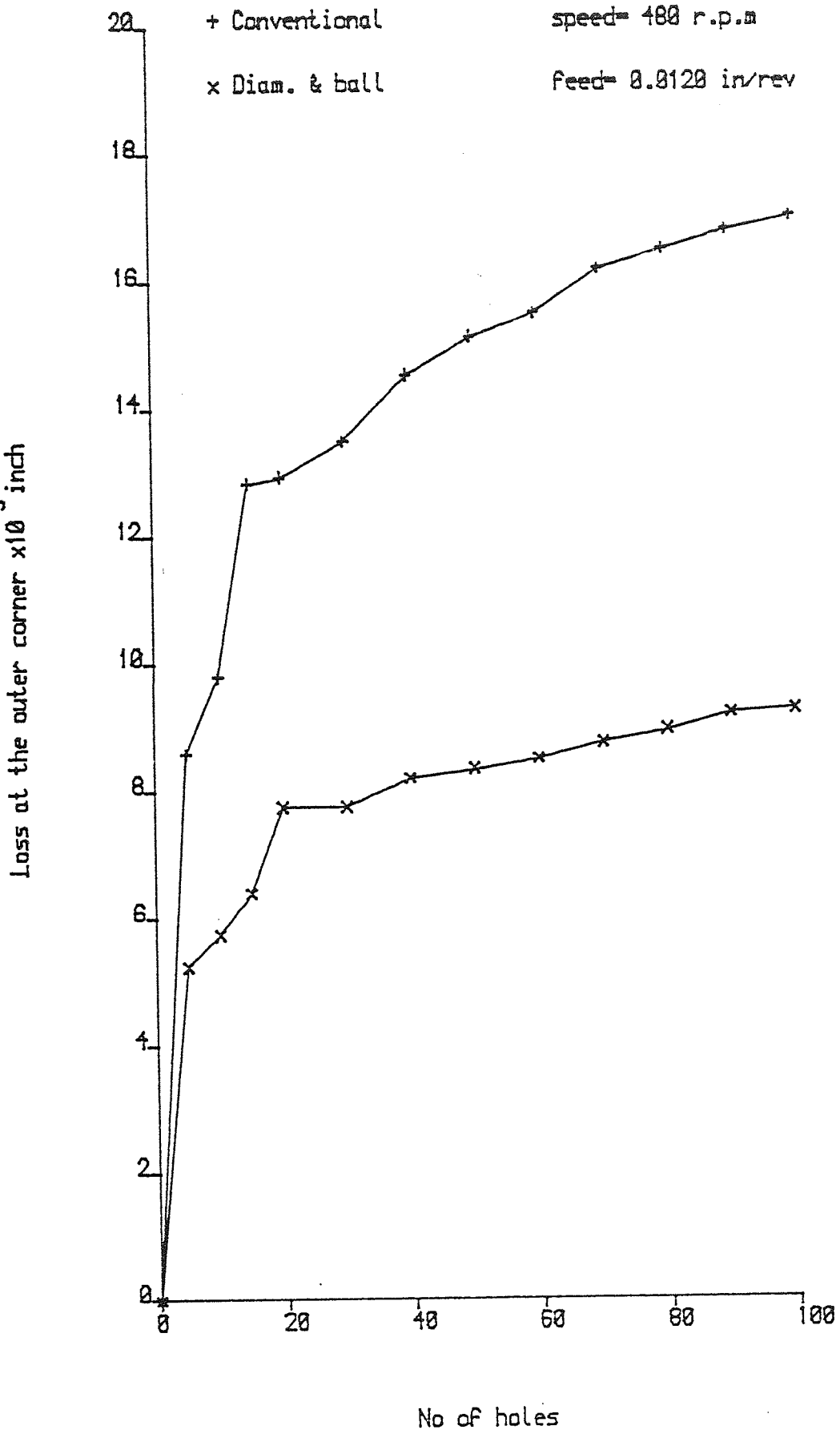

Figure 98 wear loss at the outer corner

Fig 99 Surface roughness measurement (Talysurf)

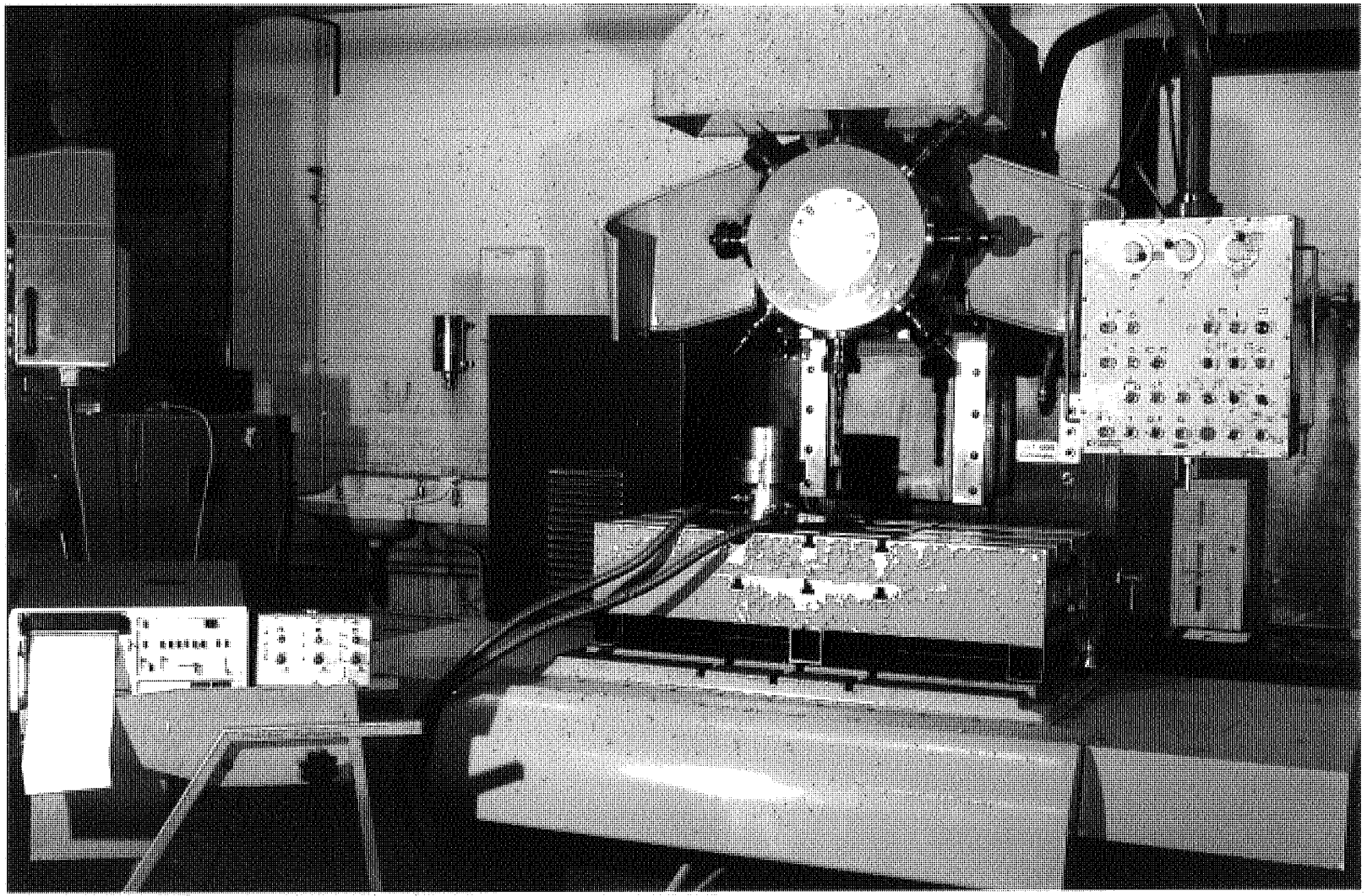

Fig 100 Cintimatic NC milling machine

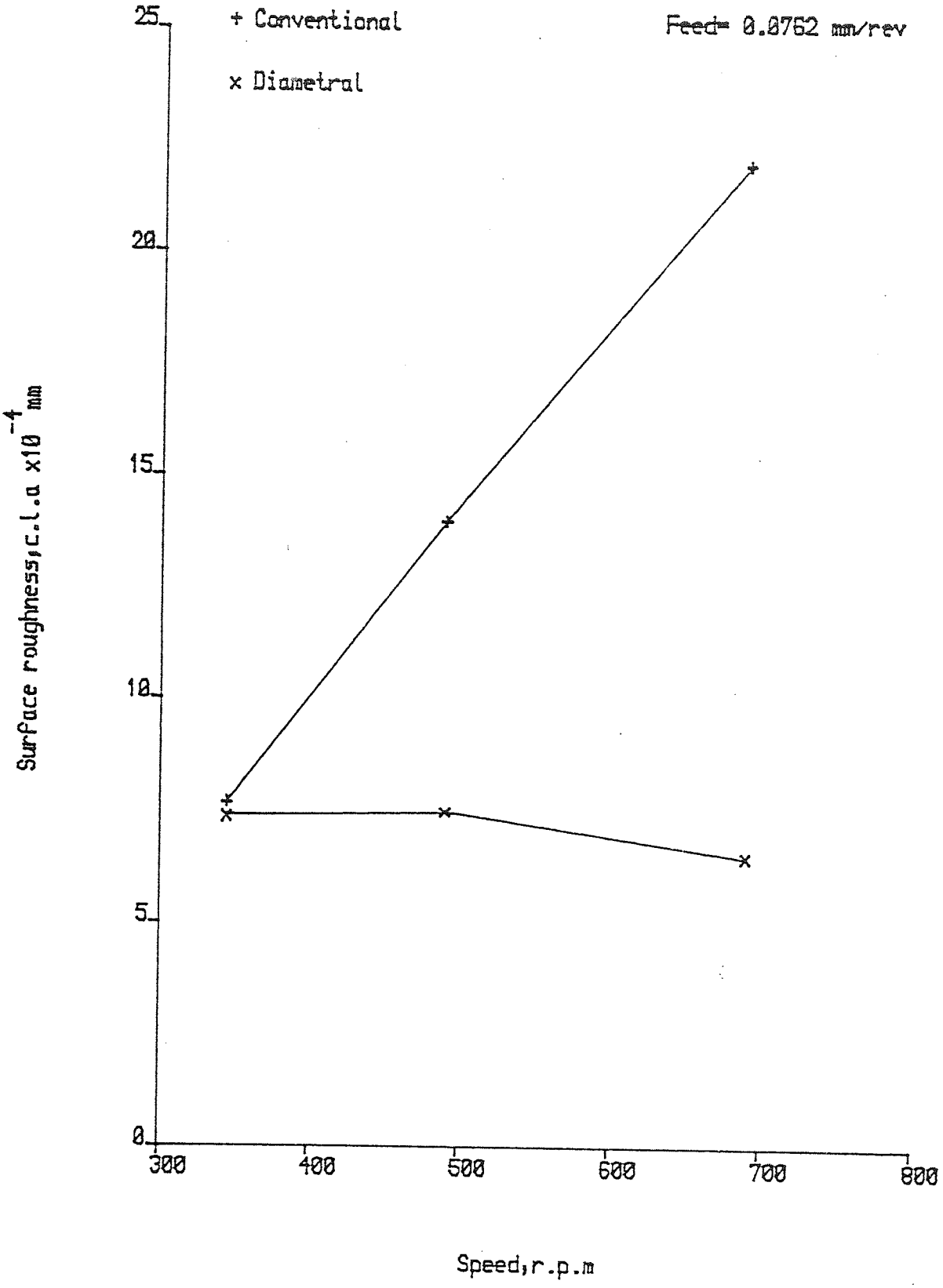

Figure 101 surface roughness comparison

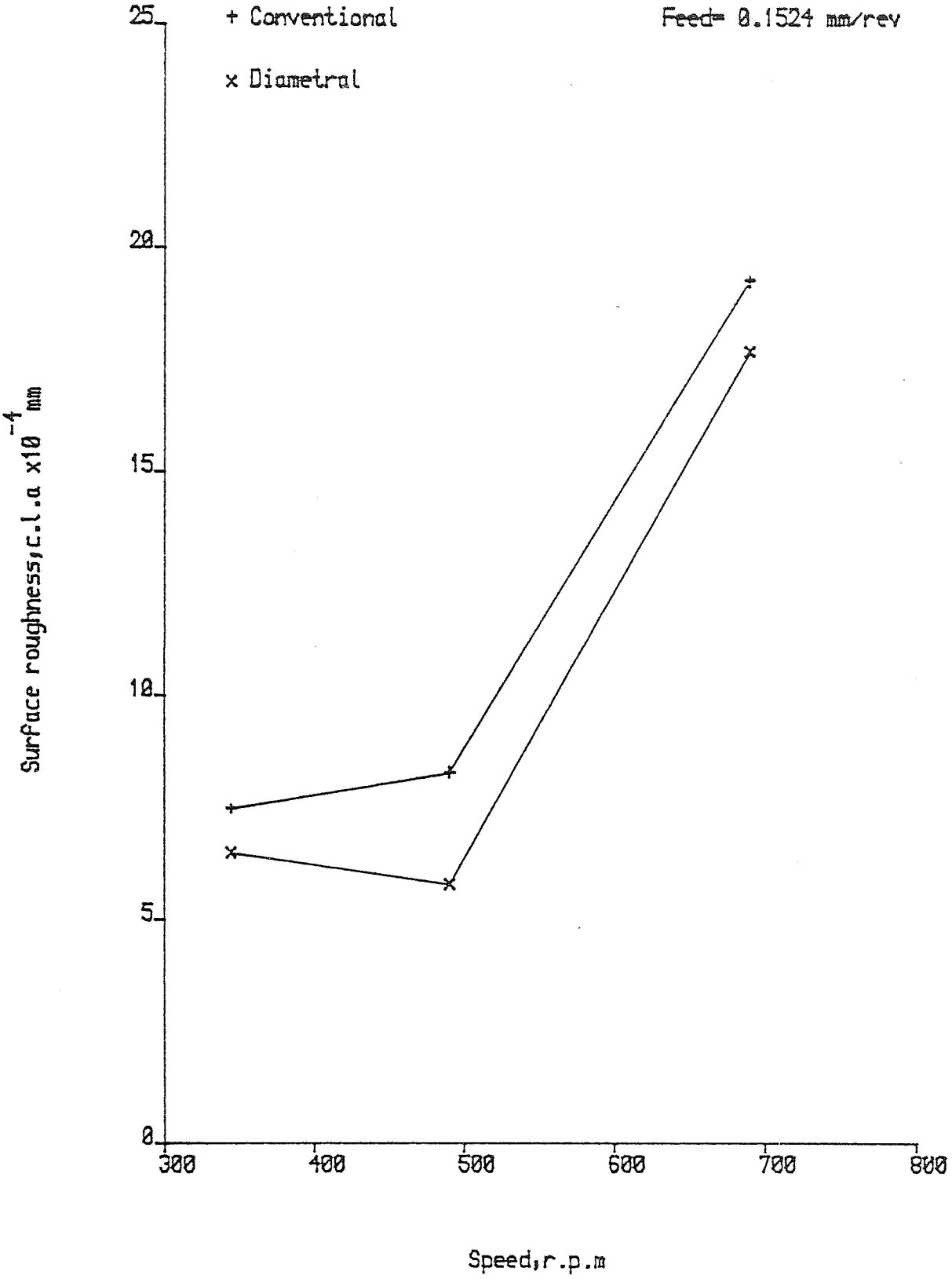

Figure 102 surface roughness comparison

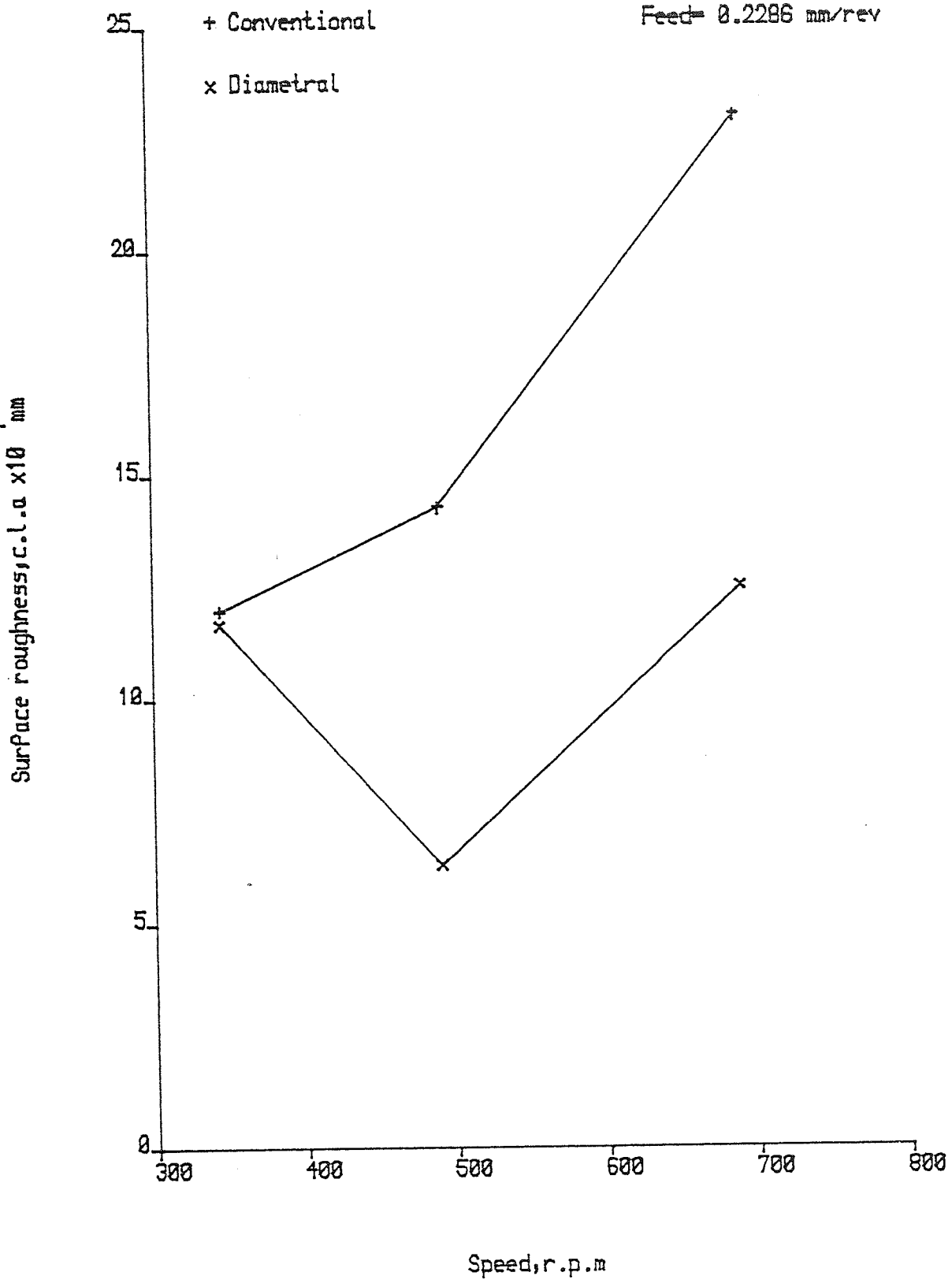

Figure 103 surface roughness comparison

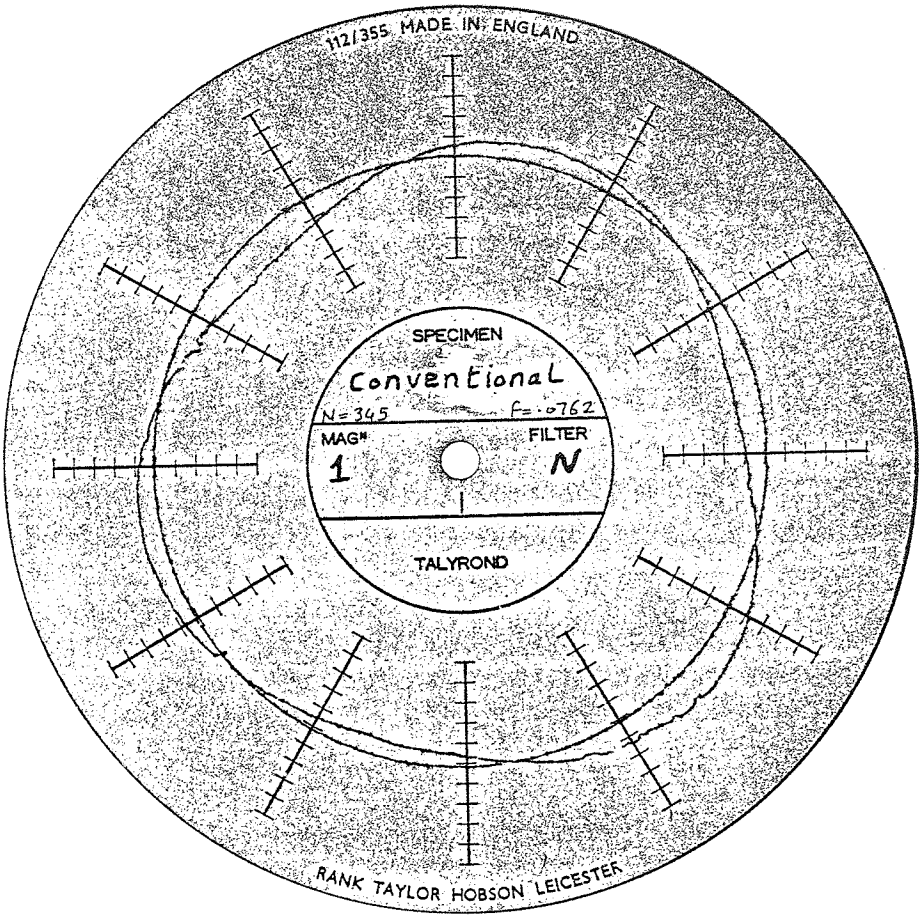

1 div. = .0005"

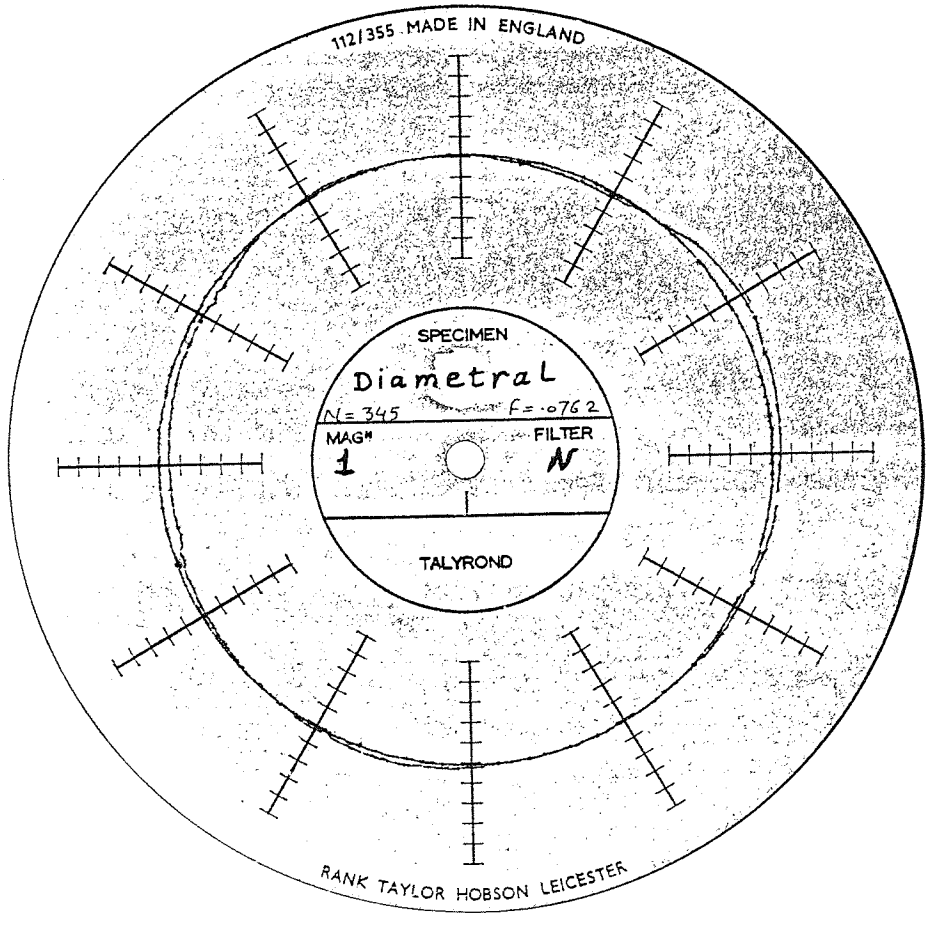

Fig 104 Talyrond trace

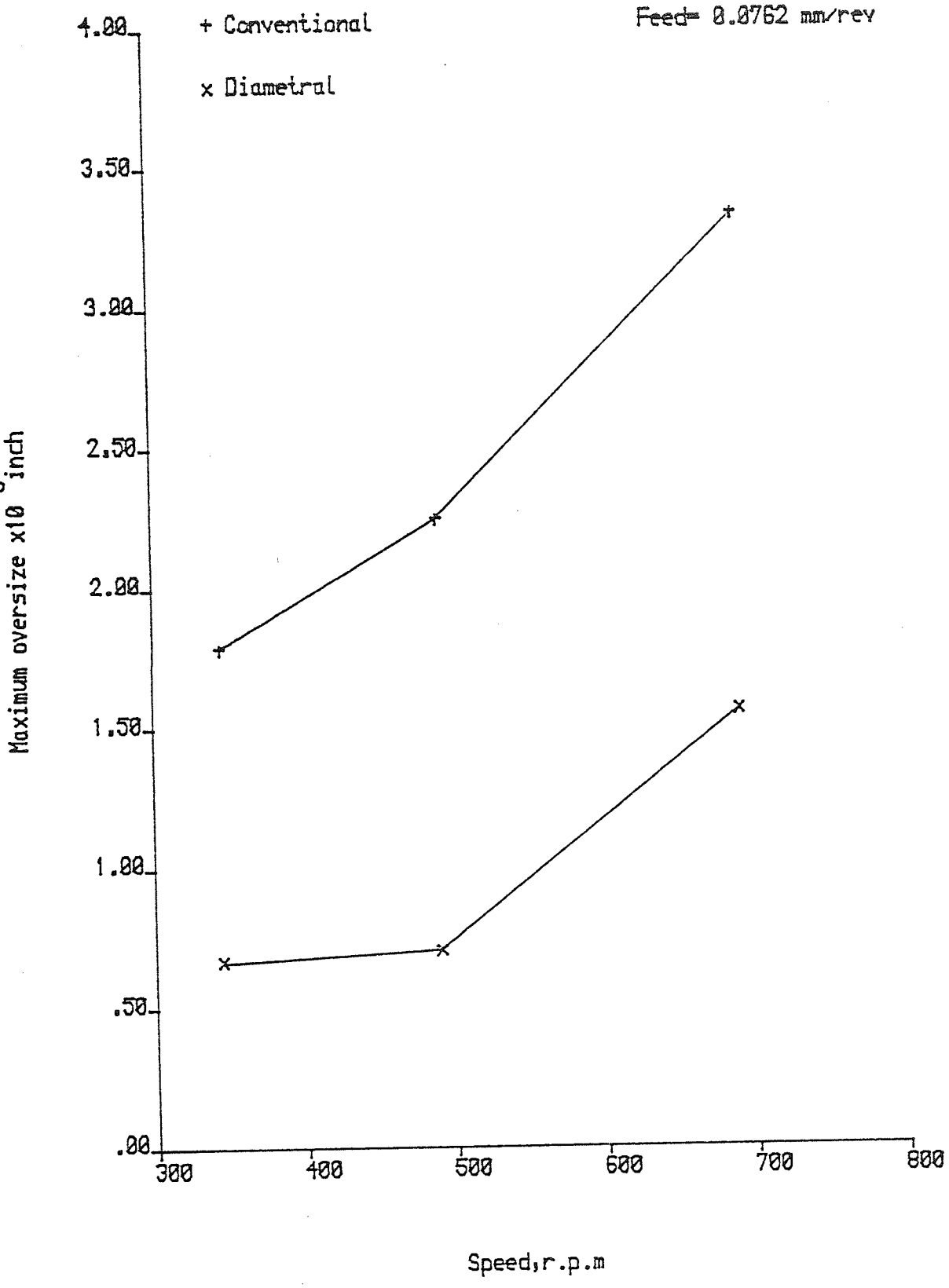

Figure 105 hole oversize comparison

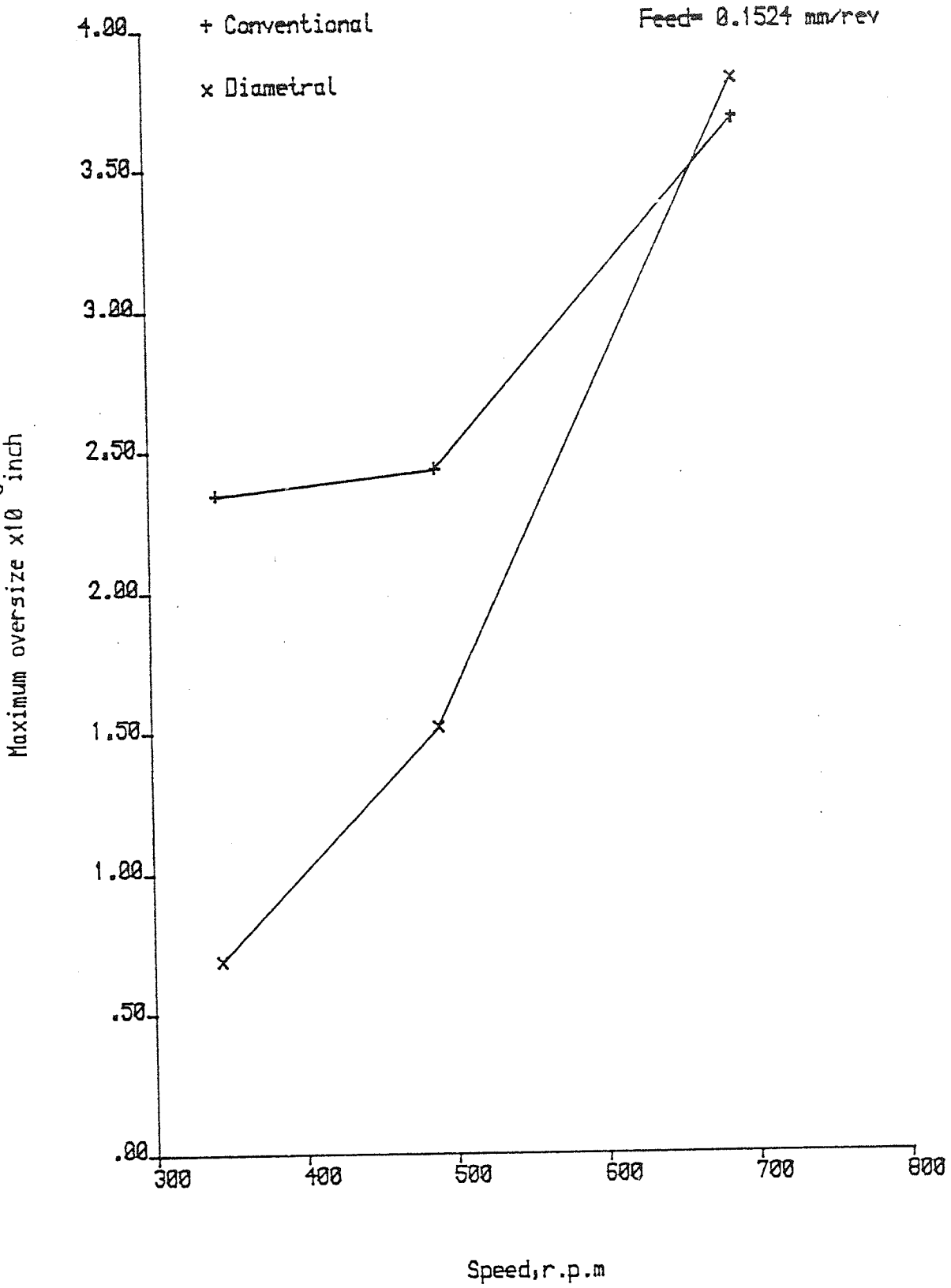

Figure 106 hole oversize comparison

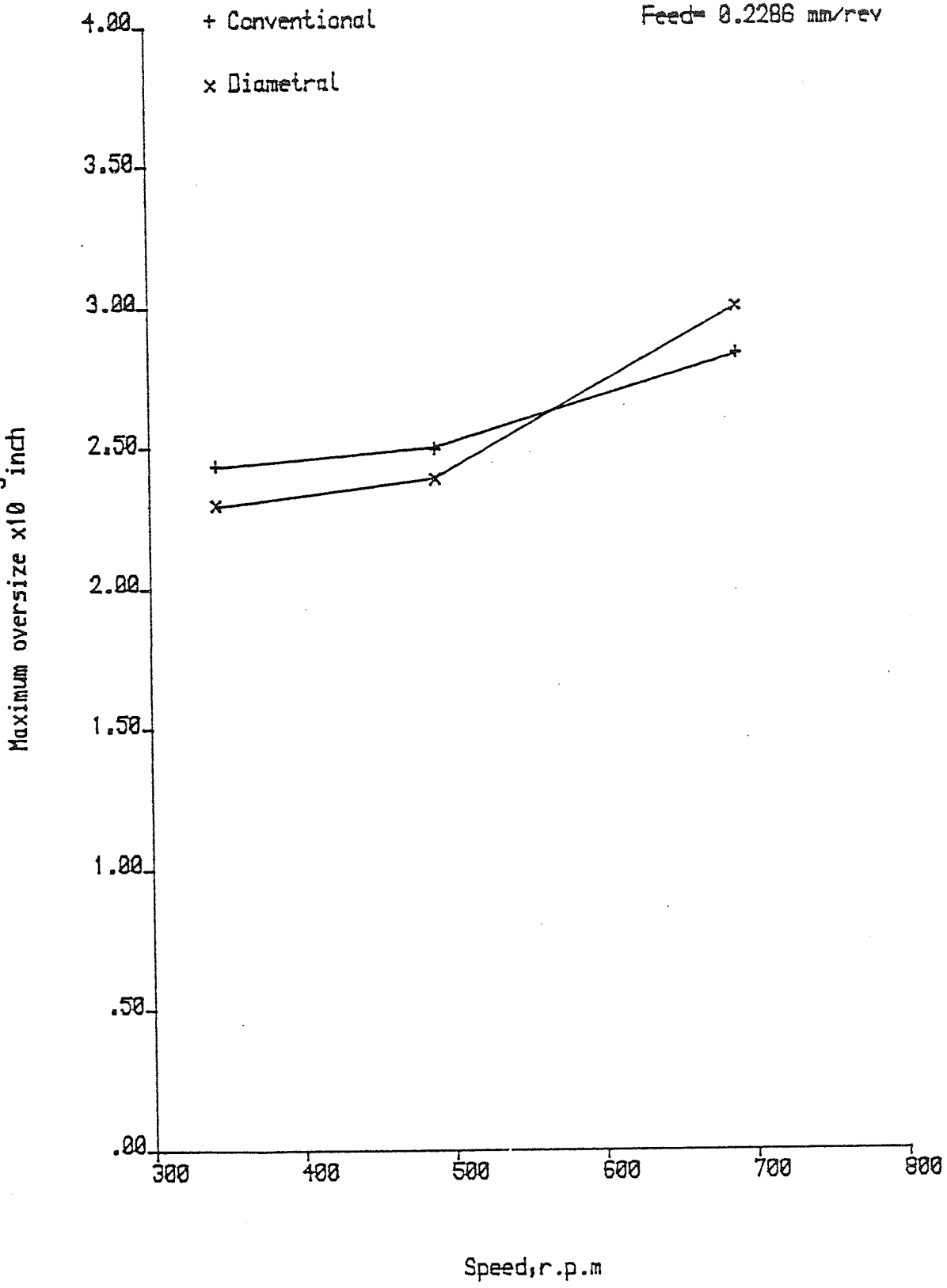

Figure 107 hole oversize comparison